



Western Washington University  
Western CEDAR

---

WWU Graduate School Collection

WWU Graduate and Undergraduate Scholarship

---

Spring 2021

## Synthesis and Reactions of Medium-Ring Silyl Ethers

Inna A. Fomina

Western Washington University, [inna.fomina01@gmail.com](mailto:inna.fomina01@gmail.com)

Follow this and additional works at: <https://cedar.wwu.edu/wwuet>

 Part of the [Chemistry Commons](#)

---

### Recommended Citation

Fomina, Inna A., "Synthesis and Reactions of Medium-Ring Silyl Ethers" (2021). *WWU Graduate School Collection*. 1030.

<https://cedar.wwu.edu/wwuet/1030>

This Masters Thesis is brought to you for free and open access by the WWU Graduate and Undergraduate Scholarship at Western CEDAR. It has been accepted for inclusion in WWU Graduate School Collection by an authorized administrator of Western CEDAR. For more information, please contact [westerncedar@wwu.edu](mailto:westerncedar@wwu.edu).

**Synthesis and Reactions  
of Medium-Ring Silyl Ethers**

By

Inna A. Fomina

Accepted in Partial Completion  
of the Requirements for the Degree  
Master of Science

ADVISORY COMMITTEE

Dr. Gregory O'Neil, Chair

Dr. James Vyvyan

Dr. Margaret Scheuermann

GRADUATE SCHOOL

David L. Patrick, Interim Dean

## Master's Thesis

In presenting this thesis in partial fulfillment of the requirements for a master's degree at Western Washington University, I grant to Western Washington University the non-exclusive royalty-free right to archive, reproduce, distribute, and display the thesis in any and all forms, including electronic format, via any digital library mechanisms maintained by WWU.

I represent and warrant this is my original work, and does not infringe or violate any rights of others. I warrant that I have obtained written permissions from the owner of any third party copyrighted material included in these files.

I acknowledge that I retain ownership rights to the copyright of this work, including but not limited to the right to use all or part of this work in future works, such as articles or books.

Library users are granted permission for individual, research and non-commercial reproduction of this work for educational purposes only. Any further digital posting of this document requires specific permission from the author.

Any copying or publication of this thesis for commercial purposes, or for financial gain, is not allowed without my written permission.

Inna A. Fomina

May 28<sup>th</sup>, 2021

**Synthesis and Reactions  
of Medium-Ring Silyl Ethers**

A Thesis  
Presented to  
The Faculty of  
Western Washington University

In Partial Fulfillment  
Of the Requirements for the Degree  
Master of Science

by  
Inna A. Fomina  
May 2021

## ABSTRACT

Olefin metathesis is a reaction that creates new carbon-carbon double bonds by rearranging two alkenes. The reaction has undergone significant development since its discovery in the 1950s, from first reports to new catalysts and industrial uses, culminating in the 2005 Nobel Prize in chemistry. Grubbs ruthenium-based catalysts are widely used for such reactions, including ring closing metathesis (RCM) that involves the rearrangement of two alkenes on a single molecule to form a ring. During the course of investigating RCM reactions to produce eight-membered ring silyl ethers, we observed double bond isomerization when using the second-generation Grubbs catalyst and the Hoveyda-Grubbs catalyst but not the first-generation Grubbs catalyst. Isomerization during metathesis reactions can be problematic, giving undesired products and signaling catalyst degradation. If controllable, however, tandem metathesis/isomerization can be of value to make compounds that would otherwise be difficult to prepare. For this reason, the RCM/isomerization we observed was studied in detail. The impact of temperature, solvent, time, and additives on the distribution of isomerized and non-isomerized products were investigated. By monitoring the reaction via nuclear magnetic resonance (NMR) at different reaction times, we were able to conclude that ring closure generally occurs first, followed by isomerization of the double bond in the ring. For systems where a single isomerization event results in formation of a silyl enol ether, this was the major product obtained (which we explain as being driven by thermodynamics). However, the direction of isomerization when using the Grubbs second-generation catalyst was not entirely selective, giving a mixture of regioisomers representing both kinetic and thermodynamic products. This thesis describes investigations aimed at understanding what drives the isomerization (e.g. the catalyst species responsible, substrate structure considerations, reaction conditions) and whether we can control the direction of isomerization.

## Acknowledgements

### Research Adviser

Dr. Gregory O'Neil

### Thesis Committee

Dr. Margaret Scheuermann

Dr. James Vyvyan

### Instrumentation

Dr. Hla Win-Piazza

Sam Danforth

### And others

A special thank you to my family who continually supported me and asked me endless questions along the lines of “so what do you really do?” To my friends who always believed in me and my success. To another special physicist friend with whom I could *actually* talk about my chemistry, who believed in me whenever I got discouraged, who always managed to boost my confidence in my abilities, and who encouraged me to take pride in my accomplishments. I could not have done this without all of you!

## Table of Contents

Abstract.....	iv
Acknowledgements.....	v
List of Tables, Figures, and Schemes.....	vii
CHAPTER 1. INTRODUCTION .....	2
1.1 Background .....	2
1.2 Catalyst development .....	3
1.3 Types of olefin metathesis .....	6
1.4 Mechanism.....	8
1.5 Drawbacks/disadvantages of RCM .....	9
1.7. Industrial Applications of Ru Metathesis Catalysts.....	10
Industrial RCM case study: Relacatib .....	12
CHAPTER 2. TANDEM DIALLYLSILANE REARRANGEMENT/RCM .....	16
2.1 Background .....	16
2.2 Initial RCM.....	17
2.3. Mechanism of isomerization.....	25
Ruthenium hydride .....	25
Ruthenium nanoparticles.....	31
CHAPTER 3. RESULTS/DISCUSSION .....	32
3.1 Solvent, time, and temperature effects.....	32
3.2 Structural features studies.....	39
3.3 Mechanistic investigations.....	46
CHAPTER 4. APPLICATIONS .....	60
4.1. Psymberin fragment synthesis.....	60
4.2. Sugar derivative synthesis.....	63
4.3. Conclusions and outlook .....	64
CHAPTER 5. EXPERIMENTALS.....	66
Spectra .....	84
Work cited.....	116

## List of Tables, Figures, and Schemes

### Figures

<b>Figure 1.1.</b> Comparison of functional group reactivity of titanium, tungsten, molybdenum and ruthenium catalysts in olefin metathesis reactions .....	4
<b>Figure 1.2.</b> Structures of common ruthenium catalysts used for metathesis .....	5
<b>Figure 1.3.</b> Variety of olefin metathesis reactions.....	7
<b>Figure 1.4.</b> Chauvin mechanism of metathesis using Grubbs catalyst .....	8
<b>Figure 1.5.</b> Examples of active pharmaceutical ingredients .....	12
<b>Figure 1.6.</b> Various reactions run by Wang et al. in the attempt to optimize RCM in relacatib synthesis. 14	
<b>Figure 2.1.</b> Crude <sup>1</sup> H NMR spectra of RCM reactions of compound <b>24</b> using GI and GII .....	21
<b>Figure 2.2.</b> COSY NMR of GII catalyzed RCM product <b>41a</b> .....	21
<b>Figure 2.3.</b> <sup>1</sup> H NMR spectrum of compound <b>41b</b> .....	23
<b>Figure 2.4.</b> COSY NMR spectrum of compound <b>41b</b> .....	23
<b>Figure 2.5.</b> <sup>1</sup> H NMR of compound <b>41d</b> .....	24
<b>Figure 2.6.</b> Proposed GII decomposition mechanism by Grubbs .....	26
<b>Figure 2.7.</b> Mechanism of C-H activation and insertion of the Grubbs and Hov-GII catalysts that contain NHC ligands. ....	27
<b>Figure 2.8.</b> Possible mechanism using Ru-Hs to form isomerization products .....	29
<b>Figure 2.9.</b> Calculated relative energies of RCM products <b>25</b> and <b>41</b> .....	30
<b>Figure 3.1.</b> Two pathways leading to RCM or olefin migration as reported by Boutgeois et al.....	32
<b>Figure 3.2.</b> Example of crude NMR of GII (5 mol %) catalyzed RCM of <b>24</b> with peaks shown for <b>41a-d</b> that were used for product distribution determination .....	34
<b>Figure 3.3.</b> NMR of product <b>24</b> run in DCM using GII run at room temperature, 0 °C, and 35 °C .....	36
<b>Figure 3.4.</b> Time study of <b>24</b> subjected under standard RCM conditions in CD <sub>2</sub> Cl <sub>2</sub> .....	38
<b>Figure 3.5.</b> Subjecting <b>41b</b> under GII conditions to observe whether conversion between products is possible .....	42
<b>Figure 3.6.</b> COSY NMR of 9-membered ring RCM product <b>61</b> catalyzed by GII.....	45
<b>Figure 3.7.</b> Proton abstraction representation of 9-membered ring vs 8-membered ring to form Ru-Hs 46	
<b>Figure 3.8.</b> NMR spectra of isolated product <b>41d</b> and the crude mixture of <b>24</b> subjected to RuClH(CO)(PPh <sub>3</sub> ) <sub>3</sub> .....	48
<b>Figure 3.9.</b> NMR spectra of isolated product <b>41a</b> , the crude mixture of <b>25</b> subjected to RuClH(CO)(PPh <sub>3</sub> ) <sub>3</sub> and crude mixture of <b>41b</b> subjected to Ru-H .....	49
<b>Figure 3.10.</b> NMR spectra of isolated <b>52</b> , <b>53a</b> and the crude mixture when <b>52</b> was subjected to RuClH(CO)(PPh <sub>3</sub> ) <sub>3</sub> .....	50
<b>Figure 3.11.</b> NMR spectra of sequential treatment of <b>24</b> with GI, followed by GII, or followed by GII and benzoquinone .....	52
<b>Figure 3.12.</b> NMR spectra of CM results of <b>64</b> and <b>65</b> with GII, <b>65</b> treated individually with GII and <b>23</b> treated with GII .....	55
<b>Figure 3.13.</b> Structures of 4 different acyclic products synthesized and treated with GII and RuClH(CO)(PPh <sub>3</sub> ) <sub>3</sub> .....	57
<b>Figure 3.14.</b> NMR spectra of <b>71</b> was treated with RuClH(CO)(PPh <sub>3</sub> ) <sub>3</sub> , GII and <b>78</b> .....	59
<b>Figure 4.1.</b> Retrosynthesis of psymberin as reported by Jiang et al.....	61

## Tables

<b>Table 3.1.</b> Influence of solvent on product distribution .....	33
<b>Table 3.2.</b> Product distribution of <b>solvent</b> studies with Grubbs II using standard conditions at room temperature as determined by NMR.....	35
<b>Table 3.3.</b> Product distribution of <b>temperature</b> studies of RCM of <b>24</b> with Grubbs II.....	37
<b>Table 3.4.</b> Product distribution of RCM with Grubbs II with different types of silane groups .....	39
<b>Table 3.5.</b> Laser test for nanoparticles using GI, GII, and Hov-GII for RCM of <b>24</b> .....	53
<b>Table 3.6.</b> Summary of results when acyclic substrates were treated with GII and RuClH(CO)(PPh <sub>3</sub> ) <sub>3</sub> .....	58

## Schemes

<b>Scheme 1.1.</b> Total synthesis of rhizoxin F as reported by Liniger et al. ....	2
<b>Scheme 1.2.</b> Electronically directed ROMP to D-A polymers adapted from Koehler et al .....	3
<b>Scheme 1.3.</b> RCM with Hov-GII leads to three possible products, as reported by Butilkov et al.....	10
<b>Scheme 1.4.</b> Alternative RCM route in the synthesis of relacatib with 96% yield .....	15
<b>Scheme 2.1.</b> Iodine-promoted rearrangement of diallyldiphenyl silane.....	16
<b>Scheme 2.2.</b> Expected oxasilacycle <b>25</b> by RCM of compound <b>24</b> compared to the more common dioxasilacycles that have been produced by RCM.....	17
<b>Scheme 2.3.</b> Synthesis of tricyclic cyclobutyl indane <b>29</b> via RCM .....	18
<b>Scheme 2.4.</b> Synthesis of dihydrobenzofuran <b>33</b> via RCM .....	18
<b>Scheme 2.5.</b> Synthesis of an 8-membered benzo-fused heterocycle by RCM with GII .....	18
<b>Scheme 2.6.</b> Synthesis of an 8-membered oxacycle .....	19
<b>Scheme 2.7.</b> Synthesis of 7-membered oxasilacycles followed by either treatment with MeLi or chemoselective epoxidation .....	20
<b>Scheme 2.8.</b> Ring closing metathesis using Grubbs I.....	20
<b>Scheme 2.9.</b> Ring closing metathesis using Grubbs II, resulting in isomerization products.....	22
<b>Scheme 3.1.</b> Synthesis of RCM precursor <b>24</b> followed by RCM with GII .....	41
<b>Scheme 3.2.</b> RCM of phenyl, hexyl and methyl substituted silanes.....	43
<b>Scheme 3.3.</b> Synthesis of 9-membered ring using RCM with GI and GII .....	44
<b>Scheme 3.4.</b> Synthesis of all carbon 7-membered RCM product .....	46
<b>Scheme 3.5.</b> Isomerization induced by RuClH(CO)(PPh <sub>3</sub> ) <sub>3</sub> as studied by Morgans et el. ....	47
<b>Scheme 3.6.</b> Three reactions used to explore isomerization in cross metathesis .....	54
<b>Scheme 3.7.</b> Successful CM in 98% yield using GII .....	56
<b>Scheme 3.8.</b> General synthesis of acyclic silanes that were then treated with GII and RuClH(CO)(PPh <sub>3</sub> ) <sub>3</sub> .....	56
<b>Scheme 4.1.</b> Synthesis of fragment <b>79</b> from the RCM product <b>6</b> .....	62
<b>Scheme 4.2.</b> Synthesis of 3-doxy-D-fructose from acetal <b>85</b> and the degradation of 3-deoxyglucosone <b>89</b> .....	63

## CHAPTER 1. INTRODUCTION

### 1.1 Background

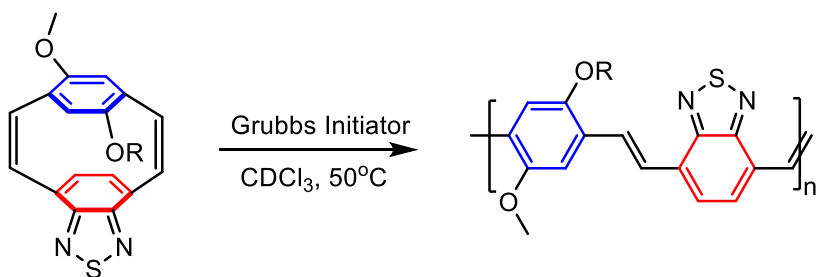
Olefin metathesis is a chemical reaction under which two olefins are exchanged to create new carbon-carbon double bonds. The first uncatalyzed metathesis reaction was reported in 1931 by Schneider and Frölich by heating propene at extreme temperatures (852°C) to obtain small amounts of 2-butene and ethylene.<sup>1</sup> In the late 1950's, catalyzed metathesis was explored, which eventually led to its breakthrough in the 1960's. The first catalysts used were molybdenum compounds supported on alumina,<sup>2</sup> but eventual catalyst development led to more efficient, stable, and selective catalysts. This greatly broadened the scope of metathesis and such chemistry has found valuable uses in synthetic organic chemistry,<sup>3</sup> pharmaceutical manufacturing,<sup>4,5</sup> material science,<sup>6</sup> and even protein modification.<sup>7</sup>

A recent publication showcased the use of ring closing metathesis (RCM, see Section 1.3 "Types of olefin metathesis") in the synthesis of bacterial macrolide rhizoxins. These naturally derived products have been shown to have cancer cell growth inhibiting properties.<sup>8</sup> In Scheme 1.1, the use of RCM is seen twice in the retrosynthesis scheme of this compound. The first time it was utilized in making the 6-membered lactone (**4**) and then a second RCM was used to form macrocyclic compound **2**. This example demonstrates several important features of modern catalytic olefin metathesis including excellent functional group tolerance (e.g. oxygen, nitrogen, and halide heteroatoms) and the ability to chemoselectively access various ring-sizes by RCM.



OLEDs and photovoltaic devices due to its enhanced solubility, as seen in Scheme 1.2.<sup>10</sup> In this study, they were able to induce metathesis using two different types of Grubbs catalysts, known as the second-generation Grubbs catalyst and the second-generation Hoveyda-Grubbs catalyst. With optimization, they were able to obtain 100% conversion, impressively, and this method is attractive compared to other polymerization methods like Stille and polycondensation due to its strict alternating pattern of the monomers.

**Scheme 1.2.** Electronically directed ROMP to D-A polymers adapted from Koehler et al.<sup>10</sup>



## 1.2 Catalyst development

Even after olefin metathesis gained popularity in the 1950's, further catalyst development was still needed to drive these reactions to their full potential. The utility of the original tungsten, molybdenum, and rhenium metathesis catalysts was limited due to the harsh conditions required such as the presence of strong Lewis acids in the reaction. As a result, they are incompatible with many functional groups and hard to initiate and control due to the difficulty in forming an active catalyst species.<sup>11</sup> Due to these challenges, interest in understanding olefin metathesis reactions resulted in further catalyst development. Despite their sensitivity to oxygen and water, molybdenum and tungsten alkylidene catalysts for olefin metathesis became more widespread due to their higher reactivity with olefins. Using ruthenium catalysts was not seriously considered until Grubbs made an interesting observation about the tolerance of ruthenium catalysts to other functional groups compared to other metals. Usually, a catalyst is considered "intolerant" to other functional groups when the catalyst

competitively binds to undesired functional groups rendering the catalyst inactive. A comparison of the reactivity of different metathesis-active metals is summarized in Figure 1.1. From this figure, Grubbs suggested that ruthenium is most suitable for olefin metathesis due to its strong reactivity with olefins and tolerance to (i.e. lower reactivity) other functional groups.<sup>12</sup>

Titanium	Tungsten	Molybdenum	Ruthenium
Acids	Acids	Acids	<b>Olefins</b>
Alcohols, water	Alcohols, water	Alcohols, water	Acids
Aldehydes	Aldehydes	Aldehydes	Alcohols, water
Ketones	Ketones	<b>Olefins</b>	Aldehydes
Esters, amides	<b>Olefins</b>	Ketones	Ketones
<b>Olefins</b>	Esters, amides	Esters, amides	Esters, amides

↑  
Increasing Reactivity

**Figure 1.1.** Comparison of functional group reactivity of titanium, tungsten, molybdenum and ruthenium catalysts in olefin metathesis reactions.<sup>12</sup>

Optimization of ruthenium (Ru) catalysts included exploration of attaching various ligands. It was observed that initiation occurs faster when the ruthenium complex contained a carbene source, obtained with the addition of ethyl diazoacetate during synthesis, as it generated active ruthenium alkylidene species. Other small molecules that were screened to determine if metathesis occurs include: diiodomethane, propylene oxide, tert-butylacetylene, and ethyl diazoacetate; however, it was observed that ethyl diazoacetate was necessary since it acts as a carbene source.<sup>13</sup> Furthermore, the discovery that the tricyclohexylphosphine (PCy<sub>3</sub>) ligand was able to increase metathesis activity led to the eventual discovery of the first-generation Grubbs catalyst (Grubbs I, GI).<sup>14</sup> This catalyst combined the bulky and strong electron-donating PCy<sub>3</sub> ligands, the readily initiated alkylidene moiety, and the functional group tolerance of ruthenium metal catalysts.

Grubbs I (GI) catalyst has had lots of applications after its discovery, which include polymerization reactions, the synthesis of heterocyclic compounds, and even fused ring systems.<sup>15</sup> However, to improve the range of accessible products, a second-generation Grubbs catalyst was

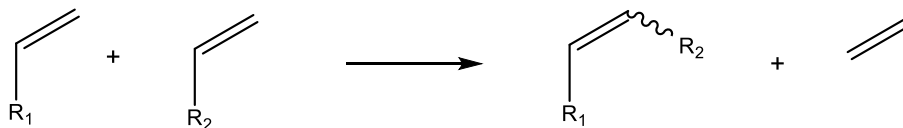


### 1.3 Types of olefin metathesis

As shown in Figure 1.3, there are a variety of different types of olefin metathesis reactions that all undergo similar mechanisms. Cross metathesis (CM) was the first metathesis reaction type observed. It involves two molecules, each with an alkene, that react together and rearrange in such a way to form one fused product and often a byproduct of ethylene if the two reacting alkenes are terminal.<sup>21</sup> If a cyclic molecule containing an alkene is opened during metathesis, this reaction is known as ring-opening metathesis (ROM). Often this process is combined with a subsequent cross metathesis resulting in a tandem ROM-CM reaction. This can be used to make polymers, or becomes ring-opening metathesis polymerization (ROMP).<sup>22</sup> On the other hand, ring-closing metathesis (RCM) has two alkenes on a single molecule and the rearrangement is intramolecular, which results in a cyclic product (and release of ethylene as a byproduct if the alkenes are terminal). Most metathesis can also be extended to alkyne functionalities and similar reactions are observed as olefin metathesis.<sup>23</sup>

### Types of Olefin Metathesis

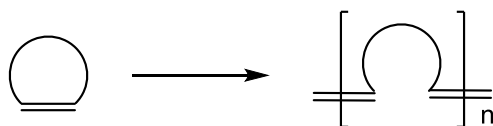
a) Cross Metathesis (CM)



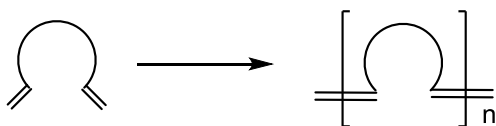
b) Ring-Closing Metathesis (RCM)



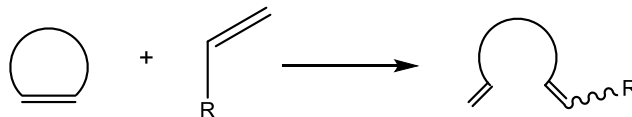
c) Ring-Opening Metathesis Polymerization (ROMP)



d) Acyclic Diene Metathesis Polymerization (ADMETP)



e) Ring-Opening Metathesis (ROM)



f) Enyne Metathesis (EYM)

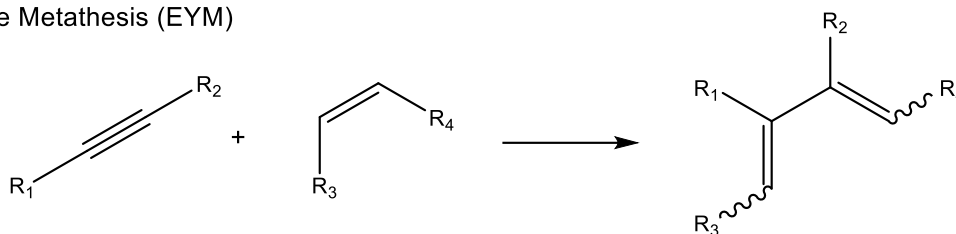


**Figure 1.3.** Variety of olefin metathesis reactions.

Work in this thesis will primarily focus on RCM. As seen in Figure 1.3, RCM occurs when a compound contains two alkenes which react in an intramolecular fashion to create ring structures. One of the key conditions to obtain an RCM product is the dilution factor, otherwise unwanted CM reactions can occur (e.g. acyclic diene metathesis polymerization (ADMET)).<sup>24</sup> This becomes more of an issue when

trying to form less stable ring structures. However, since metathesis is in principle a reversible process (see Section 1.5), ADMET oligomers can ultimately be converted to RCM products under appropriate conditions.<sup>25</sup>

### 1.4 Mechanism

The Chauvin mechanism is now widely accepted as the mechanism under which metathesis occurs. However, when Chauvin first published the proposed mechanism in 1971, not many scientists recognized this mechanism as it introduced several new ideas, including the implication of the metal-carbene in initiating the metathesis reaction, as well as the metallacyclobutane intermediate.<sup>27</sup> A decade later, in 1980, Schrock's work established the validity of the Chauvin mechanism, leading to its acceptance.<sup>26</sup> The Chauvin catalytic cycle is shown in Figure 1.4, note that each step is reversible.

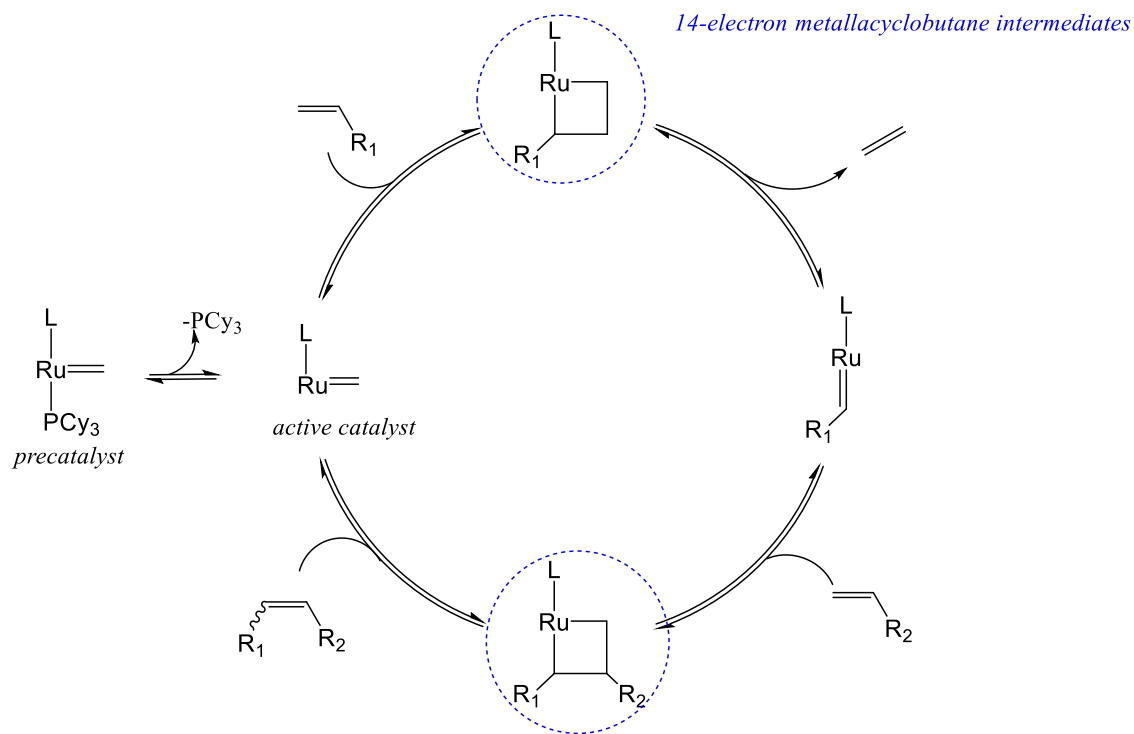


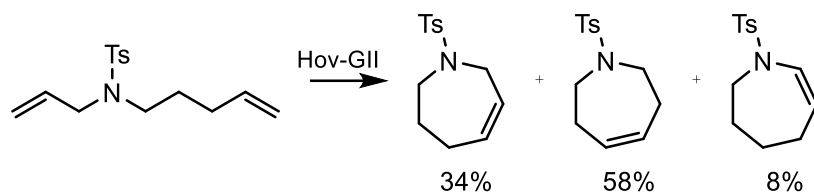
**Figure 1.4.** Chauvin mechanism of metathesis using Grubbs catalyst.

Starting with the precatalyst, one of the PCy<sub>3</sub> ligands dissociates to generate the active Ru-alkylidene metathesis initiator. The active species then binds to one of the olefins and undergoes a [2+2] cycloaddition to form a metallacyclobutane intermediate. Afterwards, the metallacyclobutane undergoes a retro-[2+2] in which ethylene is produced. When another olefin coordinates, the newly generated alkylidene will coordinate to form another metallacyclobutane intermediate, after which the metathesis product is released and the catalyst is regenerated.<sup>27</sup> Although there was prior consensus of the formation of the 14-electron metallacyclobutane intermediate, shown in blue in Figure 1.4, this intermediate species was isolated and characterized by Romero and Piers in 2005, further supporting the proposed mechanism.<sup>28</sup>

### 1.5 Drawbacks/disadvantages of RCM

Although RCM has a lot of potential in the synthesis of cyclic compounds in various ring sizes, there are a few drawbacks to this method. First, successful RCM can be dependent on the conditions under which the metathesis occurs. For instance, since Grubbs catalysts can be used in polymerization reactions as well, concentrated conditions may lead to polymerization due to intermolecular metathesis instead of intramolecular RCM. As a result, dilute conditions (typically 0.2 - 0.01 M) are generally required for RCM, which is not solvent efficient.<sup>29</sup> Secondly, the GI, GII and Hov-GII are expensive catalysts, costing \$107/gram, \$503/2 grams, and \$616/2 grams, respectively.<sup>30</sup> Another drawback is catalyst decomposition during the catalyst turnover, which can impact not only yield and catalyst loading, but can also lead to unwanted isomerization events (GII and Hov-GII are more prone to such decomposition, which is described in further detail later in the thesis). Lastly, isomerization events can occur during metathesis when using GII and Hov-GII catalysts. For example, as shown in Scheme 1.3, when *N*-allyl-4-methyl-*N*-(pent-4-en-1-yl)benzenesulfonamide is subjected to Hov-GII conditions, three different products were obtained.<sup>31</sup>

**Scheme 1.3.** RCM with Hov-GII leads to three possible products, as reported by Butilkov et al.<sup>31</sup>



Such isomerization can be problematic when trying to optimize reactions because the side reactions can be hard to control, decreasing the yield. Furthermore, since the obtained products are very similar structurally, they can be very difficult to separate. Thus, it is important to understand what drives the double bond migration and whether there are ways to suppress unwanted isomerization. Alternatively, there may be ways to induce isomerization if the desired product includes a migrated double bond.

### 1.7. Industrial Applications of Ru Metathesis Catalysts

Despite their high cost, relatively low turn-over-numbers (TON=790-10,800 depending on the catalyst loading of GII),<sup>32</sup> and potential for unwanted isomerization, ruthenium-based metathesis catalyst have been used in industry. Figure 1.5 shows nine different examples of pharmaceutical ingredients that use RCM in their total syntheses that have advanced to either clinical trials or even have been commercialized. For example, IDX316, a hepatitis C virus protease inhibitor that is currently in preclinical trials, contains a 14-membered macrocycle that is achievable with the use of the Hov-GII catalyst that able to induce RCM.<sup>33</sup> Furthermore, Danoprevir, which is also a promising protease inhibitor that can be used as an oral treatment of the hepatitis C virus, uses a first generation Hoveyda catalyst at very dilute conditions at 0.01 M in 1,2-dichloroethane to produce the macrocycle, although later improvements in RCM allowed for the reaction to be performed at 0.1-0.2 M in toluene.<sup>34</sup> For the treatment of osteoporosis and osteoarthritis, relacatib underwent clinical trials, and impressively, they were able optimize RCM in its synthesis using 0.5% Hov-GII catalyst loading to obtain 96% yield, which

was efficient enough to prepare over 200 kg of the product.<sup>35</sup> Lastly, rolapitant, which has been approved by the FDA in 2015 for the prevention of chemotherapy-induced nausea and vomiting, also includes RCM in its synthesis using Hov-GII in toluene under heating conditions (60-80 °C) to yield the RCM product in 85% yield.<sup>36, 37</sup> Clearly, there have been examples of impressive RCM applications at the industry scale, but adoption is still not widespread, due in part to the problems/drawbacks mentioned in the previous section. Additionally, at industrial scale, factors such as catalyst loading (e.g. as it relates to cost) and product selectivity (i.e. yield) become very important. Furthermore, if byproducts are formed that share similar physical properties (e.g. isomers), product separation can then be challenging which is not ideal for an industrial process. The study of unwanted isomer formation during metathesis is therefore important to help advance industrial metathesis applications.

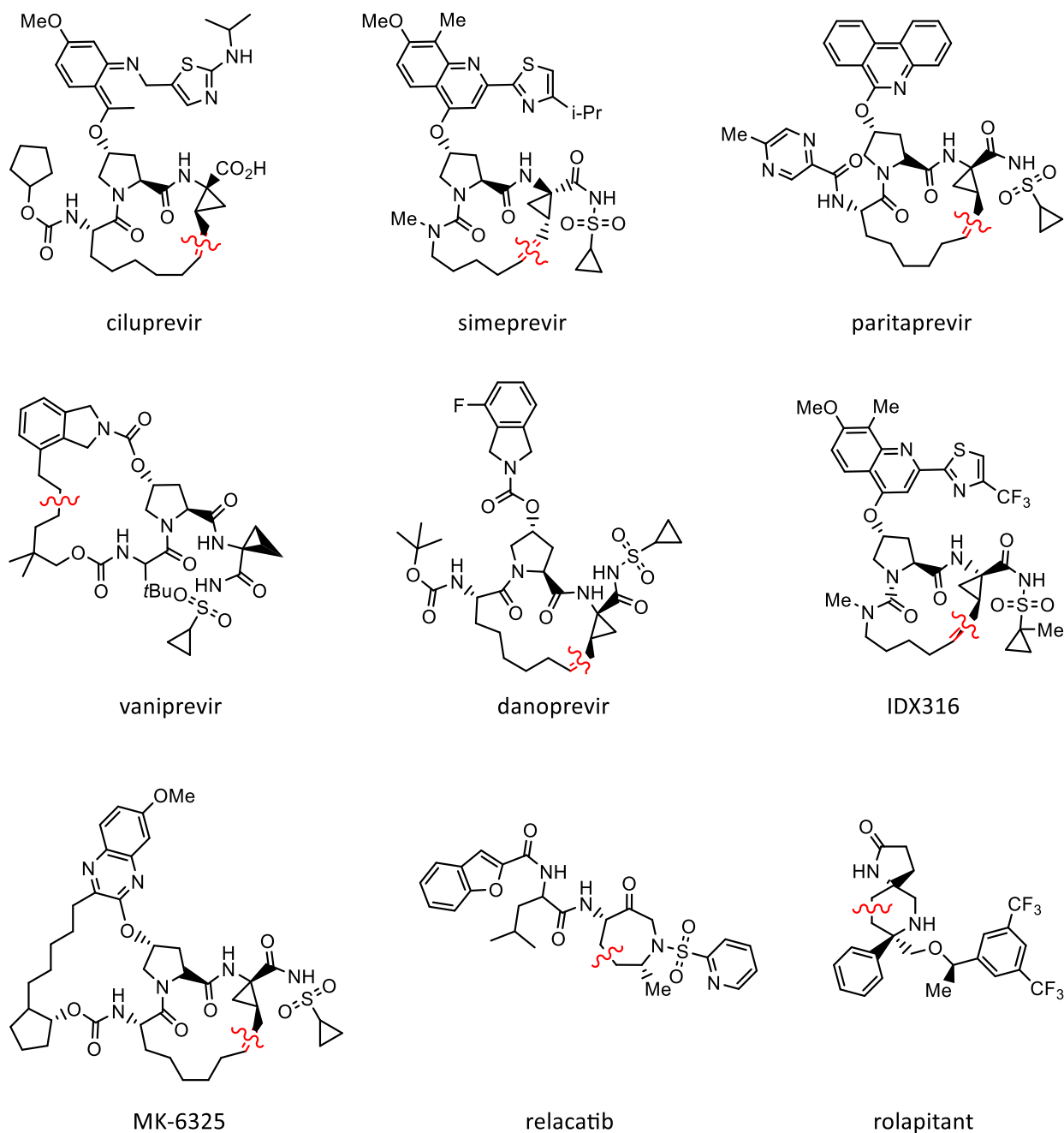


**Figure 1.5.** Examples of active pharmaceutical ingredients that either have been commercialized or advanced to clinical trials that utilize ring closing metathesis in their complete synthesis.<sup>38</sup>

**Industrial RCM case study: Relacatib<sup>35</sup>**

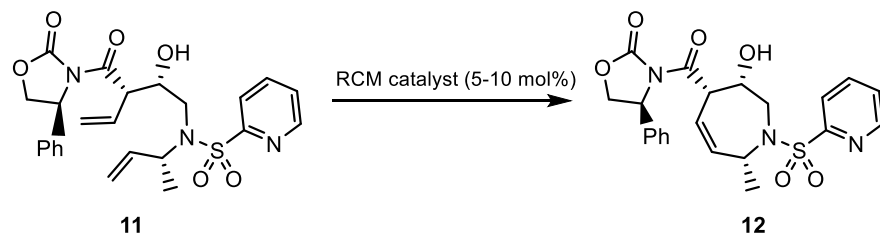
As mentioned previously, relacatib is a cathepsin K inhibitor that was used in a clinical trial in the treatment of osteoporosis and osteoarthritis. Cathepsin K is a cysteine protease synthesized by osteoclast cells which can dissolve the collagen matrix in the bone after it has been demineralized by

acid. Thus, relacatib acts as an inhibitor of cathepsin K resulting in the suppression of bone degradation. One of the challenges with relacatib synthesis is the azepinone 7-membered ring that contains two stereocenters, and one way to approach its synthesis is with RCM. Initial RCM attempts to make a substructure of relacatib were less than ideal, requiring high catalyst loading (10%) of Hov-GII (Scheme a in Figure 1.6). At 5% catalyst loading, the reaction did not go to completion and the use of additives to push the RCM led to the decomposition of the starting material. Furthermore, complete removal of Ru was very difficult as using a Ru scavenger  $P(CH_2OH)_4Cl/NaOH$  decomposed the product and proceeding with such high Ru content is impractical from a safety standpoint. Thus, a new synthetic plan was needed if RCM was to be employed. It was reasoned that the presence of the electron-rich oxazolidinone group coordinates to the Ru center and inhibits turnover, which was the reason for high catalyst loading. By subjecting the material to the Curtius reaction prior to RCM, it created a product which had no chelating pocket so it should require lower catalyst loading. However, after hydrolysis of the oxazolidinone, the Curtius reaction on the corresponding carboxylic acid with DPPA also produced some undesired double bond migration (compound **14**) resulting in low yields (eq. b, Figure 1.6). Instead, formation of the hydrazide followed by Curtius rearrangement gave the desired RCM precursor **13** in 98 % yield (eq. c, Figure 1.6). When **13** was treated with the Hov-GII catalyst (1-2 mol%) in toluene at reflux, isomerization of the RCM precursor at 20-30% was observed alongside the desired RCM product. Reducing the temperature to 60 °C suppressed the side reactions completely. However, there was still an issue of reproducibility as no one solvent gave consistent results. For example, using tetrahydrofuran at 60 °C gave a range of 37-87% conversion and 2-60% isomerization. Adding additives such as acetic acid, styrene and tricyclohexylphosphine oxide, which are supposed to suppress unwanted isomerization, did not lead to much improvement in terms of conversion or consistency between trials. However, isolating the RCM precursor as its HCl salt was able to improve the purity of this compound. Using this purified compound, they got better consistency with RCM yields (typically

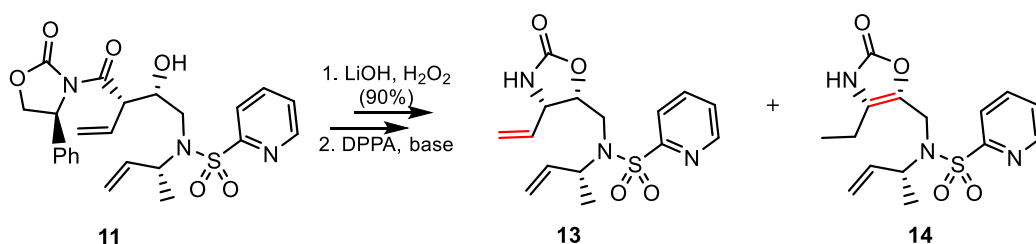
~90%), and reduced the isomerized products to less than 2% (compounds **14** and **17**, Eq. d, Figure 1.6).

The optimized RCM conditions were run in ethyl acetate as solvent (~0.5 M) at 60 °C with 1 mol% Hov-Gil catalyst for 1.5 h. The Ru was removed by extraction with a basic solution of cysteine, and purification involved crystallization to yield the desired RCM product **16** in 89% yield.

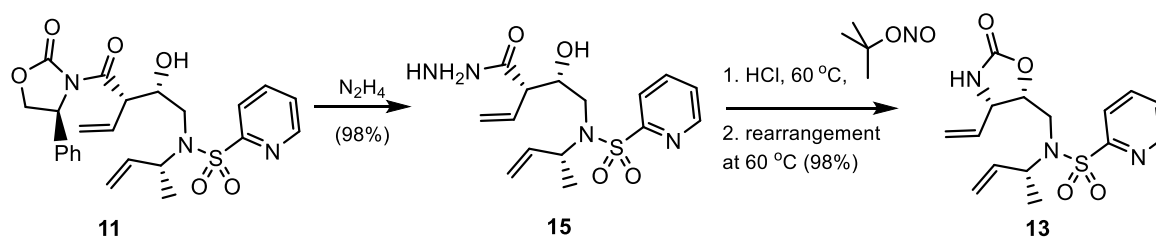
**a) Initial RCM**



**b) Curtius reaction**



**c) Oxazolidinone cleavage followed by Curtius reaction**



**d) RCM after Curtius reaction**

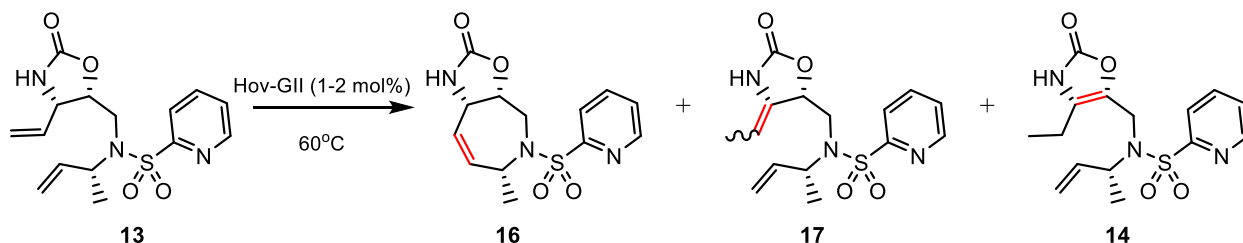
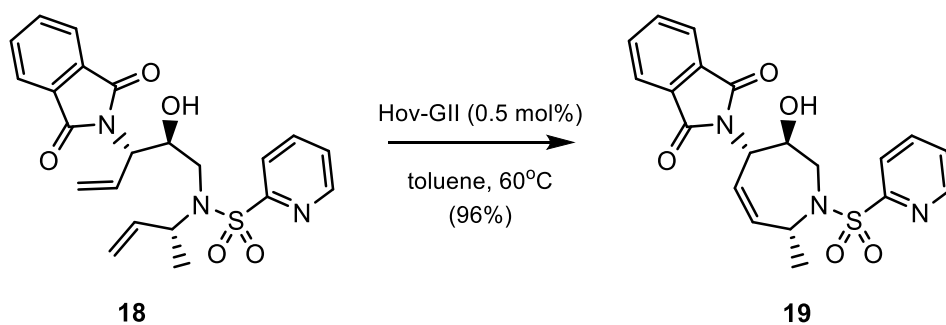


**Figure 1.6.** Various reactions run by Wang et al. in the attempt to optimize RCM in relacatib synthesis.<sup>35</sup>

Although Figure 1.6 outlines one RCM route for the synthesis of a substructure of relacatib, an alternative route was also explored with impressive yields as shown in Scheme 1.4. Treatment of phthalimide **18** in toluene at reflux with only 0.5% Hov-GII loading gave 96% yield of the desired RCM product **19**. Interestingly, the GII catalyst did not give consistent results between small- and large-scale reactions, so Hov-GII was the preferred catalyst. Surprisingly, no isomerization was observed and that has been credited to the steric bulk of the allylic substituents. This reaction has been scaled up in the production of relacatib to >200 kg.

**Scheme 1.4.** Alternative RCM route in the synthesis of relacatib with 96% yield.



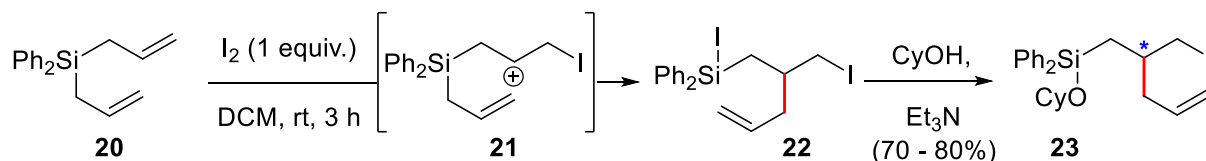
## CHAPTER 2. TANDEM DIALLYLSILANE REARRANGEMENT/RCM

### 2.1 Background

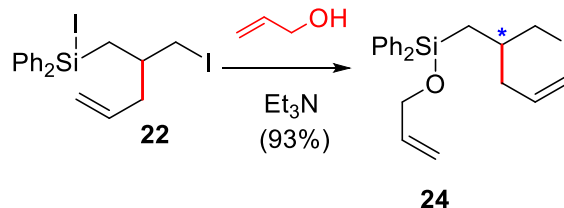
The O'Neil group recently discovered an iodine-mediated rearrangement of diallylsilanes.<sup>70</sup> The reaction is thought to proceed through formation of an intermediate cation **21**, followed by intramolecular allylation to give iodosilane **22**. Subsequent addition of an alcohol such as cyclohexanol (CyOH) or isopropanol (iPrOH) gave isolable silyl ether products featuring a new carbon-carbon bond (shown in red) and a new stereocenter (\*). Among the different diallylsilanes tested, diallyldiphenylsilane (**20**) gave the highest yields of rearrangement products (over substitution), providing compound **23** in yields consistently >70% (Scheme 2.1).

**Scheme 2.1.** Iodine-promoted rearrangement of diallyldiphenyl silane.

**Previous work:**



**This work:**



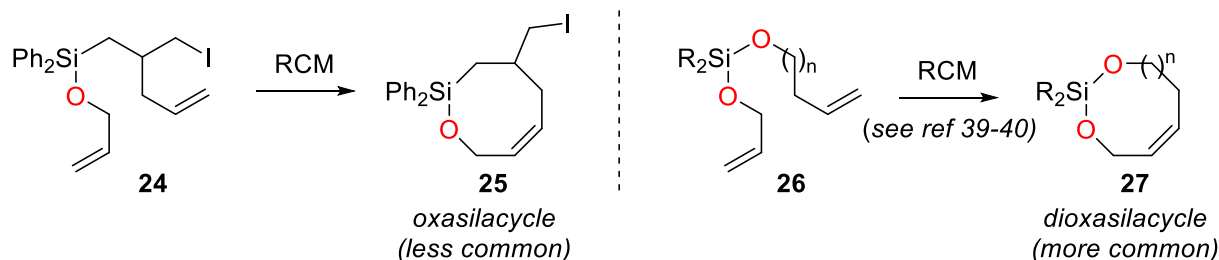
We recognized that trapping of the iodosilane intermediate with allyl alcohol would provide diene **24**, as shown in Scheme 2.1, setting the stage for a RCM reaction. To test this, we took diallyldiphenylsilane (1 equiv.), dissolved it in dichloromethane (0.1 M) and added iodine (1 equiv.), allowing the reaction to react at room temperature from 6-25 hours (extended time had no effect on the reaction), after which triethylamine (3.0 equiv.) was added at 0 °C, followed by allyl alcohol (2.0 equiv.). After letting the reaction

warm to room temperature overnight, it was quenched with DI water and purified by chromatography over silica to yield the diene in 93% yield.

## 2.2 Initial RCM

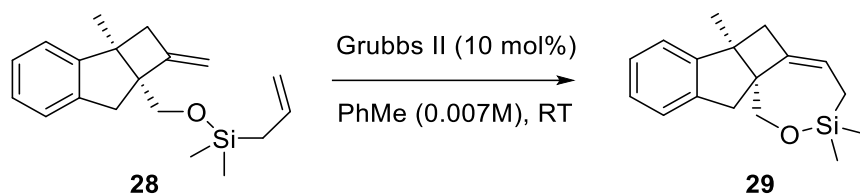
With compound **24** in hand, we then set out to investigate the RCM reaction. It was anticipated that the two alkenes present in compound **24** could undergo a metathesis reaction, resulting in an eight membered ring organosilane product **25** as shown in Scheme 2.2. Numerous examples of siloxacycle formation by RCM can be found, with the resulting products proving to be useful intermediates in synthesis.<sup>39,40</sup> Among these, RCM reactions that form medium-ring (7- and 8-membered) oxa- (as opposed to dioxo-) silacycles such as our expected product **25** are less common.<sup>41</sup>

**Scheme 2.2.** Expected oxasilacycle **25** by RCM of compound **24** compared to the more common dioxasilacycles that have been produced by RCM.



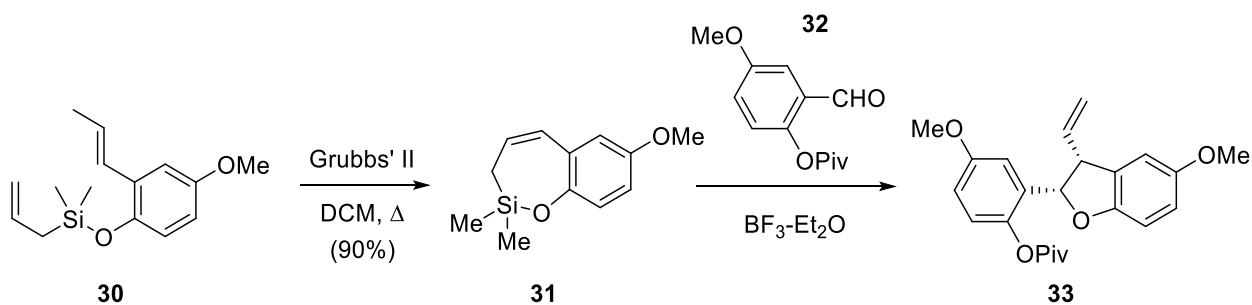
One example of medium-ring oxasilacycle formation by RCM is by Devineau et al. who reported the synthesis of a pharmacologically interesting tricyclic cyclobutyl indane structure **29** featuring the RCM of silyl ether diene **28**.<sup>42</sup> Treatment of **28** as a dilute (0.007M) solution in toluene (PhMe) with the second-generation Grubbs' catalyst (10 mol%) at room temperature gave the 7-membered siloxane **29** in yields up to 85% (Scheme 2.3). The authors reported no isomerization of the double bond was detected during the reaction.

**Scheme 2.3.** Synthesis of tricyclic cyclobutyl indane **29** via RCM.



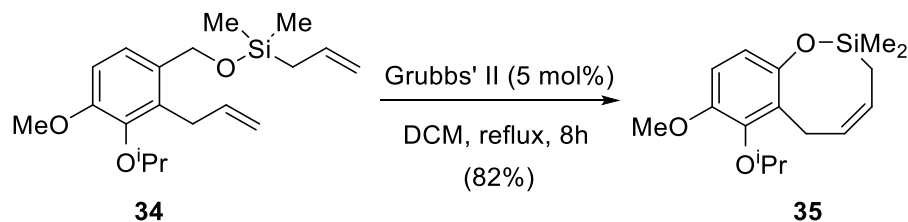
Rodríguez-García et al. reported a tandem RCM/Hosomi–Sakurai reaction in their synthesis of the pterocarpan natural products.<sup>43</sup> RCM of compound **30** delivered the benzoxasilepin **31** in excellent yield. Condensation of **31** and aldehyde **32** using  $\text{BF}_3 \cdot \text{Et}_2\text{O}$  then gave dihydrobenzofuran **33** exclusively as the *cis* stereoisomer (Scheme 2.4).

**Scheme 2.4.** Synthesis of dihydrobenzofuran **33** via RCM.



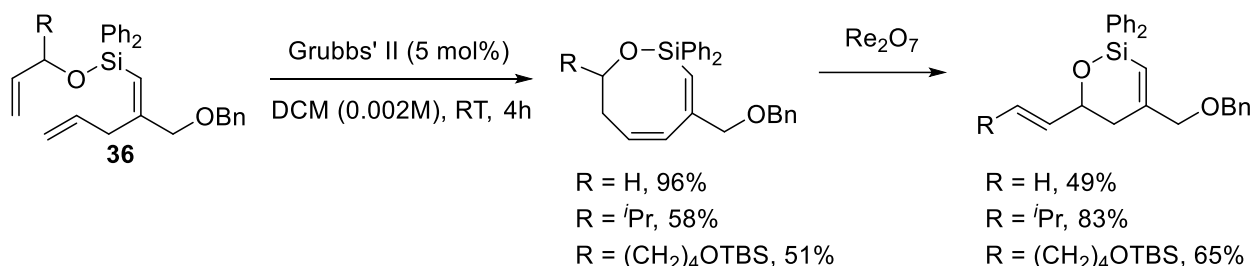
8-Membered oxasilacycles have also been prepared by RCM. Van Otterlo and co-workers used an RCM reaction to construct the 8-membered silicon-containing benzo-fused heterocycle **35** in 82% yield in refluxing DCM.<sup>44</sup>

**Scheme 2.5.** Synthesis of an 8-membered benzo-fused heterocycle by RCM with *GII*.



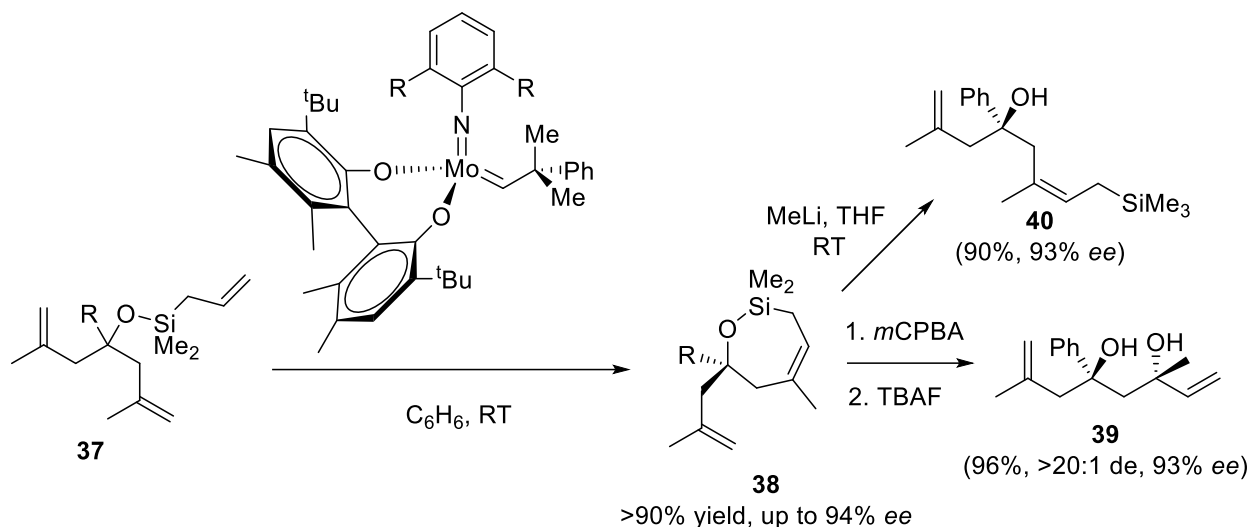
Volchkov et al. reported the synthesis of vinylsilane containing 8-membered oxacycles by chemoselective RCM of triene precursors **36**.<sup>45</sup> Yields of the RCM was sensitive to substitution at the allyl ether position, with yields being highest for the unsubstituted substrate (R = H, 96%). However, subsequent rhenium-catalyzed allylic transposition was best for RCM products with a substituent at the allyl ether position. The authors suggest that the low yield (49%) of the rhenium-promoted ring contraction when R = H is the consequence of unfavorable thermodynamics in forming terminal alkene from the internal one in the starting material.

**Scheme 2.6.** Synthesis of an 8-membered oxacycle.



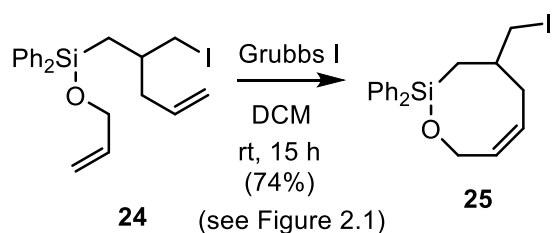
Oxasilacycle formation by RCM has also been made enantioselective. The Hoveyda group was able to prepare enantioenriched (up to 93% ee) 7-membered oxasilacycles by asymmetric RCM using a chiral molybdenum catalyst. Subsequent transformations of the of the RCM products included the addition of MeLi, affording chiral alcohol **40** containing an allylsilane group. Chemoselective epoxidation followed by desilylation with TBAF gave diol **39** essentially as a single diastereomer and enantiomer.<sup>46</sup>

**Scheme 2.7.** Synthesis of 7-membered oxasilacycles followed by either treatment with MeLi or chemoselective epoxidation.



Our RCM oxasilacycle investigations began with the treatment of iodine rearrangement product **24** with Grubbs-type catalysts under various conditions. Initial reactions were performed under a nitrogen atmosphere using either the GI or GII catalysts with 10% loading. The catalyst was added to the silane (1 equiv.) in degassed dichloromethane (0.02 M) and the mixture was stirred at room temperature overnight.

**Scheme 2.8.** Ring closing metathesis using Grubbs I.



Somewhat surprisingly, different products were obtained depending on whether GI or GII catalysts were used. The NMR spectrum from the GI reaction matched what was expected for compound **25** (see Scheme 2.8) with alkene signals at 5.79 and 5.60 ppm and the protons neighboring oxygen signaling as diastereotopic protons at 4.55 and 4.48 ppm (top spectrum in Figure 2.1).

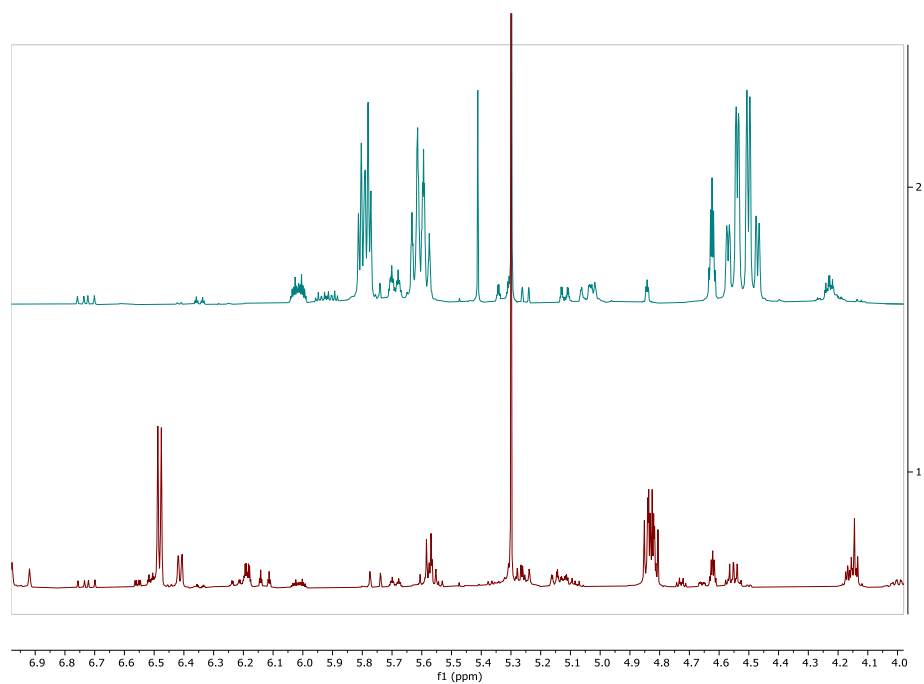


**Figure 2.1.** Crude <sup>1</sup>H NMR spectra of RCM reactions of compound **24** using GI (top) and GII (bottom).

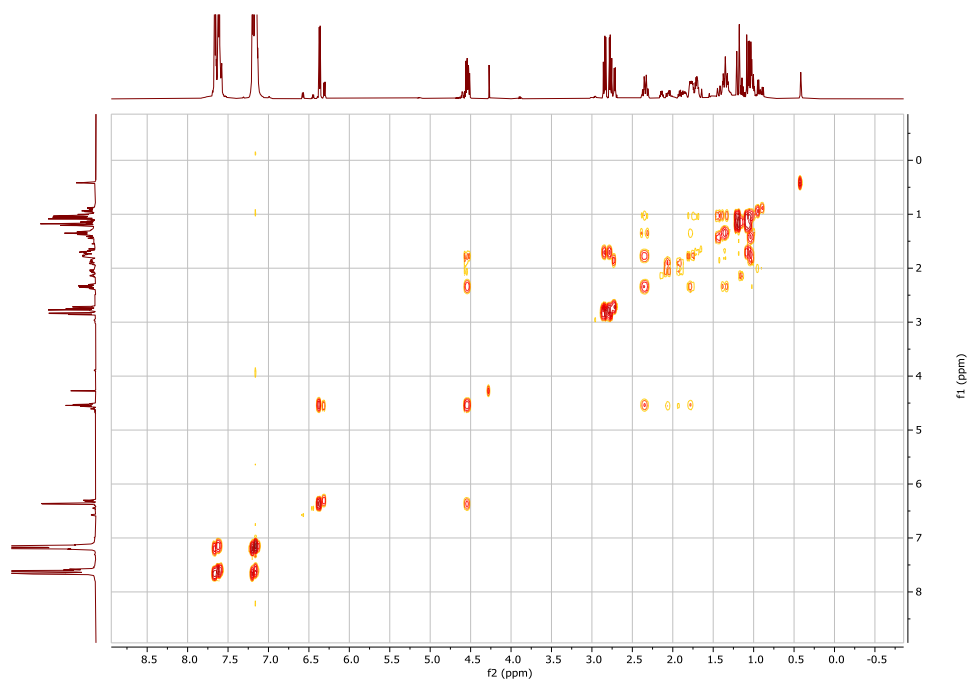
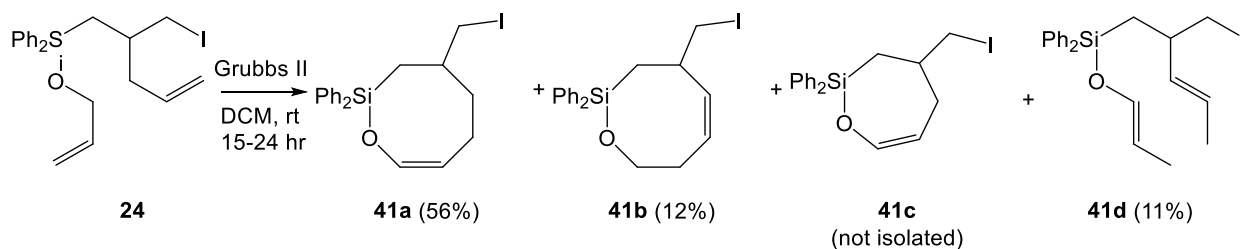


**Figure 2.2.** COSY NMR of GII catalyzed RCM product **41a**.

The NMR spectrum from the GII catalyzed reaction instead gave signals at 6.49 and 4.84 ppm that were coupled to one another according to COSY NMR (Figure 2.2). Together, these NMR signals are characteristic of an enol ether, suggesting isomerization had occurred during the GII reaction.

**Scheme 2.9.** Ring closing metathesis using Grubbs II, resulting in isomerization products.



Two different silyl enol ether RCM/isomerization products can be envisioned. If isomerization occurred before RCM, we would expect the 7-membered ring compound **41c**, as shown in Scheme 2.9. If RCM occurred and was then followed by isomerization, we would obtain the 8-membered ring compound **41a**. Ultimately detailed NMR analysis combined with high-resolution mass spectrometry confirmed that it was the 8-membered ring isomerized product that was obtained. Moreover, the isomerization was not 100% selective. Purifying the crude products over silica gel chromatography using 2:1 hexanes: dichloromethane gave several different products as shown in Scheme 2.9. Among them, was product **41b** where isomerization had occurred in a different direction. It is noteworthy that all of the shown products are all very similar in structure, which means they all have very similar polarity. Since column chromatography separates compounds based on polarity, separation was very challenging. Multiple solvent systems like ethyl acetate/hexanes, chloroform/ hexanes, were used before the optimal solvent system of hexanes:DCM was found to resolve the possible products. Also, it was found that longer columns (~25 cm) were better for separation since it provides more time for the products to separate on silica.

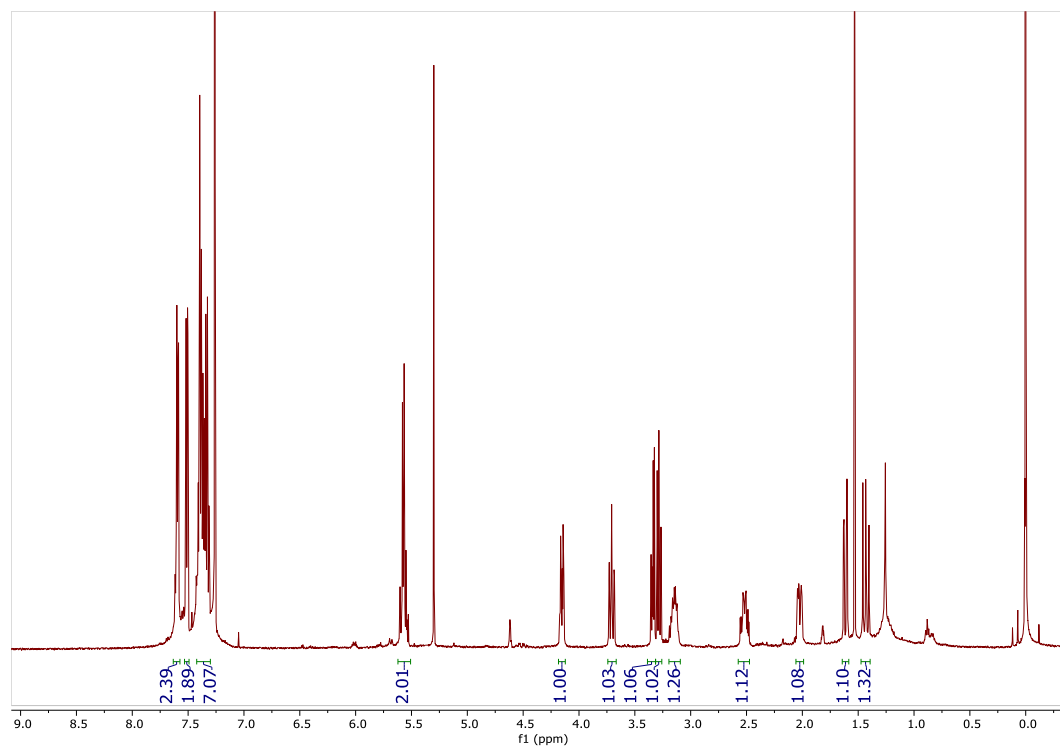


**Figure 2.3.**  $^1\text{H}$  NMR spectrum of compound 41b.

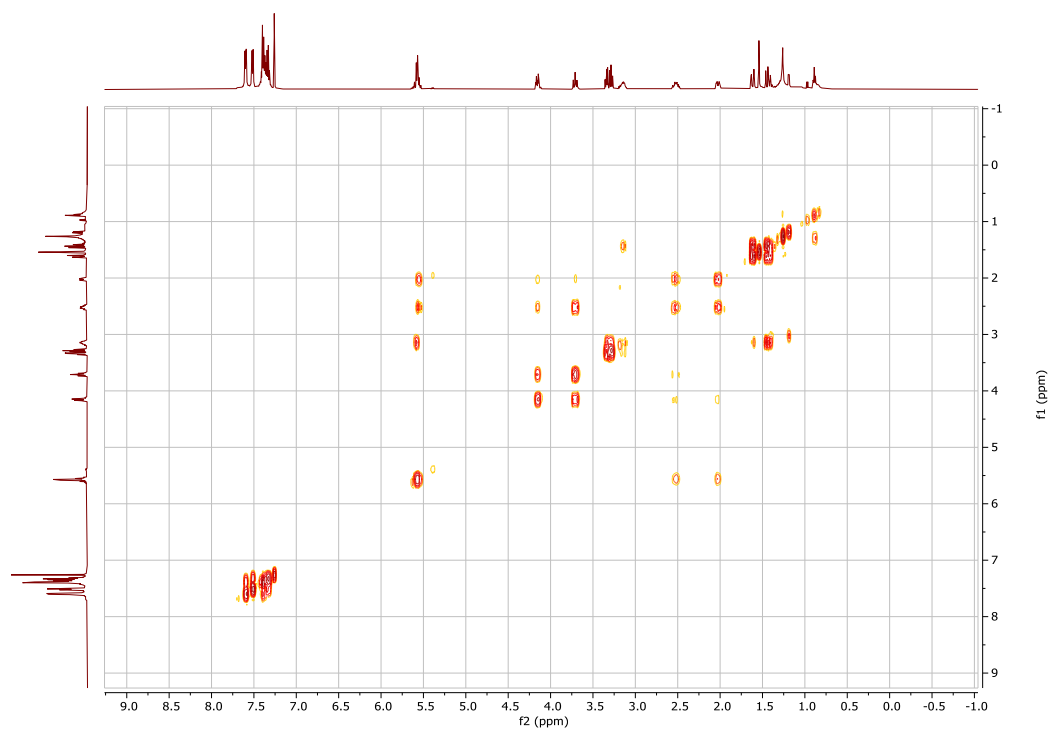


**Figure 2.4.** COSY NMR spectrum of compound 41b.

More specifically, the  $^1\text{H}$  NMR of **41b** (Figure 2.3) showed peaks at 5.57 ppm which correspond to the two alkene protons. Based on the COSY NMR (Figure 2.4), these peaks were coupled to diastereotopic protons at 2.52 and 2.03 ppm, and these protons were coupled to another pair of diastereotopic protons at 4.15 and 3.71 ppm. This suggests that the double bond is two methylene groups away from the oxygen atom, which is consistent with the structure **41b**, showing that an alternative isomerization product is also formed. From the crude  $^1\text{H}$  NMR, the ratio of isomerized products **41a** and **41b** was approximately 1.79:1.00.

Another interesting product that was isolated was compound **41d**, NMR shown in Figure 2.5. There is a total of four alkene protons, which suggest that both double bonds in compound **24** migrated to disubstituted alkenes and RCM never took place.

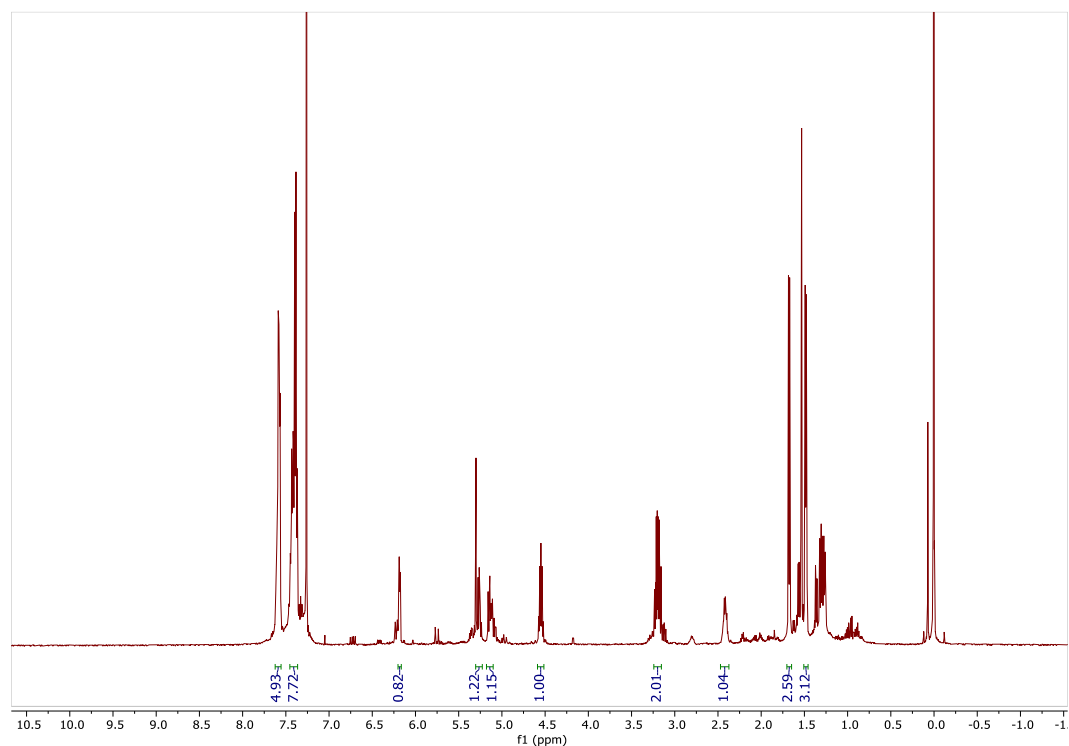


**Figure 2.5.**  $^1\text{H}$  NMR of compound **41d**.

The last potential product in GII catalyzed RCM is product **41c**, a 7-membered enol ether ring. Although it has not been isolated, mass spectrometry indicated that it is formed, unfortunately, it has the same  $R_f$  as the 8-membered product **41a**, making it inseparable by chromatography. However, it can be detected by NMR as a small peak at 6.42 ppm, while the 8-membered ring contains a peak at 6.49 ppm, both which can be seen in Figure 2.1. This product can be formed if only one of the double bonds isomerizes in compound **24**, and then it proceeds to ring close, giving the ring contracted product **41c**. Based on crude  $^1\text{H}$  NMR, the ratio between the different ring sized products **41a** and **41c** is 2.51:1.0.

Our data indicates that the isomerization event is unique to the GII and Hov-GII catalysts. In fact, sequential treatment of **24** with GI followed by reaction with GII gave identical results (including a 1.89:1.0 ratio of differentially isomerized RCM products (**41a:41b**) to the reaction with just Grubbs II. The only product not formed during this sequential GI/GII treatment is **41d**, which is understandable since prior to GII, there is no more starting material **24** that can undergo both double bonds isomerizing to form **41d**. The other surprising result is that **25** was not observed in the mixture of products that was obtained, which will be discussed in later sections.

### 2.3. Mechanism of isomerization

#### *Ruthenium hydride*

One of the leading theories for isomerization is the formation of ruthenium hydride complexes as a result of catalyst decomposition, whose mechanism is shown in Figure 2.6.<sup>47, 48</sup> GII is a precatalyst, which means that the  $\text{PCy}_3$  ligand needs to dissociate from the Ru to become the active species **42** that can catalyze RCM. However, in some cases,  $\text{PCy}_3$  attacks the carbene carbon atom, eventually leading to the elimination of phosphine ylide **43** and a 12-electron species **44**. Product **44** can then proceed to bind to the mesityl rings of **42** resulting in the chloride bridged ruthenium dimer that then decomposes to **46** with the generation of methyl tricyclohexylphosponium chloride (**45**). The last step involves oxidative

addition of the terminal alkylidyne of **46** and the migration of the two chlorides to yield the decomposed ruthenium hydride complex of **47**. Interestingly, when **47** (1.5% mol equiv.) was added to allylbenzene to act as the isomerization catalyst, isomerization product (*E*)-prop-1-en-1-ylbenzene was obtained in 76% yield.<sup>47</sup> Thus, the idea that ruthenium hydride can assist in isomerization has been supported by this study.

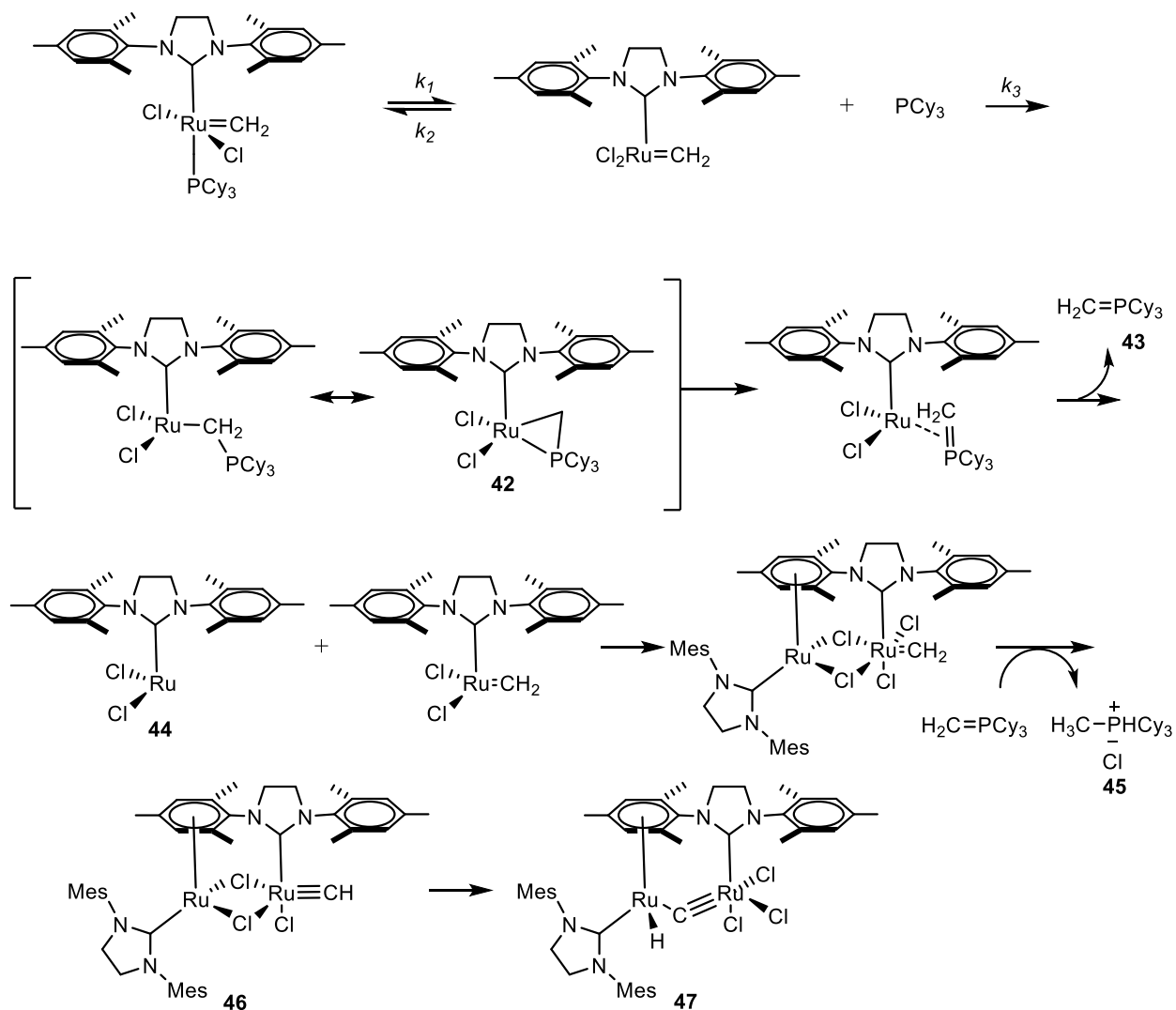


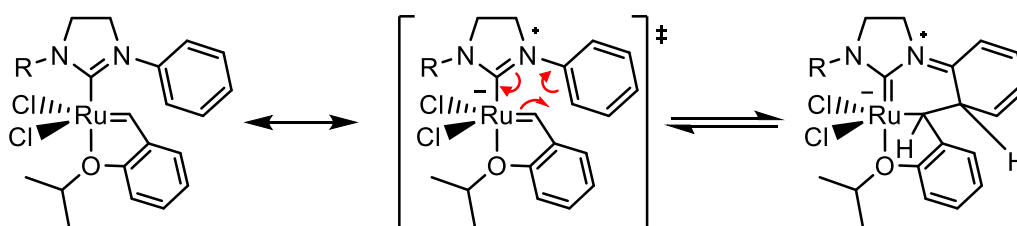
**Figure 2.6.** Proposed GII decomposition mechanism by Grubbs.<sup>48</sup>

One of the key steps in the decomposition of Grubbs II catalyst and formation of a ruthenium hydride is the binding of the 12-electron Ru species **44** to the NHC ring on another Ru molecule. Since GI

does not have the NHC ligand, it is not prone to the formation of the ruthenium hydride species via this mechanism. Therefore, isomerization tends not to be as much of an issue for the GI catalyst.<sup>48</sup> On the other hand, similar isomerization has been observed with the use of Hov-GII catalyst. Although this catalyst does not contain a PCy<sub>3</sub> ligand that is proposed to initiate the decomposition of GII, a different decomposition mechanism has been proposed which involves the byproduct ethylene generated during RCM and results in the formation of a similar ruthenium hydride.<sup>49</sup> However, intermediates along this proposed decomposition pathway have not yet been isolated or characterized.

Although Grubbs has a compelling mechanism for the formation of Ru-H, his group also proposed an alternative decomposition route via C-H bond activation. Blechert et al. built on this work to further study the decomposition of Hov-GII as shown in Figure 2.7.<sup>50,51</sup>

Hov-GII



Grubbs catalyst

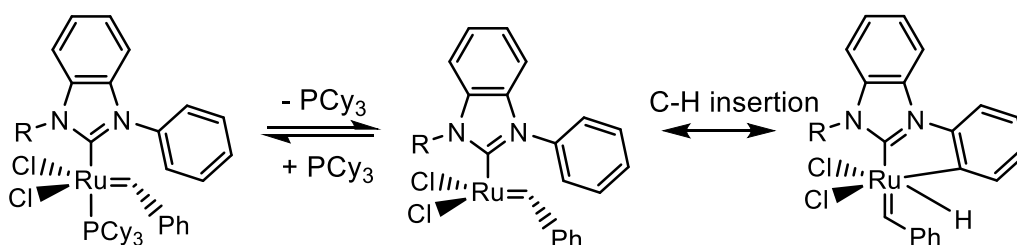


**Figure 2.7.** Mechanism of C-H activation and insertion of the Grubbs and Hov-GII catalysts that contain NHC ligands.

One of the key steps in Blechert's proposed mechanism involves a pericyclic cyclization with the NHC ligand. Since GI catalyst does not contain an NHC ligand, that could be another possible explanation why such Ru-H species are not formed with GI and isomerization is more of an issue with GII and Hov-GII catalysts.

In our case, after the Ru-H species is formed, it can proceed to add the alkene and give rise to intermediates **25a** and **25b**, as shown in Figure 2.8.<sup>52</sup> Depending on which neighboring proton is eliminated will lead to different products. For example, intermediate **25a** has two neighboring protons that are suitable for elimination, H<sup>a</sup> and H<sup>b</sup>. If H<sup>b</sup> is eliminated from **25a** to generate the Ru-H<sup>b</sup>, then the initial RCM product **25** is regenerated. On the other hand, if H<sup>a</sup> is eliminated, then enol ether **41a** would be formed. Thus, migration of the double bond has occurred. The same ideas can be applied to **25b**, where elimination of H<sup>c</sup> would regenerate the starting ring-closed product **25** while elimination of H<sup>d</sup> will lead to isomerization in a different direction. Surprisingly though, despite the possible routes to regenerate product **25** even in the presence of Ru-H species, it is not observed when the reaction is run to completion with GII and Hov-GII, while **41a** and **41b** were isolated at 56% and 12% yields.

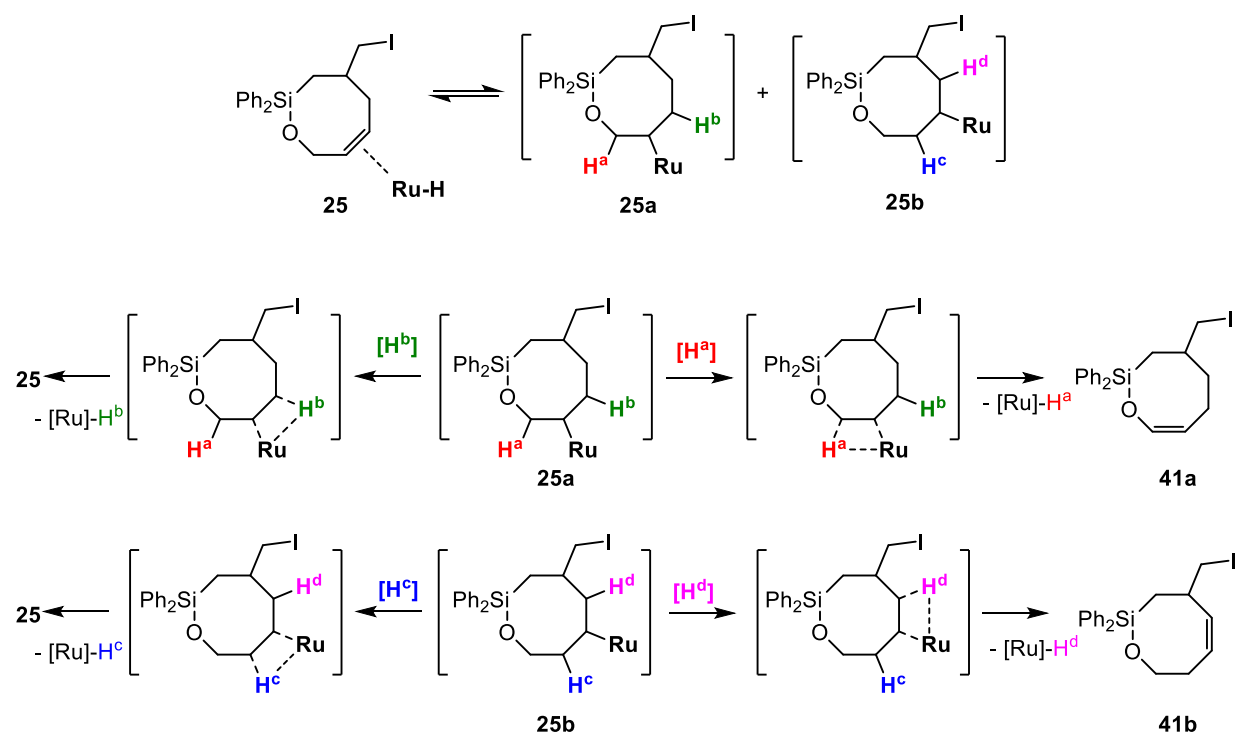


**Figure 2.8.** Possible mechanism using Ru-Hs to form isomerization products.

To better understand the product distribution from these RCM reactions, DFT calculations were performed to calculate the relative energies of the different products. Calculations were performed using the ORCA software package using the def2-TZVP basis set (valence triple-zeta polarization) with an effective core potential (ECP) for the Iodine atom. DFT Geometry optimization was first performed at using DFT using the BP86 functional followed by a geometry optimization using the B3LYP functional. Both calculations used Grimme's DFT-D3 dispersion correction with Becke-Johnson damping (D3BJ). The structure obtained using the B3LYP functional was further optimized using second order Moller-Plesset perturbation theory (MP2). Geometry optimization at the MP2 level used the resolution identity approximation (RI) that speeds up the MP2 calculation with minimal loss in accuracy. Structures shown are the final geometry optimized structure at the RI-MP2 level. For comparison of the relative energies, a single point MP2 energy calculation was performed on each of the optimized structures without the RI approximation.

All calculations were run on the SDSC Expanse supercomputer. The DFT calculations were performed on 32 cpu cores and the MP2 calculation was performed on 128 cpu cores.

### Optimized structure

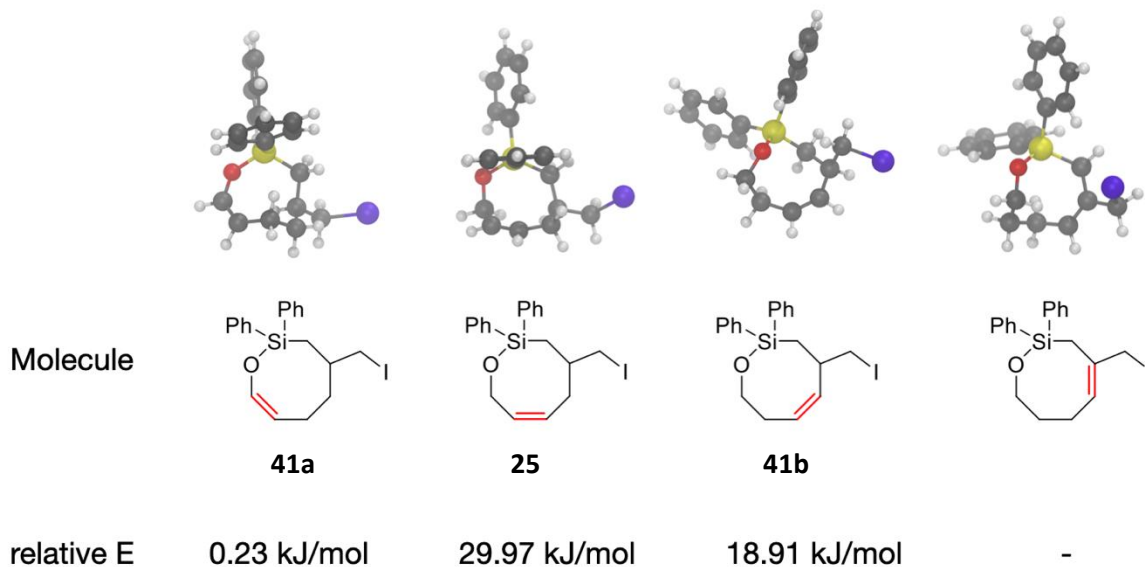


**Figure 2.9.** Calculated relative energies of RCM products **25** and **41a,b**.

Interestingly, compound **25** was calculated to be highest energy and this was not observed under isomerizing conditions (e.g. GII). The enol ether **41a** was significantly more stable than **41b** (difference of 18.68 kJ/mol), and that was the major regioisomer obtained. The most stable isomer containing a tri-substituted alkene was not observed, which we believe is the result of steric inhibition. With the calculated energies, we can compare our ratios to of **41a** and **41b** to those that are expected based on standard free-energy change and the equilibrium constant. With a different of 18.68 kJ/mol, the ratio between the two products is expected to be at the  $10^{-3}$  scale.<sup>53</sup> However, this was not observed, as our ratio between **41a** and **41b** was  $5.6 \times 10^{-1}$ .

### ***Ruthenium nanoparticles***

A study done by Fogg et al. provided another perspective on catalyst decomposition. They suggested that Ru nanoparticles (RuNPs) formed during metathesis are another factor that contributes to olefin isomerization.<sup>54</sup> By subjecting estragole to 4 different types of RuNPs, isomerization was observed in all cases, however, the most active RuNP was the one stabilized by an NHC ligand like that found on the GII catalyst. Further studies observed that commercially bought GII catalyst already contained RuNP aggregates. These NPs were isolated and used to induce isomerization in estragole, but results showed only 45% yield when compared to the 100% conversion that was seen with untreated commercially bought GII. The authors attribute the low activity of these NPs to their large size and partial oxidation, which limits the number of surface sites. A comparative study was done with commercial GII and with RNPs depleted GII by ultracentrifugation to look at the rates of metathesis and isomerization of estragole. The results showed only 15% less isomerization when using NP-depleted GII, suggesting that freshly decomposed catalyst plays a larger role in isomerization than the already-present RuNPs. To study this further, using in situ nephelometry to look at light scattering due to NPs, an increase in light scattering over the course of the reaction was observed indicating that RuNPs are formed during metathesis. This was again supported by electron microscopy that showed no RuNPs initially in styrene subjected to GII, however, after metathesis, electron microscopy showed an abundance of RuNPs. To determine whether it is the RuNPs or molecular species formed during catalyst decomposition that initiate isomerization, they performed a mercury poisoning experiment. Mercury poisoning is used to test involvement of surface-active metal(0) sites in catalysis, in other words, NPs. Their experiment showed a drop of 50% in isomerization by the introduction of mercury into the system. However, adding a substoichiometric amount of phosphine/phosphite poison, which targets RuNPS catalysis instead of molecular Ru specie catalysis, ceased isomerization completely.

## CHAPTER 3. RESULTS/DISCUSSION

### 3.1 Solvent, time, and temperature effects

Given that RCM and isomerization both occur when compound **24** is subjected to GII and Hov-GII conditions, we set out to explore what drives the isomerization and how different structural features, as well as reaction parameters, will affect the reaction results. One previous study suggested that RCM and isomerization are competitive processes. After Ru coordinates to the olefin, it can either proceed with the expected carbene exchange via metallacyclobutane intermediate (path a), or it can proceed to deprotonate the allylic proton, leading to a pi-allyl complex and eventually double bond migration (path b). These competitive reactions are illustrated in Figure 3.1.<sup>55</sup>

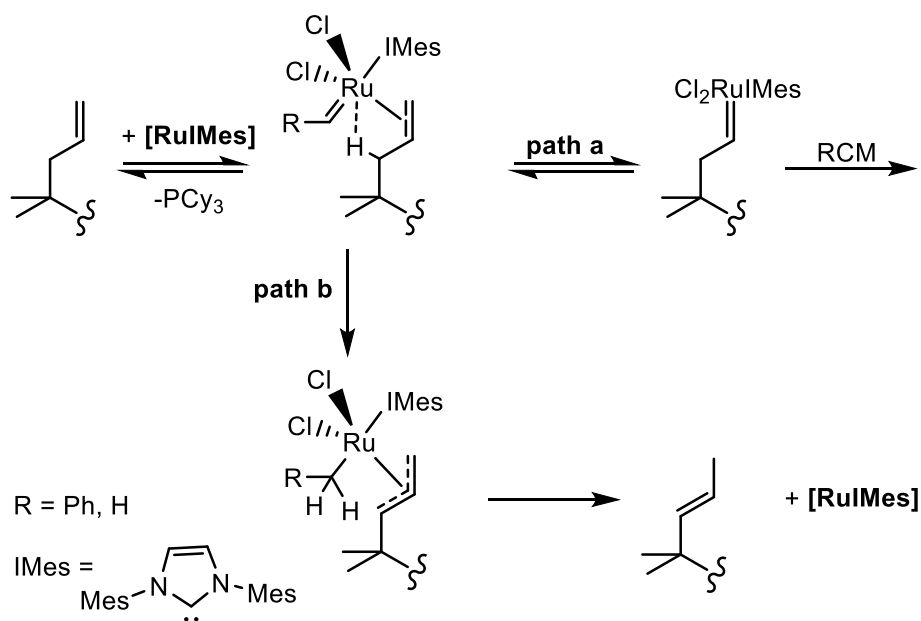


**Figure 3.1.** Two pathways leading to RCM or olefin migration as reported by Boutgeois et al.<sup>55</sup>

Considering that the ruthenium in the catalyst complex has a high oxidation state, the allylic proton is mostly likely trapped by the alkylidene carbon. Furthermore, since the NHC ligand is a strong sigma donor, it will increase the basicity of the alkylidene making GII and Hov-GII catalysts more likely to undergo that process. Since the solvent can affect the coordination between the catalyst and the

reactants, it can have a direct effect on the isomerization. Bourgeois et al. did have results that showed this relationship between solvent and isomerization, as shown in Table 3.1.<sup>55</sup>

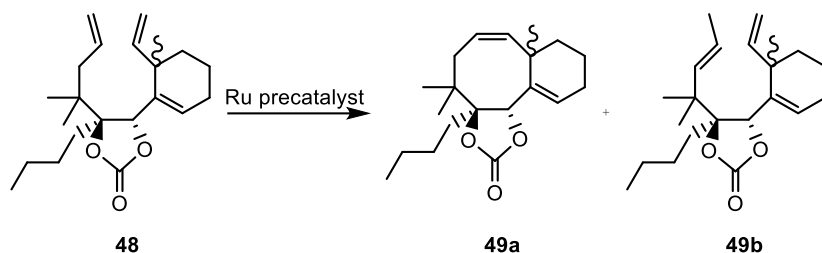


**Table 3.1.** Influence of solvent on product distribution.

Solvent	RCM (%), 49a	Isomerization (%), 49b
Benzene	50-70	30-50
Toluene	20	80
DCE	90	10
DME	0	100

The authors rationalized the results by considering the coordination activity of the solvent. If the solvent is more coordinating (e.g. dimethoxyethane (DME)) to the catalyst, the more it will prevent the second double bond from coordinating to the Ru center, making isomerization the favored reaction. However, if isomerization is slower than RCM and coordination between the substrate and Ru catalyst is sufficiently rapid, RCM will be favored. To test whether the solvent will affect the distribution between products **41a**, **41b**, **41c**, and **41d**, we ran multiple reactions under the standard RCM conditions in toluene, benzene, THF, and DCM. Our results are summarized in Table 3.2, where the product distribution was determined by NMR analysis (Figure 3.2).

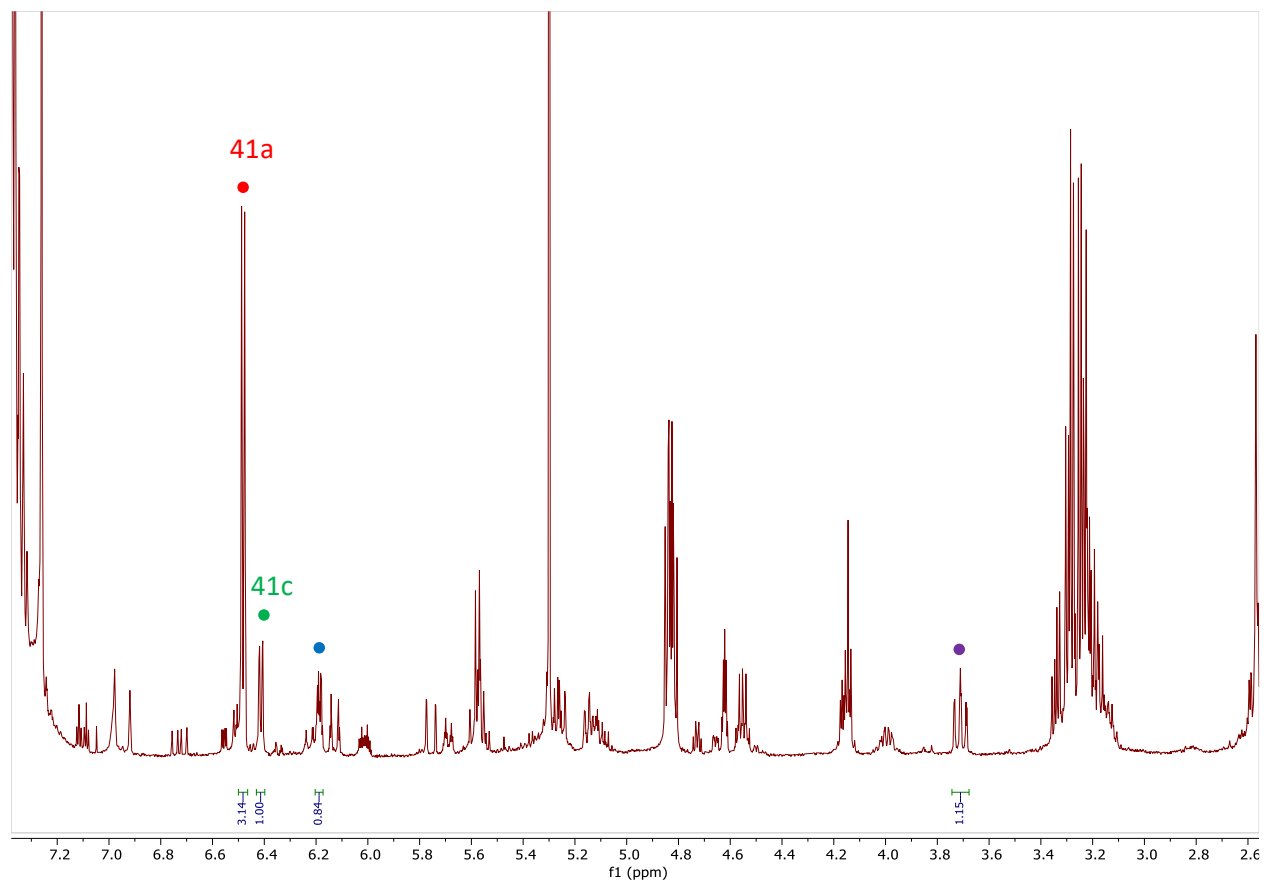


**Figure 3.2.** Example of crude NMR of GII (5 mol %) catalyzed RCM of **24** with peaks shown for **41a-d** that were used for product distribution determination, see Table 3.2.

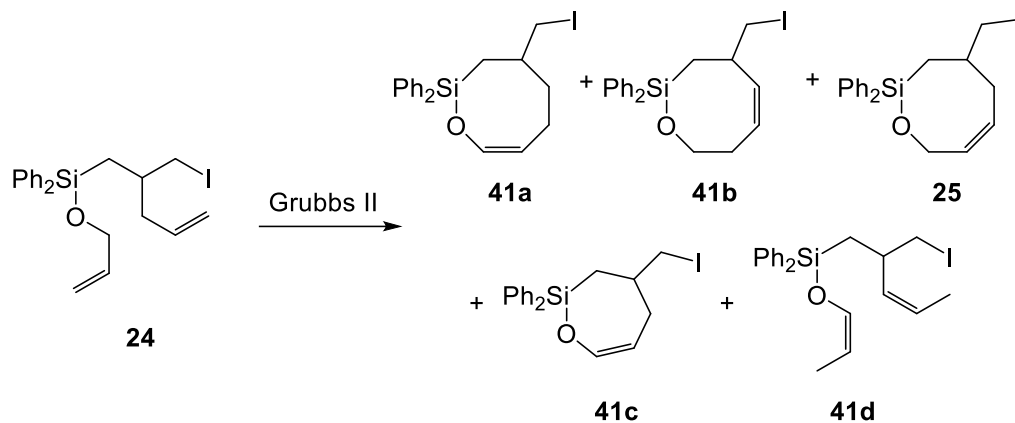


**Table 3.2.** Product distribution of *solvent* studies with Grubbs II using standard conditions at room temperature as determined by NMR.

Exp. #	Parameter	Ratio <sup>A</sup>				
		41a	41b	25	41c	41d
1	DCM, trial 1	2.51	1.40	0	1.0	0.72
2	Toluene, trial 1	2.12	0.74	0	1.0	0.58
3	Toluene, trial 2	2.28	0.79	0	1.0	0.58
4	Benzene	1.59	0.65	0.92	1.0	0.58
5	THF <sup>B</sup>	2.56	2.15	0	1.0	0

*Notes for Table:* <sup>A</sup>Product ratios were determined by integrating characteristic signals corresponding to the different products (see also Figure 3.2). <sup>B</sup>Performed in deuterated THF (THF-d8).

In general, the results from RCM gave comparable results. For instance, enol ether **41a** was the major product in all cases, the result of RCM followed by isomerization. Interestingly, comparing the ratios between **41a:41b** was different between running the trials in different solvents. For example, in DCM, the ratio is 1.79:1.00, while the average between the two toluene trials have a ratio of 2.88:1.00. However, the ratios between **41a** and **41c** are comparable between the two solvents. On the other hand, running the reaction in benzene also had an interesting effect on product distribution since **25** was observed. Based on the study conducted by Boutgeois et al., benzene is less prone to isomerization than toluene, giving only 30-50% isomerization compared to 80% isomerization observed in toluene.<sup>54</sup> Our results are consistent with this study since benzene has non-isomerized product **25** after running the RCM, suggesting that not all of **25** was isomerized to products **41a** and **41b**. In general, DCM as solvent was the most consistent and drove isomerization to 100% when run with GII. It therefore

became the preferred solvent for the rest of the experiments to study how other parameters such as temperature and substrate structural features affect tandem RCM/isomerization.

To see if isomerization can be suppressed or promoted with temperature, RCM was run at 0 °C, 35 °C and room temperature. The crude NMR spectra of the three reactions are shown in Figure 3.3.

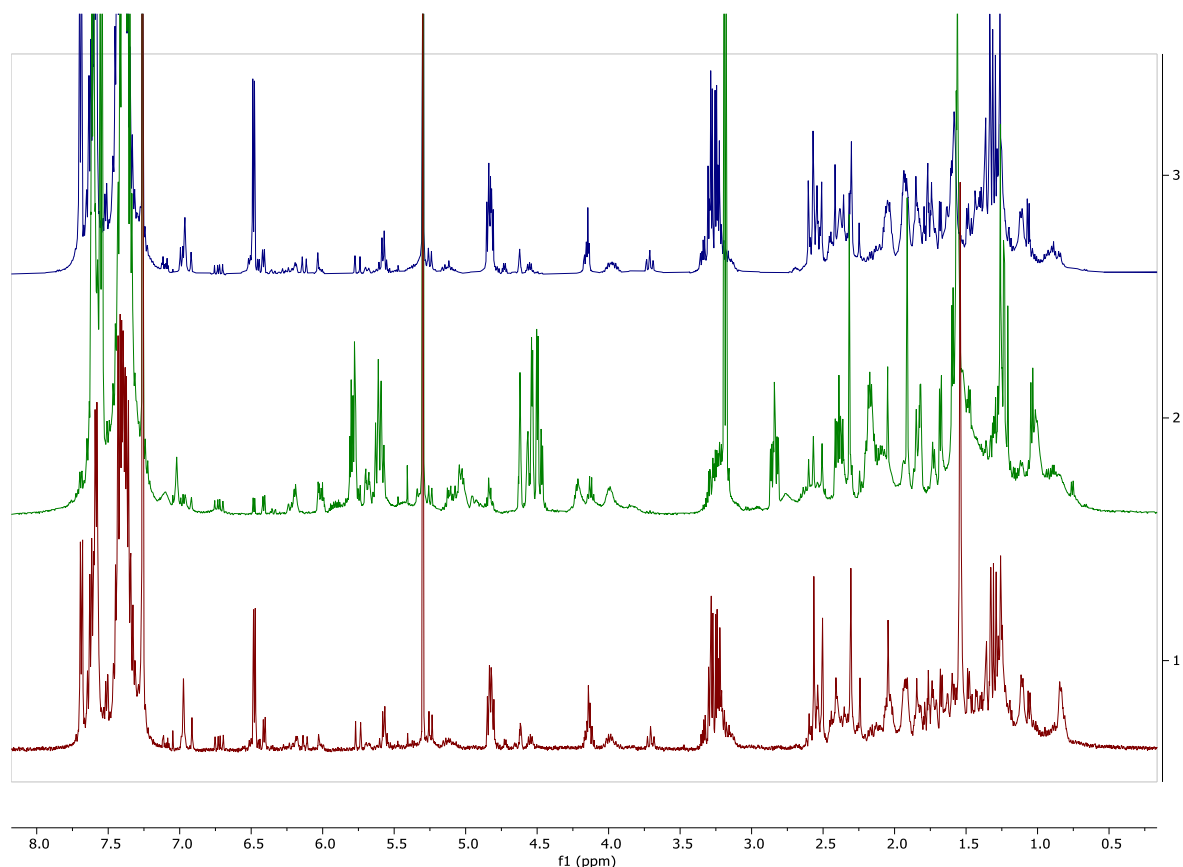


**Figure 3.3.** NMR of product **24** run in DCM using *Gli* run at room temperature (bottom), 0 °C (middle), and 35 °C (top). Presence of non-isomerized **25** detected when run at 0 °C with signals at 5.78, 5.59 and 4.52 ppm.

Interestingly, increasing the temperature to 35 °C had a profound effect on the product distribution between **41a** and **41b** (RCM/isomerization regioisomers). At room temperature, the ratio of **41a:41b** was 1.79:1.00, respectively, while at increased temperature (35 °C), the ratio changed to 3.57:1.00 (Table 3.3). This would suggest that an increase in temperature favors isomerization to enol ether **41a** instead of the other direction to **41b**. When the temperature was decreased to 0 °C, non-isomerized RCM product **25** was observed, while the ratio of **41a:41b** did not change (1.77:1.00).

However, the ratio between the 8-membered enol ether **41a** and the 7-membered ring **41c** (i.e. RCM then isomerization vs isomerization then RCM) did show a significant change between all three runs. At room temperature, the ratio of **41a:41c** was 2.51:1.00. At 35 °C, selectivity for **41a** (i.e. RCM before isomerization) increased to now 5.36:1.00, whereas at 0 °C the ratio changed the selectivity changed to favor **41c** (0.55:1.00 **41a:41c**). One possible explanation is that the lower temperatures favor a conformation of the starting material wherein the two reacting alkenes are not in close proximity, slowing down RCM and therefore increasing the amount of isomerization that occurs prior to RCM.

**Table 3.3.** Product distribution of *temperature* studies of RCM of **24** with Grubbs II as determined by NMR.

Experiment	Temperature	Ratio				
		<b>41a</b>	<b>41b</b>	<b>24</b>	<b>41c</b>	<b>41d</b>
6	room temperature (~20°C)	2.51	1.40	-	1.0	0.72
7	35 °C	5.36	1.50	-	1.0	0.70
8	0 °C	0.55	0.31	5.0	1.0	1.34

To further understand how the products are formed, a time study was conducted at room temperature in which NMR data was taken at 15 mins, 1, 2.5, 4.5, and 24 hours, as shown in Figure 3.4.

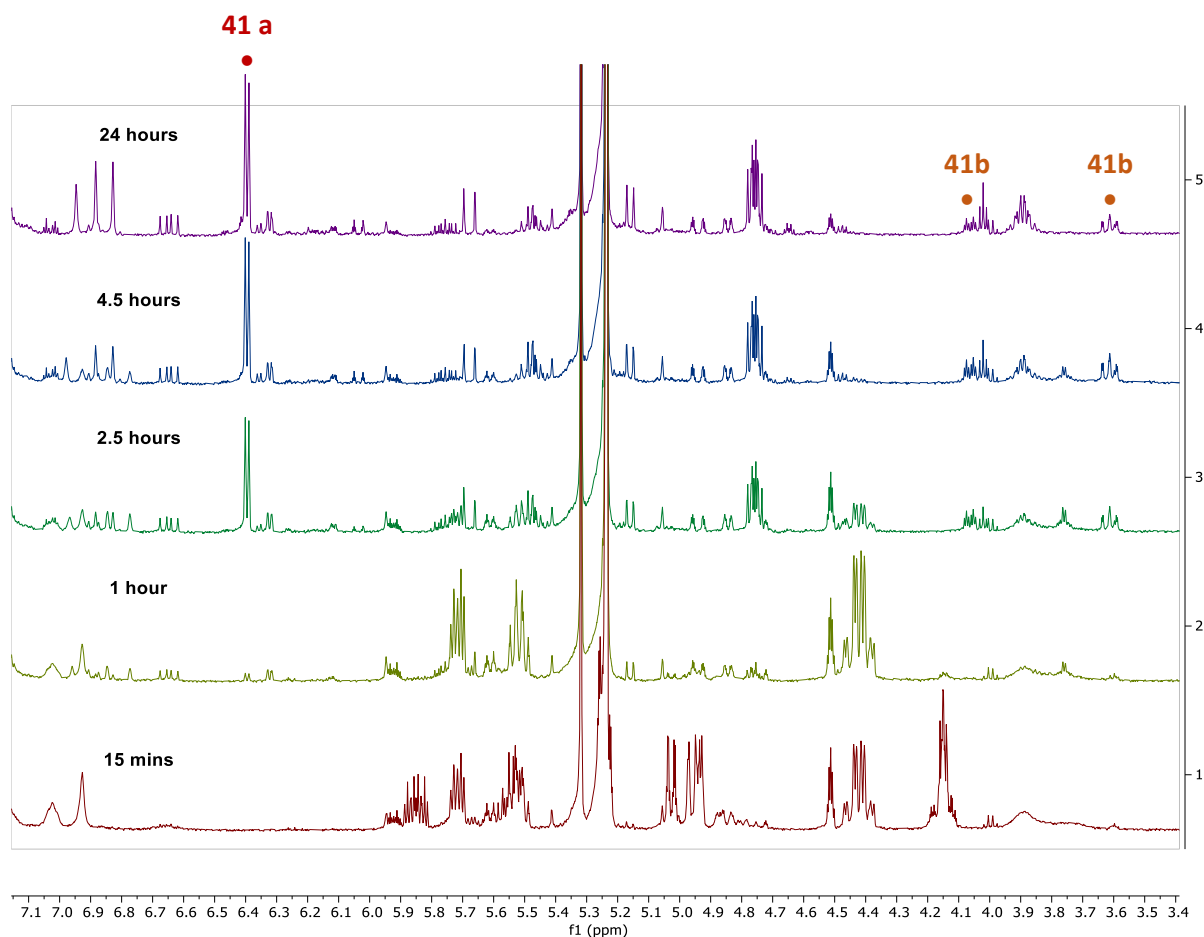


**Figure 3.4.** Time study of **24** subjected under standard RCM conditions in  $CD_2Cl_2$ .

RCM to non-isomerized product **25** (signal peaks at 5.72, 5.52, and 4.50 ppm) was very rapid, as just 15 minutes was enough to convert nearly 50% of the starting material **24** (signal peaks at 5.85, 5.01, 4.94 and 4.14 ppm). After 1 hour, **25** was predominantly observed with trace amounts of isomerized products **41a** (signal peak at 6.39 ppm) and **41c** (signal peak at 6.32 ppm). After 2.5 hours, we begin seeing **25** getting consumed and undergoing isomerization to form **41a**, **41b** (signal peaks at 4.06 and 3.60 ppm), and **41c**. Another 2 hours drove isomerization nearly to completion as trace amounts of **25** were still detected and at 24 hours no more **25** was observed. This information provides an interesting perspective as it shows that isomerization to **41a** and **41b** occurs after **24** undergoes RCM. The fact that the 7-membered **41c** is seen at 1 hour could suggest that within the hour, one of the double bonds in **24**

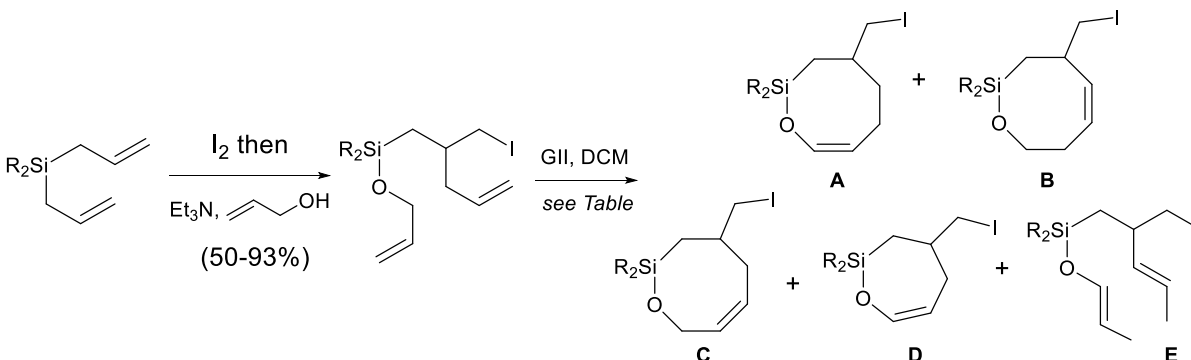
isomerized prior to RCM, resulting in the ring contraction. Additionally, the ratios between **41a**, **41b**, and **41c** were stable after 24 h and were unaffected by extra time (up to 57 h).

### 3.2 Structural features studies

Since evidence shows that Ru-H can promote isomerization by first coordinating to the alkene, exploring how structural features affect isomerization can provide interesting information on the effect of sterics. Thus, different substituted silanes were synthesized and then used in RCM (Table 3.4). These included diphenyl-, dimethyl-, and diisopropyl-substituted silanes, along with silacyclobutane.

Treatment of these compounds with GII (10 mol%) in DCM at room temperature for 15 h gave a mixture of RCM and isomerized products as summarized in Table 3.4.

**Table 3.4.** Product distribution of RCM with Grubbs II with **different types of silane groups**



The reaction scheme shows the synthesis of a diene-alkene intermediate from a diene and an alkene using I<sub>2</sub> then Et<sub>3</sub>N, with a yield of 50-93%. The intermediate is then treated with Grubbs II (GII) in DCM to yield products A, B, C, D, and E. The structures of A, B, C, D, and E are shown as substituted silacyclopentadienes with varying degrees of substitution and ring contraction.

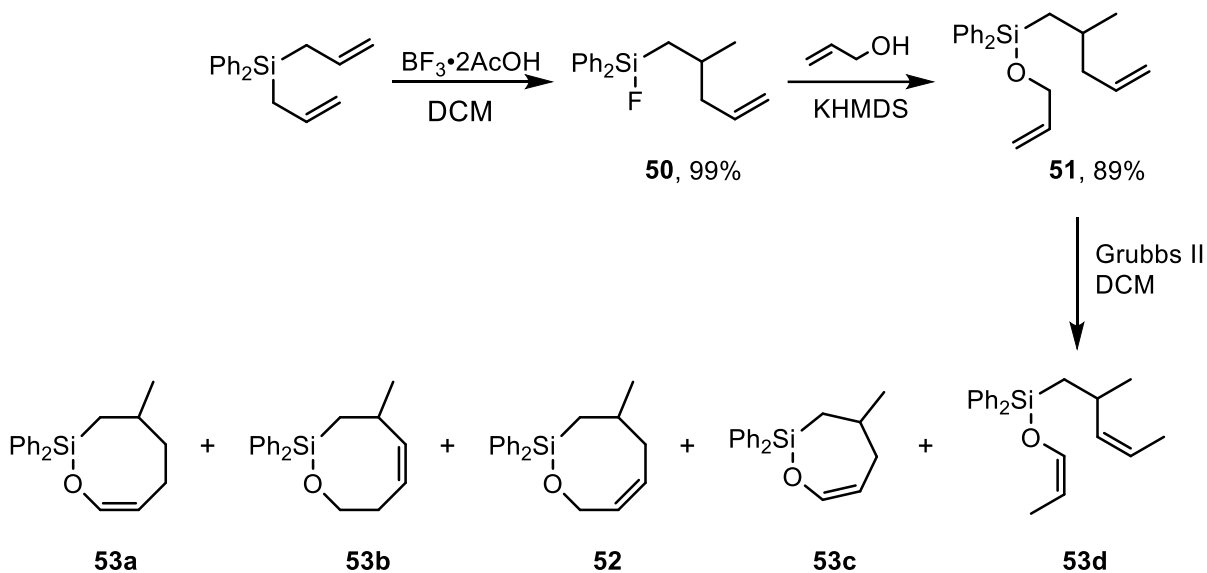
R	Catalyst loading	Yield <sup>a</sup>	A	B	C	D	E
Ph	10%	68	2.51	1.40	-	1.0	0.72
Ph	5%	56	3.14	1.15	-	1.0	0.84
Me	10%	28	2.03	1.08	-	1.0	0 <sup>b</sup>
Me	5%	--	5.08	2.81	-	1.0	0 <sup>b</sup>
<i>i</i> -Pr	10%	65	2.53	0 <sup>b</sup>	-	1.0	0 <sup>b</sup>
siletane	10%	77	6.57	1.00	-	0 <sup>b</sup>	0 <sup>b</sup>

*Notes for Table:* <sup>a</sup>All reactions were performed using Grubbs II catalyst in DCM at rt for 15 h. <sup>b</sup>Peaks corresponding to this compound were not observed in NMR spectra, however overlapping signals could have prevented the detection of very small amounts.

All four of these silanes were able to undergo RCM. Yields were generally high with the exception of the dimethyl silane. We hypothesize that larger groups on silicon aid the RCM through a Thorpe-Ingold type effect.<sup>56,57</sup> No starting material was recovered from the dimethylsilane RCM. The mass balance from that reaction is presumed to be oligomeric material. Alternatively, the dimethylsilane RCM product is less stable to purification by chromatography on silica, giving lower isolated yields. Importantly, the 8-membered ring enol ether (**A**) was the major product in cases and none of the non-isomerized RCM product (**C**) was observed. Additionally, the ratio of isomerized 8-membered ring RCM products were comparable, indicating that substitution at silicon does not affect the isomerization process.

Since **24** was a result of an iodine promoted rearrangement reaction (see Scheme 2.1), the iodine remained on the RCM precursor. To see whether its bulky nature affects the product distribution, another RCM precursor was made using the synthesis shown in Scheme 3.1, where the precursor contains just a methyl group instead of the previous iodomethyl group. Using the conditions described by Suslova et al., treatment of diallyldiphenyl silane with  $\text{BF}_3 \cdot \text{AcOH}$  gave fluorosilane **50** in excellent yield.<sup>58</sup> Substitution at fluorine for compound **51** was, as expected, more challenging than for the iodossilanes that we obtained from the iodine-promoted rearrangement. For instance, using our standard etherification conditions, (allyl alcohol, triethylamine, DCM, rt), no substitution was observed. Instead, a stronger nucleophile was first by deprotonation of allyl alcohol with KHMDS, which was then able to substitute fluorine giving ether **51** in 89% yield.

**Scheme 3.1.** Synthesis of RCM precursor **24** followed by RCM with GII.



When **51** was subjected to standard RCM conditions, the results were comparable to the iodomethyl precursor **24**, indicating that the bulky iodomethyl group has little to no effect on isomerization. The ratio of **53a**:**53b**:**53c** for the methyl substituted precursor was 2.24:1.09:1.00, while the iodomethyl gave ratios of 2.51:1.40:1.00 (**41a**:**41b**:**41c**). It is noteworthy that products **53b-d** were not isolated. Interestingly though, when **51** was subjected to RCM at 45 °C, **53b** was not observed. This could be explained if the products are in equilibrium and heating the reaction drives the equilibrium to the most stable product. It is possible that **53b** is forming, but with the increased temperature, the double bond can migrate to form **53a**. To test whether conversion between RCM products **a** and **b** is possible, **41b** was subjected to GII catalyst and the results are shown in Figure 3.5.

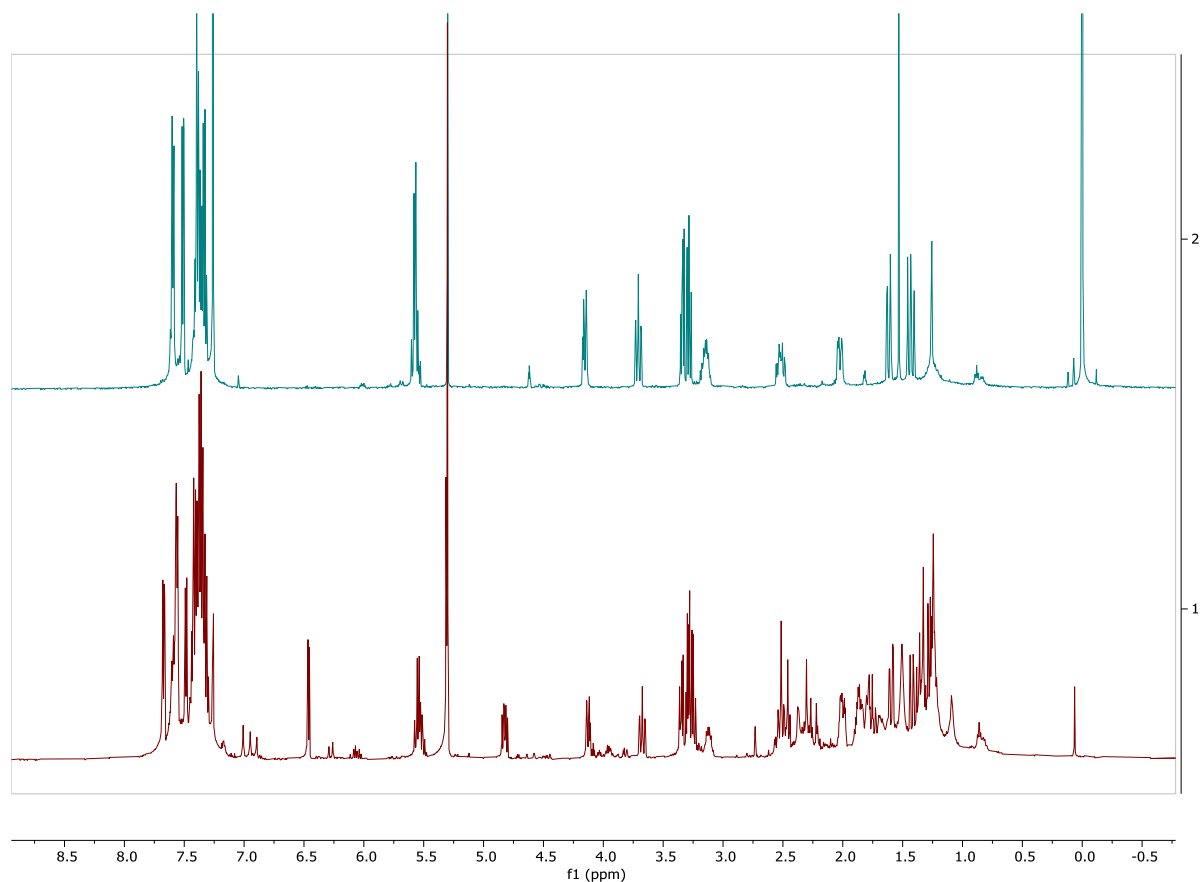
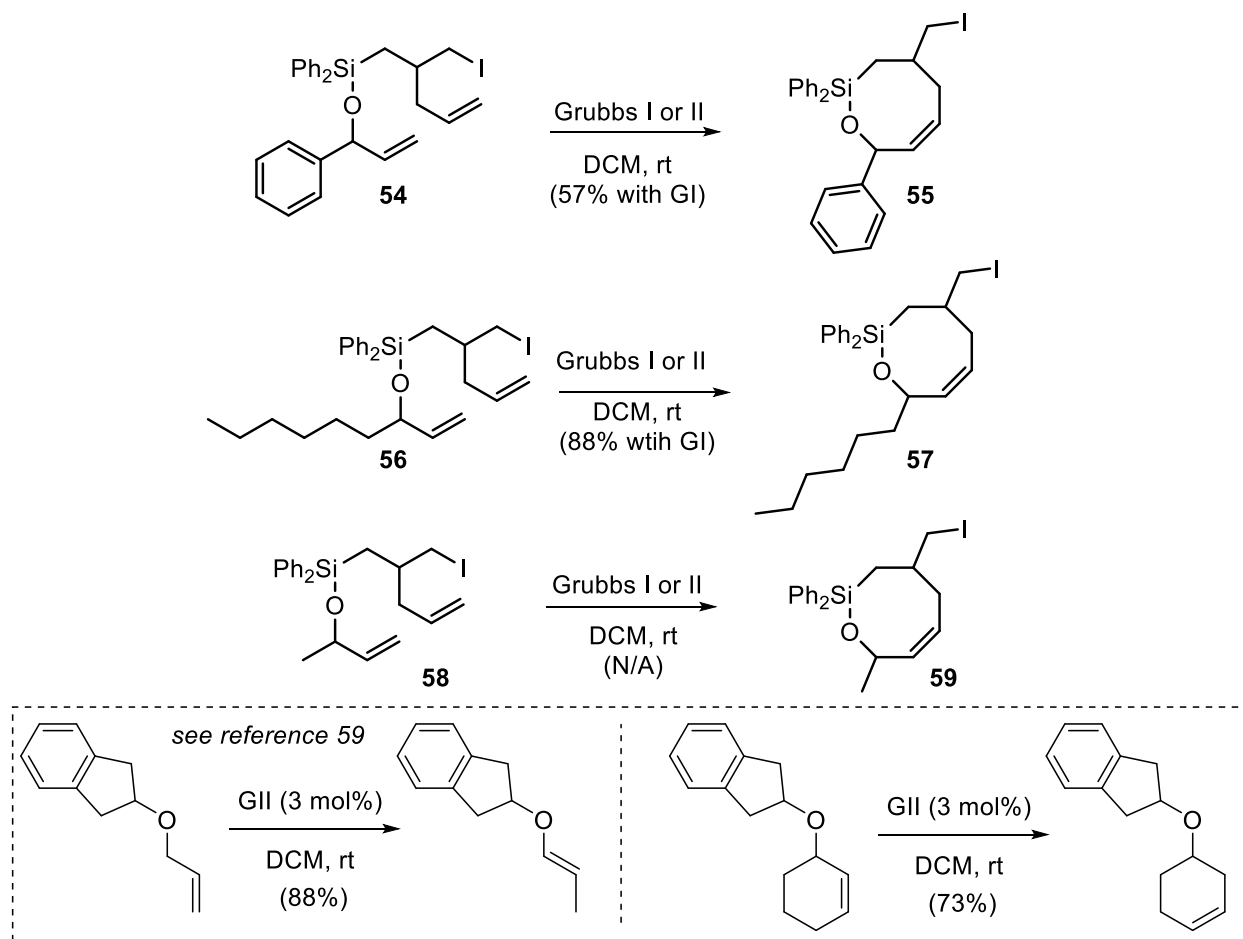


**Figure 3.5.** Subjecting **41b** under GII conditions to observe whether conversion between products is possible. Top spectrum is **41b** and the bottom spectrum is the crude NMR after 24 hours reaction time with GII.

The results were fascinating. At room temperature, **41b** was able to convert to **41a** (new peaks at 6.45 and 4.82 ppm), indicating that conversion between RCM products is possible and isomerization is a reversible process. Furthermore, running the reaction for 96 hours did not change the ratio between **41a** and **41b** when compared to 24 hours, both giving a ratio of 1:1. The fact that extending reaction time did not affect the distribution would indicate that equilibrium was reached. Another fascinating observation was that **25** was not observed at any point, even at 2.5 and 4 hours, suggesting that double bond migration can occur without going through **25** as an intermediate. This would also explain why increasing the temperature would decrease the amount of **41b** and **53b** since temperature can shift the equilibrium and conversion between products was happening at a faster rate.

Another way to determine if steric hinderance plays a role in isomerization was by attaching a phenyl, hexyl, or methyl group on the ether carbon and subjecting to RCM (Scheme 3.2). Theoretically, isomerization to a tri-substituted enol ether would be favorable since that would be the most stable product.



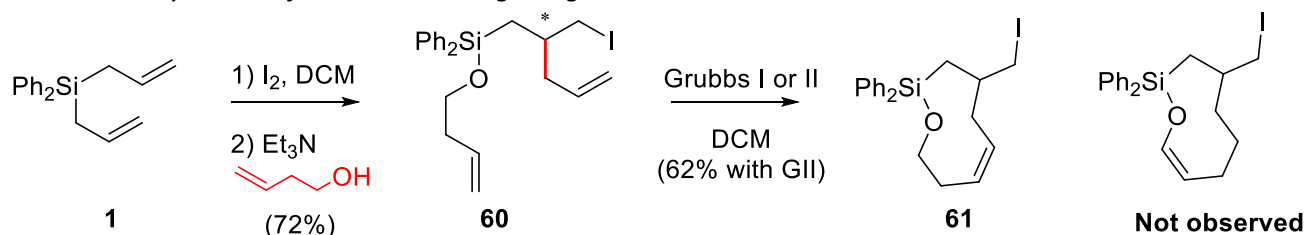
**Scheme 3.2.** RCM of phenyl, hexyl and methyl substituted silanes.

However, when **54**, **56** and **58** were all subjected to RCM using GI and GII catalysts, both catalysts gave the same non-isomerized RCM product (**55**, **57** and **59**, respectively). The lack of isomerization in these RCM reactions, even when using the GII catalyst, suggests that the phenyl, hexyl and methyl groups were able to sterically hinder the isomerization. One possible explanation is that the alkene in RCM products **55**, **57**, or **59** is unable to coordinate to the catalyst preventing formation of a Ru-H species

responsible for isomerization (see Figure 3.1). Alternatively, the Ru-H species cannot effectively bind to the alkene in RCM products **55**, **57**, or **59**. Hydrometallation could also occur, but the subsequent beta-hydride elimination to form the corresponding trisubstituted alkene enol ether is hindered in these systems so **55**, **57**, or **59** is regenerated. This could also be used to explain why we do not see any of trisubstituted alkene forming in the RCM of unsubstituted compounds, since even a methyl group on **52** was able to prevent isomerization to form a tri-substituted alkene (see Scheme 3.1). However, we would expect to see isomerization in the other direction (e.g. compound **41b**) from a Ru-H species. For instance, Cadot et al. reported a similar finding that isomerization by GII to the corresponding enol ether was prevented by substitution at C1 for allylic ethers instead giving the different regioisomer resulting from isomerization in the opposite direction (see boxed reaction in Scheme 3.2). However in our RCM reactions of compounds **54**, **56**, or **58** we simply saw no isomerization<sup>59</sup>

To determine how the ring size affects isomerization, 9-membered rings were also explored. The RCM precursors were synthesized using the same one-pot 2-step iodine rearrangement chemistry (see Scheme 2.1), except instead of trapping the intermediate iodosilane with allyl alcohol in step 2, homoallylic alcohol was used. Subjecting **60** to RCM with GI gave mostly starting material **60** with trace amount of RCM product **61**, while using GII catalyst resulted in mostly the formation of **61** (Scheme 3.3 and Figure 3.6). Interestingly, isomerization to an enol ether product did not occur to a large extent (see signals at 6.5 ppm in Figure 3.6).

**Scheme 3.3.** Synthesis of 9-membered ring using RCM with GI and GII.



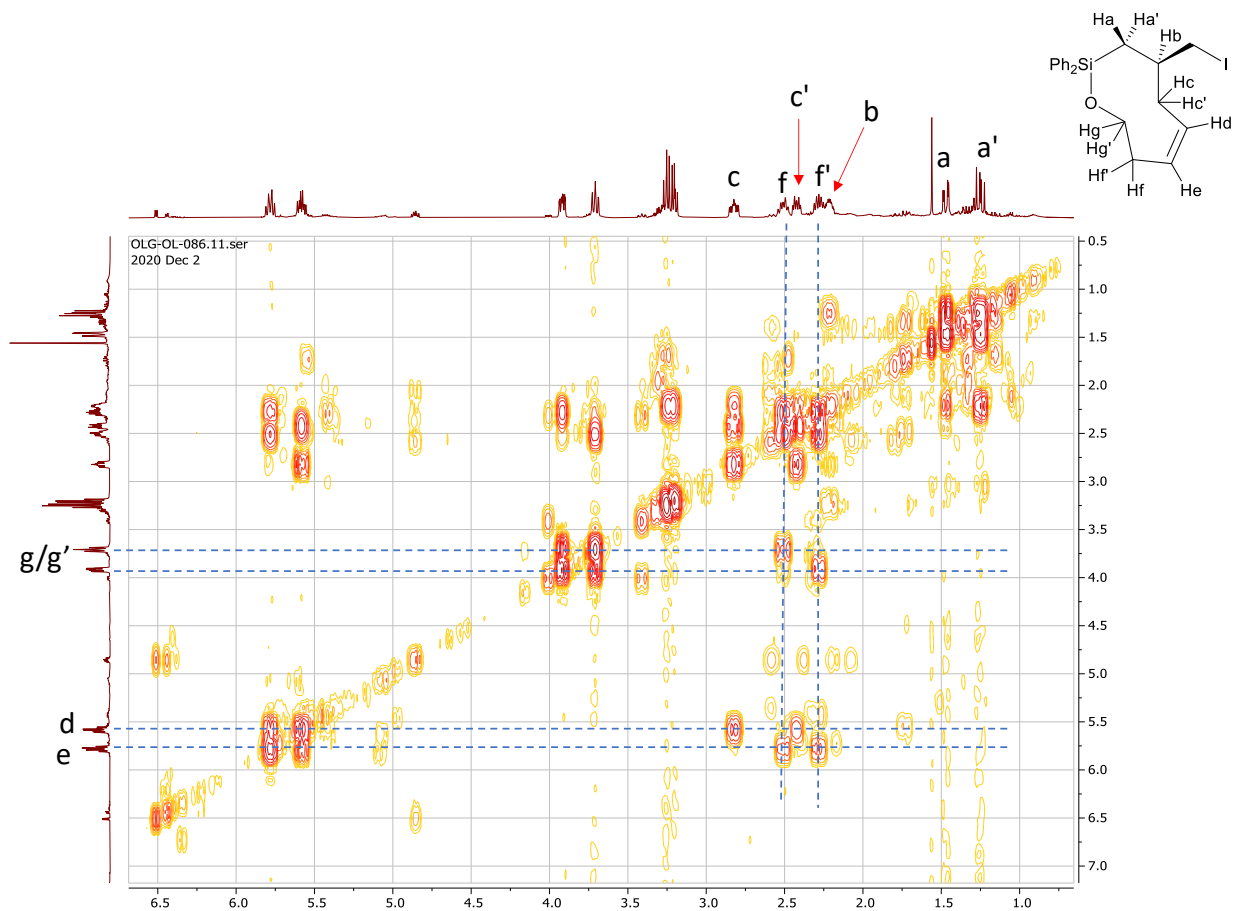


**Figure 3.6.** COSY NMR of 9-membered ring RCM product **61** catalyzed by *GII*.

One possible explanation for the lack of isomerization in this 9-membered ring RCM could be due to the lack of a neighboring acidic allylic proton that can be abstracted to form a Ru-H isomerizing species (see Figure 3.7). More specifically, in RCM product **61**, the carbons immediately adjacent to the alkene do not contain an oxygen atom that would increase the acidity of those hydrogens. Whereas the allylic position in RCM product **25** is more easily deprotonated leading ultimately to the formation of a Ru-H that can then isomerize other RCM product molecules.

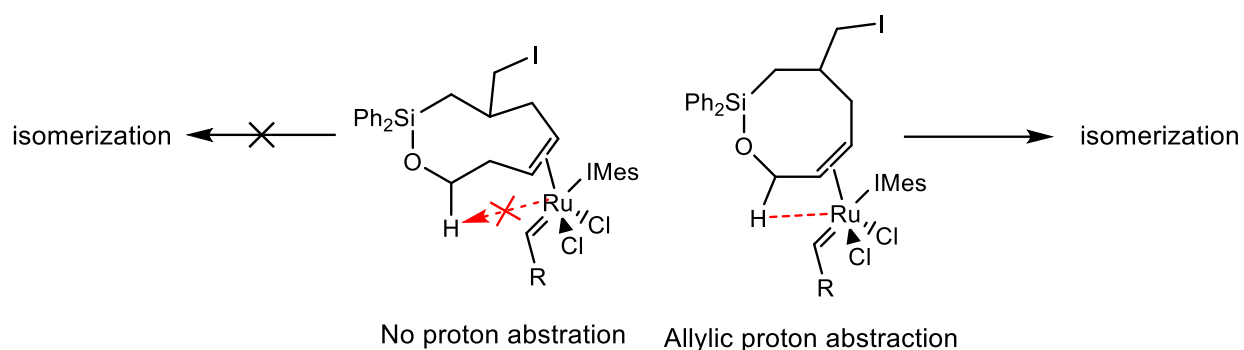
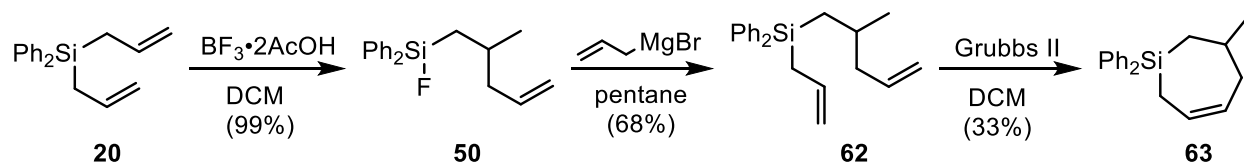


**Figure 3.7.** Proton abstraction representation of 9-membered ring vs 8-membered ring to form Ru-Hs.

The importance of the oxygen atom was also explored since other studies have demonstrated the susceptibility of allyl ethers to isomerization during metathesis,<sup>60,63</sup> we hypothesize that its removal would reduce isomerization. Although it was difficult to synthesize an 8-membered non-ether RCM precursor, the 7-membered alternative ring was more readily prepared and was therefore chosen as our target. By reacting with allyl magnesium bromide, product **62** was obtained and subjected to RCM conditions using GII (Scheme 3.4). As predicted, isomerization was not observed with **62**, instead giving the non-isomerized RCM product **63** in 33% yield.

**Scheme 3.4.** Synthesis of all carbon 7-membered RCM product.



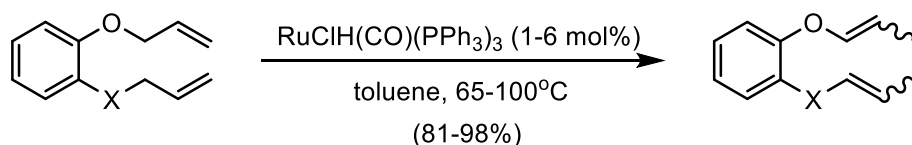
### 3.3 Mechanistic investigations

To investigate the factors that affect isomerization and catalyst decomposition, further studies were conducted. Previous studies suggest that the presence of ethylene can cause catalyst decomposition, which is known to promote isomerization.<sup>61,62</sup> There are two ways to remove the ethylene formed during metathesis, one way is by running the reaction under slight vacuum, and the other is by running the reaction under a stream of nitrogen. Attempting the latter method with **24** and

GII, only isomerization products were formed, consistent with what was observed for reactions where ethylene was not removed. However, one notable difference was the ratio of isomers **41a**:**41b**. Under standard conditions, the ratio was 1.79:1.00 in favor of the enol ether **41a**. Running the reaction under a stream of nitrogen increased the ratio to 3.39:1.00. Still, only isomerized RCM products were obtained, indicating that ethylene was not responsible for isomerization in our reactions.

Another Ru isomerization catalyst is carbonyldihydrido-tris(triphenylphosphine)ruthenium(II) ( $\text{RuClH}(\text{CO})(\text{PPh}_3)_3$ ). This complex does not promote metathesis, just isomerization. A study done by Morgans et al. studied isomerization using this catalyst in various systems with different heteroatoms to see how it affects isomerization. They have found that isomerization readily occurs in good yields, 81-89% (Scheme 3.5) in systems containing oxygen and nitrogen heteroatoms.<sup>63</sup>

**Scheme 3.5.** Isomerization induced by  $\text{RuClH}(\text{CO})(\text{PPh}_3)_3$  as studied by Morgans et al.<sup>63</sup>



X=O or  $\text{NR}_1$   
 $\text{R}_1$ = Ts, Boc or CPh

Since we suspected a ruthenium hydride was responsible for isomerization in our reactions, we set out to examine how  $\text{RuClH}(\text{CO})(\text{PPh}_3)_3$  might promote isomerization of the dialkene RCM precursor **24**, along with RCM products **25**, **41b** and **52** and compare the results to GII catalyzed reactions. When diene **24** was subjected to the isomerization conditions described by Morgan et al. using  $\text{RuClH}(\text{CO})(\text{PPh}_3)_3$ , the results showed 100% conversion of the starting material. The major product was **41d**, which we also obtained in small amounts from some GII-catalyzed reactions (see Table 3.2), where both alkenes have isomerized (Figure 3.8). RCM product **25** was also subjected to the Ru-H isomerization catalyst which yielded 100% conversion to enol ether **41a** (Figure 3.9). None of the isomeric **41b** was detected by NMR analysis from this reaction. Furthermore, when **41b** was subjected to the same conditions, isomerization to **41a** was also observed in 100% conversion (Figure 3.9). This further

corroborates the idea that conversion between isomerization products is possible, and that **41a** is favored which is in line with our relative energy calculations.

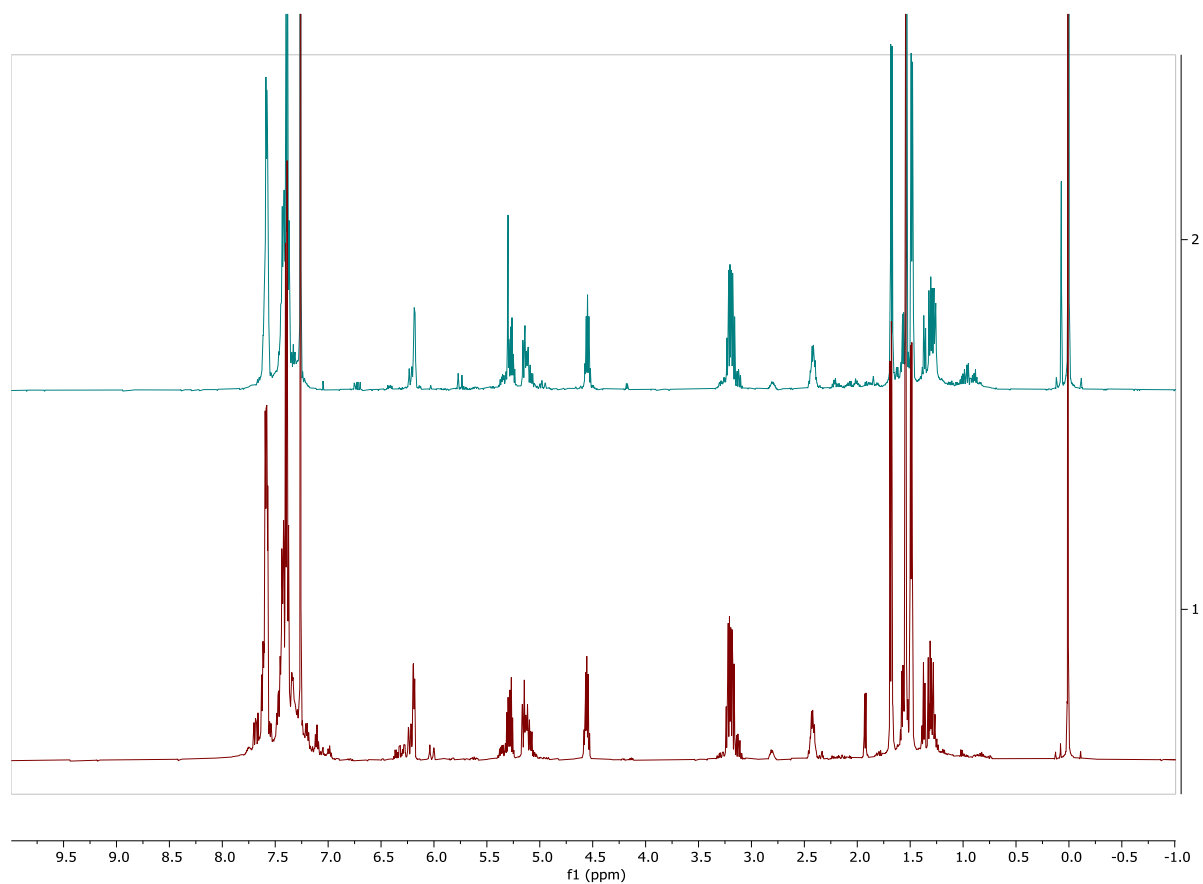


**Figure 3.8.** NMR spectra of isolated product **41d** (top) and the crude mixture of **24** subjected to  $\text{RuClH}(\text{CO})(\text{PPh}_3)_3$  (bottom).

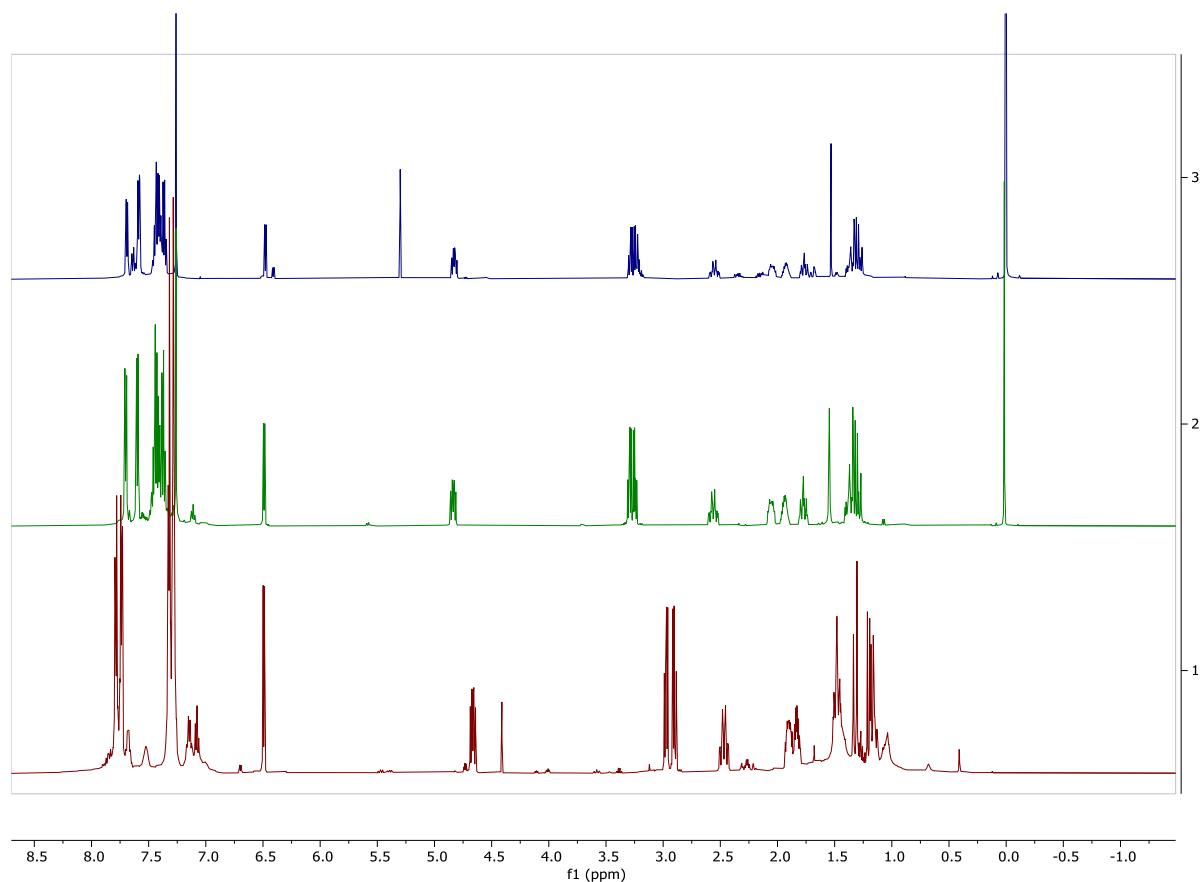


**Figure 3.9.** NMR spectra of isolated product **41a** (top) and the crude mixture of **25** subjected to  $\text{RuClH}(\text{CO})(\text{PPh}_3)_3$  (middle) and crude mixture of **41b** subjected to  $\text{Ru-H}$ , although the NMR shown is in toluene- $d_8$  (bottom) while the top two spectra are in  $\text{CDCl}_3$ .

On the other hand, whenever **52**, which contains a methyl group instead of the iodomethyl group in **25**, was taken through the isomerization route with  $\text{Ru-H}$ , isomerization to **53a** was observed but only in 30% conversion (Figure 3.10). Lübke et al. have reported that certain organic halides can impact RCM and isomerization performance, however their rationale was based on the formation of a carbocation from the organic halide which we do not think plays a major role in our system (i.e. the resulting primary carbocation would be high energy).<sup>64</sup> The reaction of **52** with  $\text{RuClH}(\text{CO})(\text{PPh}_3)_3$  was run for only 2 hours, like the previous reactions with **24**, **25** and **41b**. It is possible that with extended reaction time 100% conversion could be achieved.

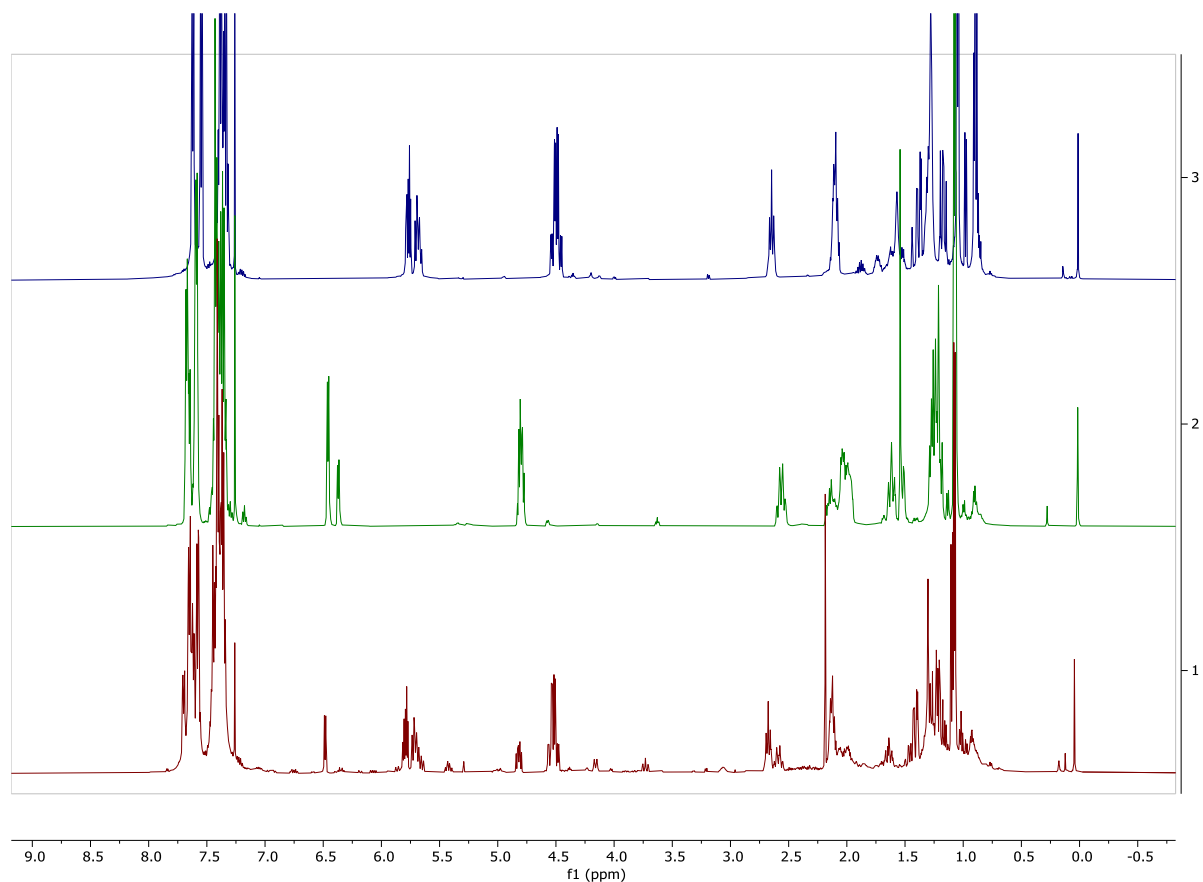


**Figure 3.10.** NMR spectra of isolated **52** (top), **53a** (middle) and the crude mixture when **52** was subjected to  $\text{RuClH}(\text{CO})(\text{PPh}_3)_3$  (bottom).

The results we obtained from experiments with  $\text{RuClH}(\text{CO})(\text{PPh}_3)_3$  provide support for a Ru-H based isomerization in our RCM reactions. However, there are some notable differences. For instance,  $\text{RuClH}(\text{CO})(\text{PPh}_3)_3$  isomerization of RCM product **25** was completely regioselective, giving exclusively enol ether **41a**. RCM reactions, in contrast, gave a mixture of **41a** and its regioisomer **41b** as an approximately 2.5:1 mixture on average. One explanation for these differences is that the nature of the Ru-H species formed during the RCM reactions, while similar to  $\text{RuClH}(\text{CO})(\text{PPh}_3)_3$ , is not identical and this GII-derived Ru-H is a less selective isomerization catalyst.

Certain additives such as benzoquinone are known to prevent isomerization, which is thought to quench any ruthenium hydrides that might form.<sup>65</sup> Although the exact mechanism for the prevention of

olefin migration is still not known, it has been proposed that either the benzoquinone prevents metal hydride formation or its rapid reaction with the generated hydrides during decomposition. This is due to the 1,4-benzoquinone being reduced to 1,4-hydroquinone upon reacting with the ruthenium hydride, which was observed by Hong et al. by NMR.<sup>65</sup>

To examine the impact of benzoquinone additive on our RCM, two reactions were set up. The control reaction involved a sequential treatment of **24** with GI, and without quenching the reaction, GII was added and allowed to react overnight (a small amount of crude was taken out of the reaction flask right before the addition of GII and used for NMR analysis). The results are shown in Figure 3.11, where the middle spectrum shows all of **24** was consumed and RCM product **25** was formed after treatment with GI. After the addition of GII, all of **25** was consumed and converted to RCM products **41a**, **41b** and **41c** (top spectrum). When compared to the standard reaction of **24** and GII, the isomerization products **41a** and **41b** were formed in comparable ratios, and about 65% less of **41c** was formed. The only isomerized product not detected was **41d** which was expected since there was no more **24** that can undergo both double bonds isomerizing without ring closing. Interestingly though, **41c** was still formed, though at a smaller quantity (~65%). It was concluded that **41c** forms by only one alkene isomerizing in **24** prior to ring closing, and when RCM happens, the resulting product is the ring-contracted **41c** product. Its formation would indicate that ring opening of **25** is possible, followed by one olefin migrating and then ring closing to form the contracted ring **41c**. For the second experiment, after treatment with GI, without quenching the reaction like before, benzoquinone and GII were added and allowed to react overnight. The NMR spectrum is shown in Figure 3.11, bottom spectrum, which shows that all with the addition of benzoquinone isomerization was ceased as only **25** was detected. This experiment would suggest that Ru-H are indeed responsible for isomerization since the addition of benzoquinone was able to prevent **25** from isomerizing.

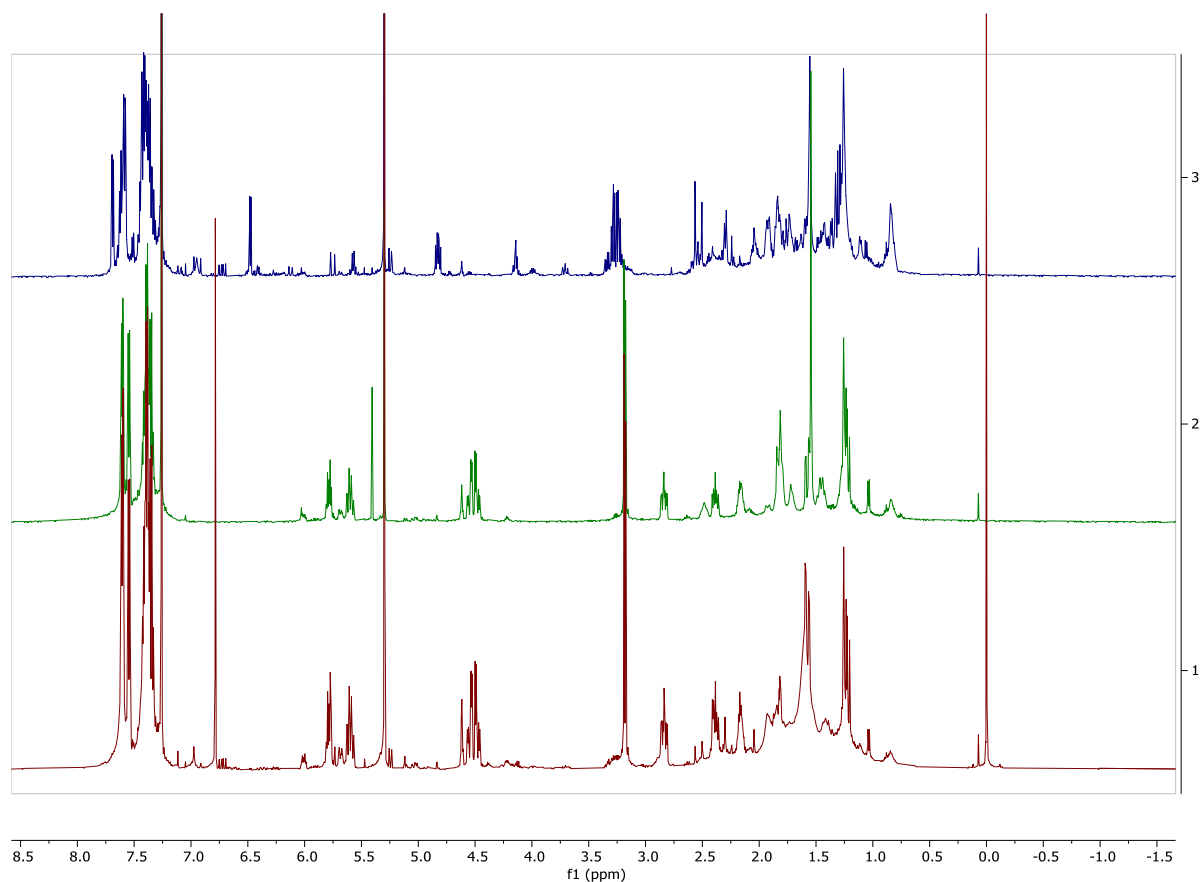


**Figure 3.11.** NMR spectra of sequential treatment of **24** with GI (middle), followed by GII (top), or followed by GII and benzoquinone (bottom), after which no isomerization was observed.

Overall, while these experiments provide support for ruthenium-hydride catalyzed isomerization during our RCM reactions; as mentioned, the regioselectivity of isomerization (i.e. ratio of regioisomers **41a** to **41b**) was different between the RCM and isomerization reactions performed using  $\text{RuClH}(\text{CO})(\text{PPh}_3)_3$ . While differences in the nature of the ruthenium hydrides (e.g. ancillary ligands) could be responsible for these differences, the possibility of a secondary ruthenium nanoparticle mediated isomerization that could occur during RCM that might result in the formation of regioisomers should also be considered. One method to test for nanoparticles is to detect them in solution using a laser via the Tyndall Effect. Since nanoparticle clusters can scatter light, shining a laser beam through a solution that contains nanoparticles will make the beam visible, and the absence of a visible beam would indicate a lack of nanoparticles present.<sup>66,67</sup> Attempting this method, we took a red laser with a

wavelength of 650 nm and at 0 mins, 30 mins, 2 hours, and 24 hours, monitored a RCM reaction with **24** and GI, GII, and Hov-GII. The result pictures are summarized in Table 3.5.

**Table 3.5.** Laser test for nanoparticles using GI, GII, and Hov-GII for RCM of **24**.

Catalyst	0 mins	30 mins	2 hour	24 hour
Grubbs I				
Grubbs II				
Hov-Grubbs II				

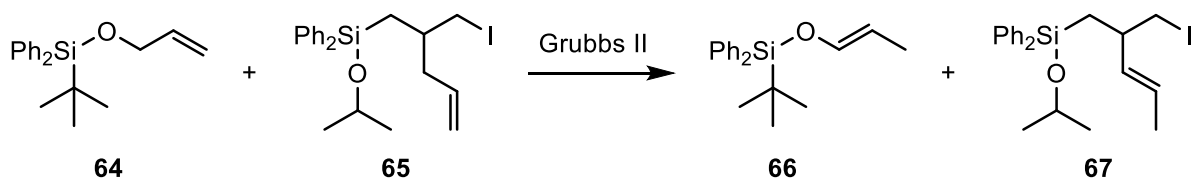
Interestingly, all the catalysts had a visible laser beam through the solution at all time increments, suggesting the presence of nanoparticles in all three catalysts. Even as 0 mins, the presence of RuNPs were detected, which is consistent with a previous report that also detected NPs in commercially bought catalysts.<sup>54</sup> These observations indicate that RuNPs could be contributors to the isomerization we observed during our RCM reactions. However, since RuNPs were detected in GI as well as GII and Hov-GII yet isomerization was not observed in GI catalyzed RCM reactions, we believe the contribution of RuNPs is minor compared to other possible isomerization mechanisms.

To explore the generality of the metathesis/isomerization we observed, we prepared compounds **64** and **65** representing both subunits of our RCM precursor **24**, and subjected each to GII individually (Eq. 2 and 3, Scheme 3.6), as well as together in an attempted cross metathesis (CM) (Eq. 1,

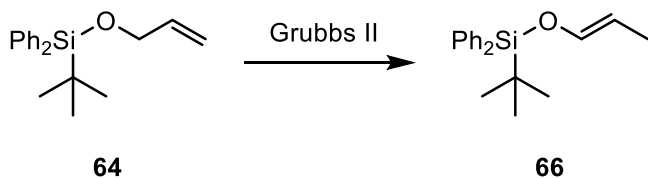
Scheme 3.6). When **64** was treated with GII, the proton NMR showed isomerization of the alkene to form an enol ether (Eq. 2, Scheme 3.6). This might explain why although other silyl-protected allyl alcohols (e.g. TBS) will undergo productive CM, no examples of successful CM reactions with **64** have been reported.<sup>68</sup> On the other hand, whenever **65** was treated using the same conditions with GII, predominately starting material was obtained with trace amounts of other unidentified products (Eq. 3, Scheme 3.6). Interestingly though, whenever **64** and **65** were subjected to CM conditions, CM did not occur, rather isomerization of both substrates occurred to give products **66** and **67** (Eq. 1, Scheme 3.6). Figure 3.12 shows the presence of **66** in the attempted CM with characteristic peaks at 6.11, 5.03, 4.40 and 3.94 ppm. Since there is another alkene peak present in the crude mixture at 5.13 ppm that does not belong to either **66** or **65**, we concluded that it belongs to isomerized product **67**.

**Scheme 3.6.** Three reactions used to explore isomerization in cross metathesis.

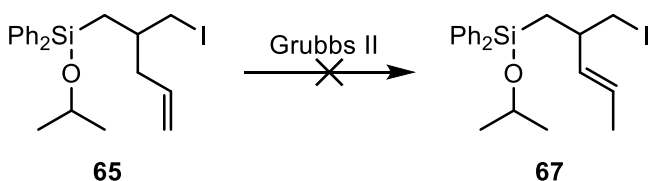
**Equation 1**



**Equation 2**



**Equation 3**



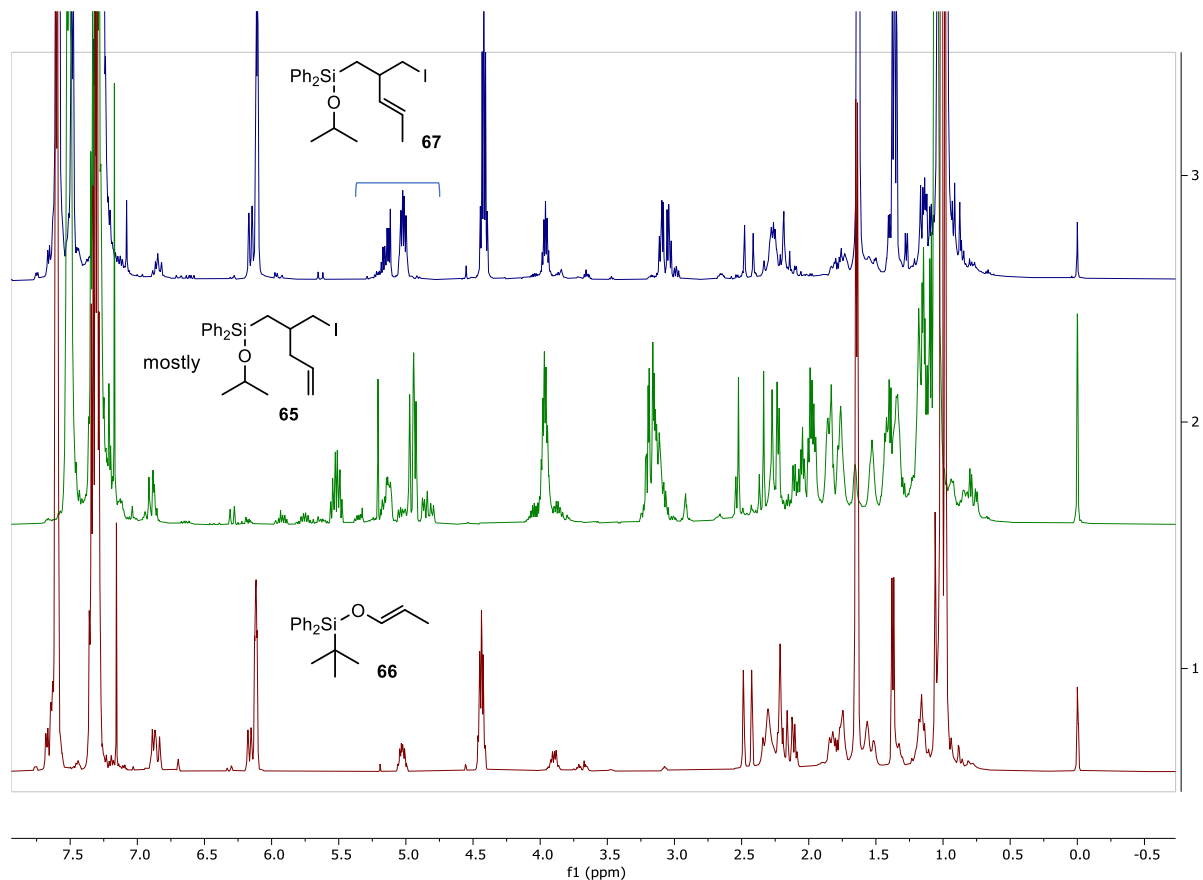
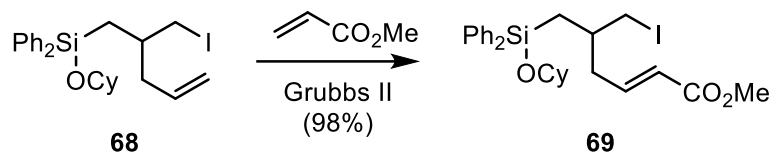


**Figure 3.12.** NMR spectra of CM results of **64** and **65** with GII (top), **65** treated individually with GII (middle) and **23** treated with GII (bottom).

One possible explanation for the lack of isomerization upon treatment of **65** with GII could be that no Ru-H isomerizing species were formed since **65** does not contain ether protons next to the alkene which can be more readily abstracted (see Scheme 3.2). However, since **64** does have ether protons in the allylic position that can be abstracted to form Ru-H, isomerization occurs to give **66**.<sup>69</sup> When **64** and **65** were subjected to CM, **64** was able to induce Ru-H formation, resulting in its isomerization to **66**, and the newly formed Ru-H proceeded to promote the isomerization of **65** to **67**. Now with two di-substituted alkenes present in the reaction mixture, metathesis becomes challenging and no CM was observed. Thus, the importance of the heteroatom for isomerization was established as it promotes proton abstraction to form Ru-H, while the attempted CM shows that isomerization is not specific to just cyclic structures. A study done O'Neil and Cummins further supports that CM can occur

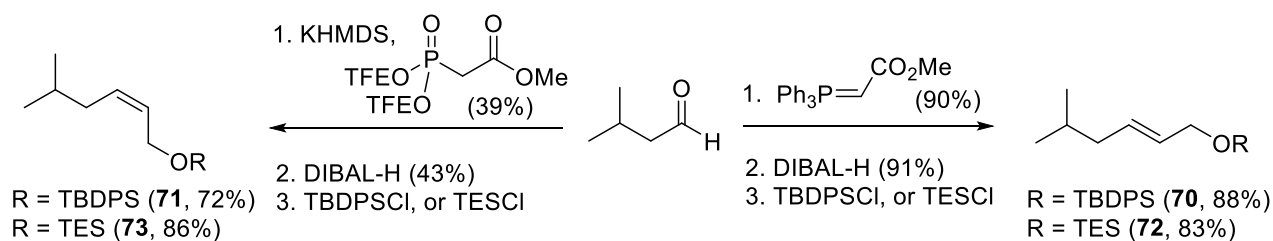
from compounds of type **65** with GII in excellent yields as long as there is no heteroatom present to induce proton abstraction (Scheme 3.7).<sup>70</sup>

**Scheme 3.7.** Successful CM in 98% yield using GII.



We also looked at whether isomerization in different directions can occur in acyclic systems when treated with either GII or  $\text{RuClH}(\text{CO})(\text{PPh}_3)_3$ . Cis and trans silyl ethers **70-73** containing either a tert-butyldiphenyl- (TBDPS) or triethyl- (TES) silane groups were prepared as outlined in Scheme 3.8. These systems contain an alkene that neighbors ether protons which can be abstracted to form Ru-H and foster isomerization. They also contain a methylene group on the other side of the alkene providing the opportunity to isomerize in a different direction without being too sterically hindered. Given these parameters, we expected that similar to the ring structures, we would see isomerization occurring in both directions after treatment with GII and only to the enol ether with  $\text{RuClH}(\text{CO})(\text{PPh}_3)_3$ .

**Scheme 3.8.** General synthesis of acyclic silanes that were then treated with GII and  $\text{RuClH}(\text{CO})(\text{PPh}_3)_3$ .



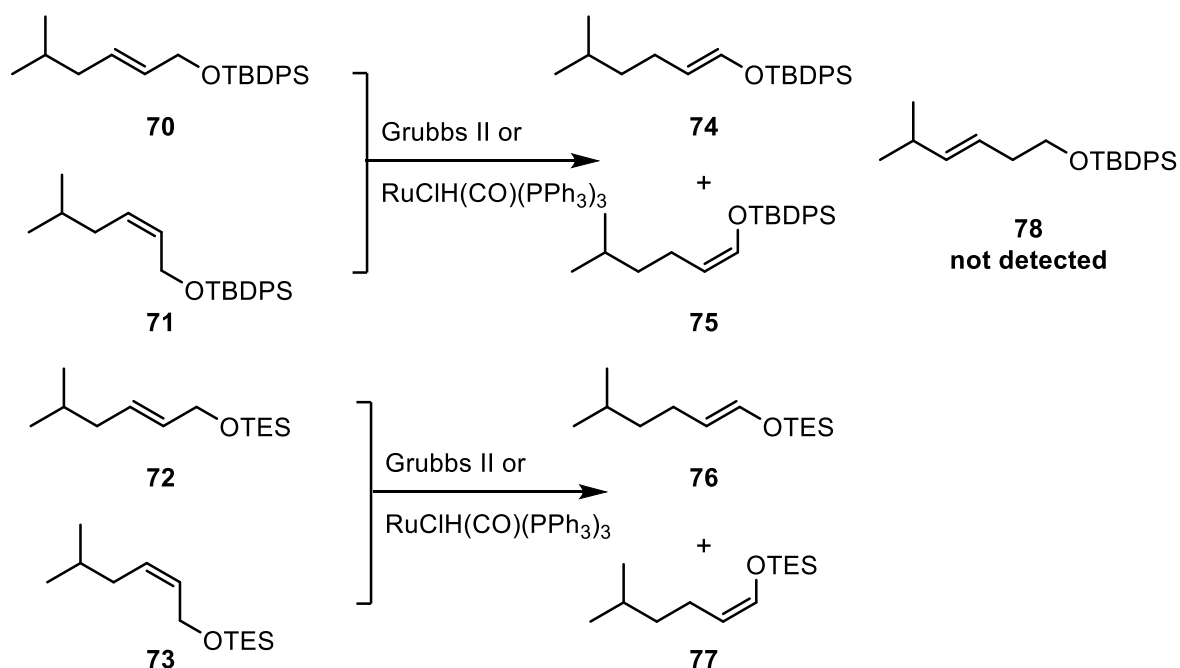


**Figure 3.13.** Structures of 4 different acyclic products synthesized and treated with GII and  $\text{RuClH}(\text{CO})(\text{PPh}_3)_3$ .

After treating the 4 different acyclic compounds (Figure 3.13) with GII or with  $\text{RuClH}(\text{CO})(\text{PPh}_3)_3$ , there was no difference in the trends observed between substrates containing either a TBDPS or TES groups (Table 3.6). Whenever trans isomers **70** and **72** were treated with GII, in both cases, isomerization to the enol ether occurred, however, not at 100% conversion as some of the starting material was still detected. On the other hand, treatment using  $\text{RuClH}(\text{CO})(\text{PPh}_3)_3$  resulted in 100% conversion to the corresponding enol ether as a 2:1 ratio of cis:trans isomers **75:74** or **76:77**. In fact, the 2:1 *trans:cis* ratio was consistent for all reactions of **70**, **71**, **72**, and **73** using  $\text{RuClH}(\text{CO})(\text{PPh}_3)_3$  and the NMR spectra were very clean with little to none other byproduct formation. Distinction between the cis and trans isomers was achieved by looking at coupling constants of the two peaks at 6.26 and 6.19 ppm (see Figure 3.14 for example). The peak at 6.26 ppm has a coupling constant of 11.9 Hz which is characteristic to trans coupling and the peak at 6.19 ppm has a much smaller coupling constant of 5.8 Hz which we have assigned as the cis isomer. Somewhat surprisingly, using GII to induce isomerization only produced the enol ether as detectable by NMR, and did not result in formation of regioisomer **78**

(compound **78** was synthesized separately and used as a reference NMR, Figure 3.14). Another interesting result was obtained upon treatment of **73** with Grubbs II. Synthesizing **73** was not 100% selective for the cis isomer and therefore a mixture of cis and trans isomers (**72** and **73**) was taken into the reaction with GII. The only starting material detected corresponded to the trans isomer **72**, indicating that the cis isomer is more prone to isomerization. This would also be consistent with the result that treatment of **70** and **72**, both of which are trans alkenes, with GII did not result in full consumption as 53% and 61% of the starting material was observed by NMR, respectively. On the other hand, the cis compounds (**30** and **32**) did give 100% conversion to isomerized products upon treatment with GII in this case.

**Table 3.6.** Summary of results when acyclic substrates were treated with GII and RuClH(CO)(PPh<sub>3</sub>)<sub>3</sub> as determined by NMR integration.

Silane	Catalyst	Starting material	Cis isomer (%)	Trans isomer (%)
<b>70</b>	Grubbs II	53	12	34
<b>70</b>	RuClH(CO)(PPh <sub>3</sub> ) <sub>3</sub>	0	70	30
<b>71</b>	Grubbs II	0	37	63
<b>71</b>	RuClH(CO)(PPh <sub>3</sub> ) <sub>3</sub>	0	69	31
<b>72</b>	Grubbs II	61	16	23
<b>72</b>	RuClH(CO)(PPh <sub>3</sub> ) <sub>3</sub>	0	68	32
<b>73</b>	Grubbs II	30 <sup>a</sup>	23	46
<b>73</b>	RuClH(CO)(PPh <sub>3</sub> ) <sub>3</sub>	0	68	32

Notes for table: <sup>a</sup>**73** starting material was present as a mixture of cis and trans, the starting material detected corresponds to the trans isomer, suggesting that all of the cis isomer was consumed.

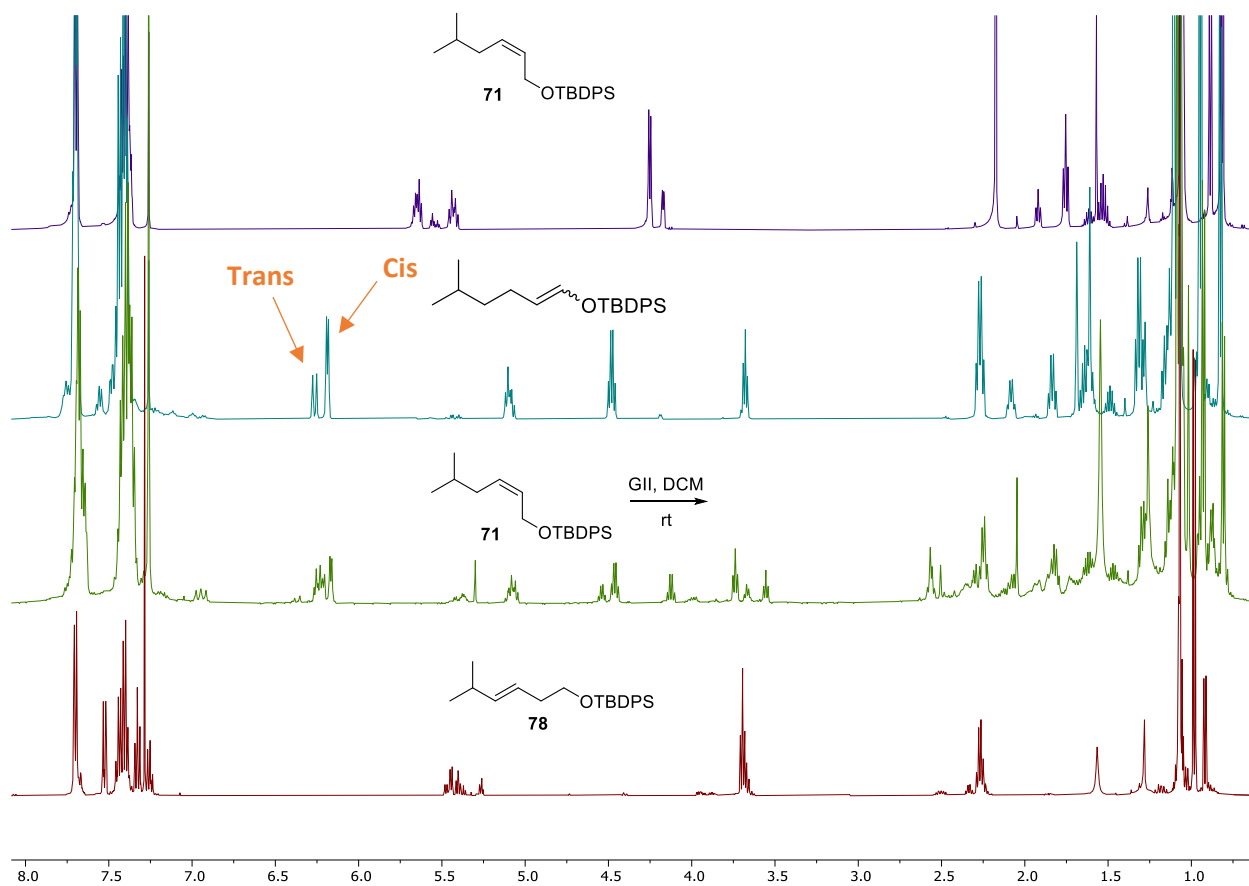


**Figure 3.14.** NMR spectra of **71** (top, purple trace) was treated with  $\text{RuClH}(\text{CO})(\text{PPh}_3)_3$  (blue trace), *GII* (green trace), and **78** (bottom, red trace) used as a reference NMR.

Thus, these conclusions provide some insight why our RCM product **25** behaved in such a characteristic way. The fact that it contains a cis alkene makes it more prone to isomerization, which can explain why we have seen 100% isomerization with the treatment of *GII*. Also,  $\text{RuClH}(\text{CO})(\text{PPh}_3)_3$  is a more selective isomerizing catalyst, which was confirmed by the treatment of **70**, **71**, **72**, and **73** with this preformed Ru-H and resulting in isomerization exclusively to the enol ether. This selective isomerization was also observed with **25** which isomerized selectively to enol ether **41b**.

## CHAPTER 4. APPLICATIONS

### 4.1. Psymberin fragment synthesis

Given that we were able to successfully synthesize functionalized medium ring silyl ethers, we looked for opportunities to make use of these compounds as synthetic intermediates and put such products into context. One such application was using **25** to synthesize psymberin, which is a rather fascinating compound with a lot of history. Psymberin belongs to the pederin family and pederin was first isolated in 1919 from *Paederus fescipes* by Netolitzky, which is a Japanese beetle with toxic effects that can lead to skin irritation.<sup>71</sup> Although the Chinese have been using the cytotoxic extracts from these beetles as early as 739 AD to cure blains and lichens,<sup>72</sup> it was not until recently that its medical potential was explored further with much enthusiasm. Whenever these beetles are harmed or injured, they release the toxic extract pederin that blocks mitosis even in small concentrations (about 1 ng/mL).<sup>73</sup> Though there can be many complications with exposure to this toxin, pederin shows cytotoxicity against various tumor cell lines in vitro and in vivo.<sup>74</sup> Further studies on this compound showed that pederin is not produced by the beetles themselves, but by symbiotic bacteria living on the beetles.<sup>75, 76</sup> Another member of the pederin family is psymberin, which was discovered in 2004 from the sponges *Psammocinia sp.* and *Ircinia ramosa* by Crews and Pettit, respectively.<sup>77,78</sup> When psymberin was tested against 60 different human cell lines, it showed impressively high cytotoxicity values for certain cancers like melanoma, breast and colon ( $LC_{50} < 2.5 \times 10^{-9}$  M), while leukemia cell lines are relatively unaffected ( $LC_{50} < 2.5 \times 10^{-5}$  M) with a difference at the  $10^4$  scale.<sup>79</sup> With this great potential antitumor activity, psymberin research became of much interest, and since it is not sustainable to extract the toxin from sponges, synthetic methods have been explored. One possible route is outlined in Figure 4.1 which was reported by Jiang et al.<sup>80</sup>

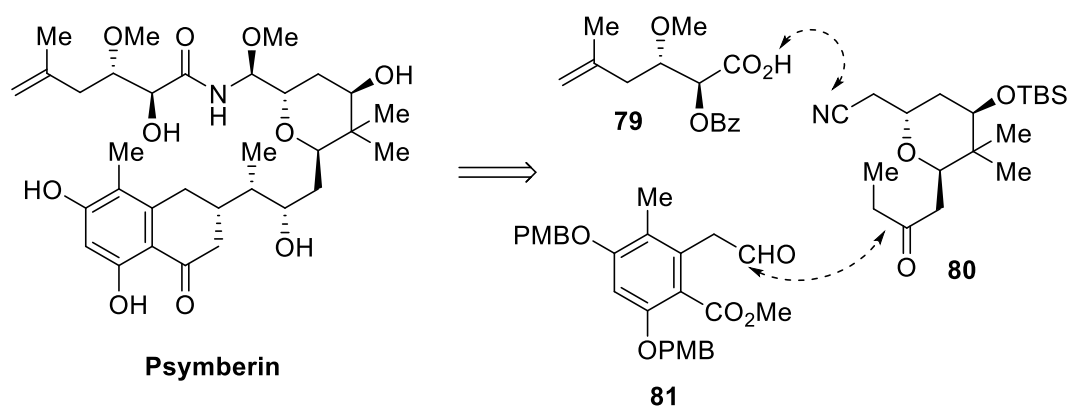
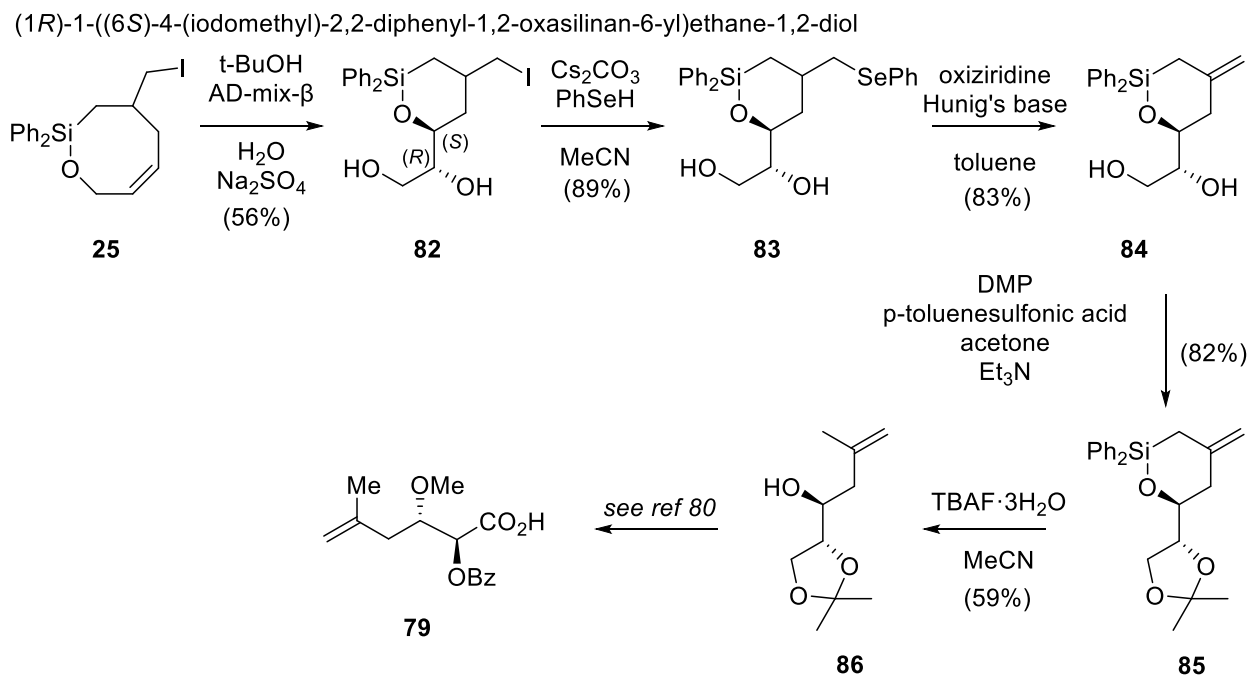


**Figure 4.1.** Retrosynthesis of psymberin as reported by Jiang et al.<sup>80</sup>

The Jiang synthesis of psymberin involves coupling fragments **79**, **80**, and **81**. We set out to investigate a synthesis of key fragment **79** from our RCM product **25** (Scheme 4.1). Compound **25** was first subjected to a Sharpless asymmetric dihydroxylation reaction (AD) using AD-mix- $\beta$ . However, with the dihydroxylation reaction, we ran into a few challenges. The first being that at 0 °C, the reaction would not initiate despite running the reaction for 72 hours, only starting material was obtained. Even with the addition of methanesulfonamide, which has been previously shown by Junttila to accelerate the AD of aliphatic olefins regardless if they were terminal or nonterminal alkenes,<sup>81</sup> the AD failed to proceed. However, running the reaction at room temperature without the methanesulfonamide we were able to get the dihydroxylation product **82** at 56% yield. Based on Sharpless' model, we expected to obtain **82** enriched as the 2*R*,3*S*-stereoisomer which would map onto psymberin.

**Scheme 4.1.** Synthesis of fragment **79** from the RCM product **6**.



After **82** was obtained, a two-step elimination of iodine yielded **84** in (74%) for the two steps. The next step involved making an acetal to protect the hydroxyl groups, which gave **85** in 82% yield.<sup>82</sup> Finally, the silicon group was removed with tetrabutylammonium fluoride trihydrate (TBAF·3H<sub>2</sub>O) which proceeded smoothly to give **86** in 59% yield. The NMR obtained for **86** matched that reported in the literature by Jiang and all further steps to obtain psymberin fragment **79** can be followed by the procedures listed by Jiang.

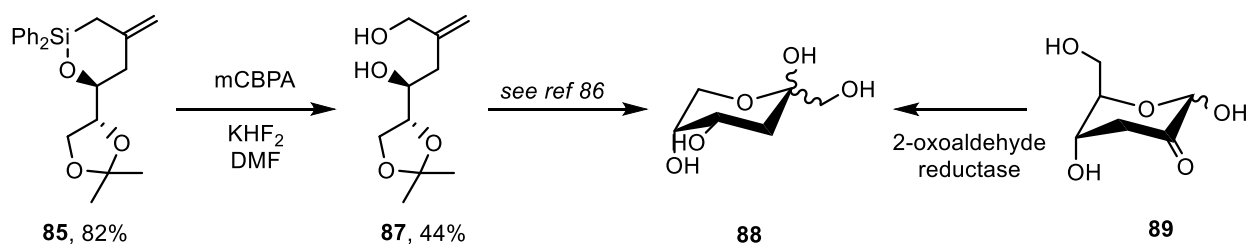
Unfortunately, we learned that there was little to no enantioselectivity for the AD. This was determined by a comparison of optical rotation data of **86**, which showed  $[\alpha]_D = -0.52$  (DCM,  $c = 0.39$ ) while Jiang et al. reported  $[\alpha]_D = +29.0$  (EtOAc,  $c = 0.224$ ). This is perhaps not surprising since it is known that *cis*-alkenes are not good substrates for AD. Disubstituted *cis* alkenes are generally lower yielding (yields not exceeding 35%) and give low enantiomeric excess.<sup>83,84</sup> The selectivity becomes even more difficult when the two substituents are similar in size since the prochiral asymmetry begins to vanish and the enantiofacial selection becomes more difficult. However, it is possible that different ligands for AD

catalysis could increase the enantioselectivity of this reaction and should be investigated further.<sup>85</sup> Nonetheless, overall yields for our sequence were good. If the dihydroxylation (or a similar reaction) could be made more enantioselective we think it represents an efficient method for synthesizing this fragment of psymberin.

#### 4.2. Sugar derivative synthesis

We also thought our chemistry could be used to synthesize the sugar derivative compound **88** (3-deoxy-D-fructose), another product that has biological importance. Compound **88** has been found in mammalian blood and urine and higher concentrations have been found in diabetics. It is a degradation product of **89** (3-deoxyglucosone), which is an intermediate in the nonenzymatic polymerization and decomposition of proteins. In mammals, a significant amount of **89** is reduced to **88** to improve its stability, thus making it less damaging to the tissue.<sup>86</sup> The synthetic route to **88**, and the degradation in the mammalian body by 2-oxoaldehyde reductase is outlined in Scheme 4.2.

**Scheme 4.2.** Synthesis of 3-deoxy-D-fructose from acetal **85** and the degradation of 3-deoxyglucosone **89**.



By taking the previously prepared acetal **85** (Scheme 4.1) and reacting with the oxidizing agent meta-chloroperoxybenzoic acid (mCPBA), potassium difluoride in dimethylformamide, the silicon-carbon bond is broken and the diphenylsilane group cleaves to yield **87** in 44% yield. Different conditions for this oxidative cleavage were screened (e.g. no KHF<sub>2</sub>, used acetonitrile as solvent, used mCPBA followed by TBAF·3H<sub>2</sub>O), however we found the original conditions proposed by Tamao in 1982 proved to be

most effective.<sup>87</sup> Though the yield was not the best, further optimizations might be possible given the continued interest in this reaction.<sup>88</sup>

### 4.3. Conclusions and outlook

With the many observations we have made concerning RCM and isomerization, there are a few key take-aways. First, GII and Hov-GII are more prone to inducing isomerization compared to GI, and this could be due to catalyst decomposition during metathesis with the formation of Ru-Hs and facilitated by the NHC ligands present on the GII and Hov-GII catalysts but not GI. Other studies have shown that Ru-Hs are active isomerization catalysts our experiments are consistent with these results. Another explanation could be the formation of RuNPs during metathesis, although further investigation is still needed. For instance, conducting a mercury poisoning experiment that inhibits NP catalysis could provide interesting data if it does decrease the extent of isomerization, as it would validate the theory of NP-induced isomerization. However, the presence of NPs in reactions with GI where no isomerization was observed would point to a minor role of NPs for inducing isomerization. The last explanation involves the abstraction of allylic protons by the catalyst which can lead to an isomerization pathway. Since the NHC ligand makes the Ru metal more basic, GII and Hov-GII are more prone to undergoing isomerization via abstraction versus GI which does not contain a NHC ligand.

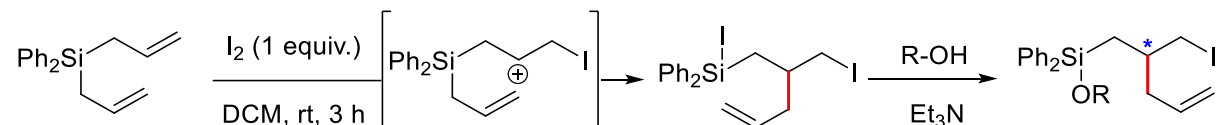
Since conversion between different isomerization products is possible, this equilibrium can be controlled by time and temperature. Decreasing the temperature prevents isomerization from occurring while the increase in temperature has shown to increase isomerization to the most stable product. Also, if the reaction time is decreased (e.g. <1 hr), not enough time is given for the reaction to undergo isomerization so non-isomerized RCM product can be obtained. Furthermore, steric hinderance can have a significant impact on determining whether isomerization occurs. Different substituents like methyl, phenyl, hexyl and iodomethyl groups were studied and each showed that isomerization to a tri-substituted alkene does not occur presumably due to hindering allylic hydrogen abstraction. Also, the

oxygen heteroatom is essential for isomerization since an oxygen-free system did not undergo isomerization. Increasing the ring size resulted in an alkene that is further away from oxygen influence and isomerization was not detected for that compound either. Lastly, we looked at the generality of isomerization and whether acyclic compounds have similar trends as observed for ring-structures. From those studies, we determined that cis alkenes are more prone to isomerization than trans alkenes, although isomerization in both directions was not observed in the same way 8-membered rings were.

Future work could involve investigating RuNP effects and how those differ between GI, GII and Hov-HII. Also, by conducting deuterium labeling experiments, it may be possible to distinguish between the different isomerization pathways by monitoring where deuterium is incorporated into the final products. We also explored the synthetic utility of our non-isomerized RCM product in synthesizing a pismberin fragment as well as a sugar derivative, although enantioselectivity of the AD remains to be optimized. Given the multiple functional groups present in our RCM products (e.g. alkene, enol ether, alkyl halide, C-Si bond), we expect these compounds can serve as useful intermediates to access a variety of important structures which remains to be explored.

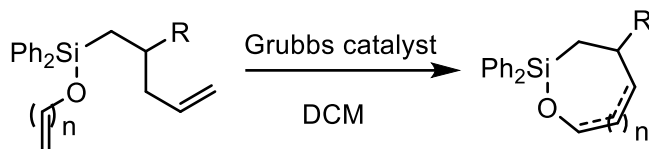
## CHAPTER 5. EXPERIMENTALS

### General procedure A- iodine rearrangement



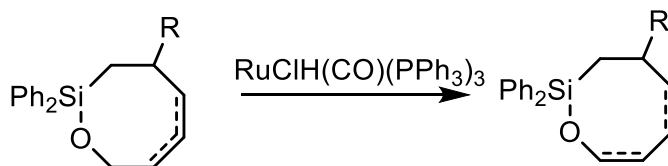
Into a flame dried flask under nitrogen, diallyldiphenyl silane (1 equiv.) and dry dichloromethane (0.1 M) was added, followed by iodine while stirring (1 equiv.). The solution was stirred at room temperature overnight, then cooled to  $0^\circ\text{C}$ . Triethylamine was added (3.0 equiv.) followed by the alcohol (2 equiv.) and the solution was allowed to warm to room temperature overnight while stirring. The reaction was quenched with deionized water, extracted with  $\text{DCM}$  three times, dried over  $\text{MgSO}_4$ , and concentrated by rotary evaporation. The crude product was purified by silica gel chromatography using 10:1 hexanes:ethyl acetate solvent system to yield product as an oil.

### General procedure B- ring closing metathesis



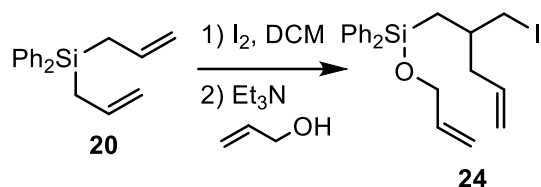
Into a flame dried flask under nitrogen, the substrate (1.0 equiv.) was added, followed by dry dichloromethane (0.02 M). The solution was degassed three times by freezing in liquid nitrogen, pumping with vacuum, and thawing under nitrogen. While stirring, the Grubbs catalyst was added (5-10 mol %) and allowed to stir at room temperature overnight. The reaction was concentrated by rotary evaporation, followed by column chromatography with silica gel using 2:1 hexanes:dichloromethane solvent system.

### General procedure C- isomerization using Ru-H catalyst



The following reaction was performed in a dry NMR tube. The substrate (1.0 equiv. ) was added to dry NMR tube under a nitrogen atmosphere. In a separate flame dried flask under nitrogen, dry toluene- $d_8$  or benzene- $d_6$  (0.2 M) was added and the solvent was degassed three times by freezing in liquid nitrogen, pumping with vacuum, and thawing under nitrogen. The degassed solvent was then added via syringe to the NMR tube containing the substrate under nitrogen, followed by  $\text{RuClH}(\text{CO})(\text{PPh}_3)_3$  catalyst (5 mol %). The NMR tube was capped and sealed using parafilm and placed into preheated sand at  $100^\circ\text{C}$  and allowed to heat for 2 hours. NMR data was collected directly from this sample.

### (allyloxy)(2-(iodomethyl)pent-4-en-1-yl)diphenylsilane (**24**)

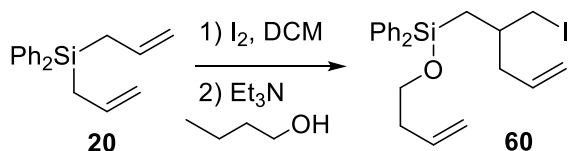


Following general procedure A, the diallyl product was obtained by reacting diallyldiphenyl silane (5.0 mL, 19 mmol) with iodine (4.8002 g, 18.913 mmol) in dichloromethane (190 mL), followed by triethylamine (7.9 mL, 57 mmol) and allyl alcohol (26 mL, 38 mmol). The crude product was purified by chromatography on silica (10:1 hexanes:ethyl acetate,  $R_f = 0.5$ ) to yield **24** (7.8387 g, 93%) as an oil.

<sup>1</sup>H NMR (500 MHz, CDCl<sub>3</sub>) δ 7.61 (dq,  $J = 6.4, 1.2$  Hz, 4H), 7.42 (m, 6H), 5.82 (ddt,  $J = 17.1, 10.2, 6.8$  Hz, 1H), 5.63 (ddt,  $J = 17.2, 10.2, 7.2$  Hz, 1H), 5.05 (m, 3H), 3.74 (m, 2H), 3.29 (h,  $J = 5.1$  Hz, 2H), 2.33 (qt,  $J = 6.7, 1.4$  Hz, 2H), 2.17 (m, 1H), 2.10 (m, 1H), 1.53 (m, 1H), 1.27 (m, 2H).

<sup>13</sup>C NMR (126 MHz, CDCl<sub>3</sub>) δ 132.7, 131.6, 130.7, 126.2, 124.1, 113.5, 110.7, 60.6, 37.3, 30.5, 15.7.

### (But-3-en-1-yloxy)(2-(iodomethyl)pent-4-en-1-yl)diphenylsilane (**60**)

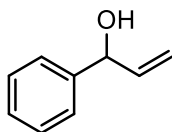


Following general procedure A, the diallyl product was obtained by reacting diallyldiphenyl silane (0.5 mL, 1.9 mmol) with iodine (0.48 g, 1.89 mmol) in dichloromethane (19 mL), followed by triethylamine (0.80 mL, 5.67 mmol) and 3-buten-1-ol (0.27 g, 3.78 mmol). The crude product was purified by chromatography on silica (20:1 hexanes:ethyl acetate,  $R_f = 0.7$ ) to yield **60** (0.63 g, 72%) as an oil.

<sup>1</sup>H NMR (500 MHz, CDCl<sub>3</sub>) δ 7.58 (m, 4H), 7.40 (m, 6H), 5.80 (ddt,  $J = 17.1, 10.2, 6.8$  Hz, 1H), 5.60 (ddt,  $J = 17.2, 10.2, 7.2$  Hz, 1H), 3.72 (m, 2H), 3.27 (m, 2H), 2.31 (qt,  $J = 6.7, 1.4$  Hz, 2H), 2.15 (m, 1H), 2.07 (m, 1H), 1.50 (m, 1H), 1.23 (m, 2H).

<sup>13</sup>C NMR (126 MHz, CDCl<sub>3</sub>) δ 135.6, 135.2, 134.7, 134.7, 134.7, 134.7, 130.0, 130.0, 127.9, 127.8, 117.3, 116.6, 63.2, 41.3, 37.1, 34.5, 19.7, 19.5.

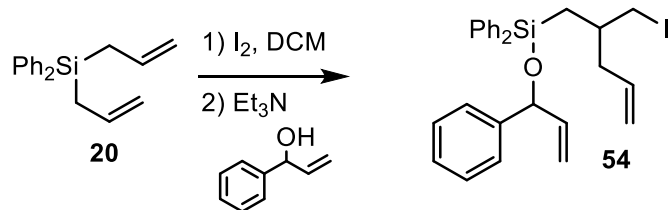
### 1-phenylprop-2-en-1-ol



**1-phenylprop-2-en-1-ol** was prepared by adding benzaldehyde (0.96 mL, 9.4 mmol) into a flame dried flask under nitrogen, followed by tetrahydrofuran (47 mL) and the solution was cooled to 0 °C in an ice bath. Vinyl magnesium bromide, 1.0 M solution in THF, (11.3 mL, 11.3 mmol), was added dropwise and the solution was stirred at 0°C for one hour and then allowed to warm to room temperature for 3-4 hours while stirring. The reaction was quenched using saturated ammonium chloride, extracted with ethyl acetate three times, followed by washing with brine and drying over MgSO<sub>4</sub> and concentrating by rotary evaporation. The crude alcohol was purified by silica gel chromatography using 4:1 hexanes:ethyl acetate solvent to yield product in 39% yield (0.4970 g) as an orange oil.

<sup>1</sup>H NMR (500 MHz, CDCl<sub>3</sub>) δ 7.35 (m, 5H), 6.06 (ddd, J = 17.1, 10.2, 6.0 Hz, 1H), 5.36 (dt, J = 17.1, 1.4 Hz, 1H), 5.21 (m, 2H). NMR matched previously reported data.<sup>89</sup>

**(2-(iodomethyl)pent-4-en-1-yl)diphenyl((1-phenylallyl)oxy)silane (54)**

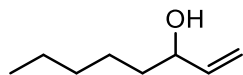


Following general procedure A, the diallyl product was obtained by reacting diallyldiphenyl silane (0.2496 g, 0.9439 mmol) with iodine (0.2407 g, 0.9483 mmol) in dichloromethane (9.5 mL), followed by triethylamine (0.39 mL, 2.8 mmol) and the previously prepared 1-phenylprop-2-en-1-ol alcohol (0.1990 g, 1.476 mmol). The crude product was purified by chromatography on silica (10:1 hexanes:ethyl acetate, R<sub>f</sub> = 0.6) to yield product in 70% yield (0.3458 g) after purification.

<sup>1</sup>H NMR (500 MHz, CDCl<sub>3</sub>) δ 7.42 (m, 10H), 5.94 (m, 1H), 5.50 (m, 1H), 5.18 (m, 2H), 5.02 (m, 2H), 3.15 (m, 2H), 2.00 (m, 2H), 1.44 (m, 1H), 1.21 (m, 2H).

<sup>13</sup>C NMR (126 MHz, CDCl<sub>3</sub>) δ 135.6, 135.5, 134.8, 130.0, 128.3, 127.9, 127.9, 127.8, 127.4, 126.4, 126.4, 117.3, 117.2, 114.2, 114.2, 41.3, 41.0, 34.3, 34.2, 20.2, 20.1, 19.9 19.8.

**1-octene-3-ol**

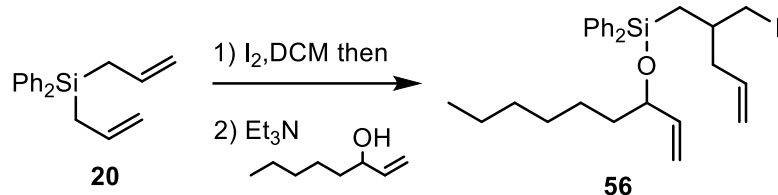


**1-octene-3-ol** was prepared by adding hexanal (1.23 mL, 9.98 mmol) into a flame dried flask under nitrogen, followed by tetrahydrofuran (48 mL) and the solution was cooled to 0 °C in an ice bath. Vinyl magnesium bromide, 1.0 M solution in THF, (12.0 mL, 12.0 mmol), was added dropwise and the solution was stirred at 0°C for one hour and then allowed to warm to room temperature for 3-4 hours while stirring. The reaction was quenched using saturated ammonium chloride, extracted with ethyl acetate three times, followed by washing with brine and drying over MgSO<sub>4</sub> and concentrating by rotary

evaporation. The crude alcohol was purified by silica gel chromatography using 4:1 hexanes:ethyl acetate solvent ( $R_f = 0.4$ ) to yield product in 39% yield (0.5042 g) as a yellow oil.

$^1\text{H NMR}$  (500 MHz,  $\text{CDCl}_3$ )  $\delta$  5.869 (ddd,  $J = 16.9, 10.4, 6.2$  Hz, 1H), 5.218 (dt,  $J = 17.1, 1.4$  Hz, 1H), 5.100 (dt,  $J = 10.4, 1.4$  Hz, 1H), 4.097 (m, 1H), 1.412 (m, 8H), 0.889 (t,  $J = 6.9$  Hz, 3H). NMR data matches that reported previously.<sup>90</sup>

**(2-(iodomethyl)pent-4-en-1-yl)(non-1-en-3-yloxy)diphenylsilane (56)**

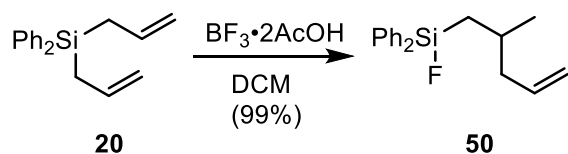


Following general procedure A, the diallyl product was obtained by reacting diallyldiphenyl silane (0.2516 g, 0.9514 mmol) with iodine (0.2406 g, 0.9480 mmol) in dichloromethane (9.5 mL), followed by triethylamine (0.39 mL, 2.8 mmol) and the previously prepared 1-octene-3-ol (0.2426g, 1.892 mmol) to yield product at 76% yield (0.3831 g) as an oil after purification with silica gel chromatography (10:1 hexanes: ethyl acetate,  $R_f = 0.5$ ).

$^1\text{H NMR}$  (500 MHz,  $\text{CDCl}_3$ )  $\delta$  7.61 (dtd,  $J = 9.5, 4.7, 2.4$  Hz, 4H), 7.41 (m, 6H), 5.82 (dddd,  $J = 17.2, 10.4, 6.8, 3.6$  Hz, 1H), 5.61 (ddt,  $J = 17.2, 10.2, 7.2$  Hz, 1H), 5.03 (m, 4H), 4.14 (qd,  $J = 6.7, 2.5$  Hz, 1H), 3.28 (ddd,  $J = 9.5, 7.0, 4.1$  Hz, 1H), 3.20 (dt,  $J = 9.5, 5.5$  Hz, 1H), 2.14 (m, 1H), 2.06 (m, 1H), 1.53 (m, 1H), 1.45 (m, 1H), 1.24 (m, 10H), 0.85 (td,  $J = 7.3, 1.5$  Hz, 3H).

$^{13}\text{C NMR}$  (126 MHz,  $\text{CDCl}_3$ )  $\delta$  140.9, 140.9, 135.7, 135.6, 135.2, 135.0, 134.9, 134.5, 129.9, 128.0, 127.8, 127.8, 127.6, 117.3, 114.7, 75.1, 41.4, 41.1, 37.7, 34.4, 31.7, 24.5, 22.6, 20.1, 19.9, 14.0.

**Fluoro(2-methylpent-4-en-1-yl)diphenylsilane (50).**

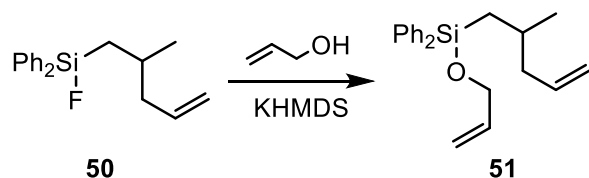


Into a flame dried flask under nitrogen, diallyldiphenyl silane (0.2075 g, 0.7843 mmol) and dry dichloromethane (1.5 M, 0.50 mL). Into a separate flame dried flask under nitrogen,  $\text{BF}_3 \cdot 2\text{AcOH}$  (0.1480 g, 0.7876 mmol) and dichloromethane (1.0 M, 0.76 mL) were added to make a diluted solution, which was added slowly over the course of 10 mins to the flask containing the silane. The solution was stirred at room temperature for 4.5 hours. Reaction was quenched using DI water, extracting with DCM three times, dried over  $\text{MgSO}_4$ , and concentrated by rotary evaporation to give product in 99% yield as an oil. No purification followed.

**<sup>1</sup>H NMR** (500 MHz, CDCl<sub>3</sub>) δ 7.53 (m, 10H), 5.73 (dtd, *J* = 17.2, 10.4, 7.0, 2.6 Hz, 1H), 4.98 (m, 2H), 2.08 (m, 1H), 2.02 (m, 1H), 1.89 (dtd, *J* = 18.2, 9.0, 5.0, 4.0, 2.1 Hz, 1H), 1.37 (dddd, *J* = 18.5, 11.0, 5.6, 3.1 Hz, 1H), 1.11 (dddd, *J* = 15.6, 9.1, 6.6, 2.9 Hz, 1H), 0.96 (dd, *J* = 6.8, 2.7 Hz, 3H).

**<sup>13</sup>C NMR** (126 MHz, CDCl<sub>3</sub>) δ 137.1, 134.5, 134.0, 132.1, 130.5, 128.3, 128.0, 116.2, 44.5, 28.5, 22.5, 21.9, 21.8.

#### (allyloxy)(2-methylpent-4-en-1-yl)diphenylsilane (51)

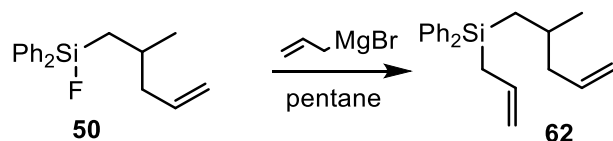


Into a flame dried flask under nitrogen, allyl alcohol (0.02 mL, 0.25 mmol) and tetrahydrofuran (0.88 mL) were added and cooled to 0 °C. Potassium bis(trimethylsilyl)amide (KHMDS) (0.50 mL, 0.5 M solution in toluene) was added and then stirred at 0 °C for 30 mins, after which the fluorosilane (0.0496 g, 0.1744 mmol) was added. The solution was allowed to warm to room temperature overnight. The reaction was quenched with deionized water, extracted with methyl tert-butyl ether three times, dried over MgSO<sub>4</sub>, and concentrated by rotary evaporation. The crude mixture was purified with silica gel column chromatography using 10:1 hexanes: ethyl acetate solvent system (*R*<sub>f</sub>=0.3) to yield the product in 83% yield (0.0562 g) as an oil.

**<sup>1</sup>H NMR** (500 MHz, CDCl<sub>3</sub>) δ 7.62 (dt, *J* = 8.0, 1.7 Hz, 4H), 7.41 (m, 6H), 5.94 (ddt, *J* = 17.1, 10.4, 4.6 Hz, 1H), 5.73 (ddt, *J* = 17.2, 10.2, 7.1 Hz, 1H), 5.35 (dq, *J* = 17.0, 1.9 Hz, 1H), 5.13 (dq, *J* = 10.4, 1.7 Hz, 1H), 4.97 (m, 2H), 4.23 (dt, *J* = 4.6, 1.7 Hz, 2H), 2.08 (m, 1H), 1.97 (dtt, *J* = 13.6, 6.9, 1.1 Hz, 1H), 1.82 (m, 1H), 1.34 (dd, *J* = 15.2, 5.0 Hz, 1H), 1.08 (dd, *J* = 15.2, 8.7 Hz, 1H), 0.93 (d, *J* = 6.7 Hz, 3H).

**<sup>13</sup>C NMR** (126 MHz, CDCl<sub>3</sub>) δ 137.5, 136.8, 135.4, 135.3, 134.7, 129.8, 127.8, 115.9, 114.4, 64.3, 44.7, 28.7, 22.6, 21.5.

#### allyl(2-methylpent-4-en-1-yl)diphenylsilane (62)



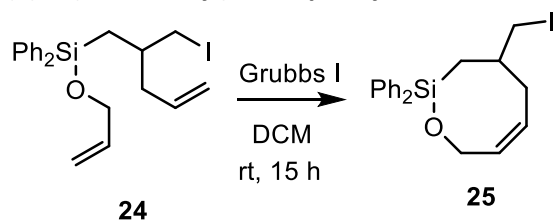
Into a flame dried flask under nitrogen, the fluorosilane (0.0551 g, 0.1937 mmol) and pentanes (0.35 mL) were added and cooled to -78 °C. Allylmagnesium bromide (0.21 mL, 1.0 M solution in ether) was added dropwise and then stirred at 0 °C for 2 hours, after which it was allowed to warm to room temperature overnight. The reaction mixture was diluted in hexanes and then quenched in ammonium chloride and extracted with hexanes three times, dried over MgSO<sub>4</sub>, and concentrated by rotary evaporation. The

crude mixture was purified by silica gel column chromatography using 10:1 hexanes:MTBE solvent system ( $R_f=0.5$ ) to yield the product in 68% yield (0.0405 g) as an oil.

$^1\text{H NMR}$  (500 MHz,  $\text{CDCl}_3$ )  $\delta$  7.537 (m, 4H), 7.391 (m, 6H), 5.772 (m, 2H), 4.933 (m, 4H), 2.159 (ddd,  $J = 6.7, 3.0, 1.5$  Hz, 2H), 2.031 (dddt,  $J = 12.9, 7.1, 5.7, 1.3$  Hz, 1H), 1.926 (m, 1H), 1.781 (dddd,  $J = 13.9, 12.3, 7.1, 4.3$  Hz, 1H), 1.295 (dd,  $J = 15.0, 5.0$  Hz, 1H), 1.012 (m, 1H), 0.850 (d,  $J = 6.6$  Hz, 2H).

$^{13}\text{C NMR}$  (126 MHz,  $\text{CDCl}_3$ )  $\delta$  137.44, 135.00, 134.09, 133.73, 129.47, 129.22, 127.74, 115.89, 114.73, 114.49, 44.91, 29.14, 22.76, 21.31, 20.02, 19.86.

**(Z)-4-(iodomethyl)-2,2-diphenyl-3,4,5,6-tetrahydro-2H-1,2-oxasilocine**

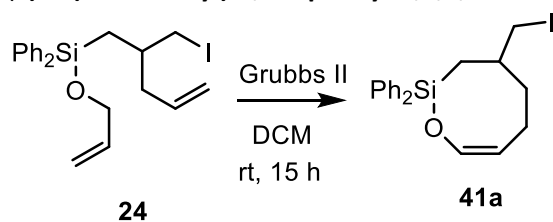


Following general procedure B, diallyl silane **24** (3.0028 g, 6.6996 mmol) was added to dichloromethane (335 mL), degassed, followed by the addition of first-generation Grubbs catalyst (0.2752 g, 0.3344 mmol). The product was obtained at 74% (2.0960 g) yield as an oil after purification on silica gel chromatography using 2:1 hexanes:DCM ( $R_f=0.3$ ).

$^1\text{H NMR}$  (500 MHz,  $\text{CDCl}_3$ )  $\delta$  7.61 (m, 2H), 7.55 (m, 2H), 7.38 (m, 6H), 5.79 (dt,  $J = 11.2, 4.7$  Hz, 1H), 5.60 (dddt,  $J = 11.3, 9.8, 8.2, 1.6$  Hz, 1H), 4.55 (dd,  $J = 15.5, 4.5$  Hz, 1H), 4.48 (dd,  $J = 15.6, 5.2$  Hz, 1H), 3.18 (d,  $J = 7.7$  Hz, 2H), 2.84 (ddd,  $J = 13.7, 9.6, 4.3$  Hz, 1H), 2.39 (ddd,  $J = 13.5, 8.3, 5.5$  Hz, 1H), 2.17 (ddtd,  $J = 11.3, 9.7, 7.1, 4.3$  Hz, 1H), 1.58 (ddd,  $J = 14.9, 4.3, 1.0$  Hz, 1H), 1.23 (dd,  $J = 14.9, 10.9$  Hz, 1H).

$^{13}\text{C NMR}$  (126 MHz,  $\text{CDCl}_3$ )  $\delta$  135.7, 134.9, 134.1, 131.8, 130.0, 128.0, 127.3, 62.2, 37.4, 31.8, 19.4, 16.9.

**(Z)-4-(iodomethyl)-2,2-diphenyl-3,4,5,6-tetrahydro-2H-1,2-oxasilocine (41a)**

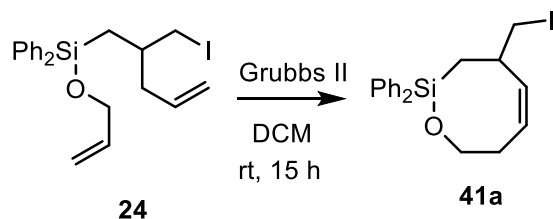


Following general procedure B, diallyl silane **24** (1.9999 g, 4.4601 mmol) was added to dichloromethane (323 mL), degassed, followed by the addition of second-generation Grubbs catalyst (0.1898 g, 0.2236 mmol). The product was obtained at 56% (1.0413 g) yield as an oil after purification on silica gel chromatography using 2:1 hexanes:DCM ( $R_f=0.5$ ).

$^1\text{H NMR}$  (500 MHz,  $\text{CDCl}_3$ )  $\delta$  7.70 (dd,  $J = 7.6, 1.6$  Hz, 2H), 7.60 (m, 2H), 6.49 (d,  $J = 5.8$  Hz, 1H), 4.84 (ddd,  $J = 9.8, 7.3, 5.8$  Hz, 1H), 3.30 (dd,  $J = 9.5, 5.6$  Hz, 1H), 3.25 (dd,  $J = 9.5, 5.3$  Hz, 1H), 2.56 (tdd,  $J = 13.3, 9.8, 3.7$  Hz, 1H), 2.05 (m, 1H), 1.94 (m, 1H), 1.77 (tt,  $J = 12.9, 3.7$  Hz, 1H), 1.35 (m, 3H).

$^{13}\text{C NMR}$  (126 MHz,  $\text{CDCl}_3$ )  $\delta$  141.4, 134.5, 133.9, 130.2, 130.2, 128.2, 127.9, 112.8, 36.1, 33.7, 21.5, 21.2, 20.9.

**(Z)-4-(iodomethyl)-2,2-diphenyl-3,4,7,8-tetrahydro-2H-1,2-oxasilocine (41b)**

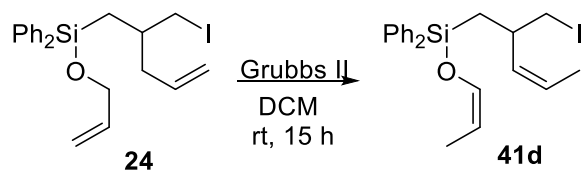


Following general procedure B, diallyl silane **24** (1.9999 g, 4.4601 mmol) ) was added to dichloromethane (323 mL), degassed, followed by the addition of second-generation Grubbs catalyst (0.1898 g, 0.2236 mmol). The product was obtained at 12% (0.2242 g) yield after purification on silica gel chromatography using 2:1 hexanes:DCM ( $R_f=0.3$ ).

$^1\text{H NMR}$  (500 MHz,  $\text{CDCl}_3$ )  $\delta$  7.60 (m, 2H), 7.51 (m, 2H), 7.37 (m, 6H), 5.57 (m, 2H), 4.15 (dt,  $J = 11.0, 3.4$  Hz, 1H), 3.71 (ddd,  $J = 12.6, 11.1, 1.8$  Hz, 1H), 3.34 (dd,  $J = 9.5, 5.3$  Hz, 1H), 3.28 (dd,  $J = 9.5, 7.6$  Hz, 1H), 3.15 (m, 1H), 2.52 (m, 1H), 2.03 (m, 1H), 1.61 (dd,  $J = 14.7, 2.6$  Hz, 1H), 1.43 (dd,  $J = 14.7, 12.7$  Hz, 1H).

$^{13}\text{C NMR}$  (126 MHz,  $\text{CDCl}_3$ )  $\delta$  137.2, 134.8, 134.0, 129.8, 129.7, 128.1, 127.8, 127.4, 64.7, 35.9, 31.6, 25.5, 16.7.

**((Z)-2-(iodomethyl)pent-3-en-1-yl)diphenyl(((Z)-prop-1-en-1-yl)oxy)silane (41d)**

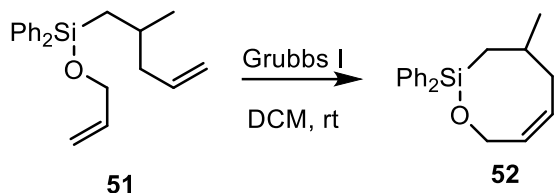


Following general procedure B, diallyl silane **24** (1.9999 g, 4.4601 mmol) ) was added to dichloromethane (323 mL), degassed, followed by the addition of second-generation Grubbs catalyst (0.1898 g, 0.2236 mmol). The product was obtained at 11% (0.2143 g) yield after purification on silica gel chromatography using 2:1 hexanes:DCM ( $R_f=0.6$ ).

$^1\text{H NMR}$  (500 MHz,  $\text{CDCl}_3$ )  $\delta$  7.58 (ddt,  $J = 8.0, 4.2, 1.6$  Hz, 5H), 7.40 (m, 7H), 6.18 (dp,  $J = 5.5, 1.6$  Hz, 1H), 5.29 (m, 1H), 5.13 (m, 1H), 4.55 (p,  $J = 6.6$  Hz, 1H), 3.20 (m, 2H), 2.42 (m, 1H), 1.68 (dd,  $J = 6.7, 1.8$  Hz, 3H), 1.49 (dd,  $J = 6.4, 1.6$  Hz, 3H).

<sup>13</sup>C NMR (126 MHz, CDCl<sub>3</sub>) δ 137.2, 134.8, 134.0, 129.8, 129.7, 128.1, 127.8, 127.4, 64.7, 35.9, 31.6, 25.5, 16.7.

**(Z)-4-methyl-2,2-diphenyl-3,4,5,8-tetrahydro-2H-1,2-oxasilocine (52)**

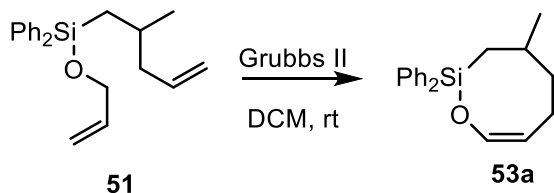


Following general procedure B, diallyl silane **51** (0.0524 g, 0.1625 mmol) was added to dichloromethane (7.8 mL), degassed, followed by the addition of first-generation Grubbs catalyst (0.0092 g, 0.0112 mmol). The product was obtained at 84% (0.0402 g) yield as an oil after purification on silica gel chromatography using 10:1 hexanes:ethyl acetate ( $R_f=0.5$ ).

<sup>1</sup>H NMR (500 MHz, CDCl<sub>3</sub>) δ 7.65 (dd,  $J = 7.4, 1.8$  Hz, 2H), 7.57 (dd,  $J = 7.6, 1.5$  Hz, 2H), 7.39 (dddd,  $J = 18.6, 9.4, 4.4, 2.8$  Hz, 6H), 5.79 (dt,  $J = 10.7, 5.2$  Hz, 1H), 5.71 (dt,  $J = 11.1, 8.6$  Hz, 1H), 4.52 (qd,  $J = 14.8, 5.1$  Hz, 2H), 2.67 (m, 1H), 2.13 (m, 2H), 1.41 (dd,  $J = 15.2, 4.0$  Hz, 1H), 1.20 (dd,  $J = 15.2, 10.1$  Hz, 1H), 1.07 (d,  $J = 6.3$  Hz, 3H).

<sup>13</sup>C NMR (126 MHz, CDCl<sub>3</sub>) δ 134.4, 134.2, 134.0, 130.6, 130.5, 130.0, 129.6, 129.6, 128.1, 128.1, 127.9, 127.8, 116.3, 61.6, 34.6, 29.5, 25.2, 21.6.

**(Z)-4-methyl-2,2-diphenyl-3,4,5,6-tetrahydro-2H-1,2-oxasilocine (53a)**

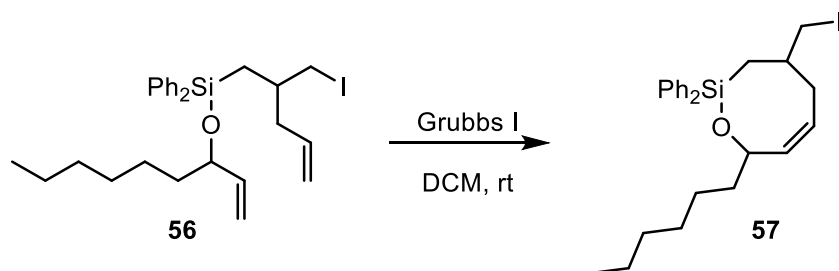


Following general procedure B, diallyl silane **51** (0.0719 g, 0.02230 mmol) was added to dichloromethane (10.9 mL), degassed, followed by the addition of second-generation Grubbs catalyst (0.0099 g, 0.0117 mmol) and heated at 45 °C overnight. The product was obtained at 74% (0.0486 g) yield as an oil after purification on silica gel chromatography using 2:1 hexanes:DCM ( $R_f=0.4$ ).

<sup>1</sup>H NMR (500 MHz, CDCl<sub>3</sub>) δ 7.66 (m, 2H), 7.57 (dt,  $J = 6.5, 1.6$  Hz, 2H), 7.38 (m, 6H), 6.44 (d,  $J = 5.8$  Hz, 1H), 4.78 (ddd,  $J = 9.9, 7.2, 5.8$  Hz, 1H), 2.55 (tdd,  $J = 13.2, 9.5, 3.6$  Hz, 1H), 2.03 (m, 1H), 1.97 (ddq,  $J = 14.3, 7.7, 4.2, 3.5$  Hz, 1H), 1.60 (tt,  $J = 13.0, 3.9$  Hz, 1H), 1.22 (m, 3H), 1.06 (d,  $J = 6.6$  Hz, 3H).

<sup>13</sup>C NMR (126 MHz, CDCl<sub>3</sub>) δ 141.1, 134.5, 133.9, 129.9, 128.1, 127.9, 113.2, 38.1, 27.1, 26.6, 21.9, 21.7.

**(Z)-8-hexyl-4-(iodomethyl)-2,2-diphenyl-3,4,5,8-tetrahydro-2H-1,2-oxasilocine (57)**



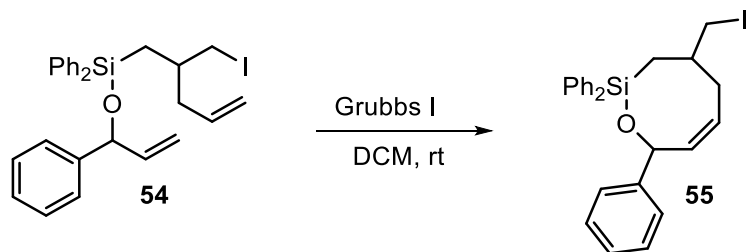
Following general procedure B, diallyl silane **51** (0.1401 g, 0.2631 mmol) was added to dichloromethane (13.2 mL), degassed, followed by the addition of first-generation Grubbs catalyst (0.0218 g, 0.0265 mmol) at room temperature. The product was obtained at 88% (0.1240 g) yield as an oil after purification using an automated column on silica gel ( $R_f=0.5$  in 2:1 hexanes:DCM).

*Spectral data for the mixture of diastereomers:*

$^1\text{H NMR}$  (500 MHz,  $\text{CDCl}_3$ )  $\delta$  7.58 (tt,  $J = 7.9, 1.9$  Hz, 6H), 7.52 (m, 2H), 7.36 (m, 12H), 5.78 (dd,  $J = 11.0, 6.2$  Hz, 1H), 5.60 (ddd,  $J = 16.9, 11.0, 6.7$  Hz, 2H), 5.44 (dt,  $J = 11.2, 8.9$  Hz, 1H), 4.57 (dq,  $J = 12.8, 6.2$  Hz, 2H), 3.23 (qd,  $J = 9.5, 6.7$  Hz, 2H), 3.10 (m, 2H), 2.79 (ddd,  $J = 12.8, 8.9, 3.5$  Hz, 1H), 2.54 (dt,  $J = 13.1, 6.6$  Hz, 1H), 2.46 (m, 1H), 2.40 (m, 1H), 2.24 (ddd,  $J = 13.2, 8.8, 6.4$  Hz, 1H), 1.97 (m, 1H), 1.74 (m, 2H), 1.61 (m, 3H), 1.29 (m, 12H), 0.89 (td,  $J = 7.0, 2.9$  Hz, 6H).

$^{13}\text{C NMR}$  (126 MHz,  $\text{CDCl}_3$ )  $\delta$  136.7, 136.3, 134.2, 134.0, 133.9, 129.9, 129.7, 129.6, 129.5, 128.2, 127.8, 127.8, 127.6, 71.2, 69.5, 38.4, 38.0, 37.7, 37.1, 32.6, 32.3, 31.8, 25.3, 25.2, 22.7, 20.6, 19.5, 18.5, 15.6, 14.1.

**(Z)-4-(iodomethyl)-2,2,8-triphenyl-3,4,5,8-tetrahydro-2H-1,2-oxasilocine (55)**



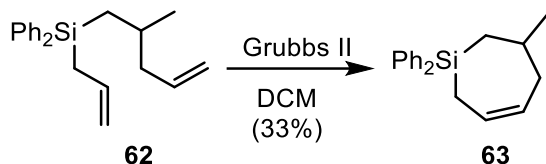
Following general procedure B, diallyl silane **54** (0.0801 g, 0.1527 mmol) was reacted with the first-generation Grubbs catalyst (0.0118 g, 0.0143 mmol) dichloromethane (7.0 mL). The product was obtained at 57% (0.0436 g) yield as an oil after purification in 2:1 hexanes:DCM solvent system ( $R_f=0.5$ ).

*Spectral data for the mixture of diastereomers:*

$^1\text{H NMR}$  (500 MHz,  $\text{CDCl}_3$ )  $\delta$  7.63 (m, 9H), 7.41 (m, 24H), 6.00 (dd,  $J = 10.8, 6.8$  Hz, 1H), 5.76 (m, 5H), 5.56 (ddd,  $J = 11.2, 9.6, 8.3$  Hz, 1H), 3.31 (qd,  $J = 9.6, 6.7$  Hz, 3H), 3.17 (dd,  $J = 7.5, 1.9$  Hz, 2H), 2.91 (ddd,  $J = 12.8, 9.0, 3.4$  Hz, 1H), 2.67 (dt,  $J = 13.3, 6.4$  Hz, 1H), 2.59 (m, 1H), 2.51 (m, 1H), 2.40 (ddd,  $J = 13.2, 9.0, 6.8$  Hz, 1H), 2.07 (dtp,  $J = 16.5, 6.7, 3.8, 3.4$  Hz, 1H), 1.74 (dd,  $J = 15.1, 5.3$  Hz, 1H), 1.65 (dd,  $J = 15.1, 3.4$  Hz, 2H), 1.31 (m, 6H), 0.90 (t,  $J = 6.8$  Hz, 2H).

$^{13}\text{C}$  NMR (126 MHz,  $\text{CDCl}_3$ )  $\delta$  143.8, 143.3, 136.5, 135.7, 134.7, 134.2, 134.1, 134.0, 133.9, 130.2, 129.9, 129.8, 129.7, 128.8, 128.4, 128.0, 127.9, 127.9, 127.2, 127.1, 125.9, 125.8, 72.6, 70.6, 38.5, 37.1, 32.9, 32.2, 20.9, 19.9, 18.5, 15.4.

### 3-methyl-1,1-diphenyl-2,3,4,7-tetrahydro-1H-silepine (63)

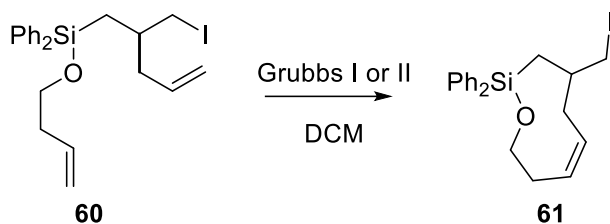


Following general procedure B, diallyl silane **62** (0.0658 g, 0.2147 mmol) was reacted with the second-generation Grubbs catalyst (0.0179 g, 0.0211 mmol) in dichloromethane (9.4 mL). The product was obtained at 33% (0.0195 g) yield as an oil after purification in 4:1 hexanes: dichloromethane solvent system ( $R_f=0.2$ ).

$^1\text{H}$  NMR (500 MHz,  $\text{CDCl}_3$ )  $\delta$  7.56 (m, 2H), 7.45 (dq,  $J = 6.7, 2.4$  Hz, 2H), 7.35 (m, 6H), 5.78 (m, 1H), 5.63 (dtd,  $J = 10.2, 7.8, 1.9$  Hz, 1H), 2.23 (ddd,  $J = 14.5, 6.7, 2.0$  Hz, 1H), 2.16 (tdd,  $J = 9.1, 7.7, 3.9$  Hz, 1H), 2.09 (ddd,  $J = 7.9, 4.0, 2.1$  Hz, 1H), 2.03 (ddd,  $J = 14.5, 8.1, 1.5$  Hz, 1H), 1.95 (m, 1H), 1.58 (ddt,  $J = 14.7, 3.3, 1.5$  Hz, 1H), 1.11 (dd,  $J = 14.8, 11.2$  Hz, 1H), 1.05 (d,  $J = 6.6$  Hz, 3H).

$^{13}\text{C}$  NMR (126 MHz,  $\text{CDCl}_3$ )  $\delta$  134.8, 134.2, 129.2, 129.1, 128.7, 127.8, 127.8, 127.1, 36.7, 29.6, 27.8, 25.4, 13.7.

### (Z)-4-(iodomethyl)-2,2-diphenyl-2,3,4,5,8,9-hexahydro-1,2-oxasilonine (61)

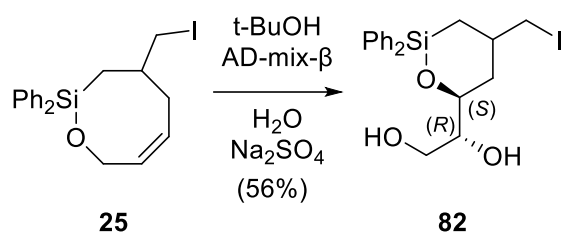


Following general procedure B, diallyl silane **60** (60 mg, 0.13 mmol) was reacted with the second-generation Grubbs catalyst (11 mg, 0.013 mmol) in dichloromethane (5 mL). The crude product was purified by chromatography on silica (20:1 hexanes:ethyl acetate) to give **61** (35 mg, 62%) as an oil.

$^1\text{H}$  NMR (500 MHz,  $\text{CDCl}_3$ )  $\delta$  7.57 (td,  $J = 7.5, 1.6$  Hz, 4H), 7.37 (m, 6H), 5.75 (m, 1H), 5.55 (td,  $J = 10.6, 6.2$  Hz, 1H), 3.89 (ddd,  $J = 10.9, 6.6, 2.0$  Hz, 1H), 3.68 (ddd,  $J = 10.7, 8.8, 1.5$  Hz, 1H), 3.20 (m, 2H), 2.79 (ddd,  $J = 14.3, 10.3, 4.8$  Hz, 1H), 2.48 (dt,  $J = 15.9, 8.4$  Hz, 1H), 2.39 (dt,  $J = 12.6, 5.6$  Hz, 1H), 2.25 (dt,  $J = 14.7, 7.5$  Hz, 1H), 2.18 (m, 1H), 1.44 (ddd,  $J = 14.7, 3.2, 1.1$  Hz, 1H), 1.22 (dd,  $J = 14.7, 10.8$  Hz, 1H).

$^{13}\text{C}$  NMR (126 MHz,  $\text{CDCl}_3$ )  $\delta$  134.4, 129.9, 129.8, 129.2, 127.9, 127.9, 64.2, 36.8, 32.2, 30.1, 19.2, 17.2.

**(1R)-1-((6S)-4-(iodomethyl)-2,2-diphenyl-1,2-oxasilinan-6-yl)ethane-1,2-diol (82)**



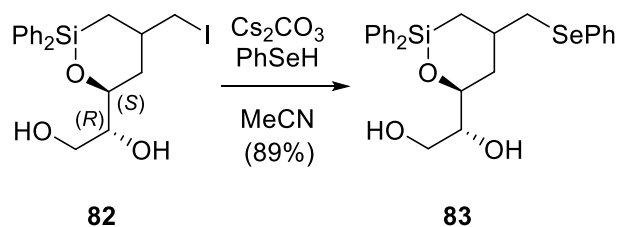
Into a round bottom flask, to a stirring solution of tert-butyl alcohol (4.47 mL) and deionized water (4.47 mL), AD-mix- $\beta$  (1.2539 g, 1.609 mmol) was added and stirred at room temperature until the solution became transparent. At 0 °C, product **25** (0.3757 g, 0.8937 mmol) was added and the solution was allowed to warm to room temperature and stirred for 70 hours. The solution was cooled to 0 °C again and sodium sulfate was added and stirred for 4 hours. After filtering over celite, the mixture was extracted with dichloromethane three times, dried over  $\text{MgSO}_4$ , and concentrated by rotary evaporation. After purifying using silica gel column chromatography with 1:2 hexanes: ethyl acetate solvent system ( $R_f=0.4$ ), the product was obtained as a mixture of diastereomers at 56% yield as an oil.

*Spectral data for the mixture of diastereomers:*

$^1\text{H NMR}$  (500 MHz,  $\text{CDCl}_3$ )  $\delta$  7.63 (dd,  $J = 7.8, 1.4$  Hz, 2H), 7.60 (dd,  $J = 8.0, 1.4$  Hz, 2H), 7.53 (m, 2H), 7.50 (m, 2H), 7.47 – 7.33 (m, 12H), 4.15 (ddd,  $J = 10.7, 6.9, 4.1$  Hz, 1H), 4.12 (dd,  $J = 14.2, 7.1$  Hz, 1H), 4.03 (ddd,  $J = 11.3, 5.2, 1.8$  Hz, 1H) 3.89 – 3.74 (m, 4H), 3.70 – 3.59 (m, 2H), 3.28 (dd,  $J = 9.7, 5.5$  Hz, 1H), 3.24 – 3.16 (m, 2H), 2.64 (bs, 1H), 2.48 (bs, 1H), 2.40 (m, 1H), 2.28 (bs, 1H), 2.12 (m, 1H), 2.08 (m, 1H), 1.91 (m, 1H), 1.80 (ddd,  $J = 14.3, 7.9, 4.0$  Hz, 1H), 1.57 – 1.50 (m, 2H), 1.30 (m, 1H), 1.26 (m, 1H), 1.18 (dd,  $J = 15.0, 8.5$  Hz, 1H), 0.86 (dd,  $J = 14.4, 13.0$  Hz, 1H).

$^{13}\text{C NMR}$  (126 MHz,  $\text{CDCl}_3$ )  $\delta$  135.26, 135.23, 134.30, 134.24, 134.22, 134.18, 134.11, 134.00, 133.24, 130.59, 130.45, 130.44, 130.36, 128.41, 128.23, 128.20, 128.18, 128.09, 76.12, 74.53, 73.62, 72.24, 63.75, 63.48, 37.81, 36.56, 35.22, 33.52, 18.85, 18.52, 17.08, 16.06.

**(1R)-1-((6S)-2,2-diphenyl-4-((phenylselanyl)methyl)-1,2-oxasilinan-6-yl)ethane-1,2-diol (83)**



Into a flame dried flask under nitrogen, the dihydroxylation product **82** (0.8479 g, 1.8661 mmol) was added, followed by acetonitrile (9.33 mL) and cesium carbonate (0.9149 g, 2.808 mmol). While the solution is stirring, benzeneselenol (0.28 mL, 2.6 mmol) was added dropwise via syringe. After stirring at room temperature for 1 hour, the reaction was quenched with ammonium chloride, extracted with methyl tert-butyl ether three times, washed with 15% sodium hydroxide solution, dried over  $\text{MgSO}_4$ ,

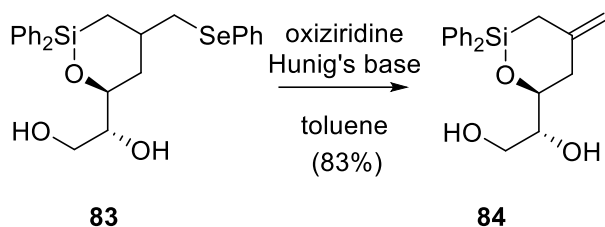
and concentrated rotary evaporation. The crude mixture was purified by silica gel column chromatography using 1:2 hexanes: ethyl acetate solvent system ( $R_f = 0.3$ ) to yield the product in 89% yield (0.8021 g) as an oil.

*Spectral data for the mixture of diastereomers:*

$^1\text{H NMR}$  (500 MHz,  $\text{CDCl}_3$ )  $\delta$  7.61 (dd,  $J = 7.7, 1.5$  Hz, 2H), 7.57 (dd,  $J = 7.6, 1.5$  Hz, 2H), 7.50 – 7.46 (m, 6H), 7.45 – 7.37 (m, 12H), 7.36 – 7.32 (m, 4H), 7.25 – 7.21 (m, 4H), 4.15 (m, 1H), 4.12 (dd,  $J = 14.1, 7.2$  Hz, 1H), 3.97 (ddd,  $J = 11.4, 5.1, 1.7$  Hz, 1H), 3.84 – 3.74 (m, 4H), 3.63 (q,  $J = 5.4$  Hz, 1H), 3.55 (p,  $J = 5.8$  Hz, 1H), 3.00 (dd,  $J = 12.2, 6.5$  Hz, 1H), 2.93 (dd,  $J = 12.0, 6.5$  Hz, 1H), 2.90 (dd,  $J = 7.5, 5.2$  Hz, 1H), 2.52 (d,  $J = 7.0$  Hz, 1H), 2.43 (m, 1H), 2.35 (d,  $J = 6.6$  Hz, 1H), 2.20 (dd,  $J = 7.7, 4.2$  Hz, 1H), 2.08 – 1.96 (m, 2H), 1.81 (ddd,  $J = 14.3, 6.9, 3.4$  Hz, 1H), 1.63 (dt,  $J = 14.3, 2.7$  Hz, 1H), 1.50 (dd,  $J = 15.0, 5.3$  Hz, 1H), 1.37 – 1.23 (m, 3H), 0.90 – 0.78 (m, 2H).

$^{13}\text{C NMR}$  (126 MHz,  $\text{CDCl}_3$ )  $\delta$  134.28, 134.18, 134.12, 133.94, 132.91, 132.77, 130.46, 130.31, 130.27, 130.20, 129.11, 128.28, 128.23, 128.08, 128.04, 126.99, 126.96, 76.44, 74.47, 73.84, 72.27, 63.68, 63.49, 60.41, 39.38, 37.74, 35.62, 34.94, 31.28, 21.07, 18.12, 16.50, 14.22.

**(1R)-1-((6S)-2,2-diphenyl-4-((phenylselenanyl)methyl)-1,2-oxasilinan-6-yl)ethane-1,2-diol (**84**)**

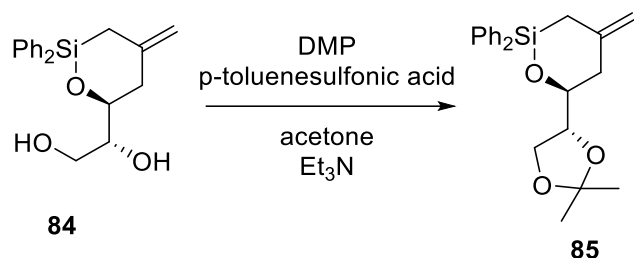


Into a flame dried flask under nitrogen, the selenium product **83** (0.8021 g, 1.6588 mmol) was added, followed by toluene (5.92 mL) and Hunig's base (1.44 mL, 8.29 mmol). 3-phenyl-2-(phenylsulfonyl)-1,2-oxiziridine (0.4773 g, 1.827 mmol) was added in three portion-wise every 10 mins. After the last addition, the solution was stirred at room temperature for 10 mins, after which it was heated to 100 °C for 5 hours and then allowed to cool to room temperature overnight. The reaction was quenched with saturated sodium bicarbonate, extracted with methyl tert-butyl ether three times, dried over  $\text{MgSO}_4$ , and concentrated by rotary evaporation. The crude mixture was purified by silica gel chromatography using 1:1 hexanes: ethyl acetate solvent system ( $R_f = 0.3$ ) to yield the product in 83% yield (0.4486 g) as a bright yellow solid.

$^1\text{H NMR}$  (500 MHz,  $\text{CDCl}_3$ )  $\delta$  7.65 (m, 2H), 7.56 (m, 2H), 7.43 (m, 6H), 4.83 (dt,  $J = 5.5, 1.8$  Hz, 2H), 4.02 (ddd,  $J = 11.0, 5.3, 2.4$  Hz, 1H), 3.84 (m, 2H), 3.71 (m, 1H), 2.50 (dt,  $J = 13.0, 2.2$  Hz, 2H), 2.34 (dd,  $J = 14.0, 1.8$  Hz, 1H), 2.29 (d,  $J = 12.2$  Hz, 1H), 2.09 (dt,  $J = 13.8, 2.3$  Hz, 1H).

$^{13}\text{C NMR}$  (126 MHz,  $\text{CDCl}_3$ )  $\delta$  142.8, 134.4, 134.2, 133.3, 130.5, 130.3, 128.1, 111.2, 77.5, 74.4, 63.5, 60.4, 40.6, 24.2, 21.1, 14.2.

**(S)-6-((R)-2,2-dimethyl-1,3-dioxolan-4-yl)-4-methylene-2,2-diphenyl-1,2-oxasilinane (85)**

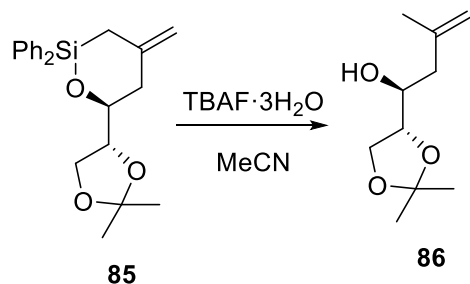


Into a flame dried flask under nitrogen, product **84** (0.0487 g, 0.149 mmol) was added, followed by reagent grade acetone (0.77 mL), 2,2-dimethoxypropane (0.08 mL (0.6 mmol)), and p-toluenesulfonic acid (0.0030 g, 0.017 mmol). After stirring for 1 hour at room temperature, triethylamine (0.05 mL) was added and the solution was concentrated by rotary evaporation. The crude product was purified by silica gel column chromatography using 4:1 hexanes: ethyl acetate solvent system ( $R_f=0.6$ ) to yield the product in 82% yield (0.0446 g) as a yellow solid.

**<sup>1</sup>H NMR** (500 MHz, CDCl<sub>3</sub>)  $\delta$  7.63 (m, 2H), 7.56 (m, 2H), 7.42 (m, 6H), 4.83 (d,  $J = 1.8$  Hz, 2H), 4.13 (m, 1H), 4.03 (m, 2H), 3.82 (ddd,  $J = 10.3, 7.8, 2.7$  Hz, 1H), 2.67 (ddd,  $J = 13.2, 2.7, 1.6$  Hz, 1H), 2.32 (dd,  $J = 13.9, 1.7$  Hz, 1H), 2.20 (dd,  $J = 13.1, 10.0$  Hz, 1H), 2.10 (dt,  $J = 13.8, 2.0$  Hz, 1H), 1.41 (s, 3H), 1.37 (s, 3H).

**<sup>13</sup>C NMR** (126 MHz, CDCl<sub>3</sub>)  $\delta$  142.7, 135.0, 134.4, 134.0, 130.3, 128.0, 110.9, 109.5, 79.1, 67.7, 41.8, 26.8, 25.4, 24.3.

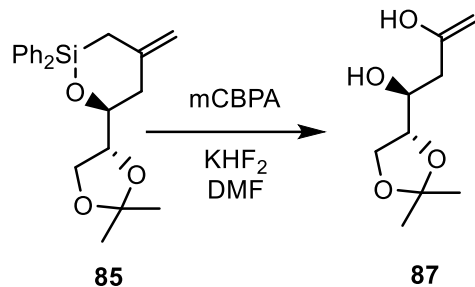
**(S)-1-((R)-2,2-dimethyl-1,3-dioxolan-4-yl)-3-methylbut-3-en-1-ol (86)**



Into a flame dried flask under nitrogen, acetal product **85** (0.0446 g, 0.122 mmol), and acetonitrile (1.22 mL) were added. While stirring, tetrabutylammonium fluoride trihydrate (0.2315 g, 0.7337 mmol) was added and heated at 65 °C for one hour. The reaction was quenched with saturated ammonium chloride, extracted with ethyl acetate three times, dried over MgSO<sub>4</sub>, and concentrated by rotary evaporation. The crude product was purified by silica gel column chromatography using 2:1 hexanes: ethyl acetate solvent system ( $R_f=0.3$ ) and the product was obtained at 59% yield (0.0133 g) as a colorless oil.  $[\alpha]_D = -0.52$  (DCM,  $c = 0.39$ )

**<sup>1</sup>H NMR** (500 MHz, CDCl<sub>3</sub>)  $\delta$  4.89 (p,  $J = 1.6$  Hz, 1H), 4.81 (dq,  $J = 2.1, 0.9$  Hz, 1H), 4.00 (m, 3H), 3.85 (dtd,  $J = 9.1, 4.4, 2.1$  Hz, 1H), 2.30 (ddd,  $J = 14.0, 4.0, 1.3$  Hz, 1H), 2.11 (ddd,  $J = 14.0, 9.4, 0.9$  Hz, 1H), 1.99 (d,  $J = 2.4$  Hz, 1H), 1.78 (t,  $J = 1.1$  Hz, 3H), 1.43 (s, 3H), 1.36 (s, 3H). NMR data matches previously reported data.<sup>91</sup>

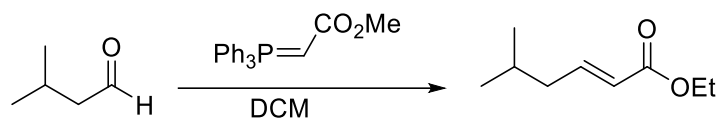
**(S)-1-((R)-2,2-dimethyl-1,3-dioxolan-4-yl)but-3-ene-1,3-diol (87)**



Into a flame dried flask under nitrogen, acetal product **85** (0.1068 g, 0.2914 mmol) was added, followed by dimethylformamide (1.46 mL). While stirring, potassium bifluoride (0.0458 g, 0.0586 mmol) was added, followed by meta-chloroperoxybenzoic acid (0.1260 g, 0.7301 mmol). After stirring at room temperature for 3 hours, the reaction was quenched using saturated sodium bicarbonate, extracted with ethyl acetate three times, dried over MgSO<sub>4</sub>, and concentrated by rotary evaporation. The crude product was purified by silica gel column chromatography using 4:1 hexanes: ethyl acetate solvent system ( $R_f=0.1$ ) to yield the purified product in 44% yield (0.0260 g) as an oil.

<sup>1</sup>H NMR (500 MHz, CDCl<sub>3</sub>)  $\delta$  5.12 (s, 1H), 4.99 (s, 1H), 4.08 (m, 2H), 4.00 (m, 2H), 3.91 (m, 1H), 3.78 (ddd,  $J = 9.3, 5.2, 3.1$  Hz, 1H), 2.43 (ddd,  $J = 14.3, 3.1, 1.1$  Hz, 1H), 2.14 (ddd,  $J = 14.3, 9.3, 1.0$  Hz, 1H), 1.40 (s, 3H), 1.33 (s, 3H). NMR data matches previously reported data.<sup>92</sup>

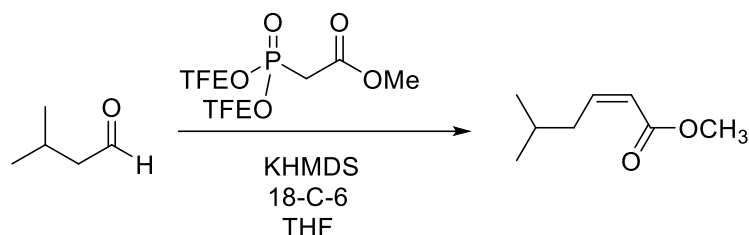
**ethyl (E)-5-methylhex-2-enoate (90)**



Into a flame dried flask under nitrogen, isovaleraldehyde (0.5 mL, 4.6 mmol) and dichloromethane (23 mL) were added, followed by (carbethoxymethylene)triphenylphosphorane (1.9174 g, 5.5033 mmol). The solution was stirred at room temperature overnight and then concentrated by rotary evaporation. Crude product was purified by silica gel column chromatography using 10:1 hexanes: ethyl acetate ( $R_f=0.3$ ) to give the product in 90% yield (0.6428 g) as an oil.

<sup>1</sup>H NMR (500 MHz, CDCl<sub>3</sub>)  $\delta$  6.94 (dt,  $J = 15.3, 7.5$  Hz, 1H), 5.80 (dt,  $J = 15.6, 1.5$  Hz, 1H), 4.18 (q,  $J = 7.1$  Hz, 2H), 2.08 (td,  $J = 7.1, 1.5$  Hz, 2H), 1.75 (p,  $J = 6.7$  Hz, 1H), 1.29 (t,  $J = 7.1$  Hz, 3H), 0.92 (d,  $J = 6.6$  Hz, 6H). NMR data is consistent with previously reported data.<sup>93</sup>

### methyl (Z)-5-methylhex-2-enoate (91)

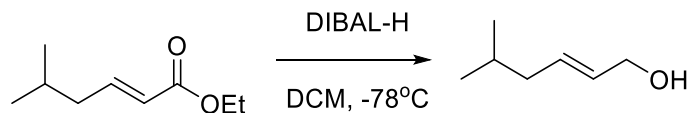


Into a flame dried flask under nitrogen, 18-crown-6 (0.9671 g, 3.659 mmol) and tetrahydrofuran (37 mL) was added and cooled to  $-78^{\circ}\text{C}$ . Phosphonoacetate (0.78 mL, 3.7 mmol) was added, followed by potassium bis(trimethylsilyl)amide (KHMDS) (7.3 mL, 3.7 mmol, 0.5 M solution in toluene) and isovaleraldehyde (0.40 mL, 3.7 mmol). The reaction was allowed to warm to room temperature overnight. The reaction was quenched using saturated ammonium chloride, extracted with methyl tert-butyl ether, dried over  $\text{MgSO}_4$ , and concentrated by rotary evaporation. The crude product was purified by silica gel column chromatography using 10:1 hexanes: ethyl acetate ( $R_f=0.4$ ) to yield the product in 39% yield (0.2236 g) as an oil which contained 1:1 cis:trans isomers.

$^1\text{H NMR}$  (500 MHz,  $\text{CDCl}_3$ )  $\delta$  6.25 (dt,  $J = 11.6, 7.5$  Hz, 1H), 5.81 (d,  $J = 11.6$  Hz, 1H), 3.71 (s, 3H), 2.56 (td,  $J = 7.2, 1.8$  Hz, 2H), 1.74 (m, 1H), 0.94 (d,  $J = 6.6$  Hz, 6H).

$^{13}\text{C NMR}$  (126 MHz,  $\text{CDCl}_3$ )  $\delta$  166.91, 149.83, 119.76, 50.94, 37.74, 28.51, 22.32.

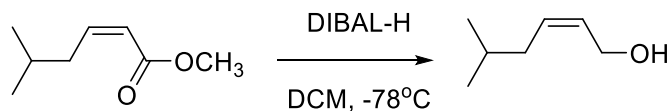
### (E)-5-methylhex-2-en-1-ol (93)



Into a flame dried flask under nitrogen, the ester **90** (0.6428 g, 4.114 mmol) and dichloromethane (21 mL) was added and cooled to  $-78^{\circ}\text{C}$ . Diisobutylaluminum hydride (DIBAL-H) (10.3 mL, 10 mmol, 1.0 M solution in hexanes) was added slowly and the solution was stirred for 1 hour at  $-78^{\circ}\text{C}$ . To quench the reaction, 50 mL of ethyl acetate was added to dilute the solution and 50 mL of Rochelle's solution was added into another round bottom flask. The diluted ethyl acetate solution was added to the flask containing the Rochelle's solution and the combined mixture was stirred vigorously for 45 min, or until the layers were visible separated. The organic layer was collected, dried over  $\text{MgSO}_4$  and concentrated by rotary evaporation to give desired product in 91% yield. The crude product was used directly without further purification.

$^1\text{H NMR}$  (500 MHz,  $\text{CDCl}_3$ )  $\delta$  5.65 (m, 2H), 4.09 (d,  $J = 5.3$  Hz, 2H), 1.94 (m, 2H), 1.63 (p,  $J = 6.7$  Hz, 1H), 1.29 (m, 1H), 0.89 (m, 6H). NMR matches previously reported data.<sup>94</sup>

### (Z)-5-methylhex-2-en-1-ol (94)

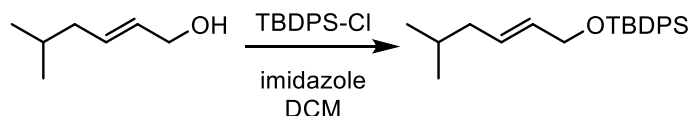


Into a flame dried flask under nitrogen, the ester **91** (0.2236 g, 1.431 mmol) and dichloromethane (7.2 mL) was added and cooled to  $-78^{\circ}\text{C}$ . Diisobutylaluminium hydride (DIBAL-H) (3.6 mL, 3.6 mmol, 1.0 M solution in hexanes) was added slowly and the solution was stirred for 1 hour at  $-78^{\circ}\text{C}$ . To quench the reaction, 20 mL of ethyl acetate was added to dilute the solution and 20 mL of Rochelle's solution was added into another round bottom flask. The diluted ethyl acetate solution was added to the flask containing the Rochelle's solution and the combined mixture was stirred vigorously for 45 min, or until the layers were visible separated. The organic layer was collected, dried over  $\text{MgSO}_4$  and concentrated by rotary evaporation. The crude product was purified using silica gel column chromatography with 4:1 hexanes: ethyl acetate solvent system ( $R_f=0.2$ ) to give a 3:1 cis:trans isomers of the product in 43% yield (0.0704 g) as an oil.

$^1\text{H NMR}$  (500 MHz,  $\text{CDCl}_3$ )  $\delta$  5.65 (m, 1H), 5.55 (m, 1H), 4.19 (d,  $J = 7.3$  Hz, 2H), 1.96 (m, 2H), 1.63 (dpd,  $J = 13.3, 6.7, 1.6$  Hz, 1H), 0.90 (d,  $J = 6.7$  Hz, 6H).

$^{13}\text{C NMR}$  (126 MHz,  $\text{CDCl}_3$ )  $\delta$  131.88, 129.05, 58.65, 36.45, 28.50, 22.25.

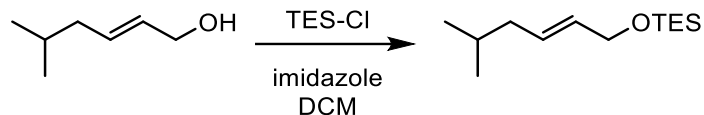
### (E)-tert-butyl((5-methylhex-2-en-1-yl)oxy)diphenylsilane (70)



Into a flame dried flask under nitrogen, the alcohol **93** (0.1010 g, 0.8845 mmol), dichloromethane (4.4 mL) and imidazole (0.1191 g, 1.752 mmol) were added and cooled to  $0^{\circ}\text{C}$ . Either tert-butylchlorodiphenylsilane (0.25 mL, 0.96 mmol) was added and the solution was allowed to come to room temperature over 2 hours while stirring. The reaction was quenched with saturated aq. sodium bicarbonate, extracted with dichloromethane three times, dried over  $\text{MgSO}_4$ , and concentrated by rotary evaporation. The crude mixture was purified by silica gel column chromatography using 10:1 hexane:ethyl acetate solvent system ( $R_f=0.5$ ) to give the product in 88% yield (0.2742 g) as an oil.

$^1\text{H NMR}$  (500 MHz,  $\text{CDCl}_3$ )  $\delta$  7.69 (dt,  $J = 6.6, 1.6$  Hz, 4H), 7.38 (m, 6H), 5.64 (m, 1H), 5.54 (m, 1H), 4.17 (dd,  $J = 5.0, 1.4$  Hz, 2H), 1.91 (td,  $J = 6.9, 1.3$  Hz, 2H), 1.61 (dp,  $J = 13.4, 6.7$  Hz, 1H), 1.05 (s, 9H), 0.88 (d,  $J = 6.6$  Hz, 6H).

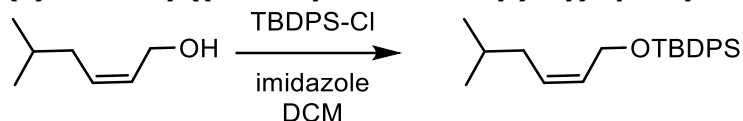
$^{13}\text{C NMR}$  (126 MHz,  $\text{CDCl}_3$ )  $\delta$  135.6, 134.0, 130.0, 129.8, 129.5, 127.6, 64.7, 41.6, 28.3, 26.9, 22.3, 19.2.

**(E)-triethyl((5-methylhex-2-en-1-yl)oxy)silane (72)**

Into a flame dried flask under nitrogen, the alcohol **93** (0.1006 g, 0.8810 mmol), dichloromethane (4.4 mL) and imidazole (0.1192 g, 1.755 mmol) were added and cooled to 0 °C. Either tert-chlorotriethylsilane (0.16 mL, 0.96 mmol) was added and the solution was allowed to come to room temperature over 2 hours while stirring. The reaction was quenched with saturated aq. sodium bicarbonate, extracted with dichloromethane three times, dried over MgSO<sub>4</sub>, and concentrated by rotary evaporation. The crude mixture was purified by silica gel column chromatography using 10:1 hexane:ethyl acetate solvent system (R<sub>f</sub>=0.6) to give the product in 83% yield (0.1680 g) as an oil.

<sup>1</sup>H NMR (500 MHz, CDCl<sub>3</sub>) δ 5.63 (m, 1H), 5.54 (m, 1H), 4.12 (dd, *J* = 5.5, 1.2 Hz, 2H), 1.92 (td, *J* = 6.8, 1.2 Hz, 2H), 1.62 (m, 1H), 0.96 (t, *J* = 8.0 Hz, 9H), 0.88 (d, *J* = 6.6 Hz, 6H), 0.61 (q, *J* = 8.0 Hz, 6H).

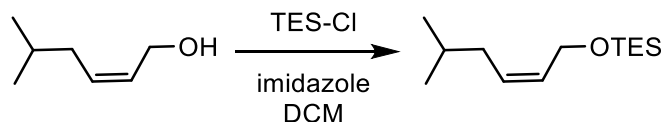
<sup>13</sup>C NMR (126 MHz, CDCl<sub>3</sub>) δ 130.5, 130.2, 63.8, 41.6, 28.3, 22.3, 6.8, 6.4, 4.5.

**(Z)-tert-butyl((5-methylhex-2-en-1-yl)oxy)diphenylsilane (71)**

Into a flame dried flask under nitrogen, the alcohol **94** (0.0357 g, 0.313 mmol), dichloromethane (1.6 mL) and imidazole (0.0426 g, 0.625 mmol) were added and cooled to 0 °C. Either tert-butylchlorodiphenylsilane (0.09 mL, 0.34 mmol) was added and the solution was allowed to come to room temperature over 3 hours while stirring. The reaction was quenched with saturated aq. sodium bicarbonate, extracted with dichloromethane three times, dried over MgSO<sub>4</sub>, and concentrated by rotary evaporation. The crude mixture was purified by silica gel column chromatography using 10:1 hexane:ethyl acetate solvent system (R<sub>f</sub>=0.6) to give the product in 72% yield (0.079 g) as an oil with a 3:1 mixture of cis:trans isomers.

<sup>1</sup>H NMR (500 MHz, CDCl<sub>3</sub>) δ 7.72 (dd, *J* = 7.7, 1.5 Hz, 4H), 7.47 – 7.38 (m, 6H), 5.67 (dddd, *J* = 12.6, 6.3, 4.4, 2.8 Hz, 1H), 5.45 (dtt, *J* = 11.0, 7.5, 1.7 Hz, 1H), 4.28 (d, *J* = 6.2 Hz, 2H), 1.78 (td, *J* = 7.3, 1.5 Hz, 2H), 1.55 (sept, *J* = 6.7 Hz, 1H), 1.07 (s, 9H), 0.84 (d, *J* = 6.7 Hz, 6H).

<sup>13</sup>C NMR (126 MHz, CDCl<sub>3</sub>) δ 135.6, 134.0, 129.1, 129.6, 127.6, 60.3, 36.6, 28.5, 26.9, 26.8, 22.3.

**(Z)-triethyl((5-methylhex-2-en-1-yl)oxy)silane (73)**

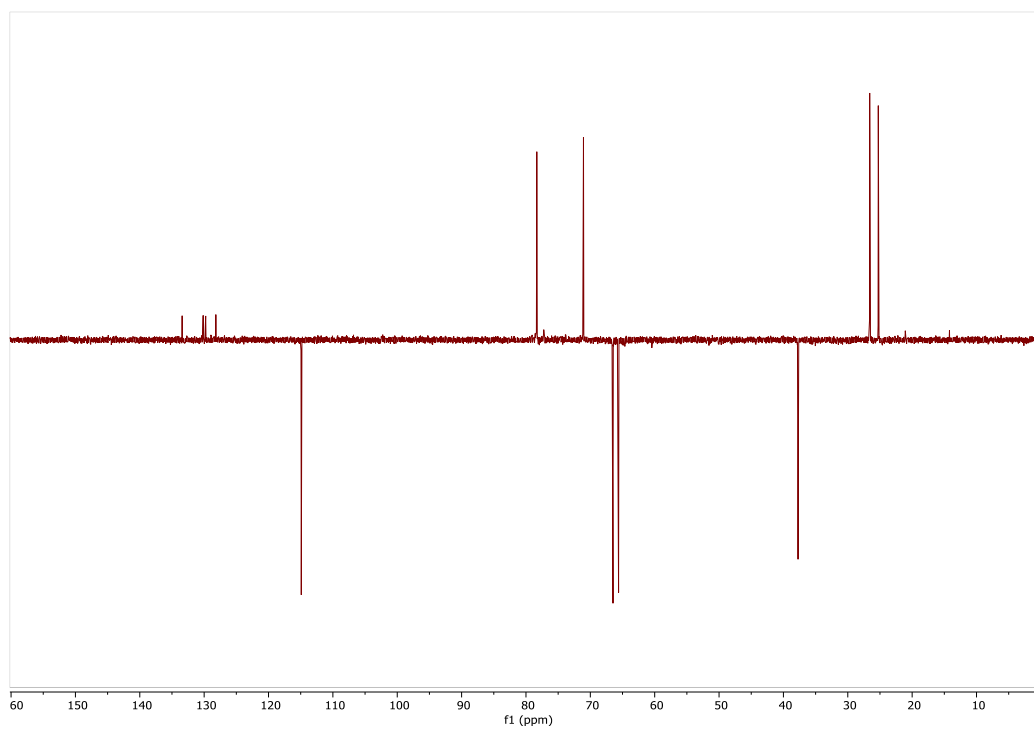
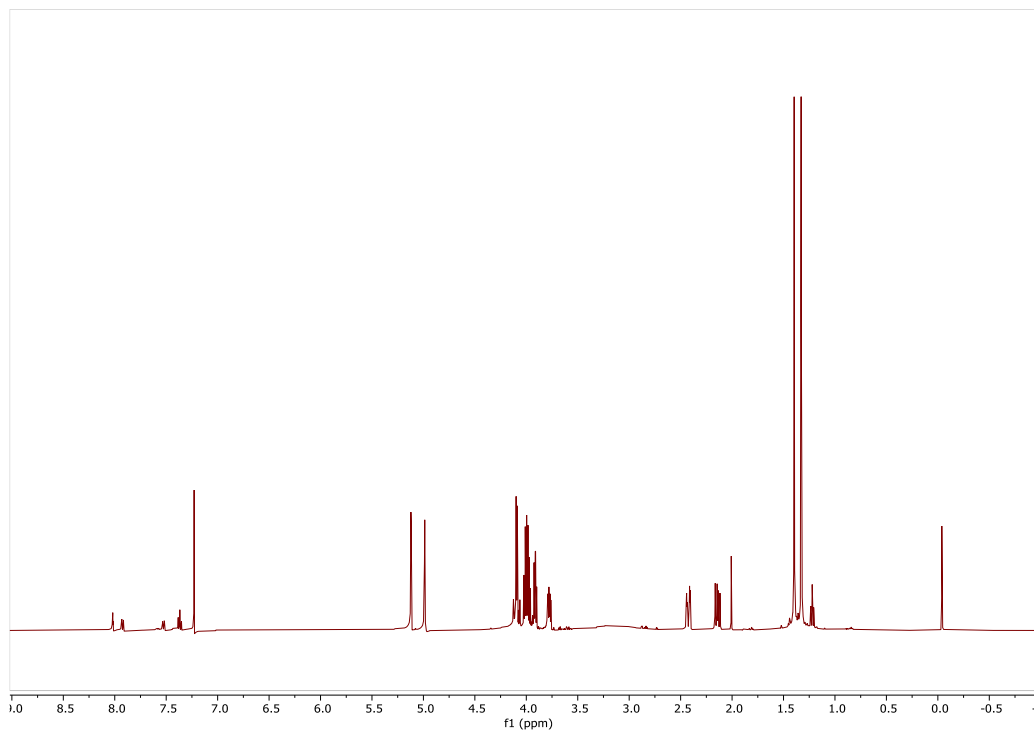
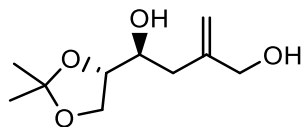
Into a flame dried flask under nitrogen, the alcohol **94** (0.0357 g, 0.313 mmol), dichloromethane (1.6 mL) and imidazole (0.0429 g, 0.651 mmol) were added and cooled to 0 °C. Chlorotriethylsilane (0.06 mL,

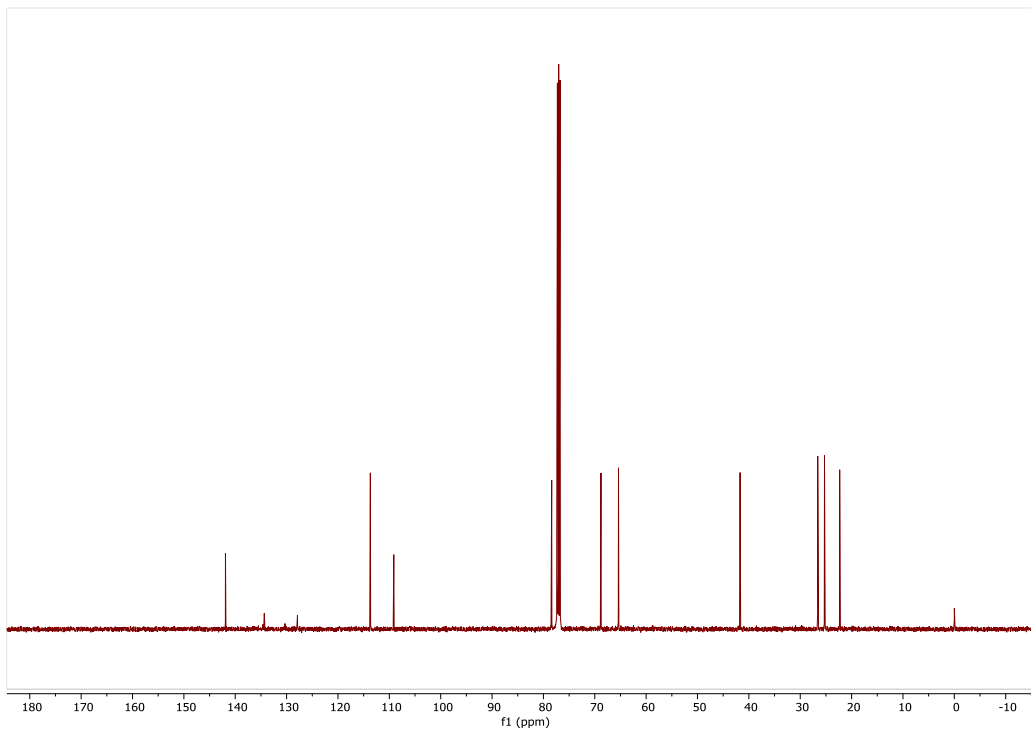
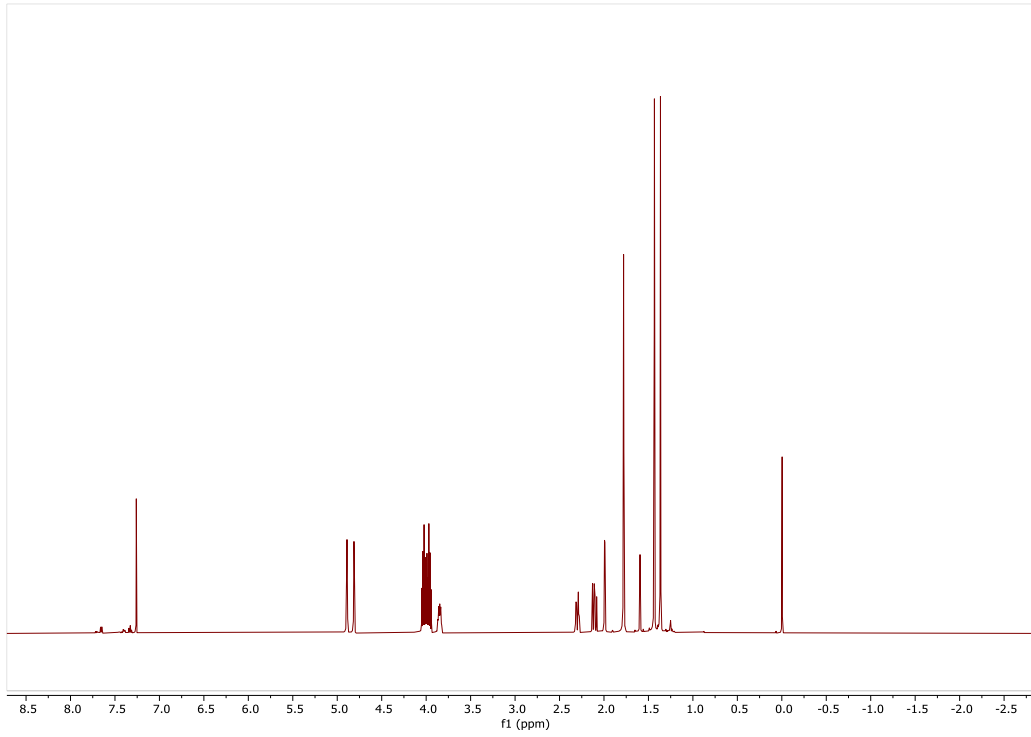
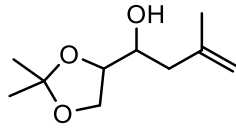
0.34 mmol) was added and the solution was allowed to come to room temperature over 3 hours while stirring. The reaction was quenched with saturated aq. sodium bicarbonate, extracted with dichloromethane three times, dried over  $\text{MgSO}_4$ , and concentrated by rotary evaporation. The crude mixture was purified by silica gel column chromatography using 10:1 hexane:ethyl acetate solvent system ( $R_f=0.6$ ) to give the product in 86% yield (0.0611 g) as an oil with a mixture of 3:1 cis:trans isomers.

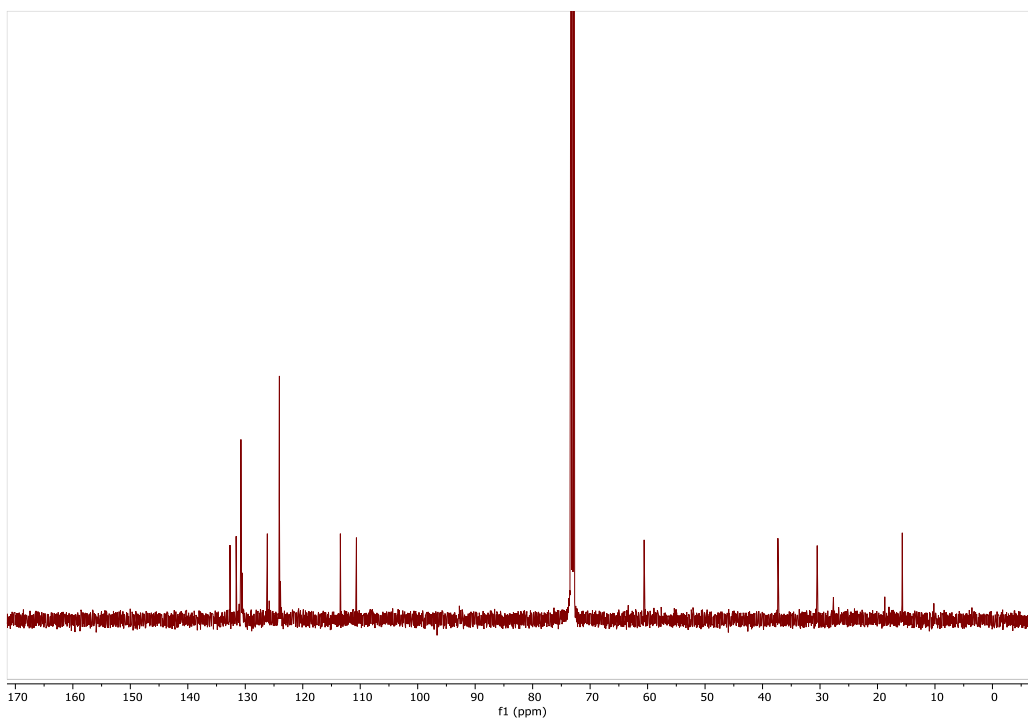
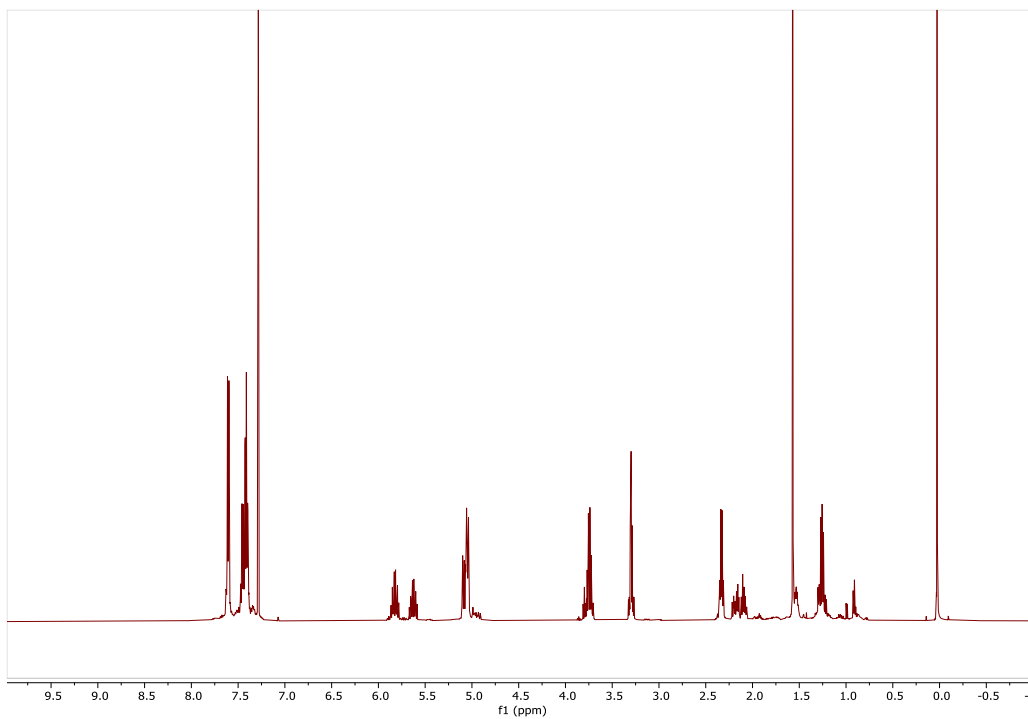
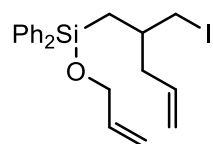
$^1\text{H NMR}$  (500 MHz,  $\text{CDCl}_3$ )  $\delta$  5.57p (m, 1H), 5.45 (dtt,  $J = 10.9, 7.5, 1.6$  Hz, 1H), 4.21 (m, 2H), 1.92(m, 2H), 1.62 (dtd,  $J = 13.4, 6.7, 1.9$  Hz, 1H), 0.96 (t,  $J = 6.8$  Hz, 9H), 0.89 (d,  $J = 6.6$  Hz, 6H), 0.61 (q,  $J = 7.8$  Hz, 6H).

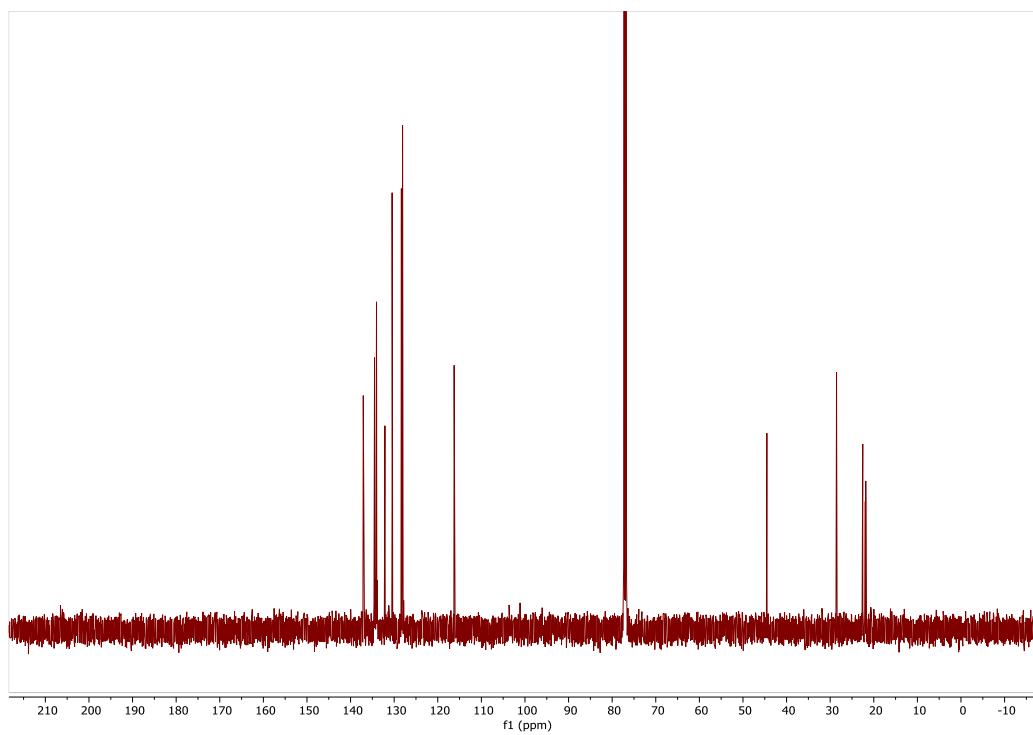
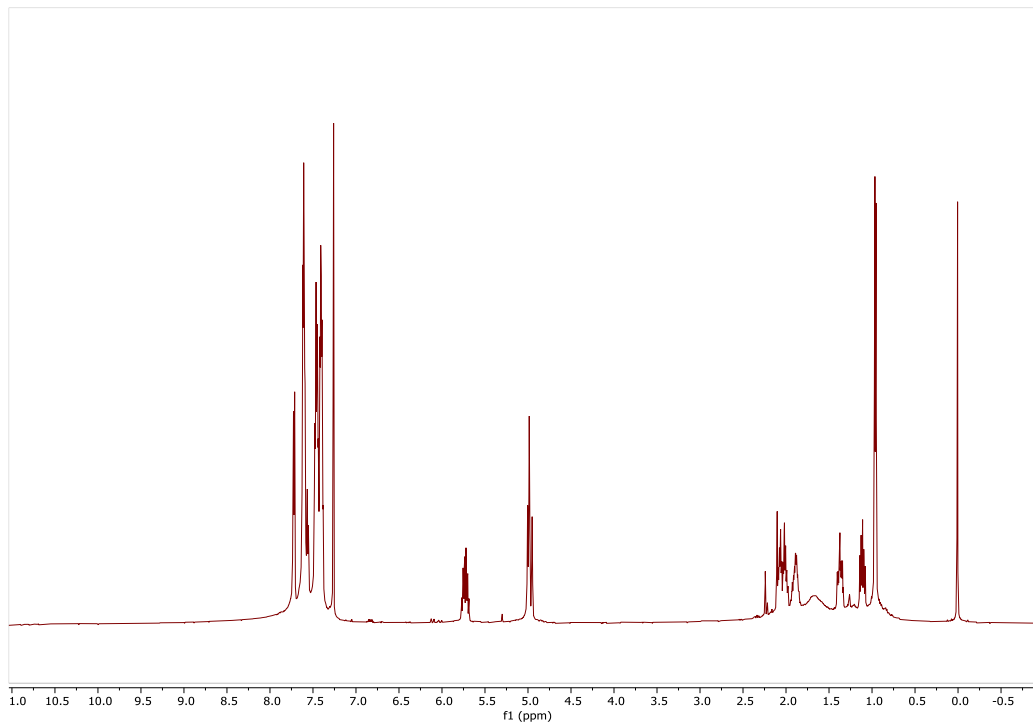
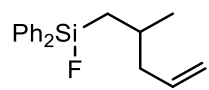
$^{13}\text{C NMR}$  (126 MHz,  $\text{CDCl}_3$ )  $\delta$  130.1, 129.7, 59.0, 36.6, 28.6, 22.3, 6.8, 4.5.

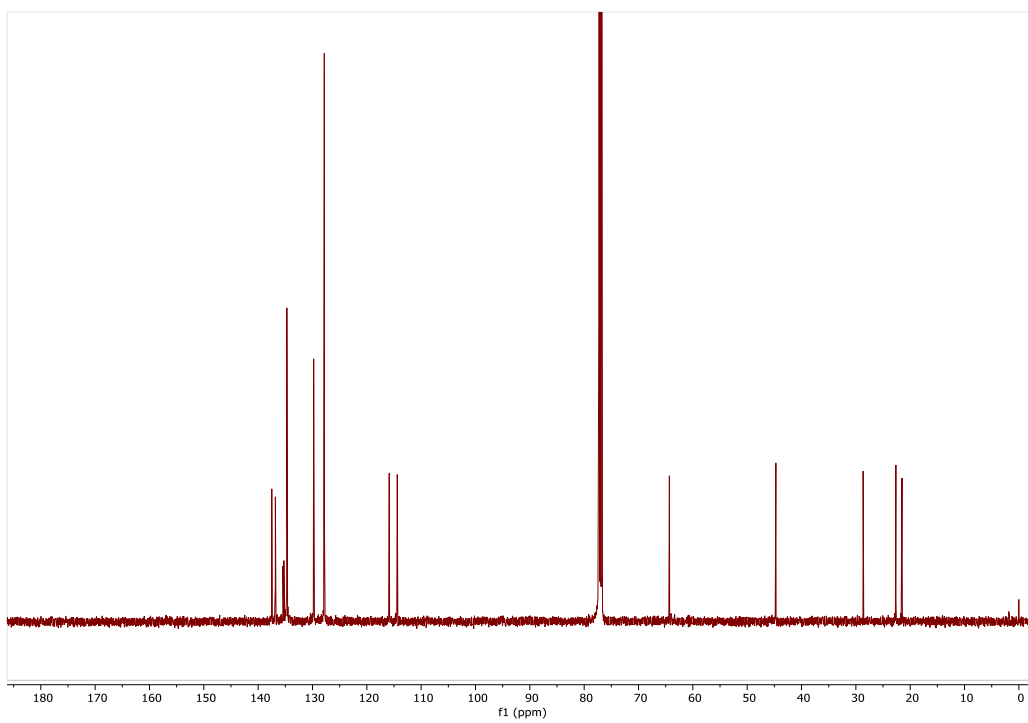
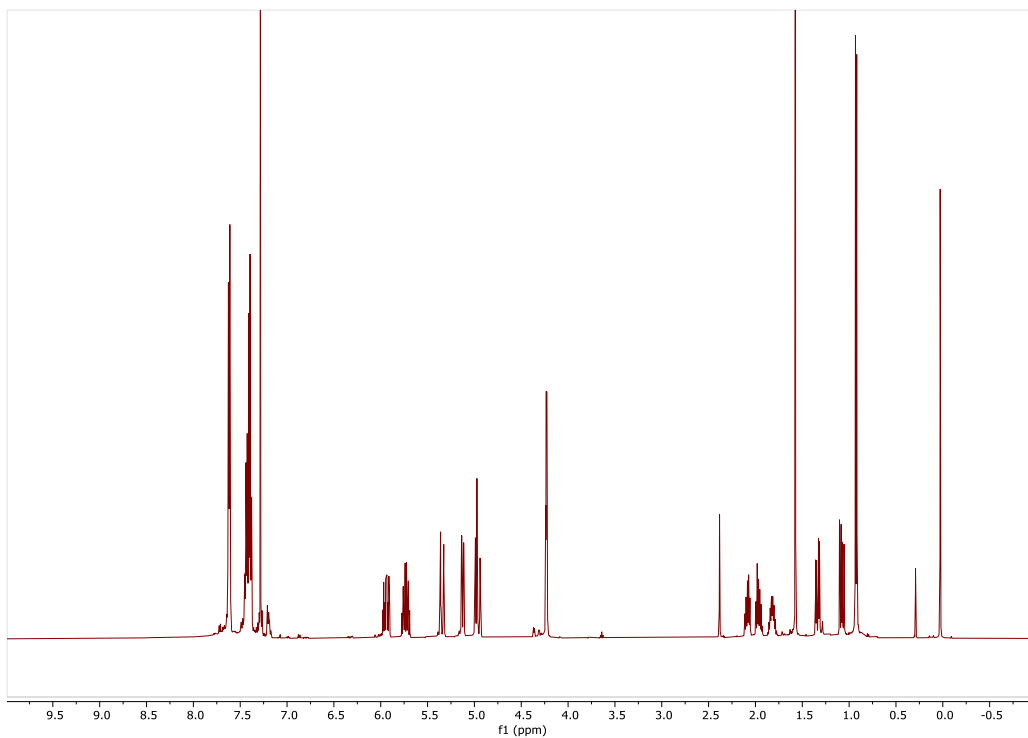
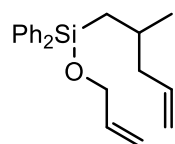
# SPECTRA

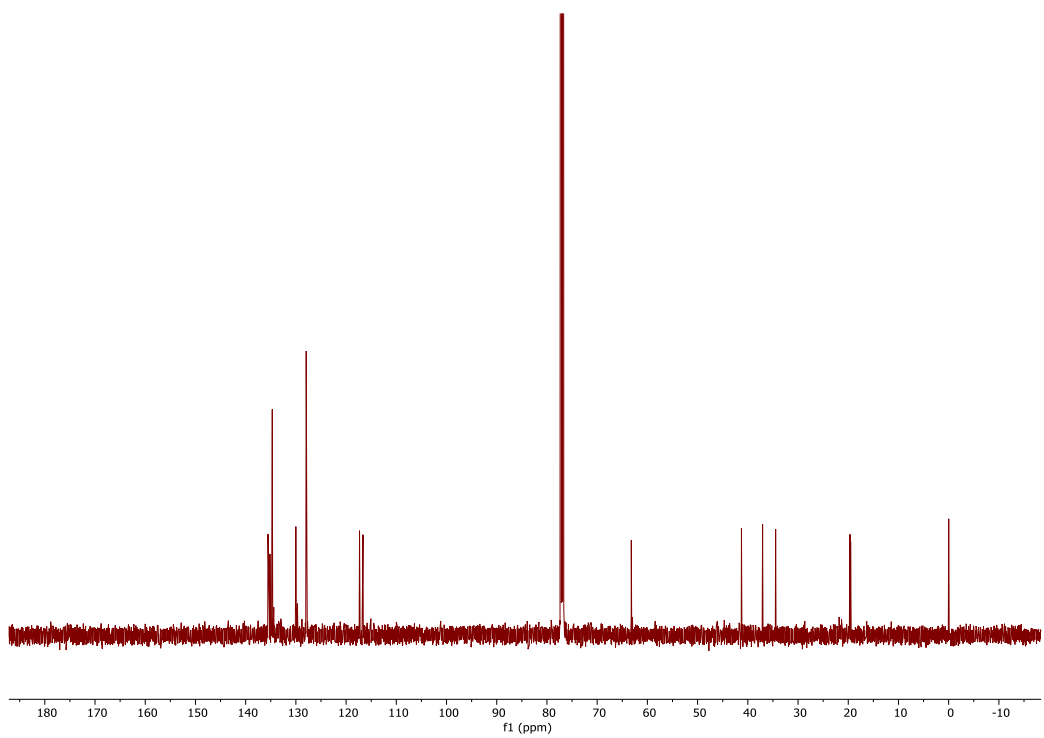
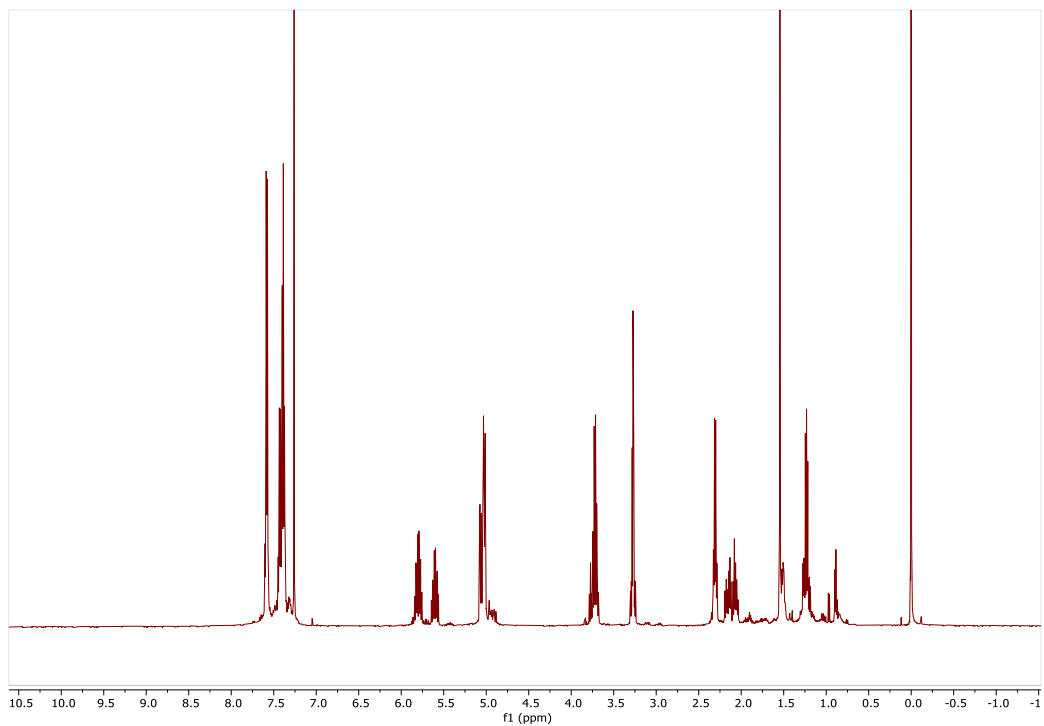
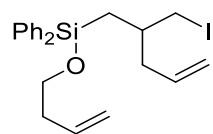


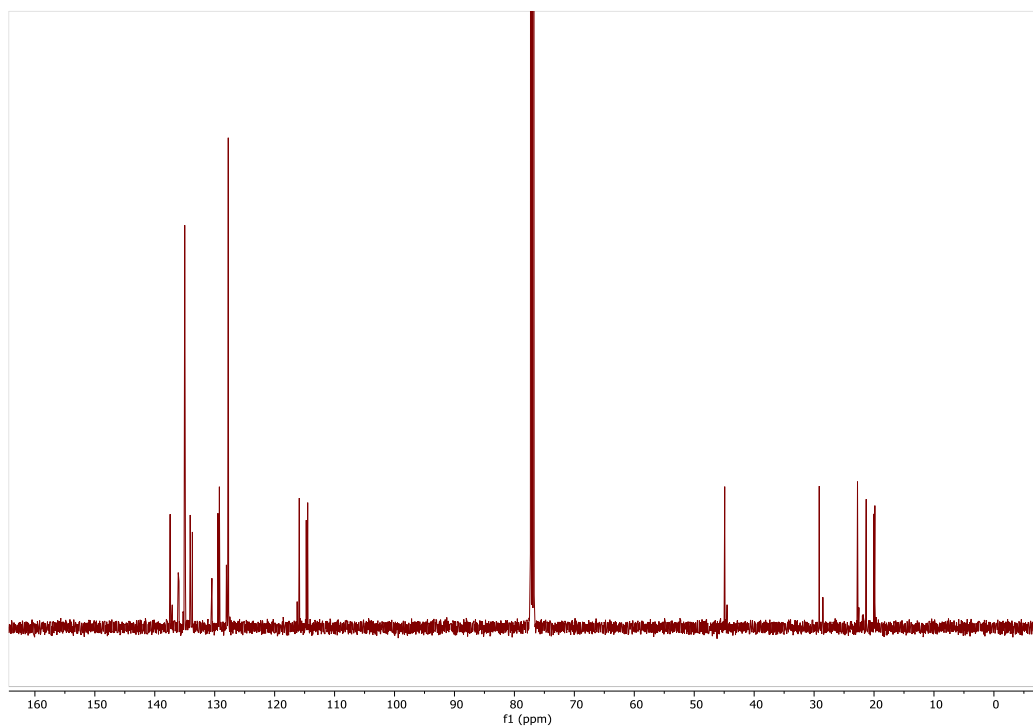
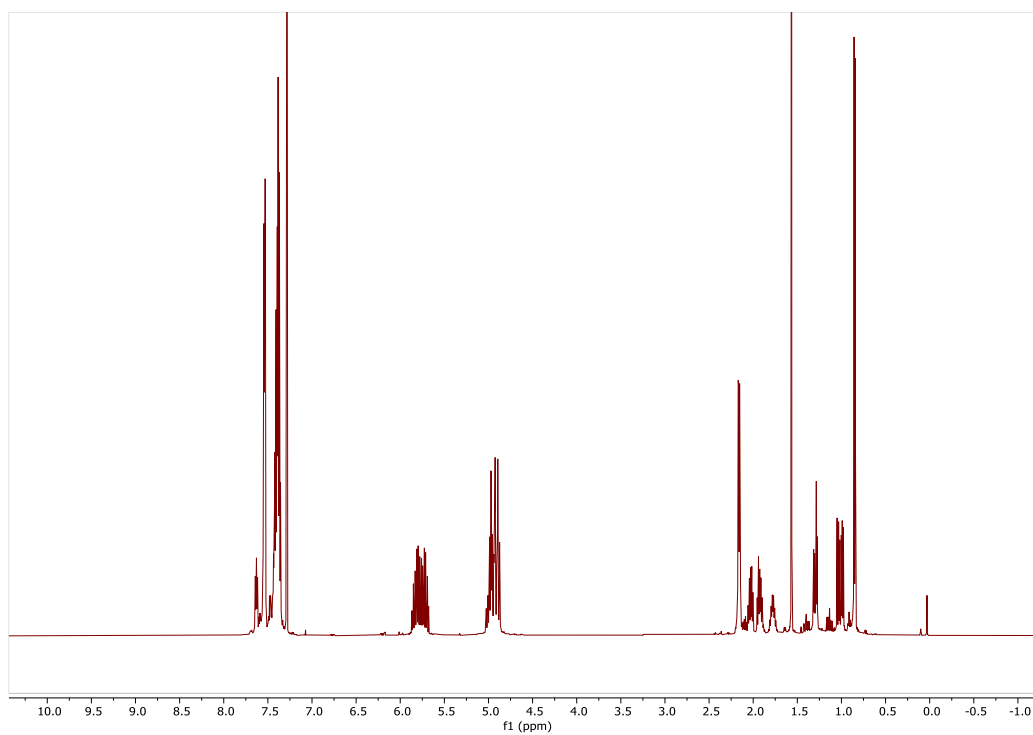
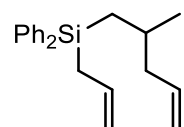


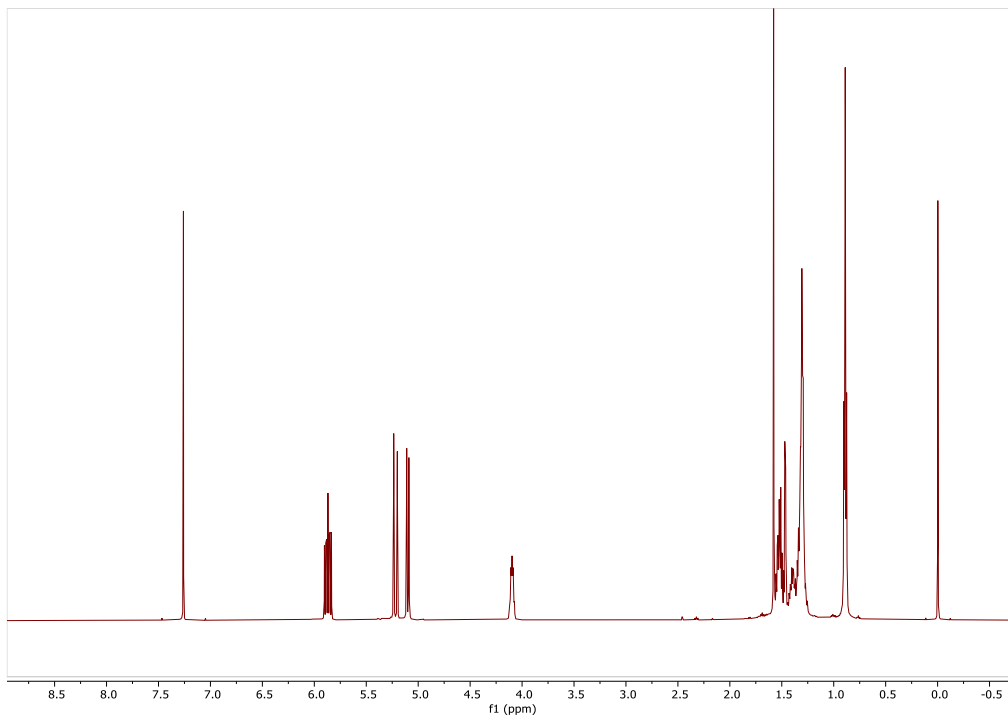
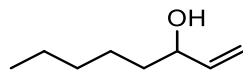
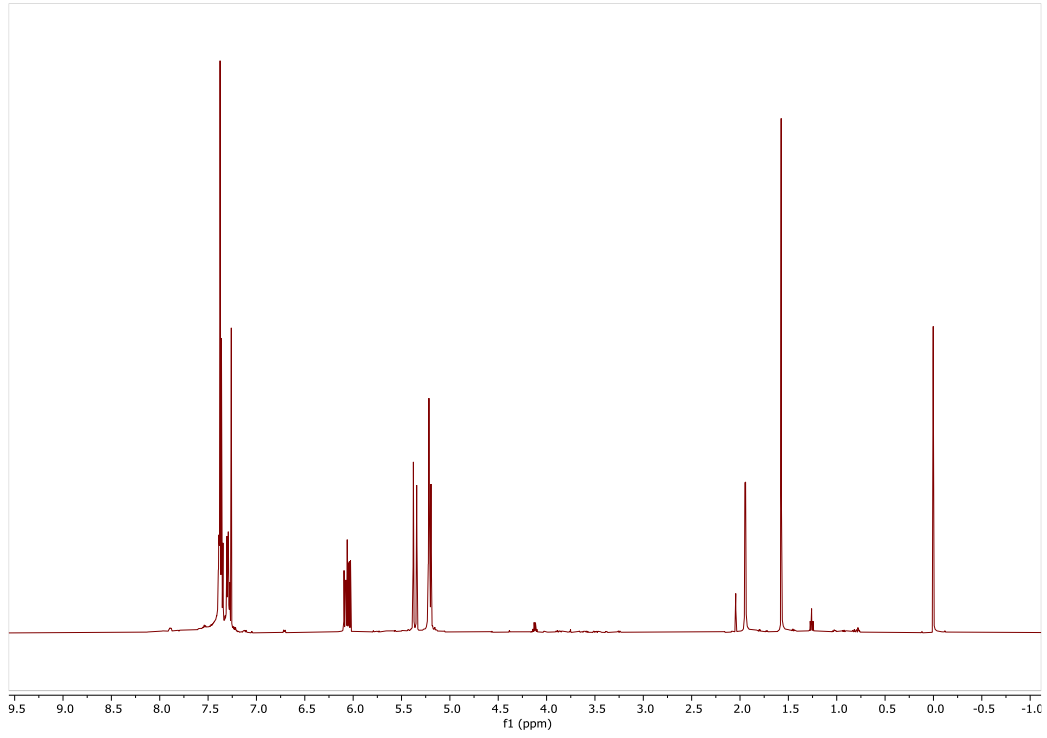
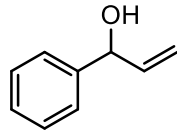


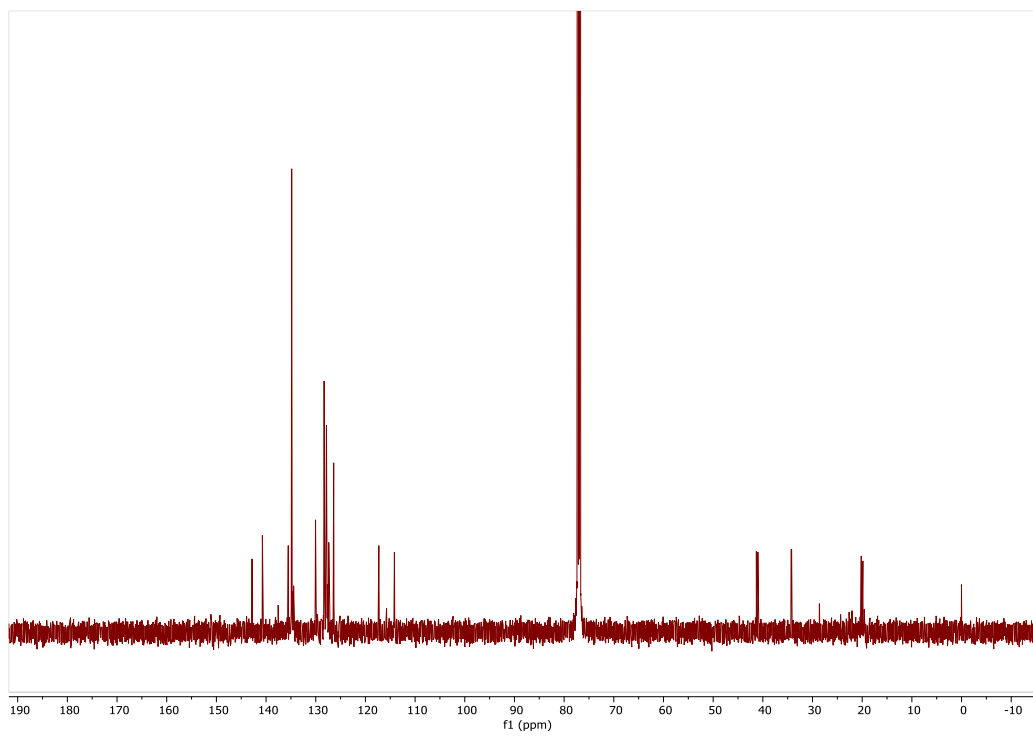
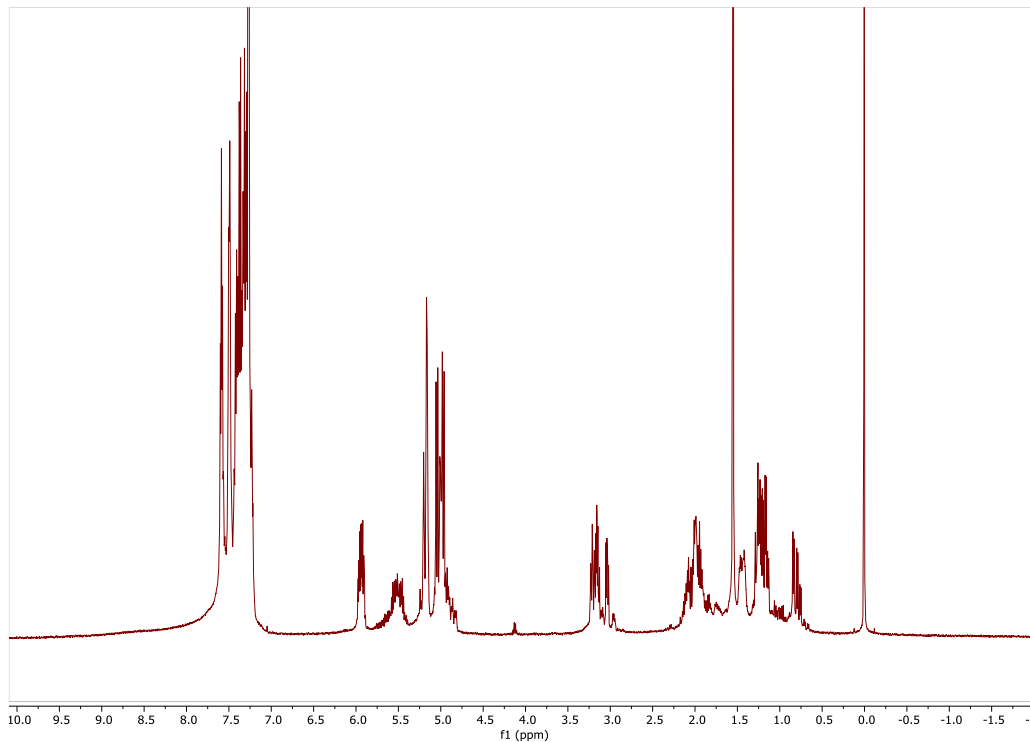
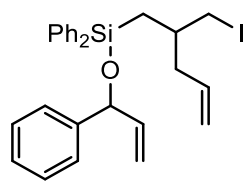


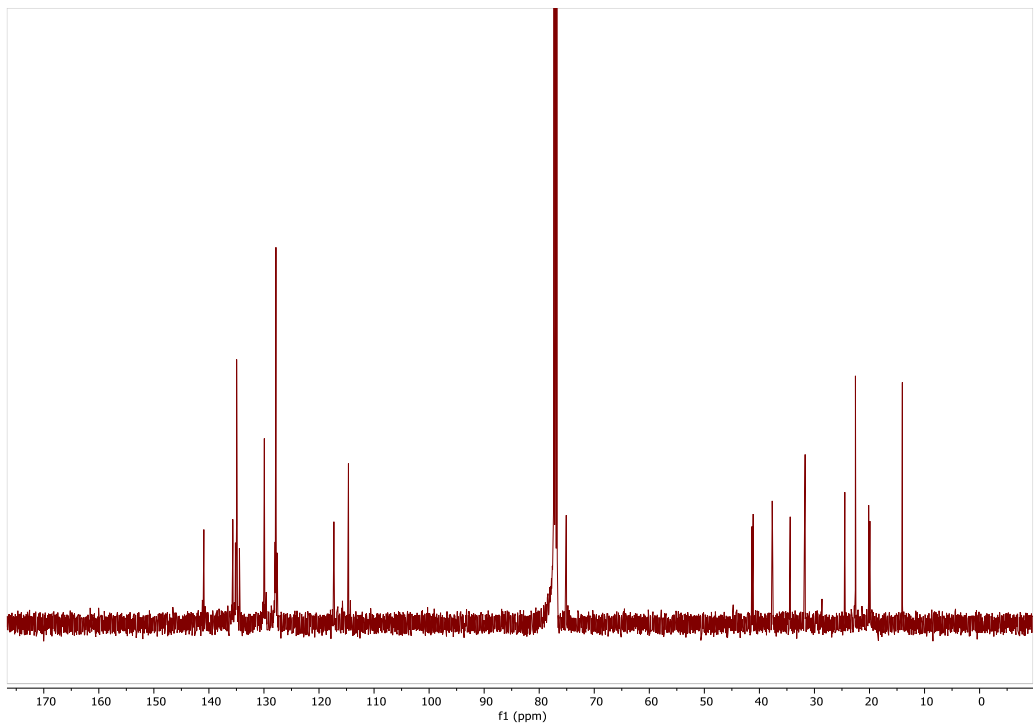
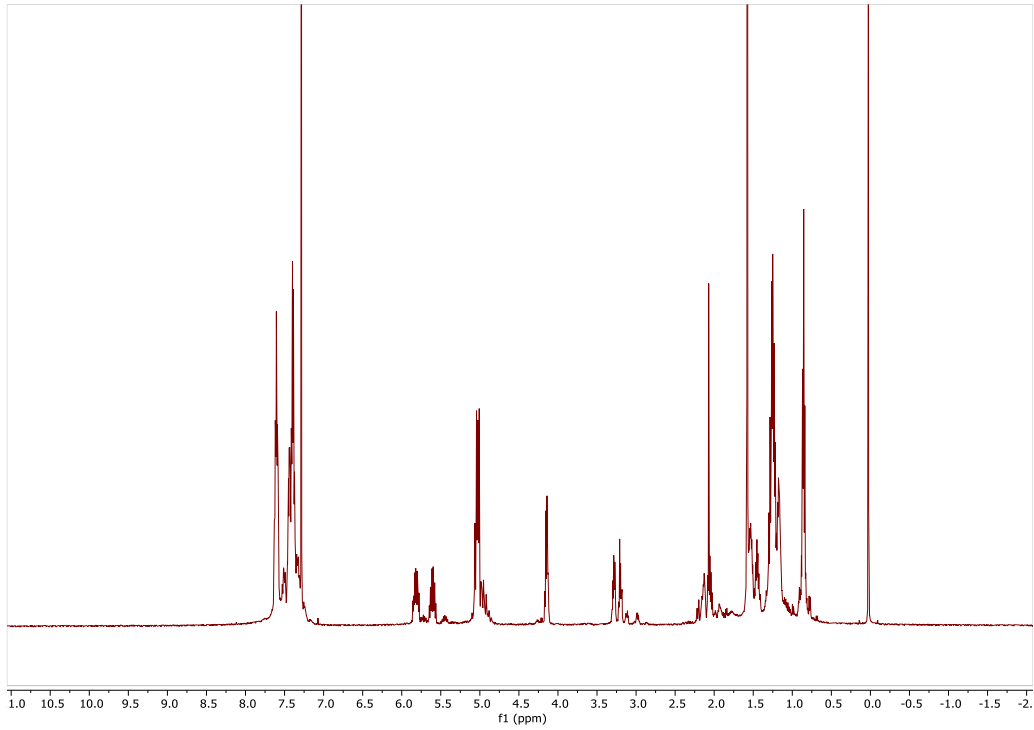
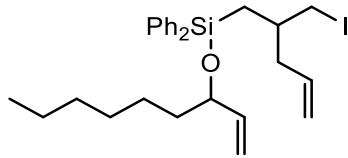


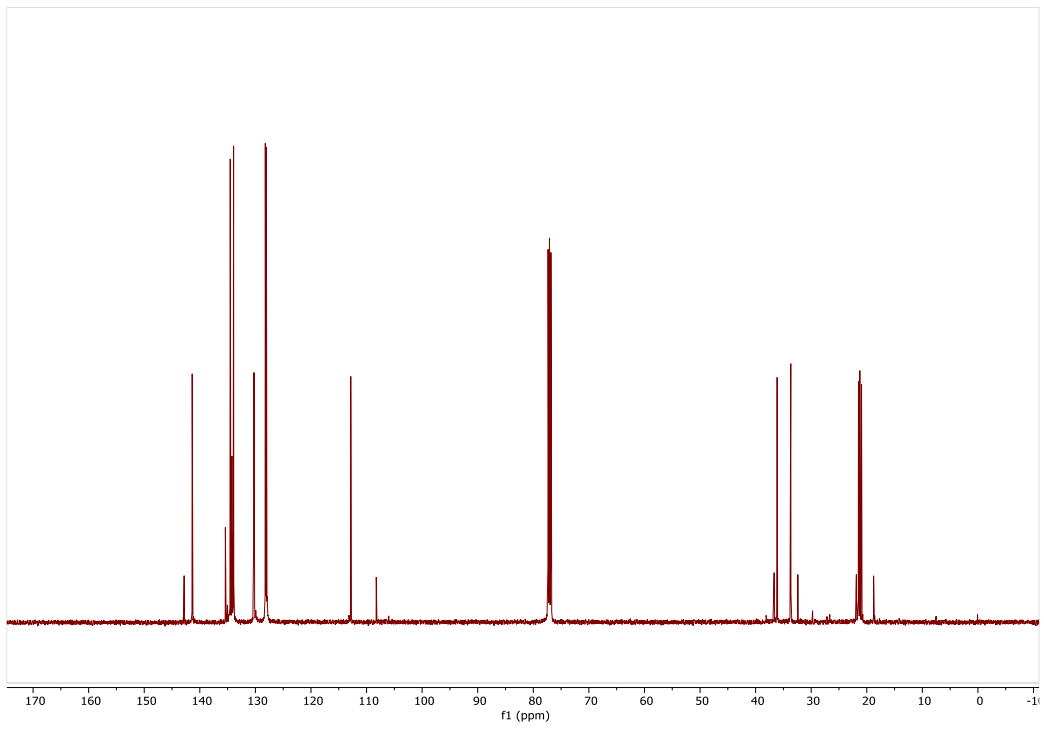
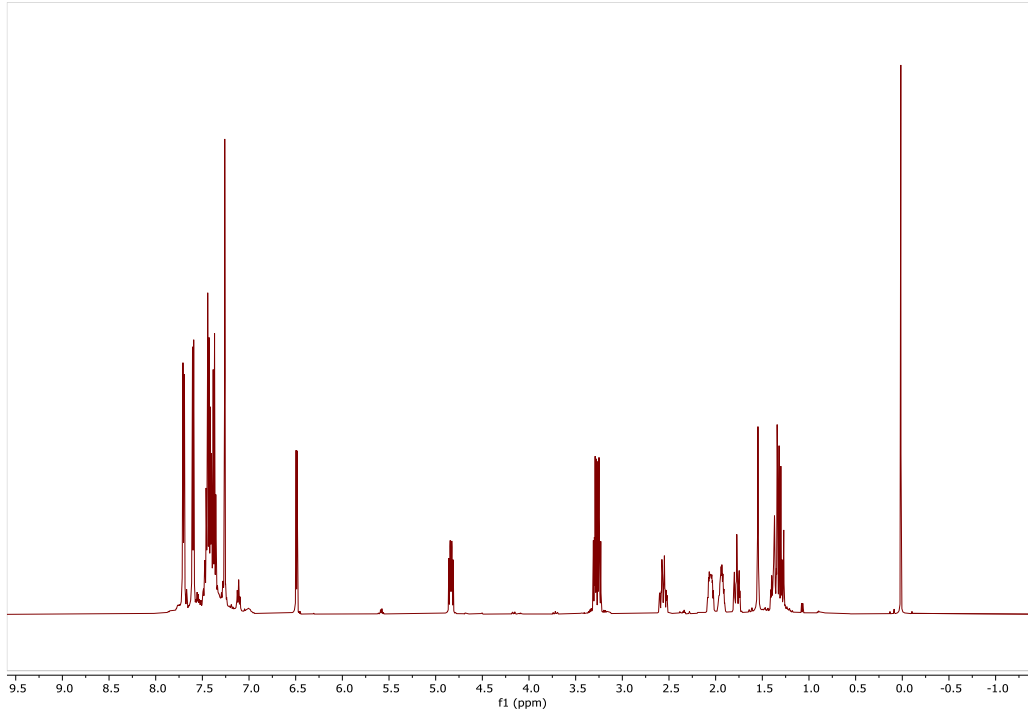
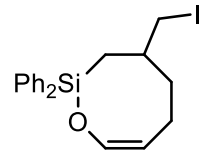


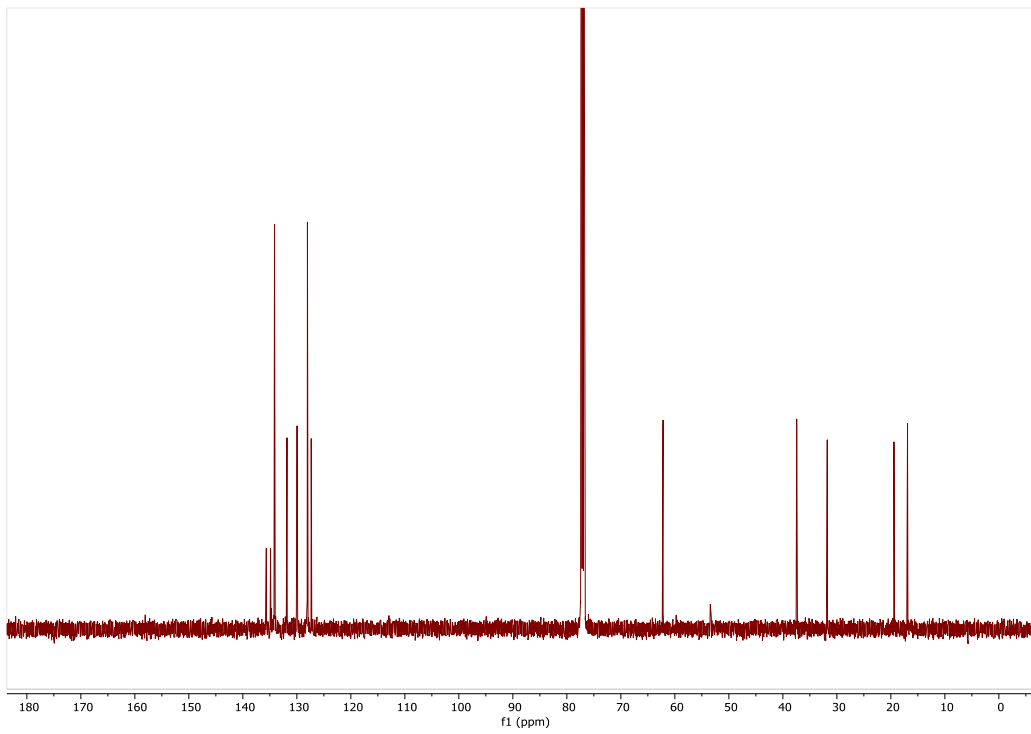
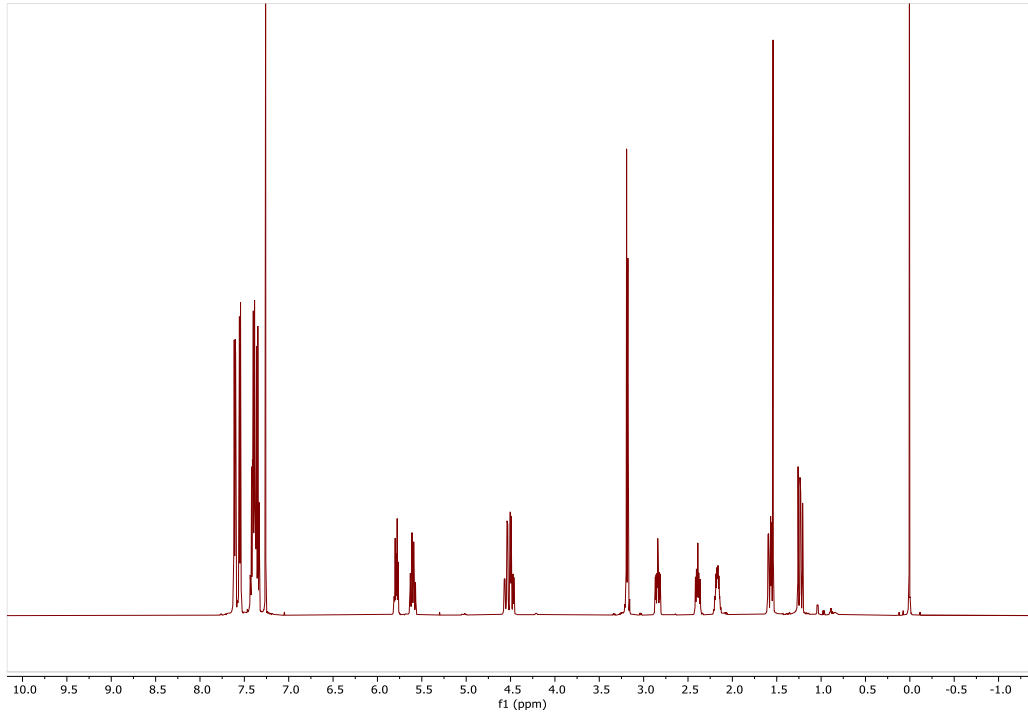
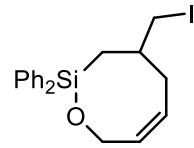


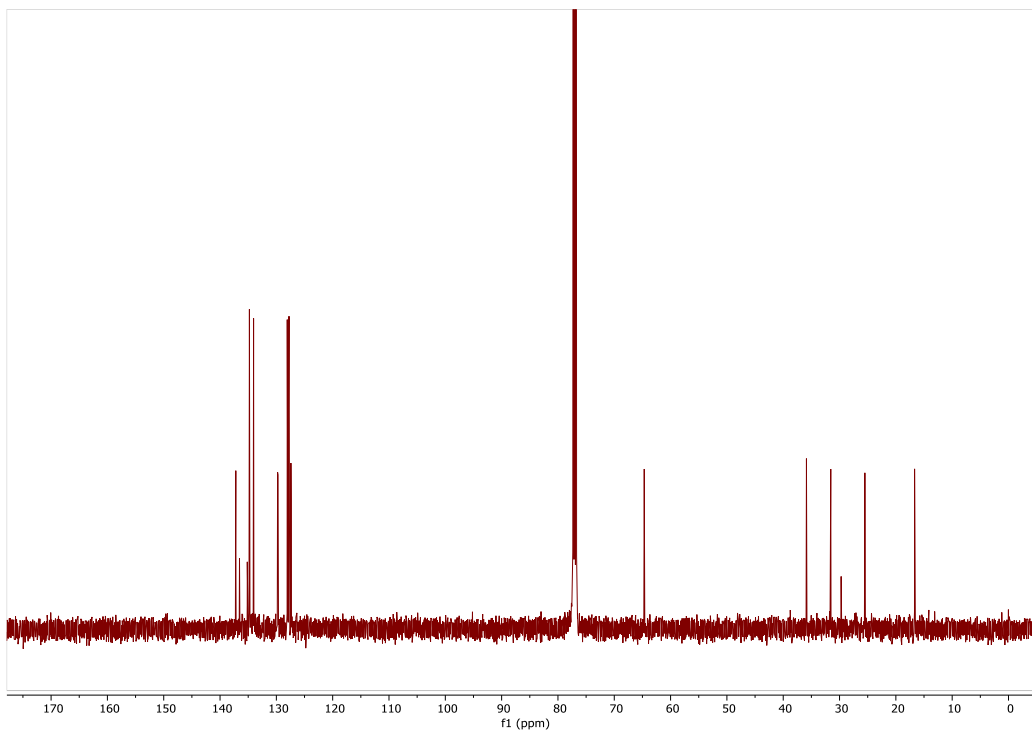
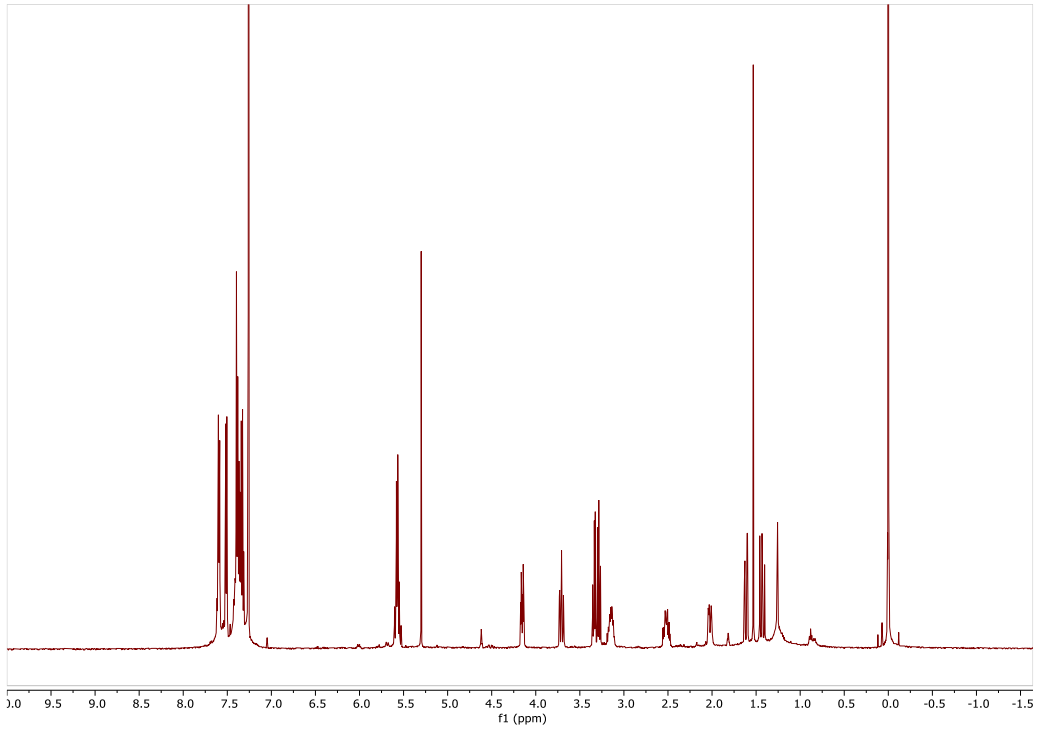
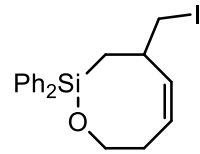


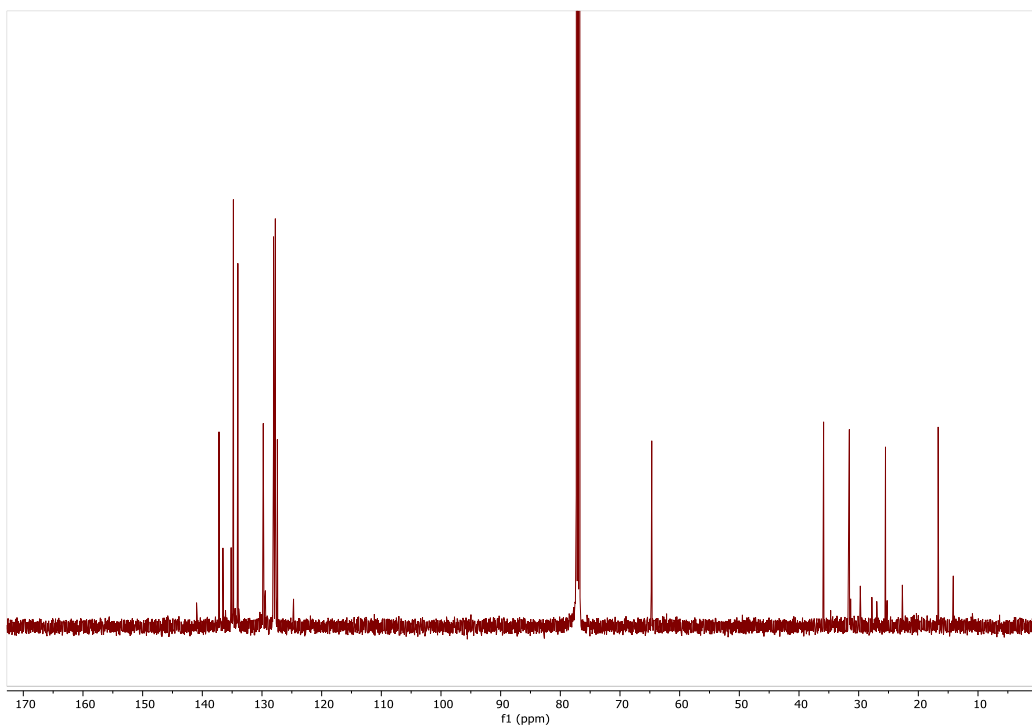
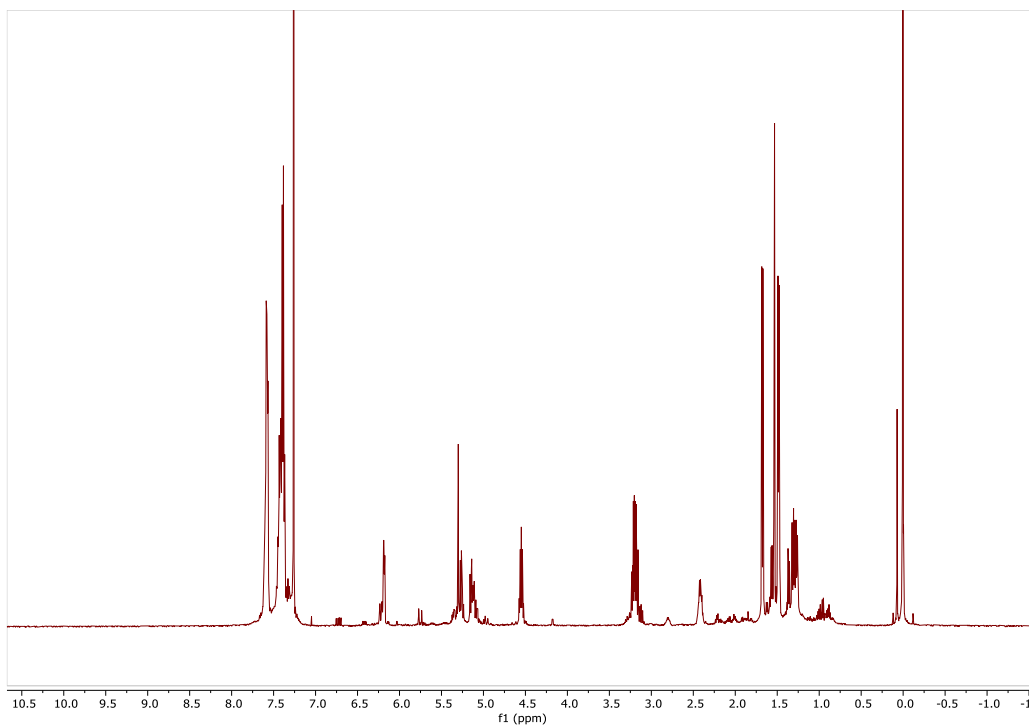
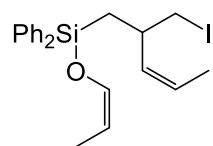


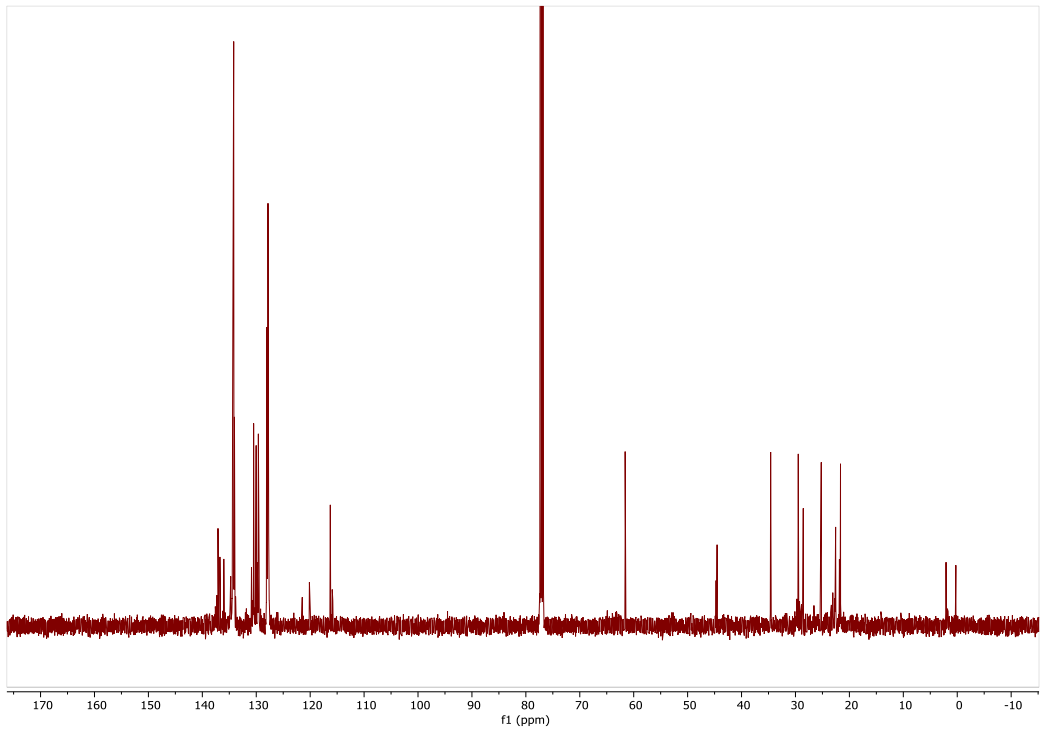
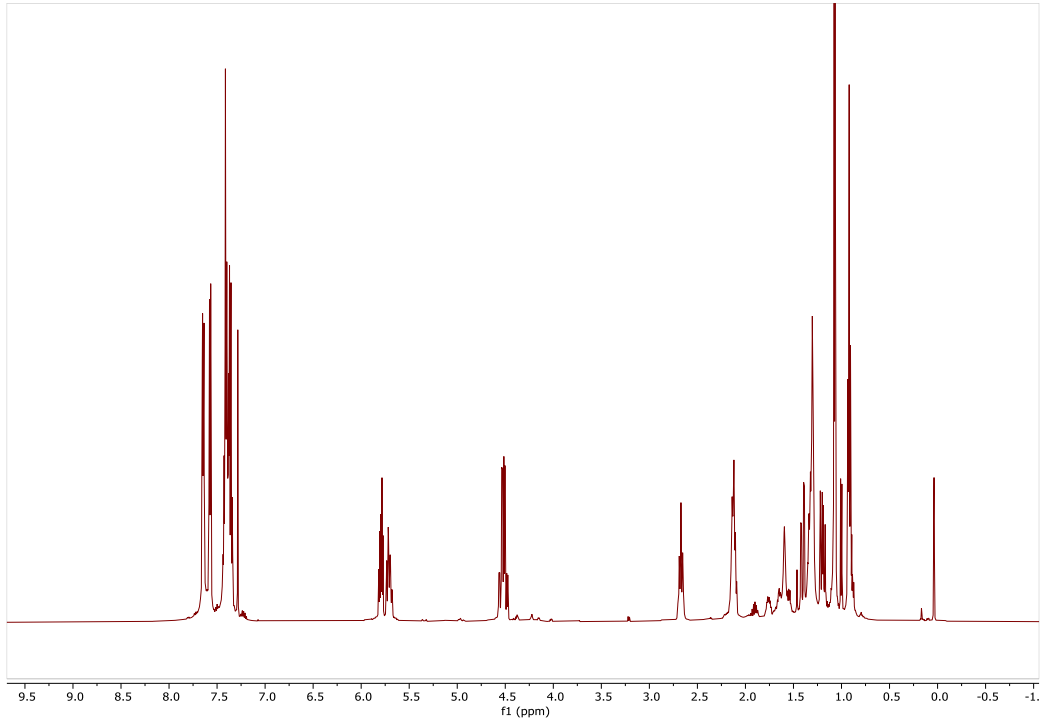
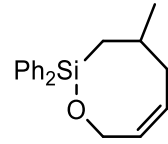


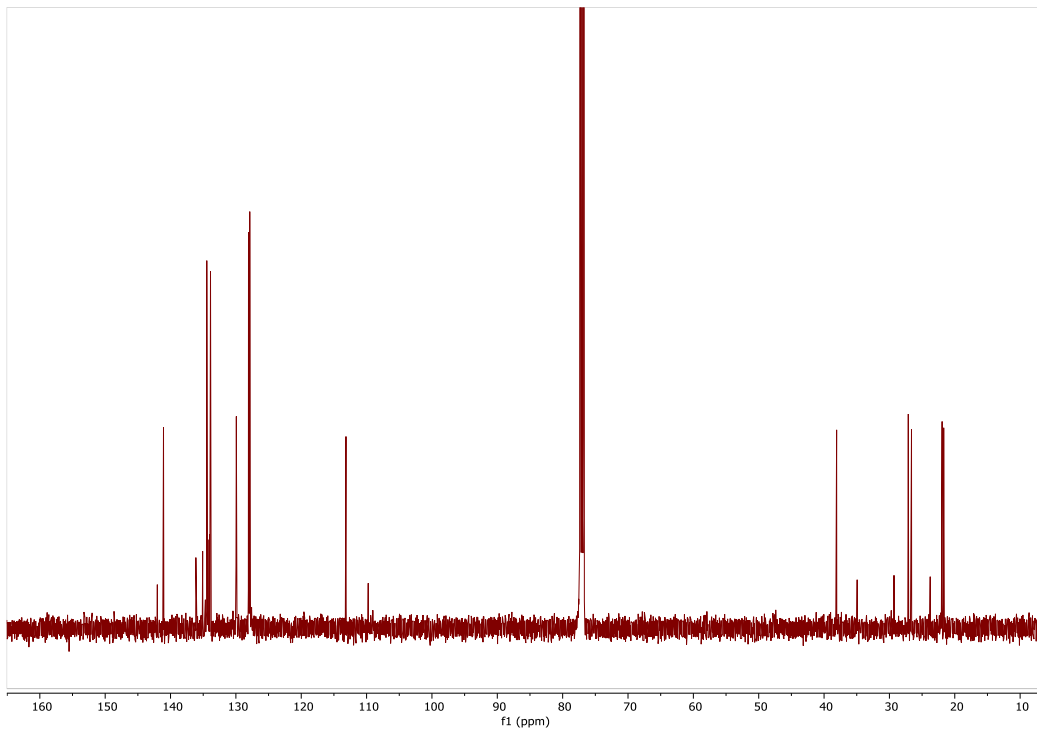
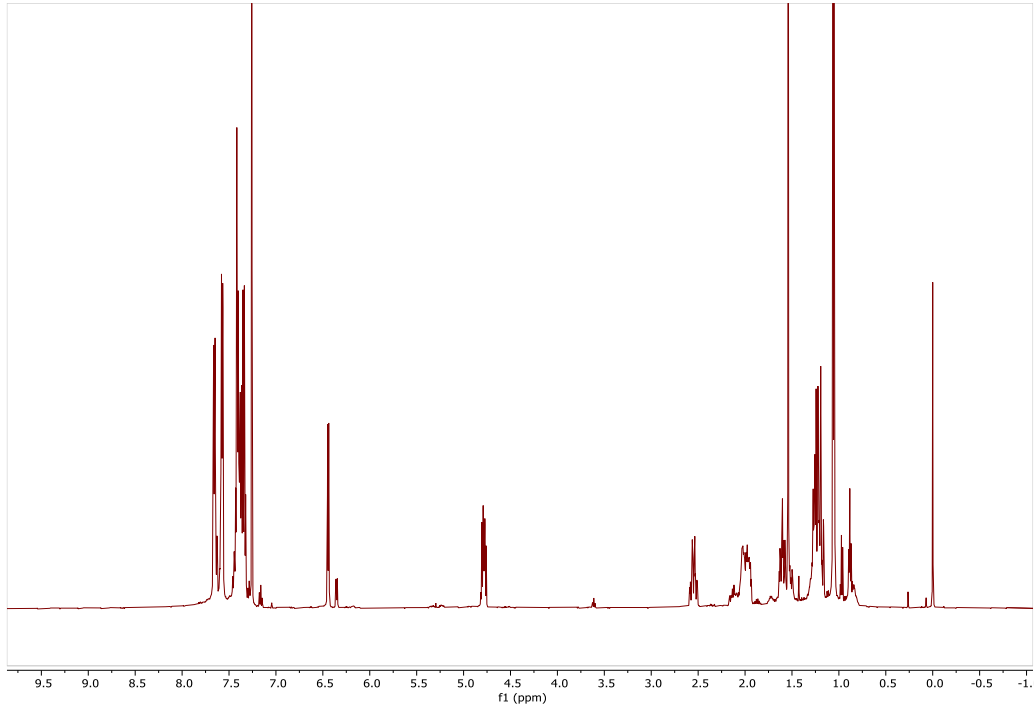
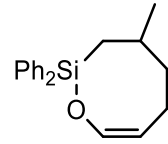


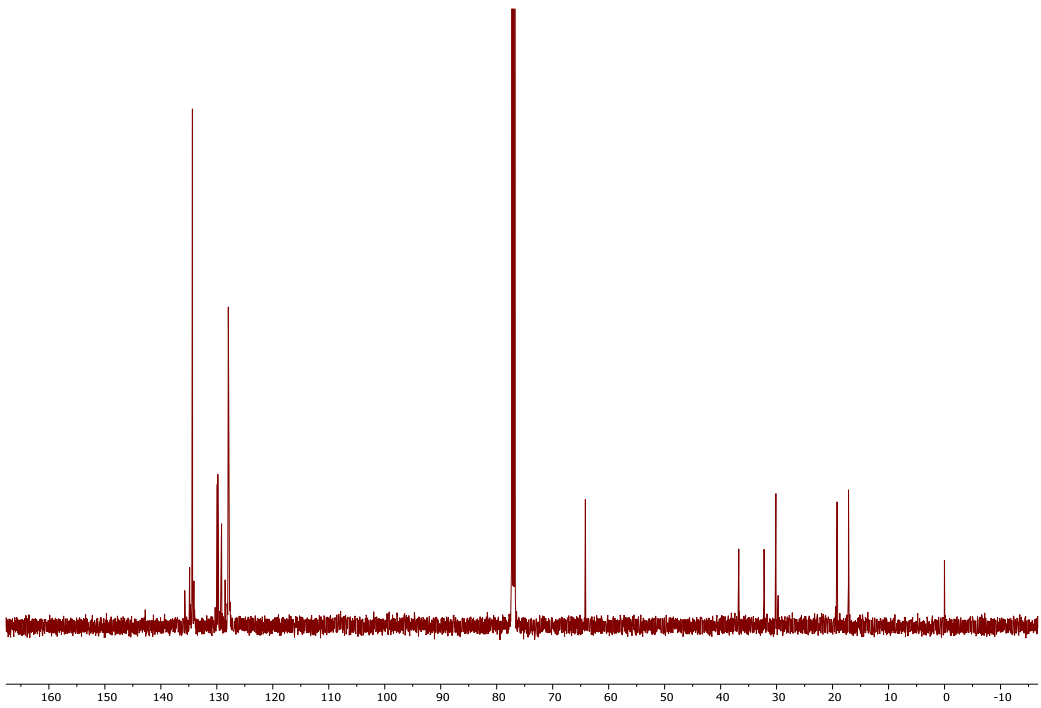
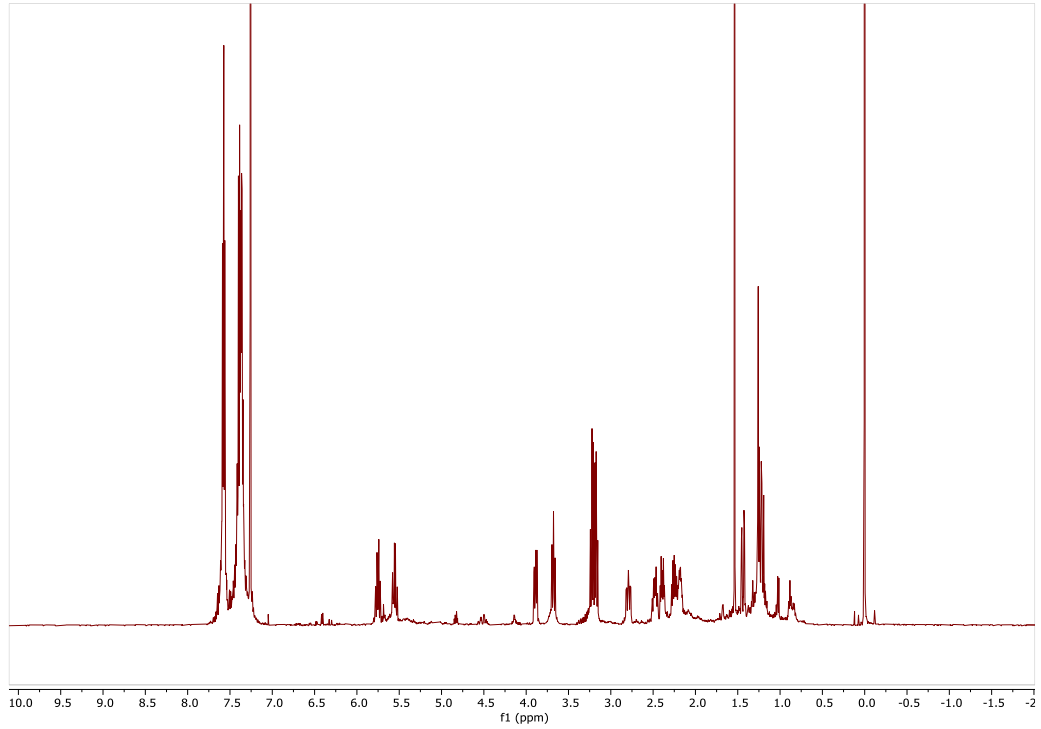
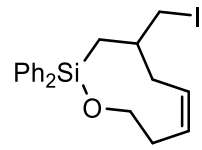


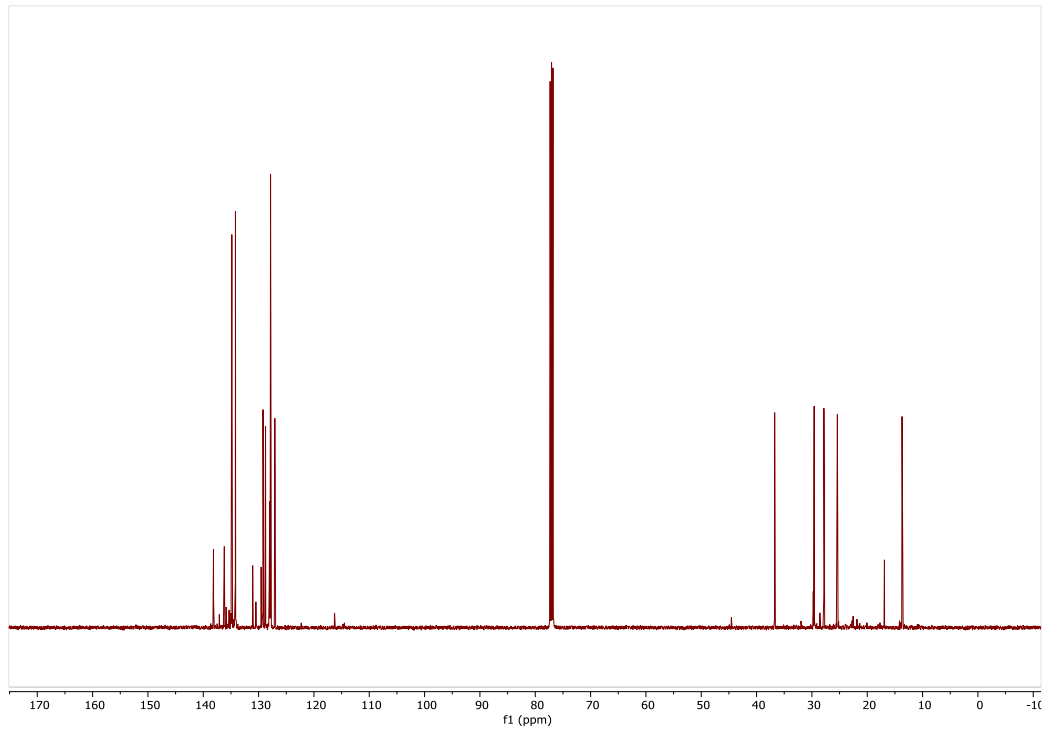
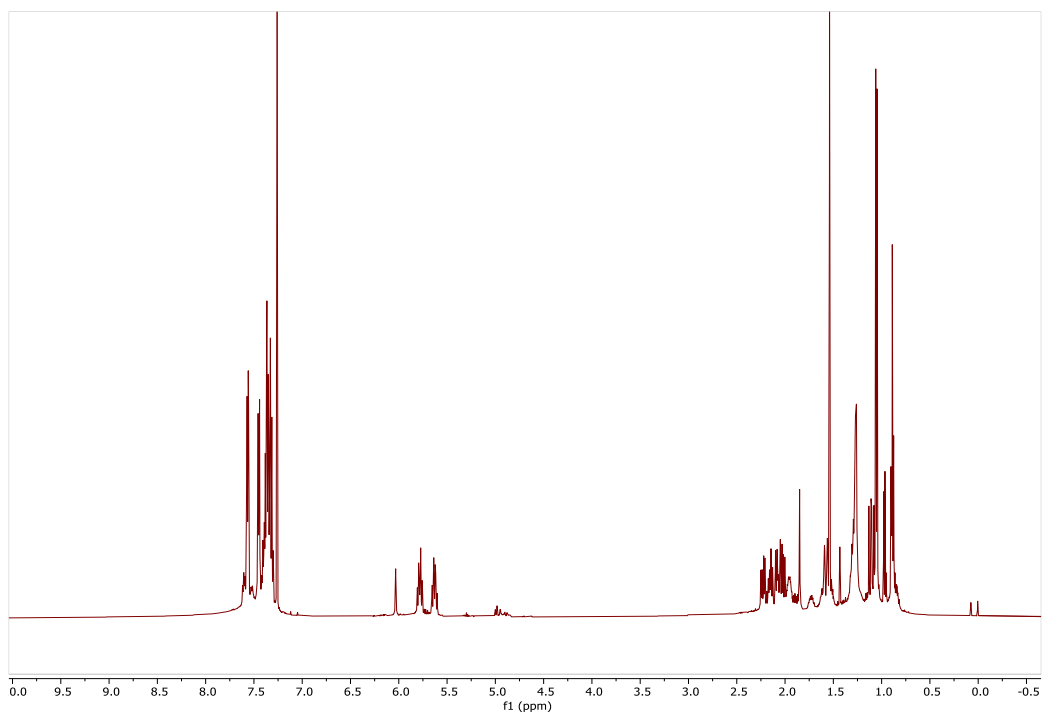
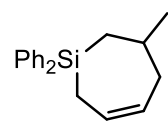


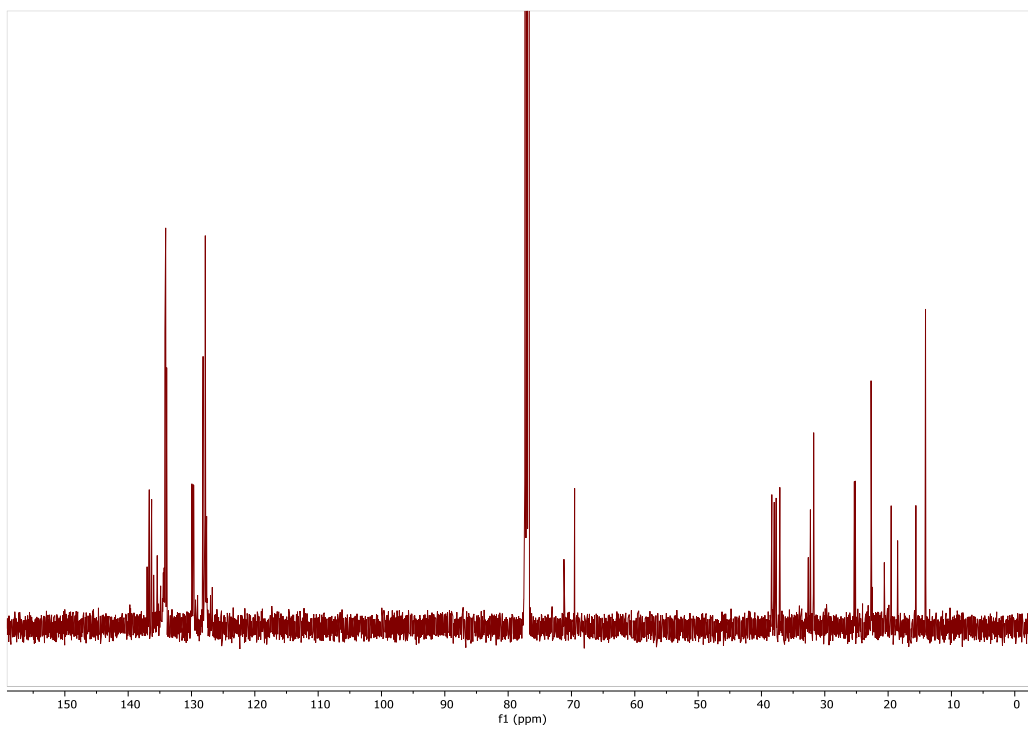
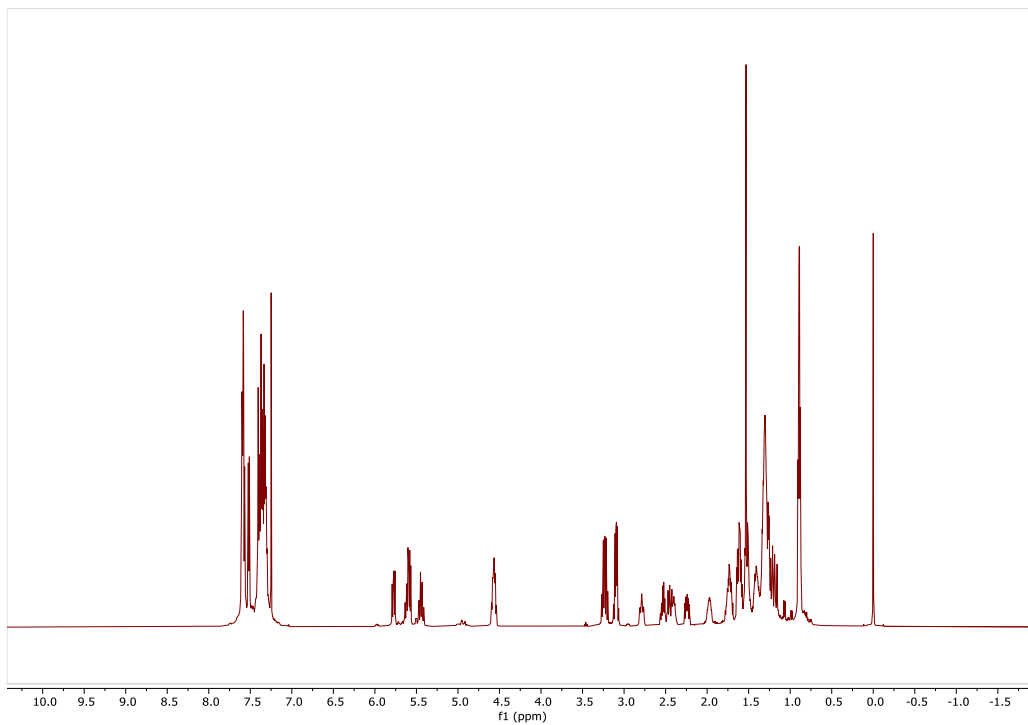
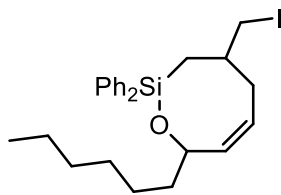




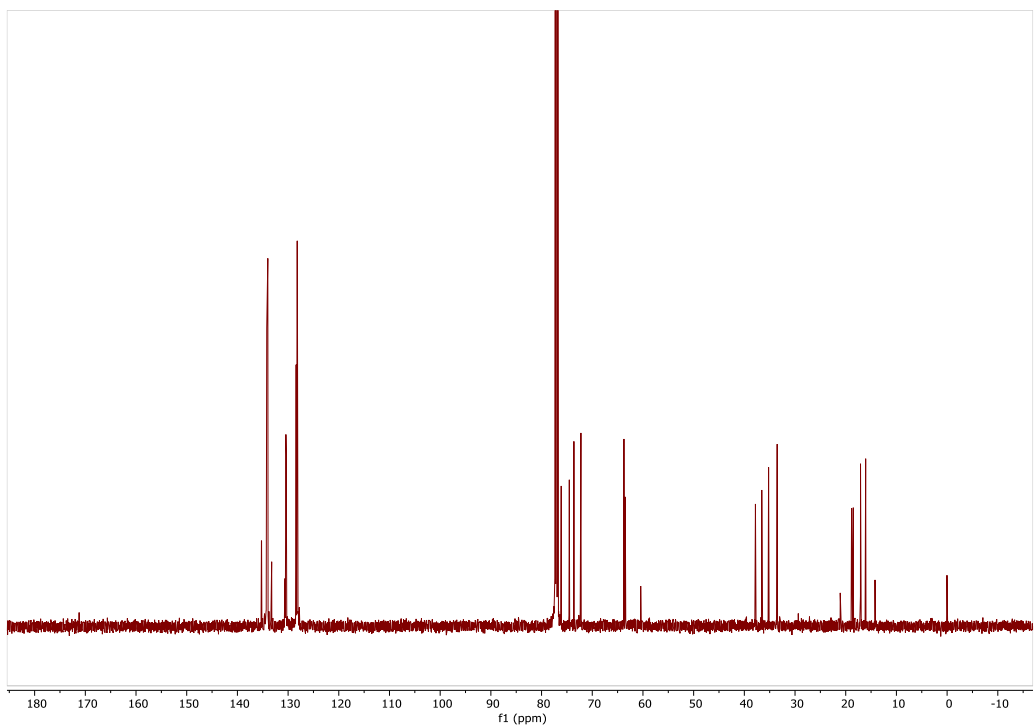
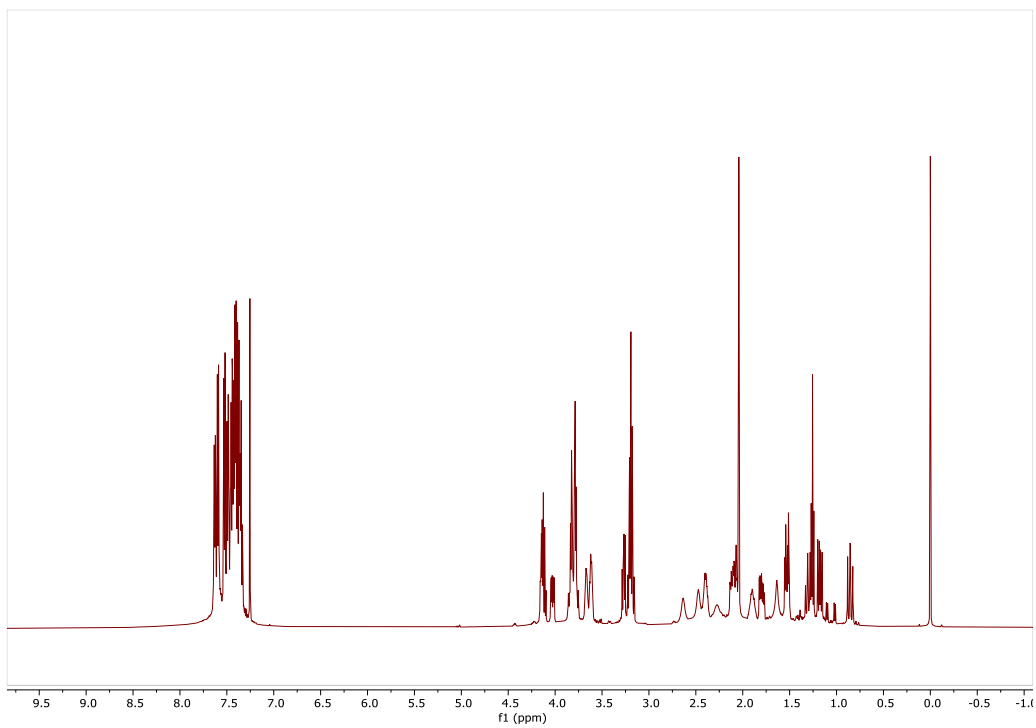
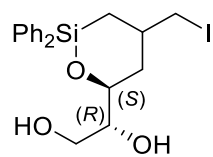


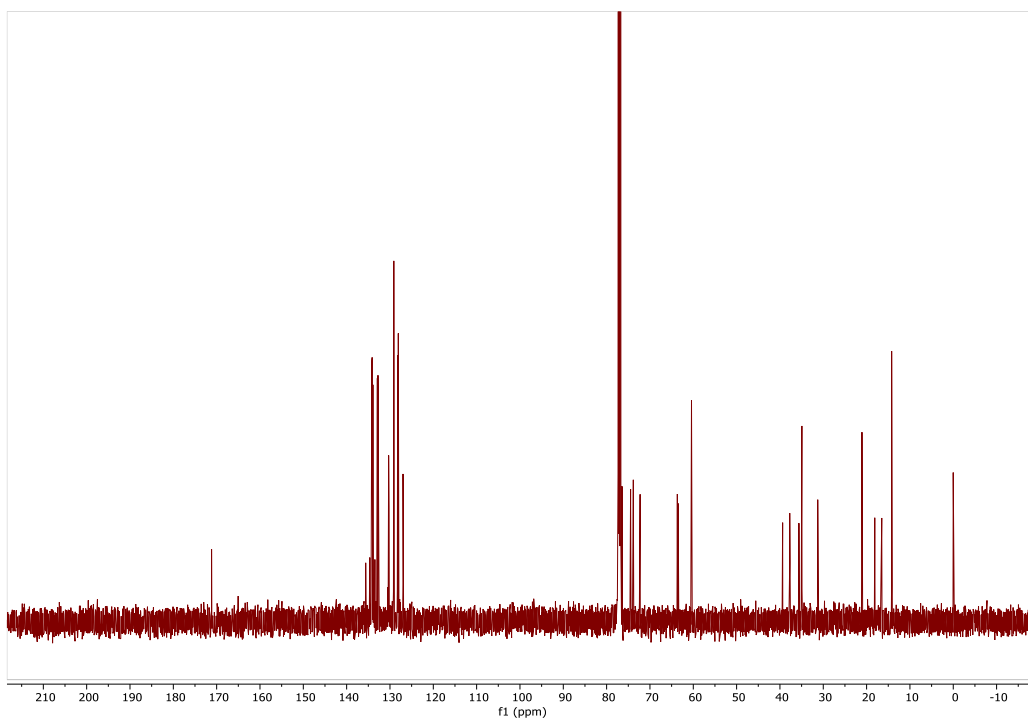
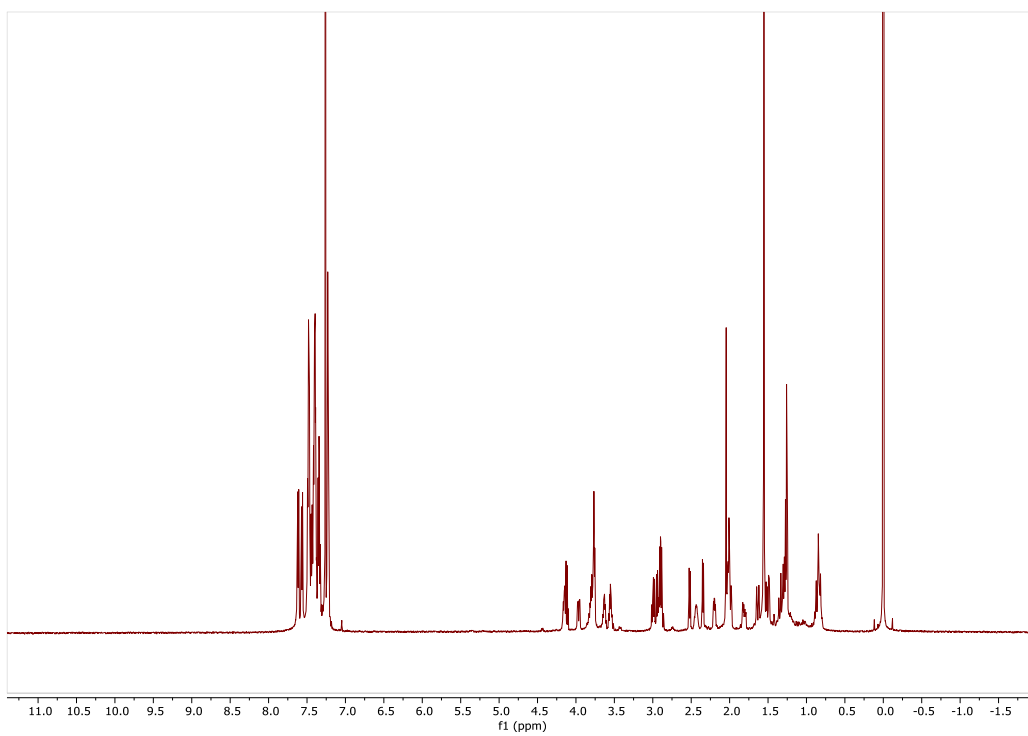


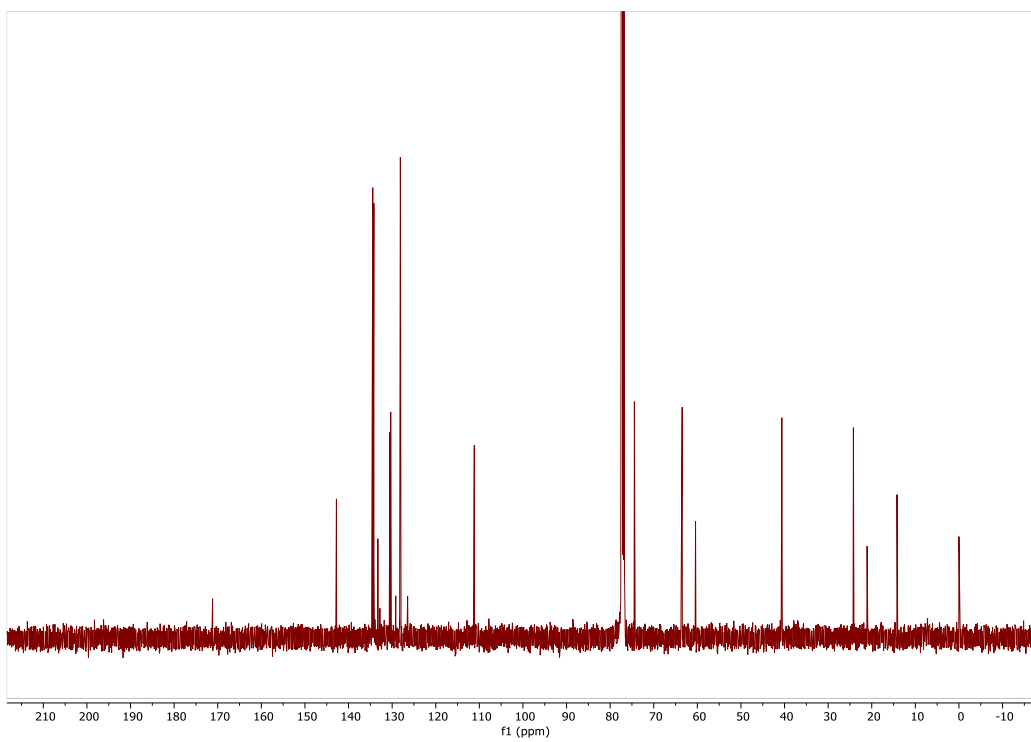
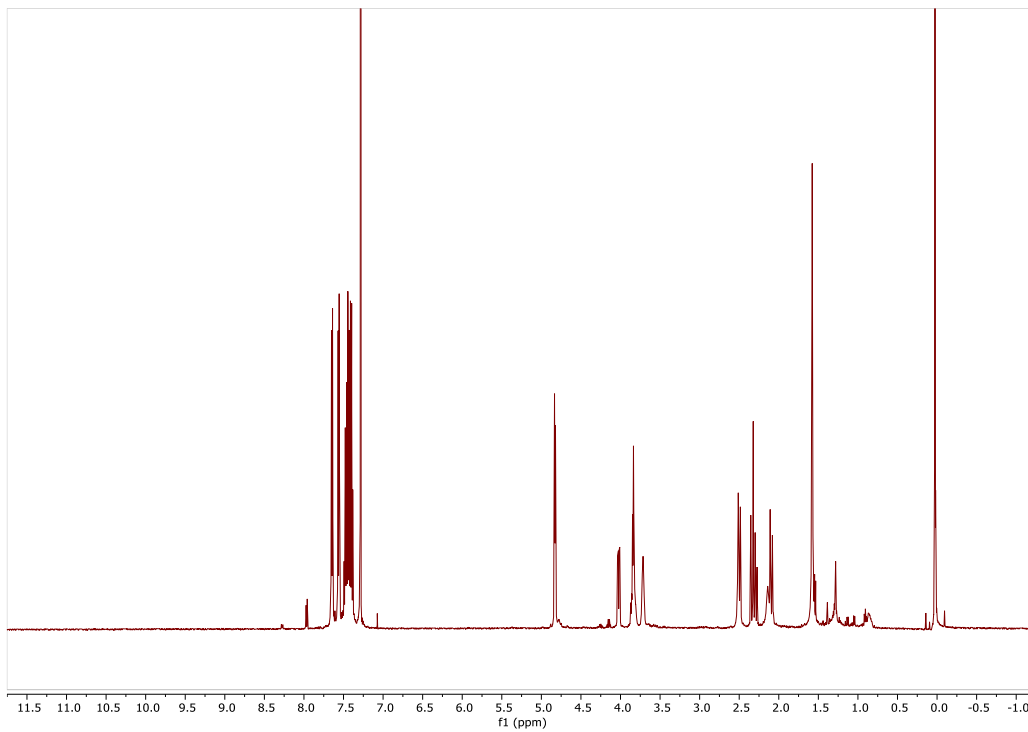
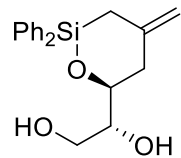


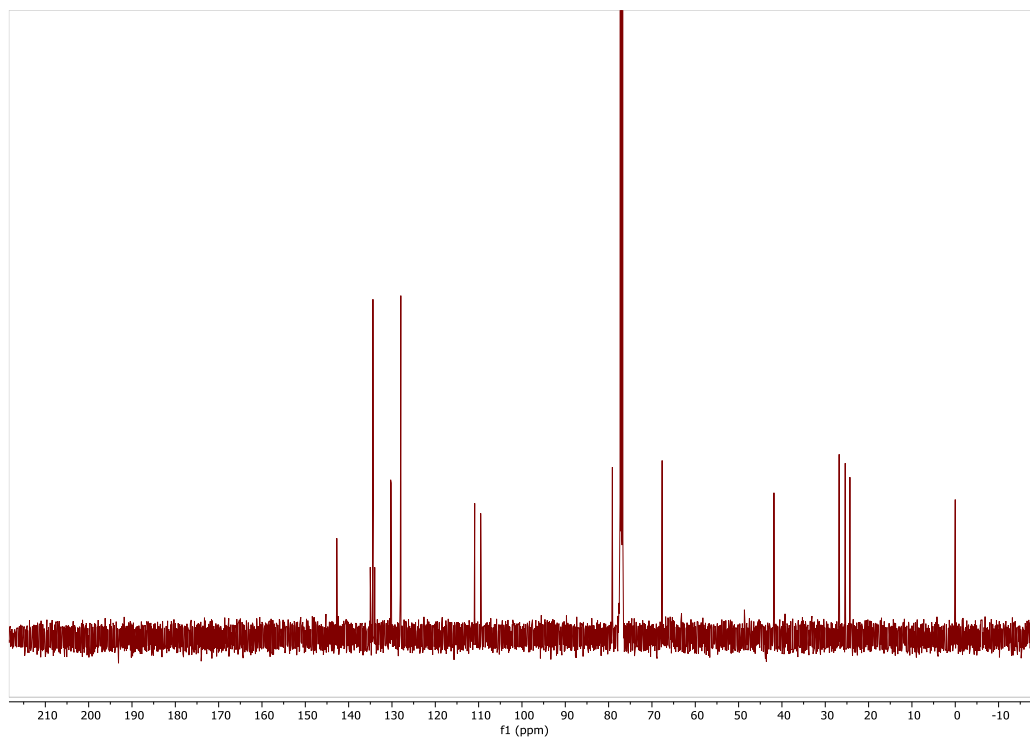
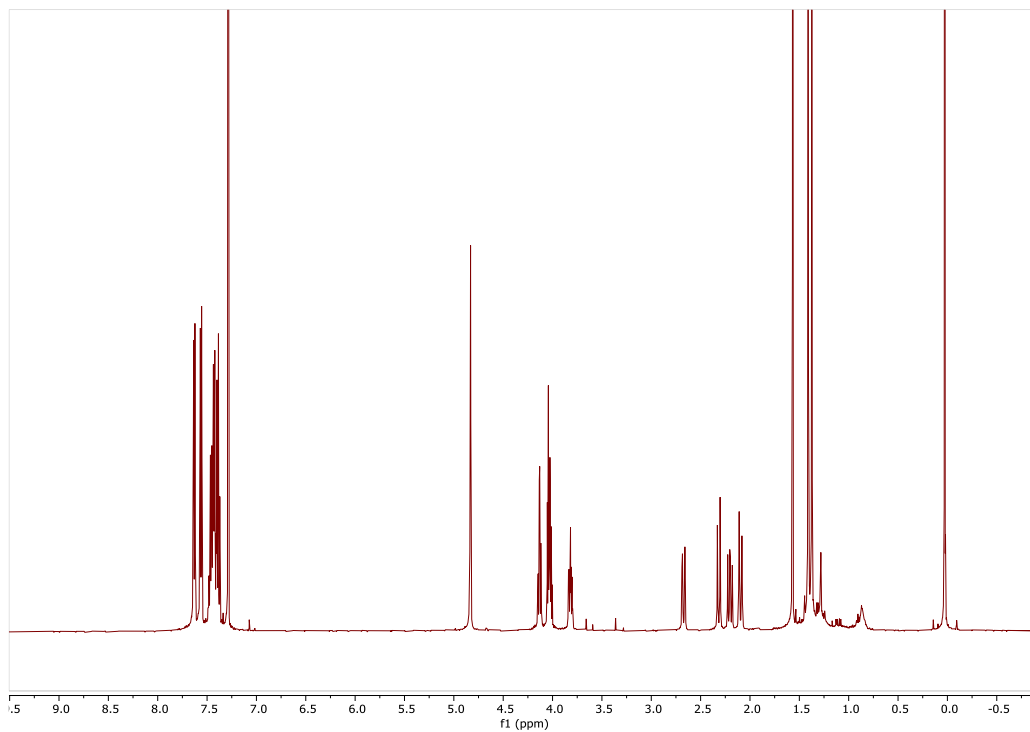
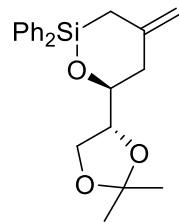


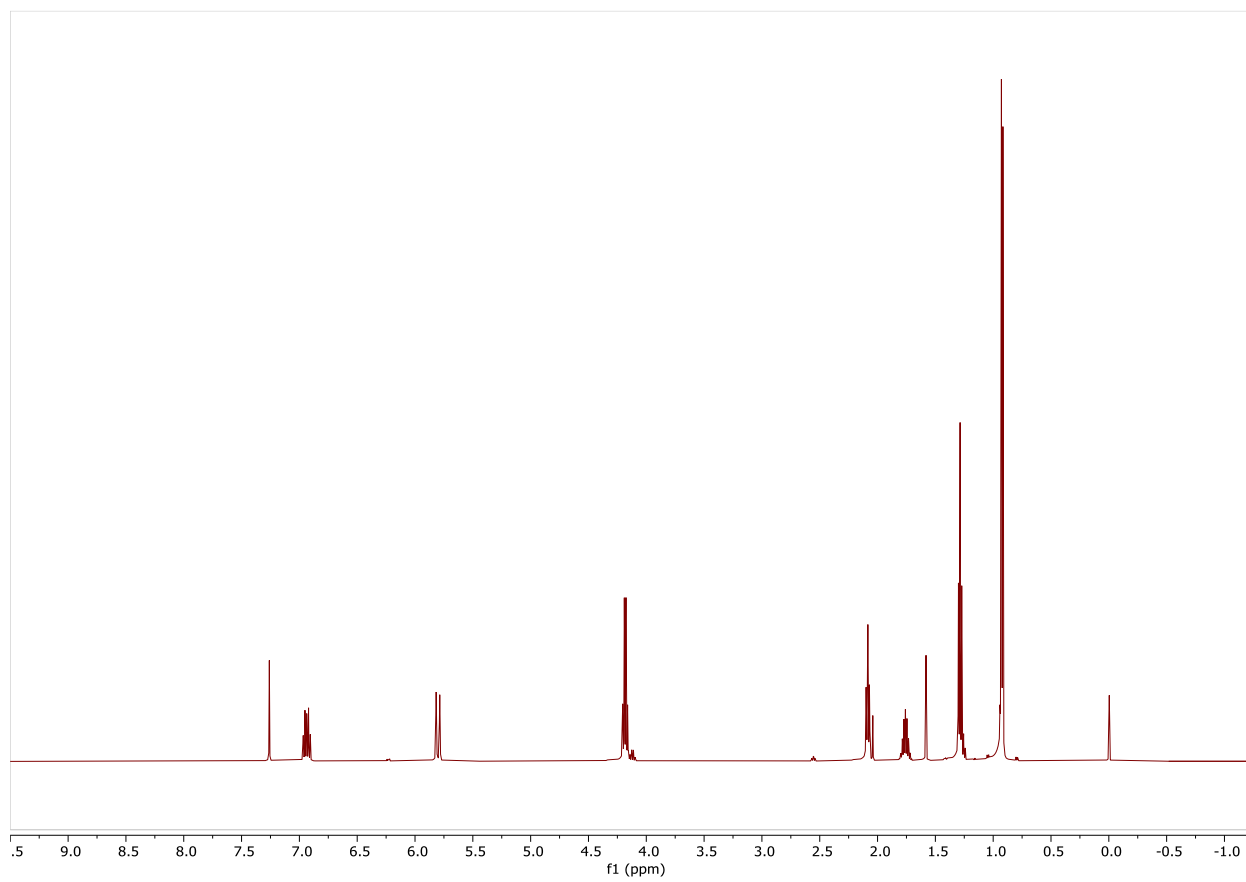
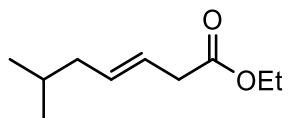


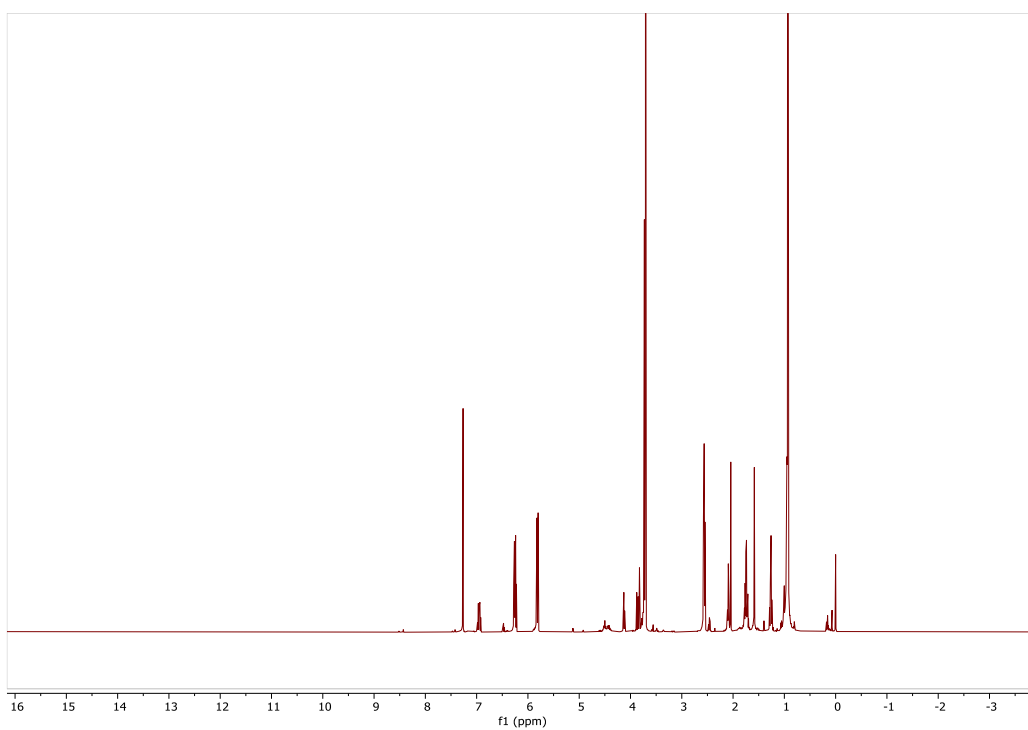
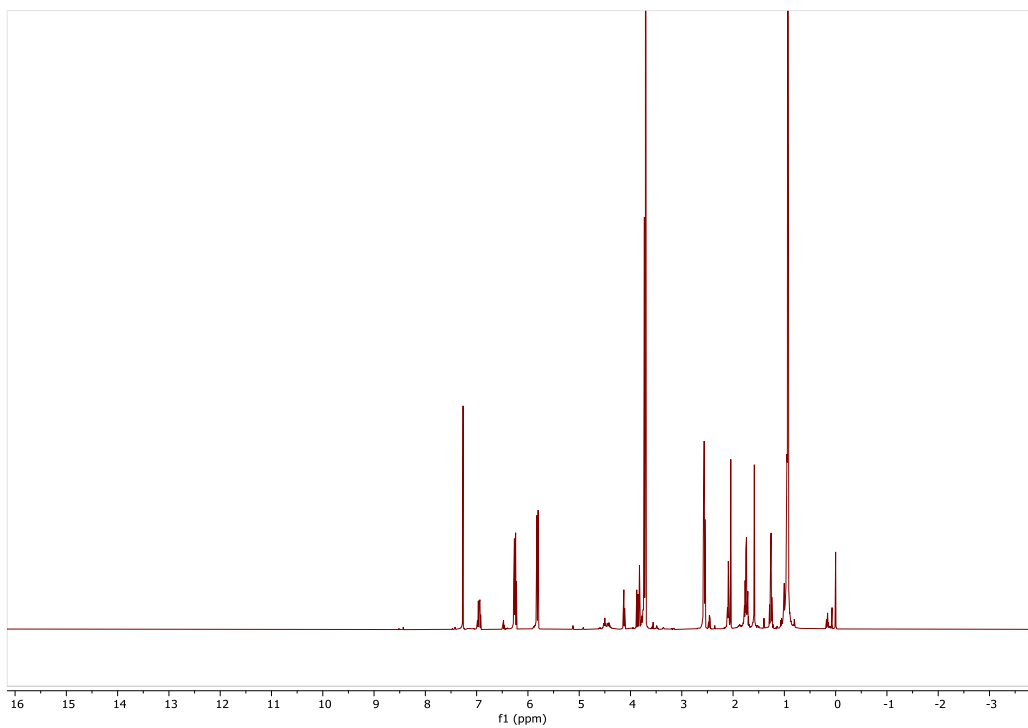
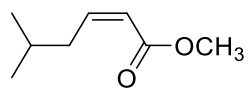


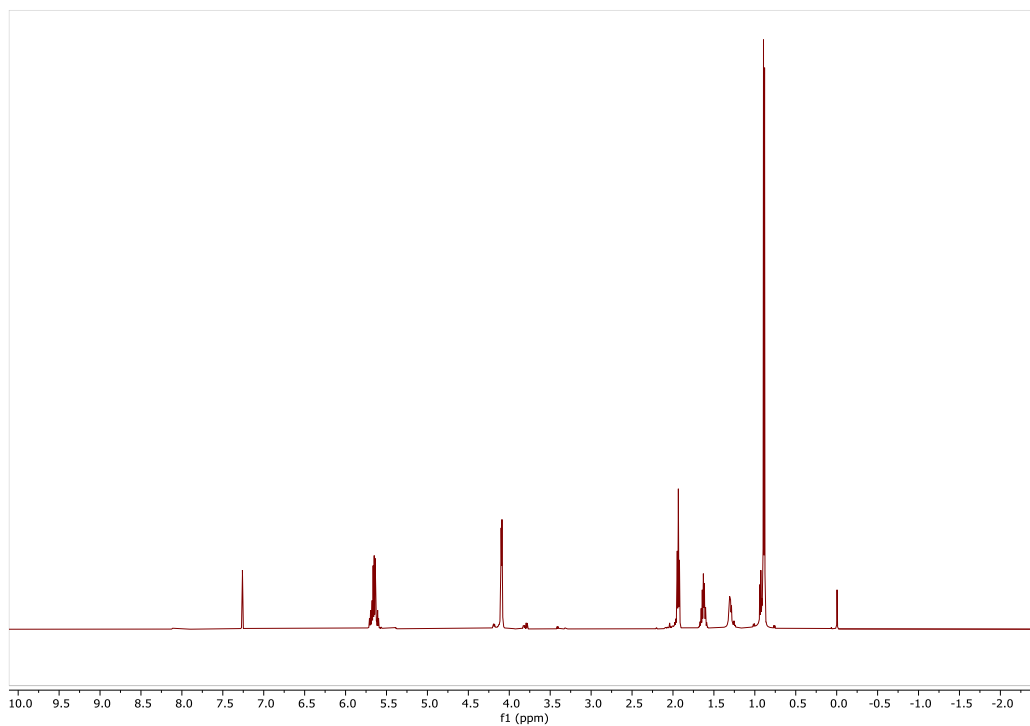
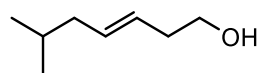


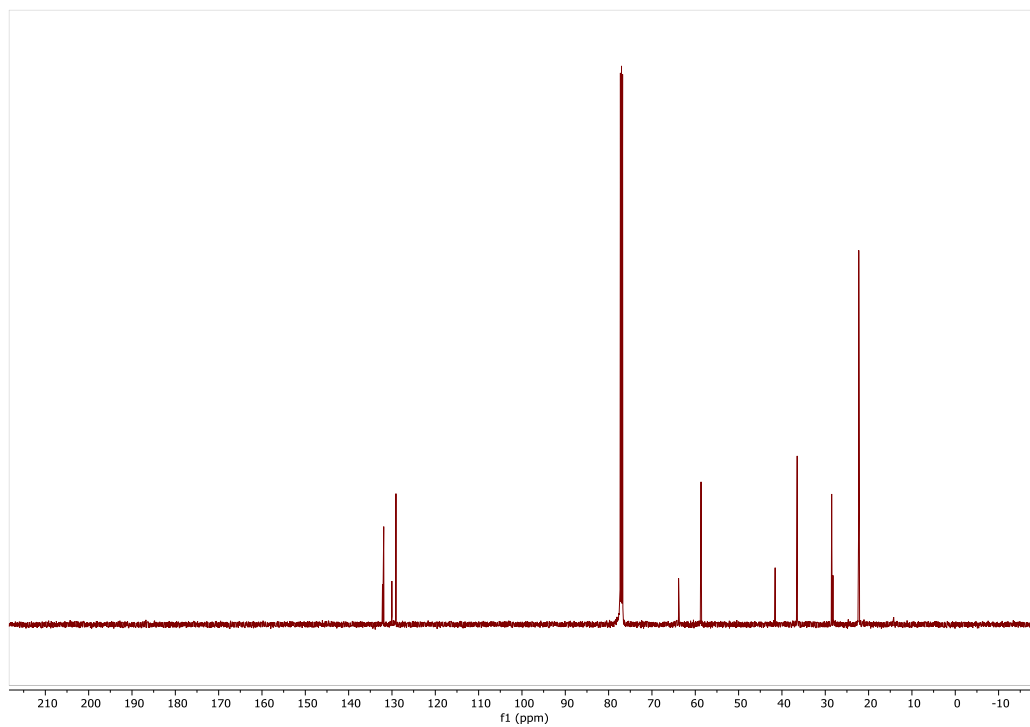
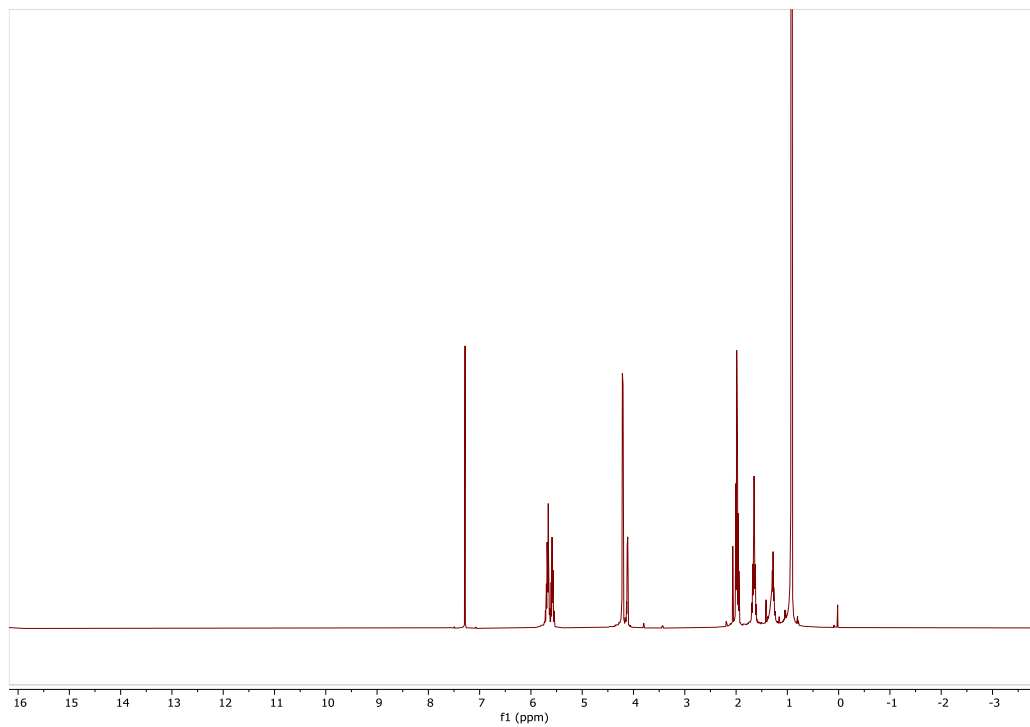
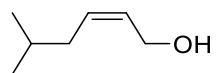


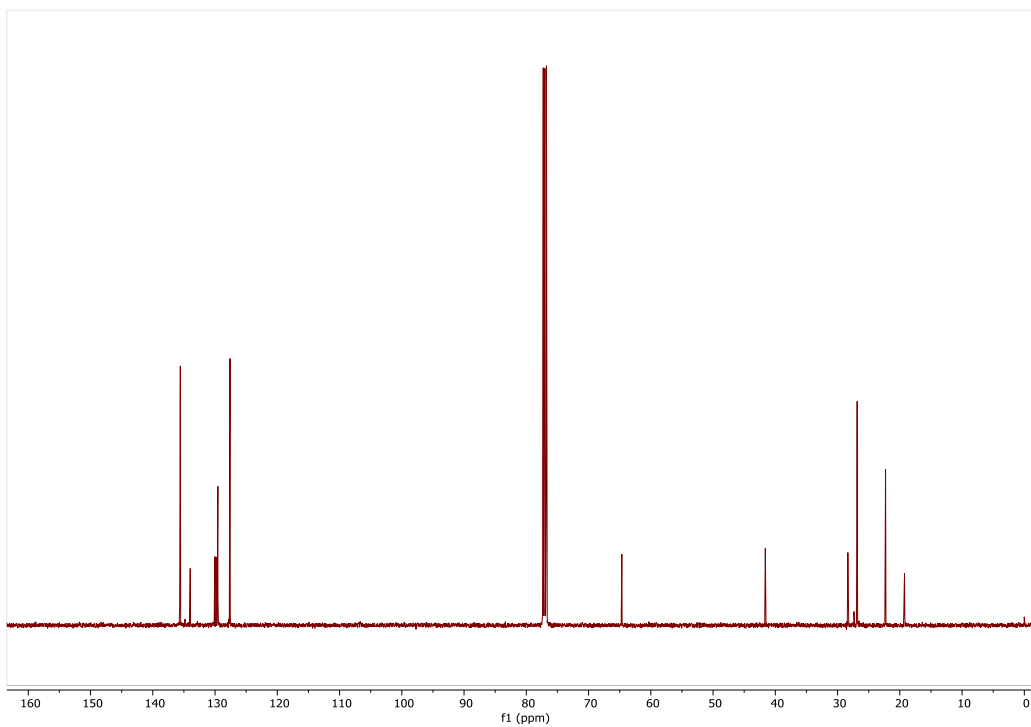
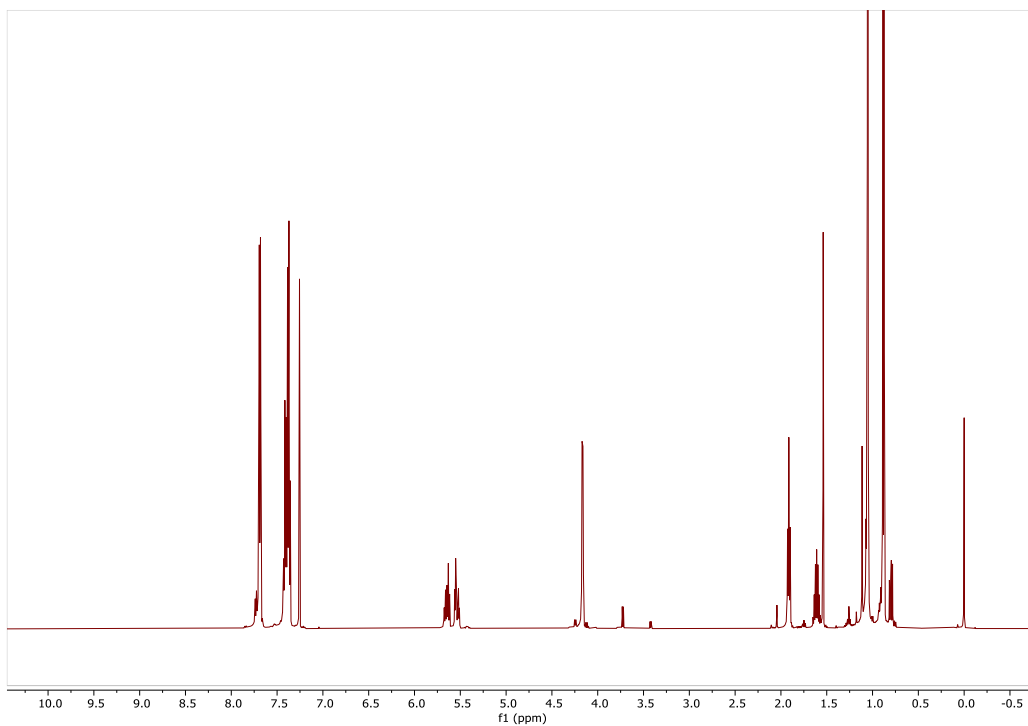
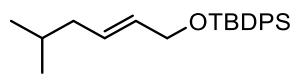


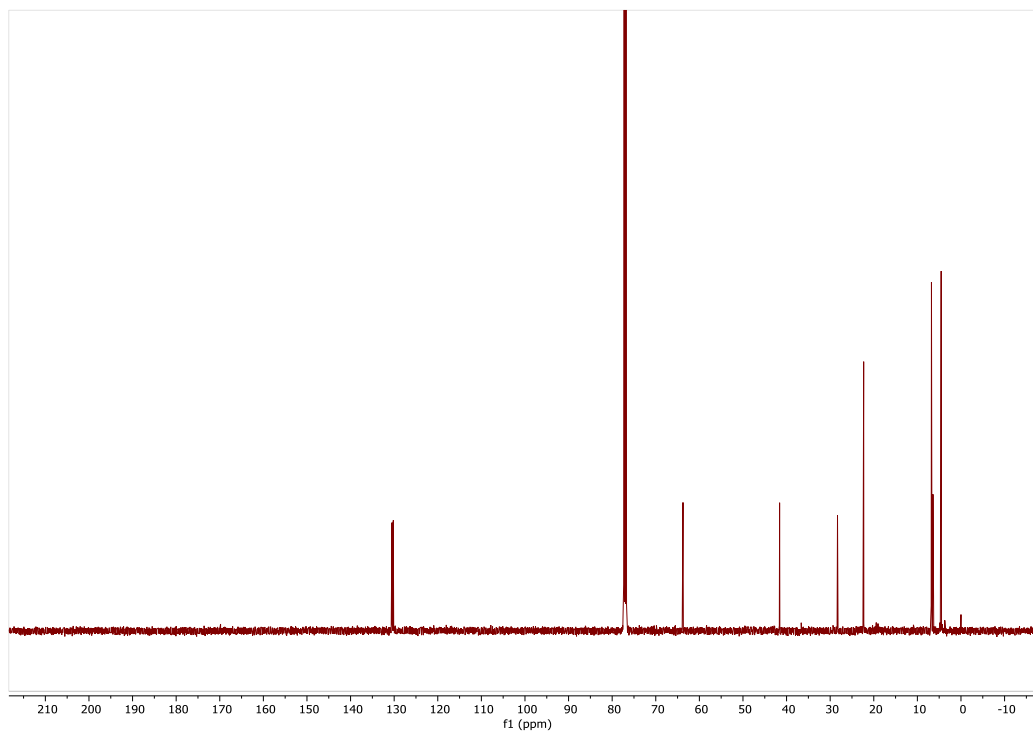
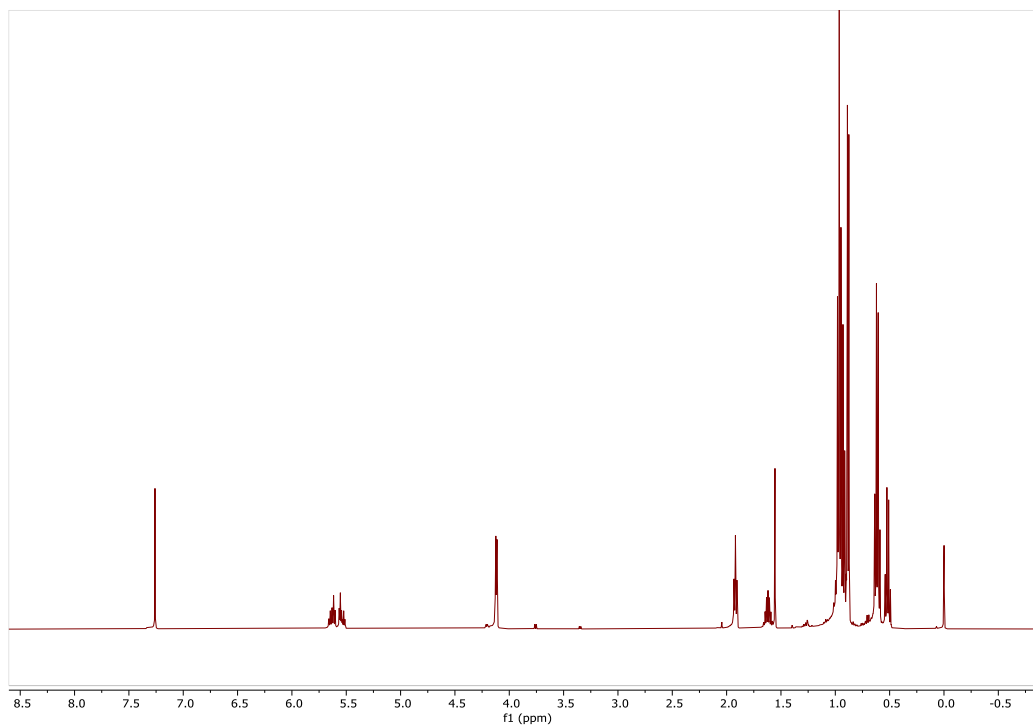
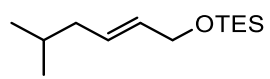


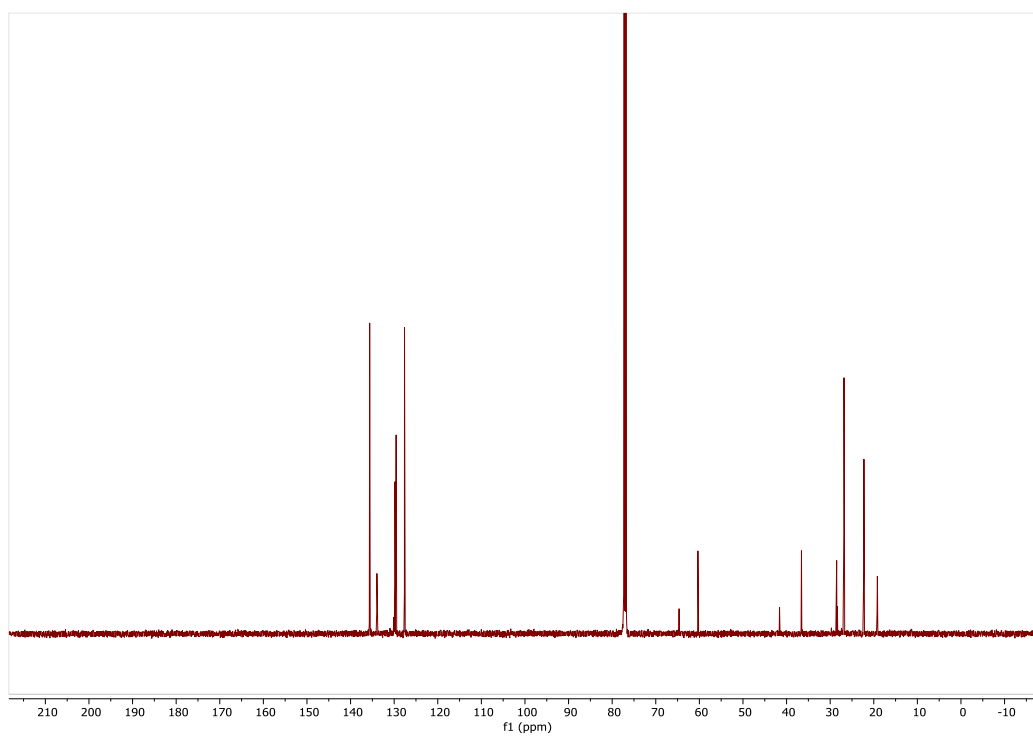
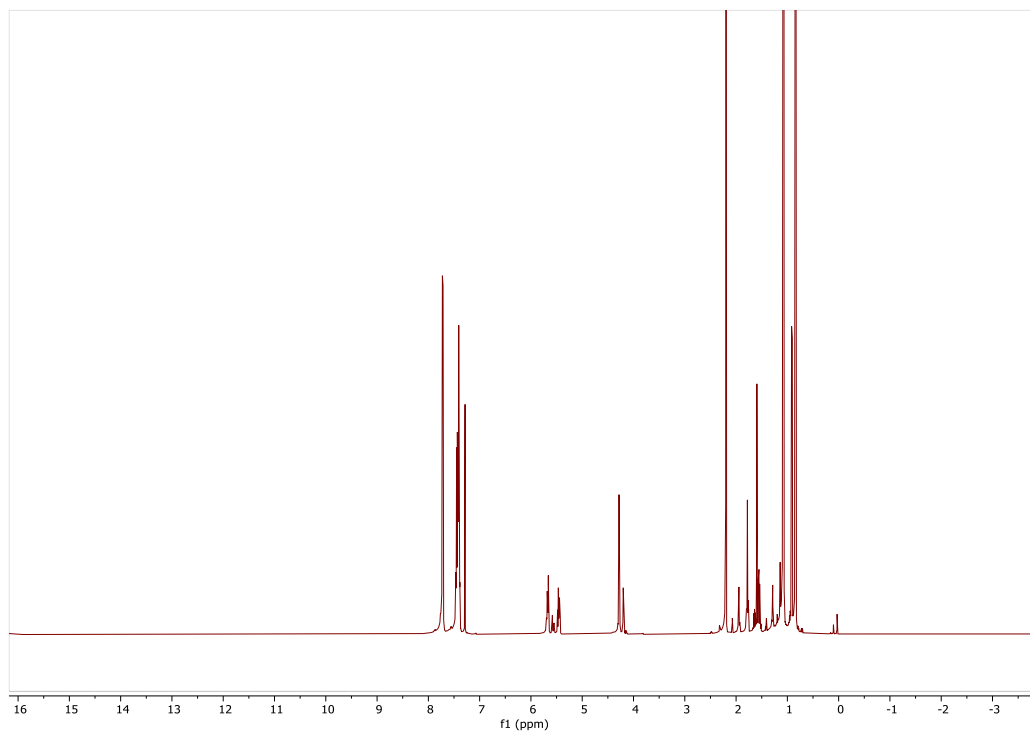
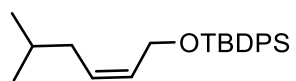


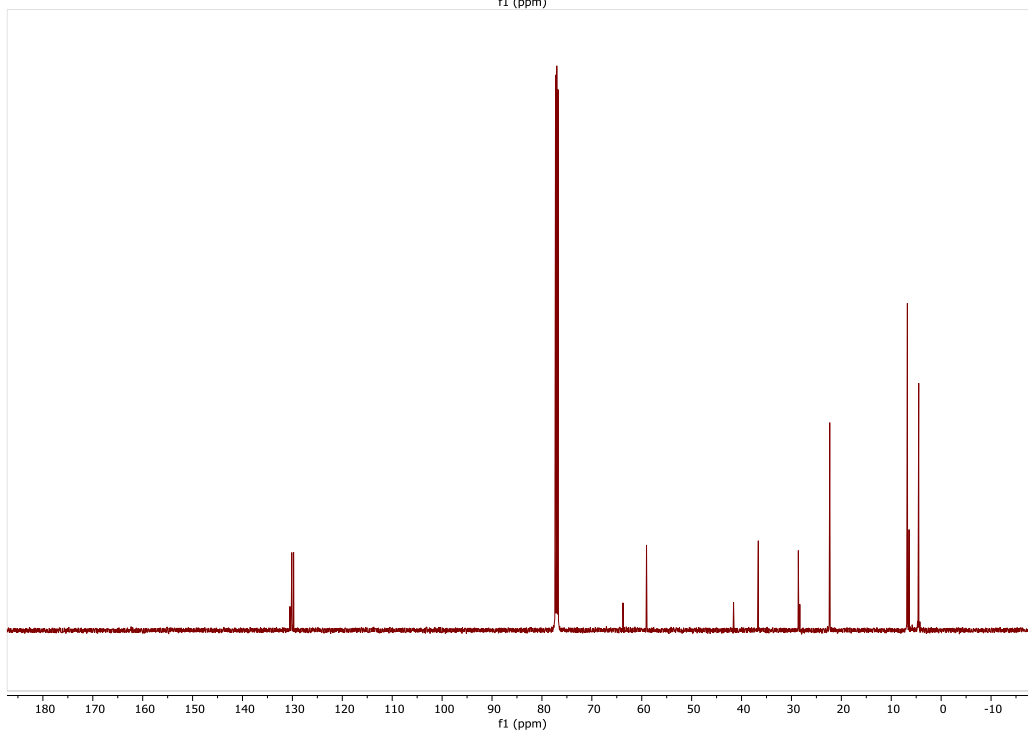
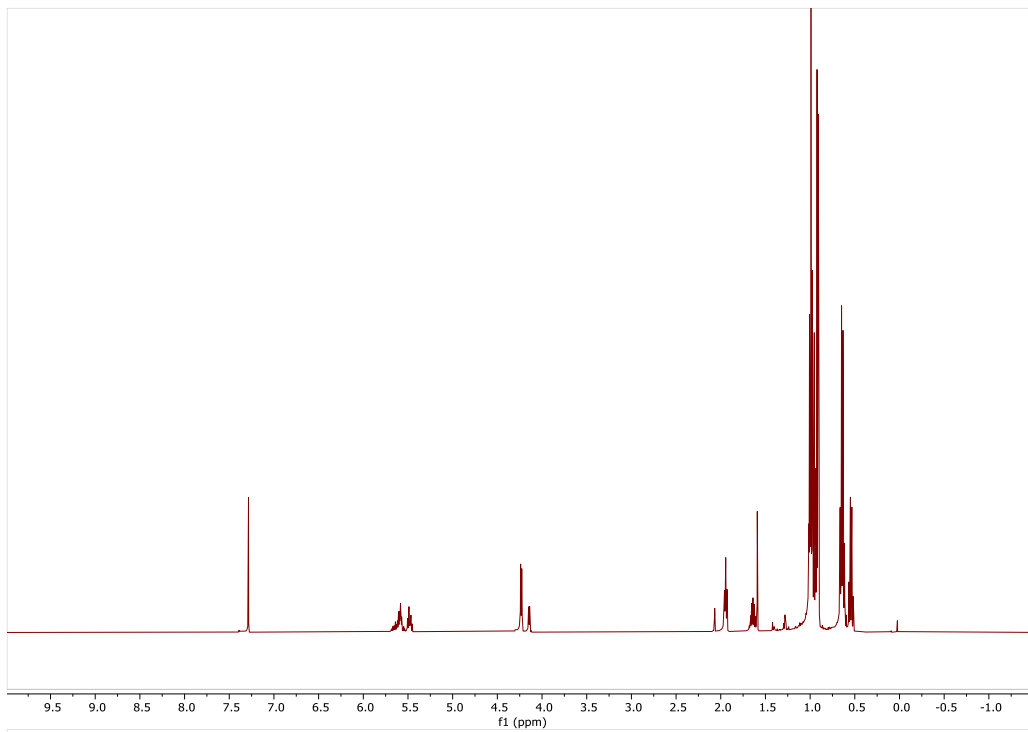
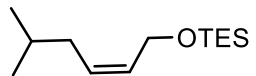












## WORK CITED

- 
- <sup>1</sup>Schneider, V. and Frölich P. K. *Industrial and Engineering Chemistry*. **1931**, 23, 1405-1410.
- <sup>2</sup>Banks, R. L. and Bailey G. C. *Industrial and Engineering Chemistry Product Research and Development*. **1964**, 3 (3), 170-173.
- <sup>3</sup>Handbook of Metathesis, 2nd ed. (Eds.:R.H.Grubbs, A. G. Wenzel), Wiley-VCH, Weinheim, **2015**.
- <sup>4</sup>Hughes, D.; Wheeler, P. and Ene, D. *Organic Process and Development*. **2017**, 21 (12), 1938-1962.
- <sup>5</sup>Higman, C. S.; Lummiss, J. A. M. and Fogg, D. E. *Angewandte Chemie International Edition*. **2016**, 55, 3552–3565.
- <sup>6</sup>Theunissen, C.; Ashley, M. A. and Rovis T. *Journal of the American Chemical Society*. **2019**, 141 (17), 6791-6796.
- <sup>7</sup>Mesina, M. S. and Maynard, H. D. *Materials Chemistry Frontiers*. **2020**, 4 (4), 1040-1051.
- <sup>8</sup>Liniger, M.; Neuhaus, C. M. and Altmann, K-H. *Molecules*. **2020**, 25(19), 4527.
- <sup>9</sup>Bloom, P. W. M. *Advanced Materials Technologies*.**2020**, 5(6), 2000144.
- <sup>10</sup>Koehler, S. L.; Hu, J. and Elacqua, E. *Synlett*. **2020**, 31(15), 1435-1442.
- <sup>11</sup>Trnka, T. M and Grubbs, R. H. *Accounts of Chemical Research*. **2001**, 34, 18-29.
- <sup>12</sup>Grubbs, R. H. *Journal of Macromolecular Science, Pure and Applied Chemistry*. **1994**, A31, 1829-1833.
- <sup>13</sup>France, M. B. and Grubbs, R. H. *Macromolecules*.**1993**, 26, 4739-4741.
- <sup>14</sup>Nguyen, S. T. The Designs, Synthesis, and Applications of Well-Defined, Single Component Group VIII Olefin Metathesis Catalysts. Ph.D. Thesis, California Institute of Technology, **1995**, Chapter 8.
- <sup>15</sup>Furstner, A. *Angewandte Chemie International Edition*. **2000**, 39(17), 3012-3043.
- <sup>16</sup>Scholl, M.; Ding, S.; Lee, C. W. and Grubbs, R. H. *Organic Letters*. **1999**, 1(6), 953-956.
- <sup>17</sup>Garber, S. B.; Kingsbury, J. S.; Gray, B. K. and Hoveyda, A. H. *Journal of the American Chemical Society*. **2000**, 122(34), 8168-8179.
- <sup>18</sup>Veldhuizen, J. J. V.; Garber, S. B.; Kingsbury, J. S. and Hoveyda, A. H. *Journal of the American Chemical Society*. **2002**, 124 (18), 4954-4955.
- <sup>19</sup>Wakamatsu, H. and Blechert, S. *Journal of the German Chemical Society*. **2002**, 41(5), 794-796.
- <sup>20</sup>Imhof, S.; Randl, S. and Blechert, S. *Chemical Communications*. **2001**, 1692-1693.
- <sup>21</sup>O'Leary, D.J. and O'Neil, G.W. (2015). "Cross-Metathesis" In *Handbook of Metathesis Vol. 2: Applications in Organic Synthesis, Second Edition* (Eds R.H. Grubbs, A.G. Wenzel, D.J. O'Leary and E. Khosravi), pp 171-294. Wiley-VCH, Weinheim Germany.
- <sup>22</sup>For a review see: Bielawski, C. W.; Grubbs, R. H. *Progress in Polymer Science*. **2007**, 32, 1-29.
- <sup>23</sup>Ehrhorn, H. and Tamm, M. *Chemistry: A European Journal*. **2019**, 25(13), 3190-3208.
- <sup>24</sup>da Silva, L. C.; Rojas, G.; Schulz, M. D.; Wagener, K. B. *Progress in Polymer Science*. **2017**, 69, 79-107.
- <sup>25</sup>Conrad, J. C.; Eelman, M. D.; Silva, J. A. D.; Monfette, S.; Parnas, H. H.; Snelgrove, J. L. and Fogg, D. E. *Journal of the American Chemical Society*. **2007**, 129, 1024-1025.
- <sup>26</sup>Schrock, R.; Rocklage, S.; Wengrovius, J.; Rupprecht, G. and Fellmann, J. *Journal of Molecular Catalysis*. **1980**, 8(1-3), 73-83.
- <sup>27</sup>Astruc, D. *New Journal of Chemistry*. **2005**, 29, 42-56.
- <sup>28</sup>Romero, P. E. and Piers, W. E. *Journal of the American Chemical Society*. **2005**, 127(14), 5032-5033.
- <sup>29</sup>Sinclair, F.; Alkattan, M.; Prunet, J. and Shaver, M. P. *Polymer Chemistry*. **2017**, 8, 3385-3398.
- <sup>30</sup>Data obtained from sigmaaldrich.com on the 16<sup>th</sup> of November, 2020.
- <sup>31</sup>Butilkov D.; Frenklahm A.; Rozenberg, I.; Kozuch, S. and Lemcoff, N. G. *ACS Catalysis*. **2017**, 7(11), 7634-7637.
- <sup>32</sup>Ngo, H. L.; Jones, K. and Foglia, T. A. *Journal of the American Oil Chemists' Society*. **2006**, 83(7), 629-634.
- <sup>33</sup>Arumugasamy, J, et al. *Organic Process Research & Development*. **2013**, 17(5), 811-828.
- <sup>34</sup>Yee, N.K.; Wei, X.; Busacca, C.A.; Zeng X.; Fandrick, D.R.; Song, J.J. and Senanayake, C.H. "9.19 Synthesis of the Leading HCV Protease Inhibitors." *Comprehensive Chirality*, edited by Erick M. Carreira and Hisashi Yamamoto, Elsevier, 2012, pp. 483-506.
- <sup>35</sup>Wang, H.; Matsuhashi, H.; Doan, B. S.; Goodman, S. N.; Ouyang, X.; Clark, W. M., Jr. *Tetrahedron*, **2009**, 65 (32), 6291-6303.

- <sup>36</sup> Flcik, A. C.; Dina, H. X.; Leverett, C. A.; H=Kyne, R. E.; Lie, K.K-C.; Fink, S. J. and O'Donnell, C. J. *Journal of Medicinal Chemistry*. **2017**, 60 (15), 6480-6515.
- <sup>37</sup> Wu et al. US Patent 9, 249,144 B2, **2016**.
- <sup>38</sup> Yu, M.; Lou, S. and Gonzalez-Bobes, F. *Organic Process Research & Development*. **2018**, 22(8), 918-946.
- <sup>39</sup> Cusak, A. *Chemistry-a European Journal*. **2012**, 18, 5800-5824.
- <sup>40</sup> Hanson, P.; Maitra, S.; Chegondi, R.; Markley, J. J. "Synthesis of Heterocycles Containing Si, P, or B" in *Handbook of Metathesis, 2nd Ed.* (Eds. D. J. O'Leary and R. H. Grubbs), pp 29-34. Wiley-VCH, Weinheim Germany
- <sup>41</sup> For an example of a non RCM-based syntheses of medium ring oxasilacycles see: Greene, M. A.; Prevost, M.; Tolopilo, J.; Woerpel, K. A. "Diastereoselective Synthesis of Seven-Membered-Ring trans-Alkenes from Dienes and Aldehydes by Silylene Transfer" *J. Am. Chem. Soc.* **2012**, 134, 12482-12484.
- <sup>42</sup> Devineau, A.; Grosbois, M.; Carletti, I.; Vacher, B. *Journal of Organic Chemistry*. **2008**, 74, 757-763
- <sup>43</sup> Jimenez-Gonzalez, L.; Alvarez-Corral, M.; Munoz-Dorado, M. and Rodriquez-Garcia, I. *Chemical Communications*. **2005**, 21, 2689-2691.
- <sup>44</sup> Scalzullo, S. M.; Islam, R. U.; Morgans, G. L.; Michael, J. P. and L.van Otterlo, W. A. *Tetrahedron Letters*. **2008**, 49, 7403-7405.
- <sup>45</sup> Volchkov, I.; Park, S. and Lee, D. *Organic Letters*. **2011**, 13, 3530-3533.
- <sup>46</sup> Kiely, A. F.; Jernelius, J. A.; Schrock, R. R.; Hoveyda, A. H. *Journal of the American Chemical Society*. **2002**, 124, 2868-2869.
- <sup>47</sup> Hong, S. H.; Wenzel, A. G.; Salguero, T. T.; Day, M. W. and Grubbs, R. H. *Journal of the American Chemical Society*. **2007**, 129(25), 7961-7968.
- <sup>48</sup> Hong, S. H.; Day, M. W. and Grubbs, R. H. *Journal of the American Chemical Society*. **2004**, 126(24), 7414-7415.
- <sup>49</sup> Hong, S. H.; Wenzel, A. G.; Salguero, T. T.; Day, M. W. and Grubbs, R. H. *Journal of the American Chemical Society*. **2007**, 129(25), 7961-7968
- <sup>50</sup> Sandford, M.S.; Love, J.A. and Grubbs, R.H. *Journal of the American Chemical Society*. **2001**, 123, 6543-6554.
- <sup>51</sup> Vehlow, K.; Gessler, S. and Blechert, S. *Angewandte Chemie International Edition*. **2007**, 46, 8082-8085.
- <sup>52</sup> Fustero, S.; Sanchez-Rosello, M.; Jimenez, D.; Sanz-Cervera, J. F.; Pozo, C. and Acena, J. L. *The Journal of Organic Chemistry*. **2006**, 71 (7), 2706-2714.
- <sup>53</sup> Berg, J. M.; Tymoczko, J. L. and Stryer, L. *Biochemistry*. 5th edition. New York: W H Freeman; **2002**. Section 8.2, "Free Energy Is a Useful Thermodynamic Function for Understanding Enzymes."
- <sup>54</sup> Higman, C. S.; Lanterna, A. E.; Marin, M. L.; Scaiano, J. C. and Fogg, D. E. *ChemCatChem Communications*. **2016**, 8, 2446-2449.
- <sup>55</sup> Bourgeois, D.; Pancrazi, A.; Nolan, S. P. and Prunet, J. *Journal of Organometallic Chemistry*. **2002**, 643-644, 247-252.
- <sup>56</sup> Brown, R. F. and van Gulick, N. M. *Journal of Organic Chemistry*. **1956**, 21(9), 1046-1049.
- <sup>57</sup> O'Neill, M. J.; Riesebeck, T. and Cornella, J. *Angewandte Chemie International Edition*. **2018**, 57(29), 9103-9107.
- <sup>58</sup> (a) Suslova, E. N.; Albanov, A. I. and Shainyan, B. A. *Russian Journal of General Chemistry* **2008**, 78, 1016-1017.  
(b) Suslova, E. N.; Albanov, A. I. and Shainyan, B. A *Journal of Organometallic Chemistry*. **2009**, 694, 420-426.
- <sup>59</sup> Cadot, C.; Dalko, P. I. and Cossy, J. *Tetrahedron Letters*. **2002**, 43, 1839-1841.
- <sup>60</sup> Taher, A.; Aderibigbe, B. A.; Morgans, G. L.; Madeley, L. G.; Khanye, S. D.; van der Westhuizen, L.; Fernandes, M. A.; Smith, V. J.; Michael, J. P.; Green, I. R. and van Otterlo, W. A. L. *Tetrahedron*. **2013**, 69, 2038-2047.
- <sup>61</sup> Smit, W.; Foscatto, <; Occhipinti, G. and Jensen, V. R. *ACS Catalysis*. **2020**, 10(12), 6788-6767.
- <sup>62</sup> Hoveyda, A. H.; Lio, Z.; Qin, C.; Koengeter, T. and Mu, Y. *Angewandte Chemie International Edition*. **2020**, 59(50), 22324-22348.
- <sup>63</sup> Morgans, G. L.; Ngidi, L.; Madeley, L. G.; Khanye, S. D.; Michael, J. P.; de Koning, C. B. and van Otterlo, W. A. L. *Tetrahedron*. **2009**, 65, 10650-10659.
- <sup>64</sup> Lubbe, C.; Dymrath, A.; Neumann, H.; Schuffer, M.; Zimmermann, R.; Beller, M. and Kadyrov, R. *ChemCatChem*. **2004**, 6,684-688.
- <sup>65</sup> Hong, S. H.; Sanders, D. P.; Lee, C. W. and Grubbs, R. H. *Journal of the American Chemical Society*. **2005**, 127(49), 17160-17161.

- 
- <sup>66</sup> Xiao, W.; Deng, Z.; Huang, J.; Huang, Z.; Zhaung, M.; Yuan, Y.; Nie, J. and Zhang, Y. *Analytical Chemistry*. 2019, 91(23), 15115-15122.
- <sup>67</sup> Widegren, J. A. and Finke, R. G. *Journal of Molecular Catalysis A: Chemical*. 2003, 198, 317-341.
- <sup>68</sup> For a recent example see: Ohta, R.; Oguro, A.; Nishimura, K.; Murai, K.; Fujioka, H. and Arisawa, M. *Organic and Biomolecular Chemistry*. 2019, 17, 867-875.
- <sup>69</sup> Thomas, R. M.; Federov, A.; Keitz, B. K. and Grubbs, R. H. *Organometallics* 2011, 30, 6713-6717.
- <sup>70</sup> O'Neil, G. W. and Cummins, E. J. *Tetrahedron Letters*. 2017, 58, 3406-3409.
- <sup>71</sup> Netolitzky, Z. *Angewandte Entomologie*. 1919, 5, 252-257.
- <sup>72</sup> Frank, J. H. and Kanamitsu, K., *Journal of Medical Entomology*. 1987, 24, 155-191.
- <sup>73</sup> Qadir, S. N. R.; Raza, N. and Rahman, S. B. *Dermatology Online Journal*. 2006, 12, 9.
- <sup>74</sup> Soldati, M.; Fioretti, A. and Ghione, M. *Experientia*. 1966, 22, 176-178.
- <sup>75</sup> Piel, J. *Proceedings of the National Academy of Sciences of the USA*. 2002, 99, 14002-14007;
- <sup>76</sup> Piel, J.; Höfer, I. and Hui, D. *Journal of Bacteriology*. 2004, 186, 1280-1286.
- <sup>77</sup> Cichewicz, R. H.; Valeriote, F. A. and Crews, P. *Organic Letters*. 2004, 6, 1951-1954.
- <sup>78</sup> Pettit, G. R.; Xu, J.-P.; Chapuis, J.-C.; Pettit, R. K.; Tackett, L. P.; Doubek, D. L.; Hooper, J. N. A. and Schmidt J. M. *Journal of Medicinal Chemistry*. 2004, 47, 1149-1152.
- <sup>79</sup> Bielitz, M. and Pietruszka, J. *Angewandte Chemie International Edition*. 2013, 52(42), 10960-10985.
- <sup>80</sup> Jiang, X.; Garcia-Fortanet, J. and De Brabander, J. K. *Journal of the American Chemical Society*. 2005, 127, 11254-11255.
- <sup>81</sup> Junttila, M. H. and Hormi, O. O. E. *The Journal of Organic Chemistry*. 2009, 74(8), 3038-3947.
- <sup>82</sup> Urosa, A.; Marcos, I. S.; Diez, D.; Padron, J. M. and Basabe, P. *The Journal of Organic Chemistry*. 2015, 80, 6447-6455.
- <sup>83</sup> Wang, Z.-M.; Kakiuchi, K. and Sharpless, K. B. *The Journal of Organic Chemistry*. 1994, 59, 6895-6897.
- <sup>84</sup> Wang, L. and Sharpless, K. B. *Journal of the American Chemical Society*. 1992, 114(19), 7568-7570.
- <sup>85</sup> Becker, H.; King, S. B.; Taniguchi, M.; Vanhessche, K. P. M. and Sharpless, K. B. *Journal of Organic Chemistry*. 1995, 60(13), 3940-3941
- <sup>86</sup> Gintner, M.; Denner, C.; Schmolzer, C.; Fischer, M.; Fruhauf, P.; Kahig, H. and Schmid, W. *Monatshefte für Chemie*. 2017, 150, 849-860.
- <sup>87</sup> Tamao, K.; Ishida, N.; Tanaka, T. and Kumada, M. *Organometallics*. 1983, 2(11), 1694-1696.
- <sup>88</sup> Roy, A. and Oestreich, M. *Angewandte Chemie International Edition*. 2021, 60, 4408-4410.
- <sup>89</sup> *Org. Biomol. Chem.*, 2004, 2, 1315-1329.
- <sup>90</sup> *Org. Biomol. Chem.*, 2004, 2, 1315-1329
- <sup>91</sup> Jiang, X., Garcia-Fortanet, J. and De Brabander, J. K. Synthesis and Complete Stereochemical Assignment of Psymberin/Irciniastatin A. *J. Am. Chem. Soc.* 2005, 127, 32, 11254-11255.
- <sup>92</sup> Gintner, M., Denner, C., Schmolzer, C. *et al.* Synthesis of 3-deoxy-2-uloses via the indium-mediated allylation reaction. *Monatsh Chem*, 2019, 150, 849-860.
- <sup>93</sup> *Org. Lett.* 2013, 15, 17, 4616-461
- <sup>94</sup> *Org. Lett.* 2013, 15, 17, 4616-461